ANALYSIS OF BUBBLE FORMATION MECHANISM WITHIN TRANSFORMER INSULATION: EFFECT OF LOADING AND MATERIAL

A thesis submitted to The University of Manchester for the degree of
Doctor of Philosophy
in the Faculty of Science and Engineering

2020

JAMES P HILL

School of Engineering

Department of Electrical and Electronic Engineering

TABLE OF CONTENTS

Table of Contents

Table of Contents

Table of Contents

Table of Contents

Word Count: 53,944

LIST OF ABBREVIATIONS

Abbreviation	Meaning
AC	Alternating Current
ADMD	After Diversity Maximum Demand
ASTM	American Society for Testing and Materials
BIT	Bubble Inception Temperature
CCC	Committee for Climate Change
CI	Crystallinity Index
-COOR	Ester Functional Group
COP	Coefficient of Performance
cuen	Copper(II) Ethylenediamine
DC	Direct Current
DDP	Diamond Dotted Paper
DP	Degree of Polymerisation
DSLR	Digital Single-lens Reflex
EHP	Electric Heat Pump
EV	Electric Vehicle
GHG	Greenhouse Gases
GTL	Gas-to-Liquid
H_2O	Water
HST	Hot-spot Temperature
I^-	Negative Iodine Ion
I_2	Iodine
IB	Sample from the Inner Layer, Bottom Section
IEC	International Electrotechnical Commission
IEEE	Institute of Electrical and Electronic Engineers
IL	Sample from the Inner Layer, Lower Section
IU	Sample from the Inner Layer, Upper Section
KF	Karl Fischer
LCT	Low Carbon Technology
MATLAB	Matrix Laboratory Software
MODEL 1	Generation of Daily Demand Profile and Daily Ambient Temperature Profile
MODEL 2	Model for Calculating Transformer Hot-Spot Temperatures
MODEL 3	Model for Calculating Bubble Inception Temperatures
NTUP	Non-thermally Upgraded Paper
-O-	Oxygen Bridge Molecule
OB	Sample from the Outer Layer, Bottom Section
OD	Oil Directed Cooling
OF	Oil Forced Cooling
Ofgem	Office for Gas and Electricity Markets
-OH	Hydroxyl Bond / Functional Group
OL	Sample from the Outer Layer, Lower Section
ON	Oil Natural Cooling
OU	Sample from the Outer Layer, Upper Section
PD	Partial Discharge
PID	Proportional, Integral, Derivative (control)
RH	Relative Humidity
RoCoT	Rate of Change of Temperature
RS	Relative Saturation
TAN	Total Acid Number
tBI	Time to Bubble Inception
TUP	Thermally Upgraded Paper
UK	United Kingdom
UNFCCC	United Nations Framework Convention on Climate Change
US	United States (of America)

LIST OF SYMBOLS

Symbol	Meaning
″	Inches
%	Percentage
£	Great British Pounds
°	Degrees of Angle
A	Frequency of Effective Collisions
a	Area (meters squared)
A	Amps
B	Specific Energy Related Constant in Exponential Functions (Kelvin)
cm	Centimeters
E	Electromotive Force (Volts)
e	Exponential Function
F_{AA}	Accelerated Ageing Factor (dimensionless)
G	Gibbs Energy (Joules)
g	Grammes
g_r	Temperature Gradient between Winding and Oil / Liquid (Kelvin)
H	Enthalpy (Joules)
H_f	Host-spot Factor
hrs	Hours
Hz	Hertz
I	Current (Amps)
J	Joules
K	Kelvin
K	Rate Reaction Constant
k_{11}	Transformer Temperature Constant
k_{21}	Transformer Temperature Constant
k_{22}	Transformer Temperature Constant
kg	Kilogrammes
kV	Kilovolts
kVA	Kilovolt-Amps
kW	Kilowatts
l	Litres
L_r	Latent Heat of Water (Joules)
m	Meters
mbar	Millibars
mg	Milligrammes
min	Minutes
ml	Milliletres
mm	Millimeters
mmHg	Millimeters of Mercury
mS	Millisiemens
n	Topology Factor
N	Number of Turns in Winding
Nm	Newton-meters
ºC	Degrees Celcius
P	Power (Watts)
p	Pressure (Pascals)
p.u.	Per Unit
ppm	Parts per Million
Q	Heat Energy (Joules)
r	Radius (meters)
R	Resistance
R_L	Ratio of Load to No-load Losses
R^2	Model Fit Varianace

List of Symbols

$\bar{R}_m$	Ideal Gas Constant, Mass Basis (Joules per kilogram-Kelvin)
S	Entropy (Joules per Kelvin))
s	Seconds
T	Temperature (Kelvin or degrees Celcius)
t	Time (seconds)
TWh	Terrawatt-hours
U	Internal Energy (Joules)
V	Volts
W	Water Content in Paper (percentage)
W	Watts
W_d	Work Done (Joules)
x	Transformer Oil Exponent
y	Transformer Winding Exponent
α	Pre-exponential Temperature Factor
β	Temperature Decay Constant
γ	Gas Content in Oil (percentage)
∂	Differential Operator
Δ	Delta – Difference between Two Points
ϑ	Bubble Inception Temperature (Kelvin or degrees Celcius)
κ	Load Factor
μg	Microgrammes
μm	Micrometers
σ	Surface Tension (Newtons per meter)
τ_{co}	Oil Time Constant (min)
τ_{cw}	Winding Time Constant (min)
Φ	Magnetic Flux (Webers)

LIST OF FIGURES

List of Figures

List of Figures

List of Figures

List of Figures

List of Figures

List of Figures

LIST OF TABLES

List of Tables

ABSTRACT

High temperature in transformers is the source of much trouble, causing the transformer to undergo ageing processes which reduce its insulation lifetime, as well as giving rise to potential failures through fires, explosion, and from the formation of bubbles within the insulation. Temperatures within the existing transformers are purported to reach higher and last longer once electrification of energy occurs as part of a move toward low carbon power networks.

Analysis of transformer temperatures by simulation of potential future loading and calculation based on the IEC thermal model provides a picture of the changes in thermal behaviour of transformers. Further analysis comparing transformer temperatures to an insulation condition specific bubble inception temperature demonstrates how the risk of inception is increased compared to cases where no electrified heating load is present.

Using a bespoke set-up developed within this work, tests showed how the liquid only insulation rarely presents a bubbling (and therefore a failure) risk during high temperature overload periods of a transformer. Despite several 'worsened' conditions (including gas saturated, and high particulate content liquid), overloads causing temperatures as high as 180°C did not evolve bubbles. However, in extremely wet conditions ($\geqslant$78% relative saturation), hydrocarbon insulating liquids can cause bubbling (though synthetic esters generated no bubbles, even when completely saturated).

Testing of transformer solid insulation generated bubbles in wet paper. Key findings were that thermally upgraded paper resisted bubble formation (i.e. needed a longer time and higher temperature) than non-thermally upgraded paper; increasing the rate at which the load is applied reduced the bubble inception temperature and time to bubble inception; and when comparing the energy input to the bubble inception temperature, different shapes of load profile performed similarly.

The mechanism of bubble formation is further understood from this work. As well as being linked to temperature and load, the moisture dynamics between the solid and liquid insulation, and between solid insulation layers, where the competing drivers of temperature and concentration difference lead to a build up of moisture between layers which allows the moisture bubble to form and later release from the overlapping paper edges of the outer-most layer.

In addition to the factors of load, moisture content, and insulation type, the ageing condition of the solid insulation is an important factor. This information is incorporated into the formula used for calculating bubble inception temperatures, as well as forming part of the development of an *ab initio* formula. Basing the calculation of bubble inception temperatures on the enthalpy of desorption rather than on isotherm behaviour showed improvements, and by accounting for the degree of polymerisation of the solid insulation, a more accurate bubble inception temperature can be established for transformers, given their actual condition.

The work from this thesis is of use to transformer designers and operators in allowing them to maximise the operational capacity of the asset while protecting them from bubble induced failure.

DECLARATION

No portion of the work referred to in this thesis has been submitted in support of an application for another degree of qualification of this or any other university, or other institution of learning.

COPYRIGHT STATEMENT

DEDICATION

This thesis is dedicated to the memory of Kenneth J Hill, Janet Sutton and William J Sutton who were all sadly lost in 2020. Thank you for everything.

ACKNOWLEDGMENTS

Completion of this PhD Thesis is the culmination of four years' work. There is no way in which I could have achieved this without the help and assistance of many people over this period. Foremost among these, I thank my Supervisor, Professor Zhongdong Wang, and Co-supervisor, Dr Qiang Liu. They provided guidance, knowledge, and advice which made this piece of work infinitely better than it would have otherwise been. They provided opportunities for me to develop as a researcher and as a person. Mostly though, I thank them for always showing calm whenever I felt my work to be in crisis.

I also wish to express special thanks to Dr S. Matharage, Dr S. Tee, and Dr X. Zhang. These exceptionally knowledgeable and helpful researchers were always willing to discuss ideas, provide advice, and most importantly, would point out the flaws in my work. Dr R. Gardner and Dr V. Peesapati also deserve my thanks for their help in setting up my experiments. Thanks also to Dr James Parr for proof reading, and for regularly boosting my morale. I thank Mr Zong Yan too, a great friend throughout the four years, and who must be held accountable for my doing a PhD in the first place!

Many other friends should be mentioned here, and I refer to all members of the Transformer Research Group, to my fellow students on the EPSRC Centre for Doctoral Training in Power Networks, and the IEEE PES Student Branch Chapter at The University of Manchester. All know how it feels to undertake study of a PhD, and were witness to my own. Particularly, I wish to apologise to Dr J. Fradley, Dr H. McDonald, Dr L. Loizou, Dr S. Shen and Mr M. Han who had to continually feign interest as I unloaded my own grievances on them, over what must have felt like a long four years. My personal opinion is that research holds most value when it is useful, and then only when shared. Throughout my PhD I was fortunate to work as a member of the Transformer Research Consortium, alongside great minds from Cargill, EPRI, M&I Materials, National Grid, Scottish Power, SGB-Smit, Shell Global Solutions, TJ|H2b Analytical Services, and Weidmann Electrical Technology AG. The impact their discussions had on my research is too great to quantify.

I spent three months during this programme at Tsinghua University, China. The benefit to my work and to my personal development cannot go unrecognised. I appreciate the opportunity provided by the University and the IRES-8 Programme.

Finally, I thank my family and girlfriend for their unwavering support and admiration of the work I have carried out, especially during the times when I was particularly busy and distracted. I love you all.

THE AUTHOR

The author received an M.Eng degree in Chemical Engineering with Industrial Experience from The University of Manchester in 2013, including a final year project focussed on production of bioethanol from sugar cane as a replacement fuel in domestic vehicles. The Industrial Experience year was taken as a Production Engineer at Cargill PLC, based in Trafford Park, Manchester, UK.

After two years working as a design engineer in the oil and gas industry (working on projects including techno-economic assessment of carbon capture and storage technologies and cogeneration plant design and specification), the author returned to The University of Manchester to embark on a PhD programme funded by the EPSRC CDT in Power Networks. This programme included a year studying Power System M.Sc modules and was the beginning of a steep learning curve as the author transferred to the new field of power systems, and specifically, transformers.

The research undertaken throughout the PhD drew on fundamental material science concepts learned during undergraduate study, coupled to the electrical equipment and system knowledge gained throughout the first year of the CDT programme.

1 INTRODUCTION

1.1 PROJECT CONTEXT

In the past few decades, researchers have consistently identified that increased human activity since the beginning of the industrial revolution is leading to higher global average temperatures, and continues to do so [1-5]. This has been shown to be a result of the emission to atmosphere of so-called greenhouse gases (GHGs). The most renowned of the GHGs is carbon dioxide. This phenomenon, and its associated threat to society and global ecosystems, is not new, and has been reported on since at least 1912 [6, 7]. World leaders have come to realise that predicted scenarios of the earth's future are not palatable under the threat of such changes to its climate. It has thus been determined to restrict global average temperature rise to 'well below 2°C above pre-industrial levels'[8]. This was signed (though not ratified) by all states within the United Nations Framework Convention on Climate Change (UNFCCC) in the Paris Climate Agreement [8] (signed 22nd April 2016, effective 4th November 2016), following on from the Kyoto Protocol [9] (signed 11th December 1997, effective 16th February 2005). While this timeline appears slow, necessary changes are needed quickly. This is finally being recognised, and the United Kingdom (UK) recently updated the Climate Change Act 2008 to sign into law a commitment for 'net zero emissions' by 2050 (increasing from a previous target of 80% net emission reduction) [10, 11]. However, [11] also states that current global plans give only a 50% probability of preventing a 3°C rise ([12] suggested the even bleaker likelihood of 4%), thus if a 2°C limit is to be met then a rapid adoption of change is needed in the short term [13].

GHG emissions come from various sources. It is possible to group these roughly into the following categories: transportation (including international aviation and shipping); electricity / power generation; heating / cooling (of buildings); agricultural; industrial; waste; and fluorinated gases [11].

There are many options available which can help to reduce GHG emissions, and in turn prevent the associated global temperature rise. While the Paris Agreement has been dubbed by some as being an incentive for fossil fuel divestment [14], there are mechanisms which do include maintenance of fossil fuels for energy production (e.g. inclusion of carbon capture processes [15], or geoengineering [16]).

Introduction

One of the most popular methods of decarbonising cited is to 'electrify' the transportation and heating / cooling categories [11, 17-19]. This is based partly on the ideology that it is easier to focus on one category than to address all three separately. Electricity is viewed as the easiest category to reduce emissions from, and the technological shift required is much less complicated than conversion of appliances to alternative fuel sources. Emissions from the power sector have reduced significantly in 2018 from 2008 levels, despite continued economic growth and increases in emissions in other sectors [11].

If electrification of transportation and heating / cooling is adopted at large scale, then this would add a huge strain to the existing electrical networks, pushing many assets to or even beyond their designed capacities. Indeed, the Committee for Climate Change (CCC) consider that electricity demand in the UK could double by 2050 as a result of the electrification of other energy sectors [20]. This introduces a major issue as it is not feasible to replace electricity networks of entire countries (or entire regions) in the time available (there is not the finance, the production capability, material resource, (trained) personnel, nor transport capacity, to name but a few limitations).

In some countries, such as the UK, the electricity network is an ageing infrastructure. Some components in service today have been installed for over 60 years at all voltage levels of the network. A large proportion (over 50%) of transformers in the UK are more than 30 years old [21] (based on a study of three major UK utilities). Transformer design should last for approximately 20 years if operated at rated loading and if they are well maintained [22, 23], yet the actual expected lifetime is from 50 – 60 years [24]. This is mostly because actual loadings have generally been lower than ratings, assisted by good maintenance practices. However, if high electrification occurs, the loading on these transformers would be increased, potentially leading to premature, unexpected failures, or at least a shortening of operational life.

Loss of assets in the power network infrastructure such as transformers can lead to blackouts. The cost of blackouts can be totalled in any number of ways, normally a monetary figure is used to represent lost productivity, but it is just as important to note that often the cost can be counted in lives lost as well. In August 2019, a network outage occurred in London, UK during stormy weather; this led to 'subsequent disconnection, loss of power and disruption to more than one million consumers' [25]. Over £10 million was paid to the Ofgem Voluntary Redress Fund by the companies involved (generators and distributors) as a result of failures in this instance [25]. Luckily, nobody died during this event, but the

disruption to daily life was not insignificant, occurring as it did at rush hour on a Friday (arguably the worst time possible).

It is within this context, of the anticipated adoption of electrification as a 'silver bullet' to solving climate change, applied to an ageing electrical network which supplies both life and livelihood to almost every person around the globe, that this project finds its importance.

1.2 PROJECT BACKGROUND

Whilst many transformers operate far beyond their expected operational lifetime [26], in-service failure of transformers is a phenomenon that operators must be wary of. Failure of a transformer 'always causes irreversible damage' [27]. Transformer failure rate has been calculated at approximately 2% [28], but may in fact be lower, in the order of 0.5 – 1% with transformers of lower voltage rating failing at higher rates [29] .

Transformer failures come in many guises. Indeed, often a transformer failure leaves no evidence of its cause (given the destructive nature of failure) and so failure is attributed based on best information (following a post-mortem investigation, if conducted), although such information may be sparse [30].

It is possible to group failures in different ways. Figure 1-1 shows failures categorised by failure mode. Alternatively, as in Figure 1-2, failures can be categorised by the component deemed to be the cause of the transformer failure. Among modes of failure, dielectric, mechanical and electrical are seen to be most prevalent [29], and windings, tap changers and bushings are components which are most often the primary location of failure in transformer failures [29].

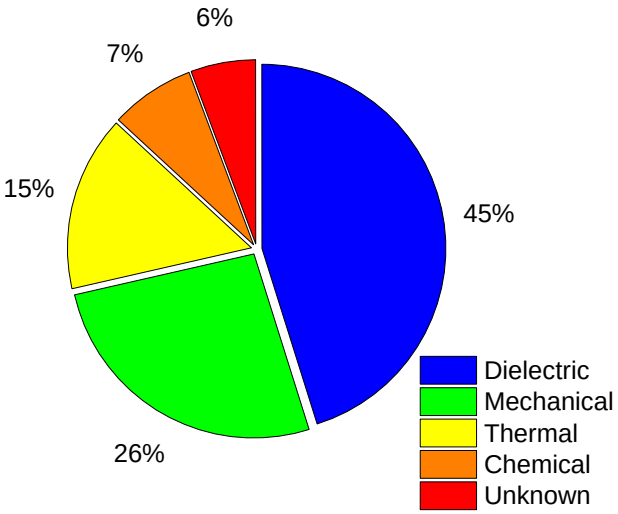

Figure 1-1 – Breakdown of transformer failure by mode [29].

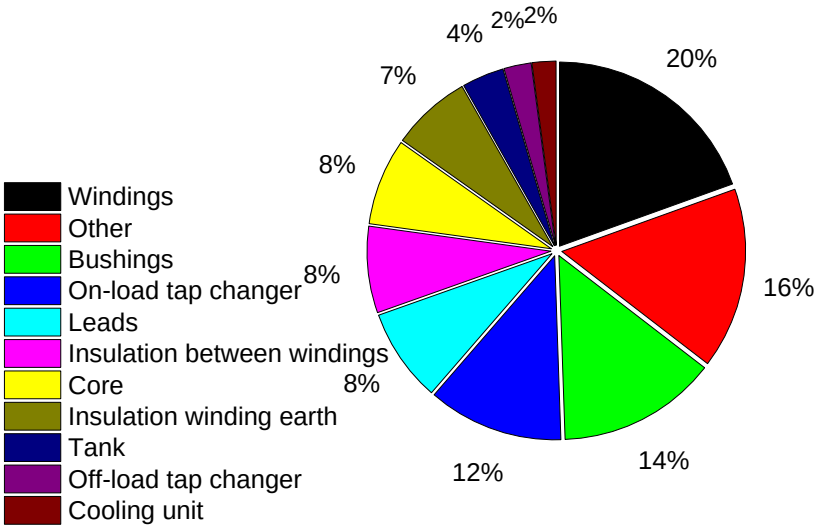

Figure 1-2 – Breakdown of transformer failure by component [29].

Due to the expected increase in loading on transformers in future, transformer operating temperatures will rise correspondingly. Multiple paths to failure exist as a result of high temperatures, and a complete list of these is unrealistic. Four prominent transformer failure pathways related to (high) operating temperatures are: fire [29], acceleration of long term ageing [31, 32], free water production [33], and bubble evolution [34].

Of these methods of failure, some are better understood than others. The ageing process can be managed, and considerable work has gone into understanding this, and although not complete, it is possible to minimise the effect of ageing through correct design

and operation (e.g. reduction of catalytic materials and ensuring flat, low load profiles), as well as techniques such as oil regeneration or replacement. Some information about transformer condition can also be gleaned through what are now routine tests, this can allow for controlled, planned replacement of transformers which are nearing their end of life.

Fire leads to instantaneous failure, however the cause of fire is directly linked to the fire triangle (heat, oxygen, fuel), and can be averted by eliminating one or more of the components required (though it is noted than many transformers can be good sources of all three). Principally, the temperature of transformers is intended to be limited far below the fire point of its components, though in certain fault or emergency scenarios such temperatures may occur.

The other listed causes of failure are less well understood, and therefore this research sets out to increase knowledge related to one of these causes, bubble formation.

Bubble formation as a result of high temperature in transformers can be assumed to follow the pathway outlined in Figure 1-3. It is important to start with a mechanism of failure, as this allows for identification of potential junctures at which failure can be arrested. Adoption of sound engineering principles such as the hierarchy of controls and risk analysis techniques (for example, those outlined in [35]) can lead to procedures which can be implemented within transformer design and operation in order to reduce failure likelihoods.

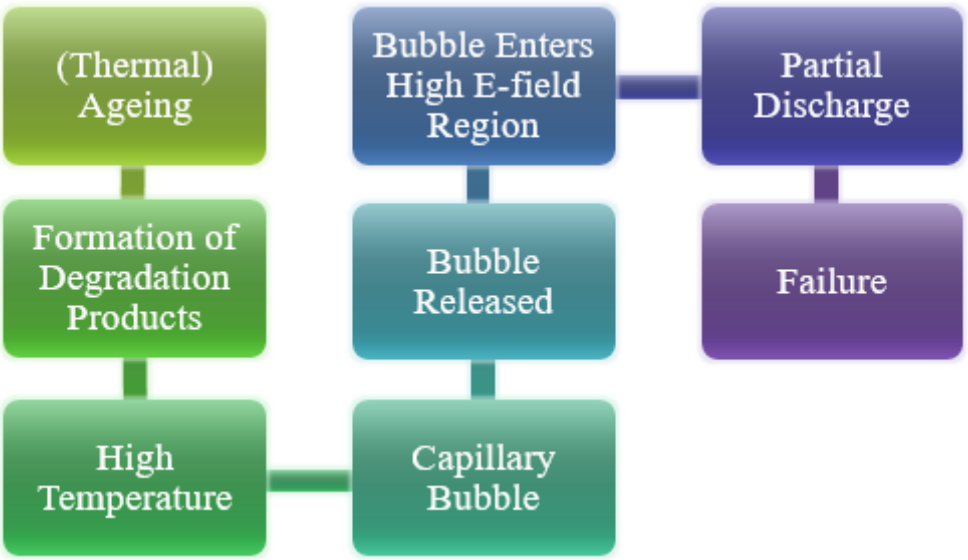

Figure 1-3 – Mechanism of transformer failure through bubble formation.

The steps in Figure 1-3 can be briefly described as follows. Initially, the transformer is essentially dry and free from contaminants. Over time, the transformer insulation is subjected to an ageing process, driven by ingress of moisture and oxygen and the increased temperature experienced during operation. This ageing produced by-products, including acids and, importantly, more moisture.

During certain conditions – such as short-term emergency overload situations – the temperature in the transformer windings and insulation can become excessively high (i.e. beyond rated temperatures). As temperature increases, the degradation products formed during the ageing process tend to migrate out of the solid insulation at the winding into the liquid insulation surrounding it, and under certain conditions, bubbles may form. The bubbles present a dielectric weakness within the insulation, if the bubble is maintained within or enters an area within the transformer of high-electric field then this can lead to partial discharges and ultimately, this can lead to instantaneous failure of the transformer through dielectric failure of the insulation.

The main source of bubbling within transformers is water vapour generated at the interface of solid and liquid insulation media. Hence this study investigates the bubbling phenomenon, with focus on the effect of insulation type (variants of solid and liquid insulation are investigated) and insulation condition (moisture content), through experimental assessment, theoretical analysis, and simulation of scenarios. It is intended to explain fundamentally the bubble effect as it relates to operation of in-service transformers, developing the understanding of the underpinning mechanism involved, as well as relating this to different loading situations.

1.3 AIMS AND OBJECTIVES

The aim of this PhD study is to establish a more thorough understanding of the bubbling phenomenon within transformer insulation systems. Further, the work aims to study the working limits for transformers that are used within standards, and provide additional insight to their suitability. This work is particularly concerned with the impact that the change in network load profiles due to integration of low carbon technologies may have on the likelihood of a failure on a transformer and the specificity of transformer limits based on individual asset condition.

The aims of the study are to be met by achievement of the following objectives:

i. Assessment of the influence of low carbon technologies on the likelihood of transformer failure: the likelihood of a transformer failure due to bubbling can be seen simply as the frequency of events where the temperature required to form a bubble is achieved, taking into account the transformer condition (i.e. moisture content, etc.) and the loading scenario (i.e. the transformer temperature). Introduction of low carbon technologies, especially those connected at the distribution level, have the potential to increase the number of times that such temperatures can be reached by adding load at peak times, and adding that load quickly.
ii. Establishment of experimental set-up: a test set-up was developed at small scale to establish a method of effectively comparing multiple parameters.
iii. Tests on a variety of insulation materials, with different moisture conditions and loading conditions, with a serious of secondary tests and analysis included to allow a greater understanding of the mechanism behind bubble formation with transformer insulation.
iv. Analysis of the formula used for calculating bubble inception temperatures, and how the ageing condition of the transformer insulation is influential in bubble temperature calculation.

1.4 THESIS OUTLINE

The thesis starts in Chapter 1 with an outline of thesis and its core contents, followed by a detailed literature review in Chapter 2. The literature review covers the background of transformers and transformer failures, as well as details of the insulation materials used in them. The purpose of the literature review is to help frame the problems that are solved through the remainder of the body of work, and to provide the technical information that is relied upon for bolstering the credibility of the results shown later.

In Chapter 3, the strategy adopted for modelling temperatures used to investigate the problems identified within the literature review is explained. The rationale for the load and temperature modelling is explained, and the key equations and parameters are discussed. This sets up the work of Chapter 4, and is recalled in Chapter 7.

Chapter 4 sets the problem in the future load scenario. While in the literature review it is shown that addressing bubble formation in transformers as a potential failure mechanism

is important for a number of reasons, the potential for increased failure rates due to adoption of low carbon technologies is shown clearly through simulation of the impact of electrified heating on transformer temperatures.

Chapter 5 includes a detailed outline of how the experimental set-up was designed and tested, with rationale given for each step, the theoretical basis for the experiments is sound, building on the knowledge gained from previous studies. The importance of this chapter is to test liquid insulation against the IEC Standard 60076-7 [23] guidance for protection against bubble formation, comparing the performance of three different types of liquid insulation.

Chapter 6 shows the results of tests conducted over various loading scenarios for different solid insulating materials. The loading scenarios are a key philosophy of this thesis in that it adds to the usual conversation about 'temperature'. Equally, referring back to the modelling work of Chapter 4, the way in which load profiles could change due to adoption of low carbon technologies may mean that loading becomes a more influential parameter to consider. As with Chapter 5, the results of the tests in Chapter 6 can be used to help set operational limits and guidance (such as that given in [23]) for the avoidance of bubbles, especially within the changed loading environment. Further, the mechanism by which bubbles form is scrutinised, with several additional tests conducted which can give insight to the way in which bubbles form within transformers.

Chapter 7 provides analysis of results that are already available in literature to tease out further bubble inception temperature (BIT) dependencies, for example based on the condition, not just the selection, of transformer insulation materials. Chiefly, the ageing condition of the insulation is considered, and this is incorporated into the formula for bubble formation. Additionally, an alternative formula for calculating BIT (also including ageing condition of the solid insulation as a factor) is developed. Finally, the profiles of Chapter 4 are reanalysed, showing how accounting for the insulation condition can draw different conclusions on where to set safe transformer temperature limits.

In Chapter 8, a summary of the main points from throughout the thesis are combined to give a final coherent conclusion as the outcome from this study. Finally, ideas for future work are suggested.

1.5 MAIN CONTRIBUTIONS

This work provides contributions that can be utilised by transformer owners / operators, allowing them to make best use of their asset while better understanding the risks of operating beyond normal limits. The UK CCC states that 'Plans for networks to be capable of meeting higher demand for electrical energy' is a priority for 2019-2020 [11], and the work covered by this thesis is therefore timely as it can help in achieving part of that aim as the UK decarbonises over the next 30 years.

Further, from this study it is possible to make more informed material selection decisions for transformer insulation during the design stage based on comparative assessments which were generally not available in literature previously.

The following eight key contributions can be extracted from the thesis:

i. Recognition that the current bubble inception formula is erroneous. An algebraic mistake from 1989 has propagated and therefore the numbers shown in the formula in the IEEE C57.91 and IEC 60076-7 standards [22, 23] are incorrect and should be updated. Updating this formula will allow for more accurate calculation of the temperatures at which bubbles might form, and so the relevant transformer protection can be better instructed.

ii. Considering future loading scenarios which include the additional loading added from the electrification of heating is shown to put transformers at increased risk of bubble formation, the severity of which is linked to the transformer insulation condition (age, moisture content, etc.). This increased risk in a future network scenario is vital for future system planning and for understanding the requirements on assets (both existing assets and as-yet-installed) assets) likely in the near future.

iii. Selection of solid insulation material is shown to be significant when considering bubble inception performance. Thermally upgraded paper insulation was better at resisting bubble formation. This indicates that the selection of materials is important when considering the operational capability of a transformer. When calculating thermal limits, it is vital to consider the actual materials in use, rather than applying blanket rules. Further, that thermally upgraded paper can resist bubbling as well as ageing at high temperatures is a bonus that ensures this material is compatible with

transformers that operate under such conditions of high load and high(er) operating temperature.

iv. Selection of liquid insulator presents an insignificant variation in bubbling performance. Indeed, without paper insulation present, it was nearly impossible to form bubbles. Such a finding not only validates the guidance provided in existing standards, but it means that transformer manufacturers can focus on other aspects of transformer materials and design when safeguarding against bubble formation. Equally, a transformer owner / operator can work in the comfort that the liquid insulation is unlikely to present a bubble risk, and so (for the purposes of bubbles) may focus more on the condition of the solid insulation instead.

v. Formation of bubbles in this manner is a process driven by temperature, but dominated by moisture migration. The trapping of moisture into pools between outermost paper layers, with the continued addition of material and energy causes bubbles to release from points of least resistance of the paper insulation, hence the abstraction of the effect of liquid insulation. This finding is helpful for transformer design, and provides a platform for improvement of the solid insulation wrapping process to help hinder formation of bubbles within transformers.

vi. While moisture content is a key variable, the rate of temperature rise, as described by the transformer loading profile is also crucial to setting limits to protect transformers from formation of bubbles. Owner / operators of transformers should therefore be aware of the load scenario faced by their transformer. Noting that a transformer may be safe now, but that if load profiles change in future, this risk must be reappraised, considering several factors.

vii. Bubble formation is dominated by the solid insulation and its condition. It has been shown that chemical thermal upgrading of solid insulation affects bubbling behaviour. Additionally, the ageing condition (measured through the degree of polymerisation of the solid insulation) has an effect on the bubble inception temperature. A method of accounting for this within the extant formulae is presented. Thus, when considering the risk of bubbling for a transformer, it is best to make use of specific data wherever possible, rather than relying on general rules that may overlook particulars.

viii. Further, the use of a desorption isotherm to model bubbling is not sound, and a formula based on enthalpy of desorption may be preferable. Whether or not this alternative formula is adopted, whichever formula is used within the standards should account for variation in bubbling based on the degree of polymerisation of the solid insulation in addition to the moisture content. To ensure that accurate temperatures representing a risk of bubbling are calculated, the correct formula should be used.

The work presented in this thesis has led to five peer-reviewed publications, listed in List of Publications section. Points i., vii. and viii. above are covered in reference [P1] of that list. Reference [P2] of that list covers points ii. and vi.. References [P3] and [P4] from that list make use of the model developed in Chapter 3, used in Chapters 4 and 7, providing confidence in the model suitability. Reference [P5] of that list provides a thorough review of the literature and experiments covering transformer bubble formation, and thus covers Chapter 2 of the thesis.

2 LITERATURE REVIEW

2.1 INTRODUCTION

This chapter provides the background to the thesis. It covers an overview of the power system, how it began, how it is today, and how it is likely to change in the near future. The changes covered are mainly to do with low carbon technologies and their influence on load profiles. For clarity, the review is restricted mainly to a detailed look only for those technologies which are expected to cause the biggest changes to the loading profile of transformers. Also for the purposes of clarity, the discussion is mostly focussed on the situation within the UK, though the points raised are common in many countries and regions.

Transformer design and operation is then discussed, with particular focus on its thermal behaviour and the insulation materials used, leading to a discussion of temperature-driven transformer failure. The information herein is useful to aid in discussions of findings in later chapters, as well as helping to identify the voids in current understanding which shines the light on the gaps in current knowledge which this thesis aims to help fill.

2.2 POWER NETWORKS

2.2.1 Purpose of the Power Network

The power network is designed to produce electricity and deliver it safely, efficiently and reliably to users (domestic and industrial users). To do this, it requires generators to generate the electricity, a transmissions system to transmit the electricity from the generator to areas where users are, and then a distribution system to distribute the electricity among the users. The network is built to serve the demand of the users, but against a number of constraints, including reliability and resilience, cost, efficiency, and safety. The concept of such a network is commonly credited to Thomas Edison, who was issued a patent for his ‘system of electric lighting’ in 1881 in the USA [36]. Edison’s network ran on direct current (DC). In 1883, Lucien Gaulard and John Dixon Gibbs established the first multi-user alternating current (AC) distribution system in Italy, serving remote, sparsely populated locations. Later, Gaulard and Gibbs patented a transformer in England in 1884, after recognising the need for high voltage for transmission of electricity and low voltage for usage, mainly because the economics of running large distribution systems based on DC

were not viable [36]. A device such as a transformer was thus required to convert voltage (and inversely, current) to the desired level at each stage of the network.

Today, power networks supply electricity to homes and businesses to a multitude of appliances. These appliances can be for comfort, communication, or combustion, for cooking, catalysis, or computing, and an infinity of other uses. Devices use electricity in different ways, and so the manner in which it is received (and thus in which it must be delivered) differs. Appliances differ in their use of electricity in several ways. For example, some devices are battery powered (e.g. a mobile phone) and charging of the battery is the main demand, which normally happens in one consistent period, with usage removed temporally from the demand. On the other hand, appliances such as kettles have a short, high demand which is made only at the point of need. This difference in demand spike (small, lengthy demand for charging; large, short demand for heating water) and the temporal dissonance between demand and point of use can place different stresses on the network. Further, the capacity of these appliances to provide service to the network (so called 'demand response', i.e. turning off or delaying demand to assist the network in peak / difficult scenarios) also differs accordingly.

Likewise, there are many different methods of generating electricity, though many techniques rely on the turning of a generator for the conversion of mechanical energy to electrical energy. Traditionally generation was performed by burning fuel to generate gases (and sometimes also steam) which then turns a turbine. More recently, other methods of turning turbines have been put to use (such as wind turbines). Other ways of generating electricity were once the norm, since went out of fashion, but are now utilised again (though maybe for different purposes, e.g. frequency response), with an example being water wheels, which may now also take the form of tidal turbines. Indeed, the development of electricity has allowed for another massive benefit – the ability to utilise power remotely from the generation location. Previously, a water wheel (for example) may have been used to turn a mill, generating useful power and turning a raw material (such as wheat) into a useful product (flour). Modern mills make use of electricity to power equipment that does the same thing, but the electricity generator does not need to be local, it just needs to be connected.

This is not a unidirectional change of use however, and recent developments have seen generation move back to the user in many cases, roof-top solar panels are a key example of where users can generate electricity local to their demand, and without the need for transmission and distribution systems to deliver the electricity (and thus the associated fees).

This understanding of why the electricity network is important and how it operates (at a high level) is essential for understanding the influence of demand on the system, and it also helps to understand the drivers behind recent changes to the system.

2.2.2 Low Carbon Technologies

Adoption of low carbon technologies (LCTs) is desirable due to the increasing need to reduce carbon emissions. Many types of LCT are already available or currently under development. Indeed, the type of technology can vary in how they reduce carbon emissions, including reduction during generation (e.g. a low carbon fuel type), post-generation (as in carbon capture and storage), or reduction in energy usage (such as demand response or improved efficiency).

Generation from coal reduced by 98 TWh in the UK in the ten years from 2008 to 2018 [11]. In the same period, low carbon generation increased to reach 54% (the highest proportion attained in the UK) of annual generation [11]. This shows the upward trend of LCT adoption.

More details on the adoption of common LCTs within traditional power system are discussed in Section 3.2.

2.3 TRANSFORMERS

Transformers are used within the power network to change the voltage of power supplied depending on the section of the system it is at, the UK network is depicted in Figure 2-1 [37]. Generation of electricity is done at a voltage of tens of kilovolts but is then boosted for transmission. For long transmission distances within the UK, 400 kV is used. The higher voltage reduces the current flow required for the same power transferred. Lower current means lower losses as resistive heat from the cables and lines that transport the electricity, which is a benefit to the system financially with less generation being required to cover the system losses. Once the electricity is close to the user, the voltage is dropped to a level which is safer, with a 3-phase voltage of 400 V being most common at the residential user.

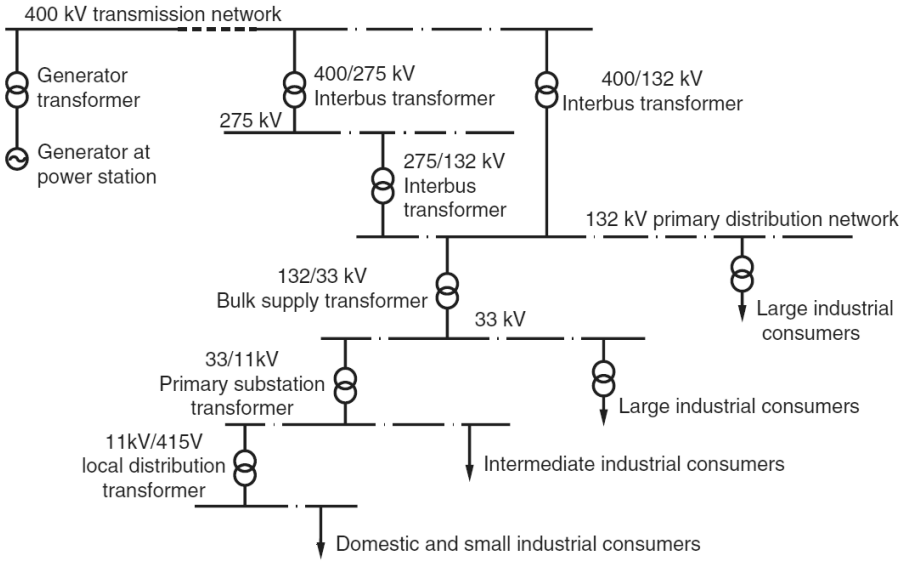

Figure 2-1 – Extant UK power network voltage levels [37].

A transformer works by making use of Faraday's Law [38], which states that electromotive force (*e*) produced is proportional to the number of turns (*N*) and the magnetic flux (φ) passing through each turn and where φ is a function of time, (*t*). This is shown in equation (2-1).

$$e = -N\frac{d\varphi}{dt} \tag{2-1}$$

For one phase of a transformer, the high and low voltage windings can be represented as in Figure 2-2, with N_1 turns on the primary side and N_2 turns on the secondary side [39]. Equation (2-1) can then be written for each side, and dividing the equation for the primary by the equation for the secondary, the following relationship is formed:

$$\frac{N_1}{N_2} = \frac{e_1}{e_2} \tag{2-2}$$

which is to say that the voltages (simplistically, the electro-magnetic force can be considered the same as voltage for an ideal transformer) are in the same ratio as the number of turns on the two windings, this is usually called the `turns ratio' of the transformer. Importantly, this therefore defines the required number of turns in the two transformer windings when the voltage levels are prescribed.

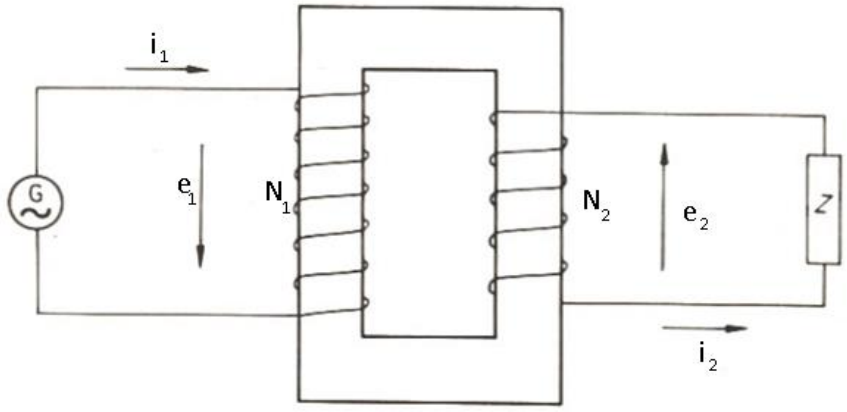

Figure 2-2 – Representation of single phase transformer windings, adapted from [39].

The principle of operation for the transformer is to have an alternating current applied to the primary side. This generates magnetic flux that passes through the core material, which then generates a current in the secondary winding. The secondary winding is connected to the load.

For an ideal transformer, there is conservation of power between the two terminals of the transformer (power entering the primary side (P_1) is equal to the power leaving the secondary side (P_2)). Using this relationship, equation (2-2) can be modified to equation (2-5), which shows the ratio in terms of current (i) instead of voltage.

$$P_1 = e_1 i_1 = e_2 i_2 = P_2 \tag{2-3}$$

$$\frac{e_1}{e_2} = \frac{i_2}{i_1} \tag{2-4}$$

$$\frac{N_1}{N_2} = \frac{i_2}{i_1} \tag{2-5}$$

In reality, transformers are not ideal machines and so the above relationships must be adjusted to account for this. The non-ideality of transformers gives rise to `losses' in the system, the pertinent effects of which are discussed in Section 2.5.2. Equation (2-6) shows how (2-3) is changed by the occurrence of losses, where losses are mostly in the form of resistive losses, described by equation (2-7) (with R the resistance of the (copper) conductor).

$$P_1 = e_1 i_1 = e_2 i_2 + P_{Loss} = P_2 + P_{Loss} \tag{2-6}$$

$$P_{Loss} = i^2 R \tag{2-7}$$

Transformers are designed and rated against a number of parameters, and as explained later in this chapter, temperature is a key limitation due to its effect on the asset lifetime.

However, the temperature is affected by loading. The transformer will be rated to a voltage class, depending on where it sits within the network described in Figure 2-1, and so the load, described in either power or current terms, will be set based on the required capacity of the transformer (i.e. how much power the transformer is required to transfer).

2.4 TRANSFORMER INSULATION

There are two types of insulation within most transformers: solid and fluid. The solid type is generally used in contact with the conducting material and has high electrical withstand strength along with good mechanical strength properties. The fluid is usually a liquid, commonly oil, which is used to cool the transformer, as well as provide dielectric strength. The fluid may also be a gas (such as air or sulphur hexafluoride). Transformers that use gas as an insulator are known as 'dry-type transformers'. Dry-type transformers are not considered within this thesis. Details pertaining to the solid and liquid insulation commonly used within transformers are given below.

2.4.1 Solid Insulation

Solid insulation serves two main purposes within a transformer. It acts as a dielectric (with electric strength in the order of 10 kV/mm, [40] specifies ≥7.0 kV/mm for new insulation), and it also provides mechanical structure [41]. The transformer windings are wrapped with paper insulation [37], and mechanical failure of the paper can lead to transformer failures. The risk of mechanical failure increases with ageing of the paper as it becomes brittle and shows reduced mechanical strength, particularly at end of life conditions [31]. Mechanical strength of paper insulation is often described through its tensile strength (which shows the resistance to failure under tension in either the machine or non-machine direction) [40] which is commonly cited as an end of life criterion [42]. Also important is the burst strength: as the electro-magnetic force in a transformer is generated radially to the winding it applies a force across the paper insulation, once the bursting strength of the insulation is reduced below this force, risk of failure is high.

Cellulosic paper is a common selection for the solid insulator in transformers. While it sufficiently meets the criteria of a good insulating material under these conditions (electrical resistance, mechanical strength, material compatibility, etc.) [37], it is inferior in its resistance to ageing and thermal breakdown compared to some other materials such as synthetic polymers. However, the relative ubiquity of the source material makes it an

attractive raw material at relatively low cost [37]. It is also a reasonably well understood material, used in many industries.

2.4.1.1 Types

There are several types of solid insulation that can be used to insulate the windings of a transformer. Mostly, they are cellulose-based, including standard non-thermally upgraded Kraft paper (NTUP), thermally upgraded Kraft paper (TUP), diamond dotted paper (DDP), and crepe paper. Additionally there are some other materials used, such as Aramid. Each of these materials is described below. Transformers also commonly contain pressboard, which is a thicker cellulosic insulator used for spacers and supports, and elsewhere for numerous duties within the transformer [43].

Non-thermally upgraded Kraft paper is the most commonly used solid insulating material in transformers [37, 41]. The manufacture of Kraft paper is from softwood (usually sourced from regions of cold climates) through a multi-step process including pulping, drying, forming and (hot) pressing stages. Full descriptions of this process are available variously in [43-46]. The process by which the paper insulation is made is designed to leave a strongly bonded fibrous structure, which is relatively dense, but the insulation will need drying before entry into service as it is still highly hydrophilic.

TUP is often used in special cases where higher loading on (and thus higher temperatures in) the transformer are desired [47]. In these cases, the ageing rate of NTUP would not allow for economic operation, and so TUP is used instead. TUP is commonly used in transformers in the United States (US) [47]. TUP is chemically ‘treated’, usually through addition of compounds containing nitrogen, such as melamine, dicyandiamide or polyacrylamide [43, 47-49]. The compounds neutralise the water forming agents within the paper [47, 48], and have been seen to reduce the amount of acid formed through the degradation of the paper as well [50]. This allows the TUP to operate at a higher temperature while maintaining the same life expectancy. The treatment process increases the initial cost of the transformer, and so this insulation is normally only used when the likelihood or necessity of high temperature in the transformer is large.

DDP is found mostly in transformers at the distribution level. It takes its name from the diamond pattern of dots that appear on its surface due to the application of a thermosetting resin. The resin is employed to provide increased mechanical strength of the

solid insulation and helps with the reduction of electrical weakness through elimination of void space between paper layers [37].

Crepe paper is produced with high extensibility (in machine direction) [51], it is used mostly at awkward sections of the transformer such as winding crossovers and terminals. Crepe paper is usually hand wrapped (unlike the other papers which are wrapped by lathe) [37]. Crepe paper is commonly produced 'to order', at different degrees of extensibility, depending on the usage requirements.

Solid insulation does not need to be manufactured from organic material. Papers such as NOMEX® are synthesised by polymerisation of chemicals commonly known as 'aramids'. The term aramid is a portmanteau of two of the main chemical groups present in the monomer; aromatics and polyamides [52]. Figure 2-3 shows a typical chemical structure of an aramid with these two chemical groups identified. Papers made from such materials tend to be able to work stably in high temperature environments [53] and are less hydrophilic than cellulosic papers [54], making them ideal as insulation in transformers.

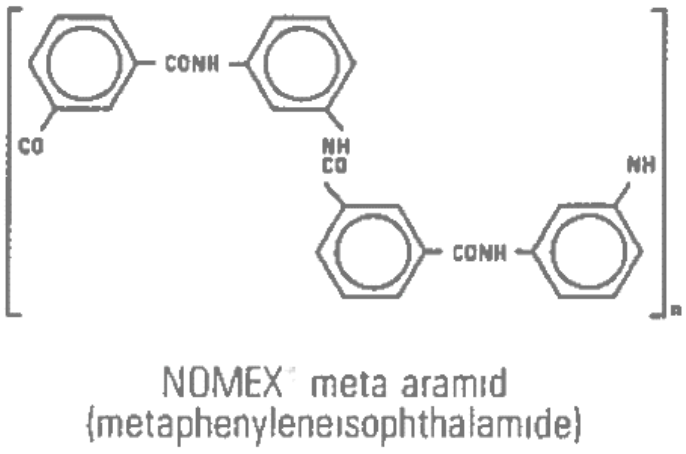

Figure 2-3 – Chemical structure of aramid polymeric insulation [52].

However, as they must be completely manufactured (unlike cellulosic papers which are refined from readily available material), chemical papers tend to be more expensive [54], and thus they are not used frequently despite their attractive properties.

2.4.1.2 Structure and Chemistry

As seen in the previous section, the dominant material for transformer solid insulation is cellulose-based paper. Cellulose is the most abundant naturally occurring polymer. It is formed of repeating monomer units as per Figure 2-4 [31]. It is important to represent the cellulose structure as in Figure 2-4 rather than as a single monomer unit as two key features

are visible from doing so. Firstly, the two end molecules terminate with an extra –OH group, and secondly, the position of the linking –O– bridge oscillates between 'upper' and 'lower' positions at each subsequent link. This latter point particularly adds value, in terms of the strength of inter-polymeric bonds, this allows for strong bonds to be formed along the length of the chain, on either side, such that the mechanical strength benefits greatly. It also makes bonding sites for moisture and other polar contaminants more readily available. The cellulose fibres link together to form a structure, in some areas of the cellulose, this occurs in well-formed crystalline patterns, whereas in others, the structure is less so, known as the amorphous region [55].

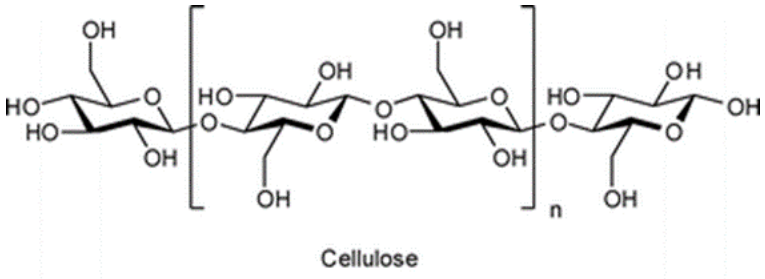

Figure 2-4 – Cellulose polymer structure [31].

The insulation is formed from wood pulp, usually softwood (which has properties preferable over hardwoods) [46]. The naturally occurring fibres of the wood consist of hemicellulose and lignin in addition to the cellulose. Hemicellulose and lignin are generally considered undesirable for the insulation, and although the final material is mainly composed of cellulose, complete extraction of hemicellulose and lignin is not technically or economically feasible. Table 2-1 shows the common final constitution of the solid insulation alongside typical values in the source material. Inorganic materials are introduced through the paper making process, and while undesirable, are difficult to fully remove [46].

Table 2-1 – Composition of cellulosic insulation and source material [46].

	Before Pulping	**After Pulping**
Cellulose	40 – 50%	75 – 80%
Hemicellulose	15 – 35%	10 – 20%
Lignin	25 – 40%	2 – 6%
Inorganics	Nil	<0.5%

The average length of cellulose chains, described by the number of monomer units is termed the degree of polymerisation (DP) of the insulation. On installation of a transformer, the solid insulation normally consists of an average of between 1000 and 1200 monomer units [41, 45], although there is no standard value for this initial value [56]. The DP of raw cellulose is normally much greater than 1200, however after the pulping and paper-making process the DP is typically around 1200. The value of DP at the transformer is less than this

(closer to 1000 and sometimes even lower [56]) as the drying and impregnation processes (which are conducted at elevated temperatures) degrade (age) the chains further slightly.

The DP is related to the mechanical strength of the paper. Mechanical strength of paper can be measured by a number of factors, such as the tensile strength, elongation, and burst strength [45]. As the paper insulation is aged, the DP decreases, and its mechanical properties reduce accordingly. Shrinking and swelling of the solid insulation can also compromise the mechanical integrity of the insulation through the service life of the transformer [45].

The relationships of several measures of mechanical strength to the cellulose DP are shown in Figure 2-5 [31]. The differences in the rate of reduction is related to how each of these measures of strength relate to the inter-fibre bonds of the cellulose. Initially, depletion of DP takes place on the amorphous region of the cellulose structure which is more easily accessible to breakdown agent. This region is less strong in terms of inter-fibre bonds which contribute to the tensile strength of the paper [57], particularly for tests on long paper samples (the shorter the sample the more the strength relies on the fibre than the inter-fibre bonding) [58]. This explains the period of slower reduction in tensile strength compared to DP in the early ageing period [59]. Conversely, the related parameter of elongation is affected oppositely, with a rapid initial drop off during the depletion of the amorphous region of the cellulose. In this case, the rigid structure of the crystalline cellulose prevents movement (but resists force) whereas the amorphous region being less rigid allowed for movement and hence elongation was possible.

Burst strength aligns more closely with the rate of reduction of DP. The most likely reason for this is that the burst strength test applies a force (hydraulic pressure) to the surface area of the material, rather than through the plane as in the tensile strength test. Thus, the force is not only put through the machine direction (or sometimes cross-machine direction) as in the tensile strength test, but in all directions, and so despite the maintenance of a crystalline structure in the early ageing period, the burst test may find a weakness in any direction as it will apply force radially from the point of contact.

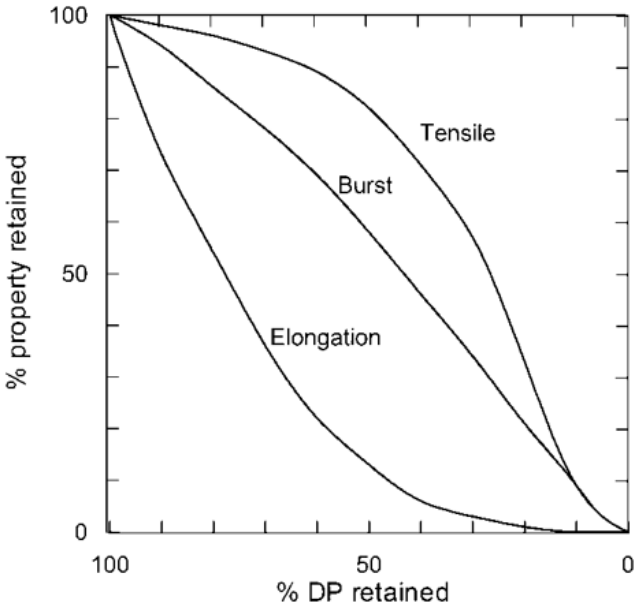

Figure 2-5 – Relationship between degree of polymerisation and various measures of mechanical strength [31].

2.4.1.3 Ageing

The inter-fibre hydrogen bonds are what provide the strength of cellulose, forming a matrix. During the ageing process, these bonds can be broken or used, thus causing the loss of mechanical strength described in Figure 2-5 [31]. There are three mechanisms of ageing which take place with cellulose-based solid insulation. Initially the paper is thought to undergo oxidation [31, 50]. Oxidation allows for the formation of moisture [60] and acids [50] which contribute to the catalysis of the primary ageing mechanism, hydrolysis [31], pronounced in NTUP over TUP [61]. Pyrolysis is considered as a third mechanism of ageing, it does not require chemical interaction with the cellulose (where oxidation requires oxygen and hydrolysis requires water), but is generally considered to be significant only at high temperatures, around 140°C and above [31]. Figure 2-6 shows the relative influence of each of these mechanisms with temperature [46]. Oxidation is most influential at low temperatures, hydrolysis dominates in the mid-range, and pyrolysis is the main ageing mechanism at higher temperatures.

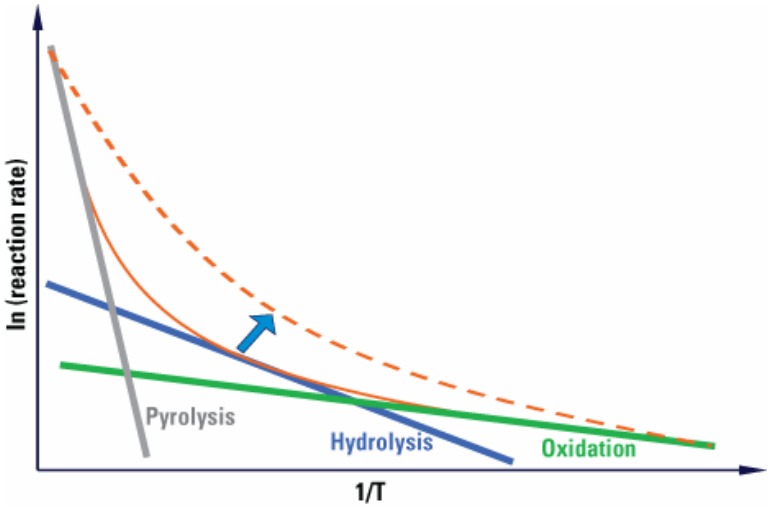

Figure 2-6 – Relative influence of cellulose ageing mechanisms with temperature (T) [46] (orange lines and blue arrow show the influence of increase temperature on reaction rate).

Ageing of the paper insulation is accelerated by two main parameters: temperature and moisture content. Moisture in paper accelerates ageing, with evidence that the ageing rate can be around 20 times faster for paper of 4% moisture than of 0.5% [56]. It has also been shown that for approximately every 6–8 K rise in temperature (within the likely transformer operating range), the ageing rate of insulation materials increases twofold [31, 62], under certain moisture, oxygen, and insulation age conditions [63]. [32] also showed the temperature dependency of cellulosic insulation life on temperature, and the presence of oxygen. Oxygen availability and moisture content are also shown to be significant factors for paper ageing in [60], irrespective of the end of life criterion selected. Free breathing transformers are seen to experience a much higher potential ageing rate under the same loading conditions as a sealed transformer.

Ultimately, the effect of ageing of insulation is loss of the mechanical strength of the insulation, leading to failure. This is caused by the reduction in DP of the insulation as it is aged, which reduces the number and strength of inter-fibre bonds, leading to loss of tensile strength and burst strength, as well as embrittlement of the paper. The relationship between these factors, and others involved in the age-strength association, is complicated. For example, high moisture content will accelerate ageing through hydrolysis, however studies have shown that some indicators of strength (e.g. tearing resistance) of paper is higher when more moisture is present [64]. An increase in tearing resistance of between 40% and 80% was observed for paper samples prepared to 55% relative saturation (RS) compared to samples prepared at 7% RS (depending on age, i.e. DP, of paper and whether the test was done in the machine direction or non-machine direction).

Not only are the mechanical properties of cellulose altered through the ageing process, but so too are its chemical properties. The paper becomes less hydrophilic as a result of the loss of available –OH bonds for binding moisture. The paper structure also changes, becoming less crystalline as the amorphous region is attacked preferentially [65]. Due to the availability of the hydrogen bonds (i.e. they are not used up in inter-fibre bonding and the fibres are less well aligned), amorphous cellulose holds moisture most easily [66]. Indeed, several studies have shown that aged paper is capable of holding less moisture than unaged paper [67-69]. The proportions of amorphous and crystalline regions define the crystallinity index (CI); the more prevalent the crystalline regions, and less amorphous regions, give a higher CI.

During ageing, many breakdown products can be evolved, particularly of concern are acids (especially low molecular weight acids, such as formic acids which can form directly from cellulose [70]) which can be autocatalytic to the hydrolysis ageing process [46, 50, 61]. Such products of ageing can affect interaction with moisture and influence results of tests such as those testing dielectric response [46].

Ageing of TUP is slower for the same conditions compared with NTUP. A chemical agent is applied to the paper which protects the –OH bonds, particularly from attack by moisture molecules (i.e. increases resistance to hydrolysis) [61]. The influence of this is profound, with the rated temperature of TUP being set at 110ºC, compared to 98ºC for NTUP [71]. In spite of this, the mechanisms and effects of ageing of the two papers are similar, and most of the by-products are the same.

2.4.2 Liquid Insulation

The liquid insulator serves several roles within the transformer. Chief among these are dielectric and cooling provisions [72, 73]. It is difficult to state which of these is primary, but given that it is often called the ‘liquid insulation’ it must be considered that the electrical insulation properties of the liquid are paramount to its utility in this application. However, although a liquid insulator must provide sufficient electrical withstand capability, its dielectric properties are lower than the solid insulator [45]. That said, the liquid insulation impregnates the solid insulation, filling voids and thus improving the dielectric performance of the insulation system as a whole [37]. The liquid also performs the role of coolant. The liquid insulator extracts heat generated from losses in the windings, core and other parts of the transformer, and transports it away to be expelled to a heat sink (commonly the

atmosphere, but sometimes secondary cooling is provided by water or other available sinks) [72]. It can do this either under the action of a naturally established thermosiphon effect, commonly referred to as oil natural (ON) cooling mode, or via pumping, termed oil forced (OF) cooling mode. Forced cooling can often be aided by directing the coolant through the windings in a particular pattern or to particular locations, and is then termed oil directed (OD) [37].

Additional to these two main roles, the liquid insulator also serves as a method of inferring the condition of the transformer insulation (therefore called an 'information carrier') [72]. Actually, the condition of the liquid insulation, while important, is secondary to that of the solid insulation in terms of transformer life. However, solid insulation is generally unavailable for testing during the service life of the transformer, only able to be measured after a failure event or decommissioning [41]. Sampling of liquid insulation can take place 'on-line', and much effort has gone into ascertaining a link between the liquid sample condition and the solid insulation condition [31, 50, 61, 74-77].

Further, while the deterioration of solid insulation can often be the life-limiting factor for a transformer, liquid insulation can be regenerated or replaced if necessary to avoid foreshortening of the transformer's useful life [78]. Poor liquid insulation condition can lead to premature failure through reduced dielectric performance [79], and in extreme cases through immediate thermal failure (e.g. in the case of the presence of sludge [79, 80] or in cold climates using high viscosity fluids [81-83]). If the cooling performance is reduced then this can lead to higher operating temperatures within the transformer windings which will contribute to the loss of transformer lifetime by increasing the rate of degradation of the solid insulation, and thus is it still desirable to maintain high quality liquid insulation conditions throughout the life of a transformer.

2.4.2.1 Types

Within the existing transformer market there are several types of insulation liquids, four of the main types are considered herein. A description of each type is provided next. For a comprehensive description of transformer insulating liquids, the reader is also directed to [82, 84] and to [73, 85, 86] for comparisons of insulating liquid properties.

2.4.2.1.1 Mineral Oils

Mineral oils are the dominant insulating liquids in the transformer insulation market. They are produced by refining of crude oil, a process which separates out the so-called

'fractions' within the crude by size (i.e. number of carbons in the molecular chain), and also removes contaminants. The final product is an oil consisting of hydrocarbon components in three forms: straight chain alkane (paraffinic), cycloalkane (naphthenic) and arene (aromatic). These are shown in Figure 2-7 [87]. The paraffins are generally not reactive, however aromatics can be, and are sometimes unstable due to their ring structure. The ring carries a small charge dipole which can also account for some of the capacity for polar compounds in mineral oils. The naphthenic molecules tend to be less reactive than aromatics, though small naphthenes can undergo nucleophilic substitution because of the tightness of their bond angles (aromatics instead tend to react through electrophilic addition).

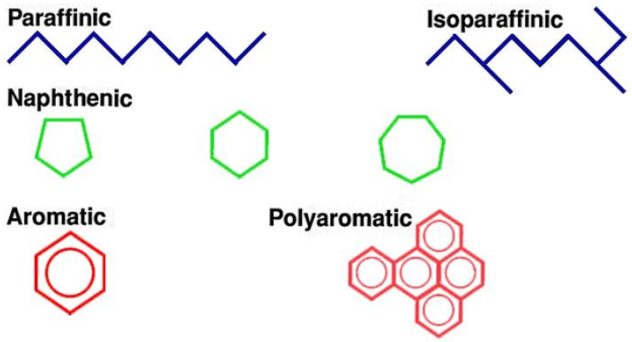

Figure 2-7 – Chemical components of mineral oil [87].

The flash point of mineral oils is approximately 140°C [88] and so transformer operation should be cautious of reaching excessively high temperatures to avoid risk of fire, especially in a free breathing transformer where an oxygen source is readily available.

2.4.2.1.2 Gas-to-Liquid Oils

Gas-to-liquid (GTL) oils are also mineral based oils, but are produced through a gas-to-liquid process where natural gas is converted to liquid (via the Fischer-Tropsch process) [84]. One of the stated advantages of GTL oils is that natural gas is a much cleaner raw material than crude oil, and so it is possible to reduce impurities in the final product. Sulphur is an impurity found in crude oil that can be eliminated from transformer oil by instead generating it from natural gas [89]. The acceptable sulphur content in mineral type insulating liquids is limited by IEC Standard 60296 [90] as sulphur promotes corrosion of copper [84] (of which there is plenty within transformers).

GTL oils are also low in aromatic compounds, and this is thought to improve their resistance to oxidation, increasing their lifetime, and hence the lifetime of the transformer. The chemical structure of GTL fluids will therefore be akin to that of the cycloalkane molecules shown in Figure 2-7. The moisture capacity of GTL oils may also therefore be

considered lower than in mineral oils due to the lack of aromatic compounds which have slight polarity (and thus affinity to water molecules) due to their ring structure [67].

As with mineral oils, GTL liquids have a flash point in the region of 140°C and hence similar caution in relation to transformer operating temperature is advisable.

2.4.2.1.3 Natural Esters

Natural esters are also known by the name ‘vegetable oils’, where ‘vegetable’ differentiates their source from ‘mineral’. While natural esters have been used in over 2 million transformers worldwide, their use is a still an area of intense research and development [91].

Natural esters are highly polar in comparison to mineral or GTL oils. This is brought about by the presence of ester groups (-COOR). Natural esters typically have three such groups (and are thus ‘triglycerides’), with a total carbon number of about 20 [85]. Their chemical structure is seen in Figure 2-8 [92]. As a result of this increased polarity, esters can hold more moisture than hydrocarbon-based liquids and can therefore better protect solid insulation from the ageing effects of moisture [91].

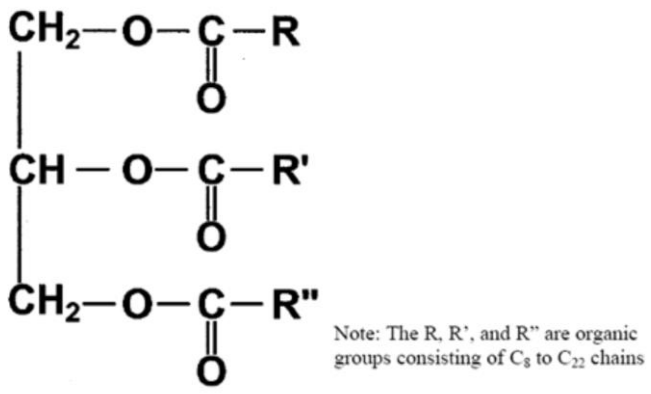

Figure 2-8 – Chemical structure of natural ester triglyceride molecule [92].

Natural esters have been shown to oxidise much more readily than mineral or GTL oils, meaning that the environment they operate in is very important and their use in free-breathing transformers is not advised [82]. However, [91] states that the effect of oxidation of natural esters can take more than five years to show any effects in real operation.

Natural esters are much more environmentally friendly than oils made from natural gas or crude oil [93]. This is considered a major benefit in case of spills and for disposal at the end of the transformer life. They also have a much higher fire point (>350°C [94]), meaning that it can be safe to operate transformers at temperatures in excess of usual thermal

limits [85]. The benefits of insulating liquids which have high fire point and do not combust easily is not a new concept, and they are well described in [95]. However the material developed in that patent did not address the environmental concerns that esters do.

2.4.2.1.4 Synthetic Esters

Recognising that natural esters are useful alternative liquids to mineral oils, a desire to produce ester liquids synthetically arose. This can be done through esterification, the reaction of alcohol and acid molecules to make esters. Crucially, the synthetic process allows for manipulation of the ester molecules (by selection of different acids / alcohols or reaction parameters). Such manipulation means that tweaks to performance can be made, allowing for improvements in certain characteristics. Additionally, this allows for liquids to be optimised against different criteria for specific situations (e.g. in some cold climates, liquids with high viscosity can present issues [83, 96]). Use of synthetic esters in operational transformers is also on the rise, although few assets have been in operation for long periods and so the understanding of their long term behaviour is not yet as well understood as for mineral oils [97].

The chemical structure of a typical synthetic ester (pentaerythritol) is shown in Figure 2-9 [92]. In contrast to natural esters, synthetic esters normally have four ester groups (-COOR), making them even more polar as a result (due to the presence of the additional oxygen molecules), this gives synthetic esters large capacity for water [98].

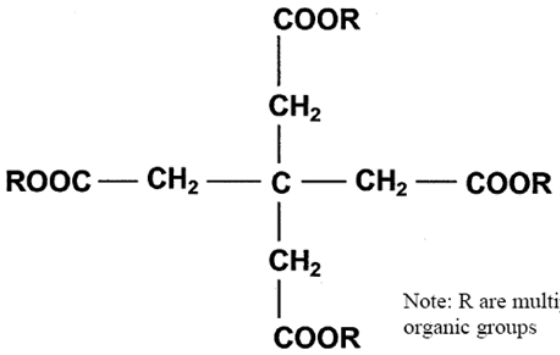

Figure 2-9 – Chemical structure of natural ester triglyceride molecule [92].

Many of the statements made for natural esters apply equally to synthetic esters: they have high fire point (> 300°C [99]), have high polarity, are environmentally friendly, and oxidise more easily (though synthetic esters are more resistant to oxidation than natural esters [100]). Due to these improved characteristics, in addition to on-par operational performance to mineral oils, synthetic ester filled transformers are now being adopted into the UK network [97]. A key barrier to their adoption has been a lack of service experience,

but with more transformers coming online, this gap in knowledge can now be filled. However, this must be supplemented by continued laboratory research.

A result of the high polarity of esters is that they can absorb more moisture. This is purported to have a benefit within transformers as moisture is present in the insulating fluid instead of the cellulose insulation where it can be more damaging to the transformer [101]. This also reduces the likelihood that 'free water' can form in the liquid during sharp temperature declines, a phenomenon that can lead to failure of the transformer [33].

2.4.2.2 Ageing

When insulating liquids age, it is usually the result of oxidation for mineral oils, and of oxidation and hydrolysis for esters. These processes lead to the degradation of the main chemical species present and the generation of acids [50]. Acids can damage cellulose insulation as they catalyse hydrolysis [31, 61]. There is also a reported relationship between acids and moisture in the liquid, where higher acidity leads to a greater capacity for moisture due to increased polarity of the fluid [46, 67].

Another issue that comes with the ageing of transformer liquid insulation is the generation of sludge. This sludge can get stuck in cooling ducts and layer the paper insulation surface, reducing cooling efficiency. This can lead to elevation of the hot–spot temperature (HST), and subsequent acceleration of the ageing process [79].

2.4.3 Moisture in Transformer Insulation

2.4.3.1 Sources of Moisture in Transformer Insulation

Transformers are dried before entering service, with typical values of moisture being less than 0.5% in paper (on an absolute mass basis) [37, 56] and less than 10% RS in the liquid [37]. The presence of moisture within transformers is detrimental to its dielectric strength, and also accelerates the ageing processes, thus foreshortening the transformer life.

Undesirably, moisture becomes more prevalent in the transformer over time [46, 90]. The main sources of moisture in transformers can be divided into external and internal. 'External' moisture is moisture which comes from the atmosphere. The transformer design can aid in reducing moisture ingress from the atmosphere, either through a sealed system or, for free breathing transformers, desiccants are used to scrub moisture from the air as it enters the transformer (these desiccants have been known to fail through saturation if not maintained properly). Even then, moisture will enter the transformer from the atmosphere

from outside through any available gaps (albeit slowly), due to the difference in concentration. For sealed transformers with inert gas blanketing, maintaining a slightly positive pressure may help in keeping moisture out through this mechanism.

Internally generated moisture is harder to prevent. Moisture is a natural breakdown product from the hydrolysis of cellulosic insulation, and in the case of esters, the esterification process (combining of alcohols and aldehydes to form esters, part of a reversible reaction) generates moisture too. Moisture content in paper through the ageing process can reach 2% after about 5 to 7 average chain scissions (i.e. a DP of around 200) based on the average measurement of moisture produced from three series of ageing tests combined in [31].

2.4.3.2 Transition of Moisture between Insulation Media

Solid insulation made of cellulose is hydrophilic (even if thermally upgraded) and thus preferentially adsorbs moisture. In cellulose, there are three potential sites for adsorption of H_2O molecules, the hydroxyl (OH) bonds at the 2-, 3- and 6- positions on the β-D-glucose (technically β-D-glucopyranose) ring, as shown in Figure 2-10.

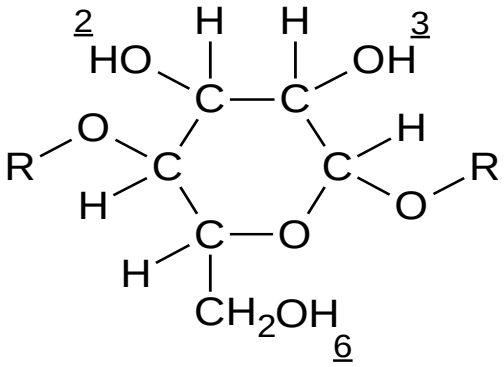

Figure 2-10 – Cellulose monomer with 2-, 3- and 6- OH groups identified.

Adsorption of moisture by cellulose takes the form of a Type II isotherm. The Type II isotherm can be broken down into three sections, marked as *x*, *y*, *z*, in Figure 2-11. The initial part of the curve for low moisture content (section *x*) rises steeply and terminates in a 'knuckle point' which is usually taken to indicate the saturation of mono-molecular adsorption to the -OH bonds on the glucose ring. Beyond this point (section *y*), the moisture is assumed to form multiple layers of moisture bonded to the previously adsorbed moisture molecules of the mono-layer [67, 102, 103]. This part of the isotherm again terminates in a knuckle point (of the inverse inflection), where the final section starts (section *z*). This final section is thought to describe the swelling of cellulose, at which point the adsorption of

moisture occurs more as a physical than chemical adsorption process, with moisture held in the capillaries of the cellulose. This point is expected to be some way beyond the normal operating moisture content of transformers. Alternatively, compelling evidence from [66] suggested that the initial uptake of moisture (section *x*) occurs preferentially on the primary OH at position 6- of the cellulose monomer glucose ring [47] (as seen in Figure 2-10) and this saturates at the first knuckle point, with positions 2- and 3- hydrating thereafter in section *y*.

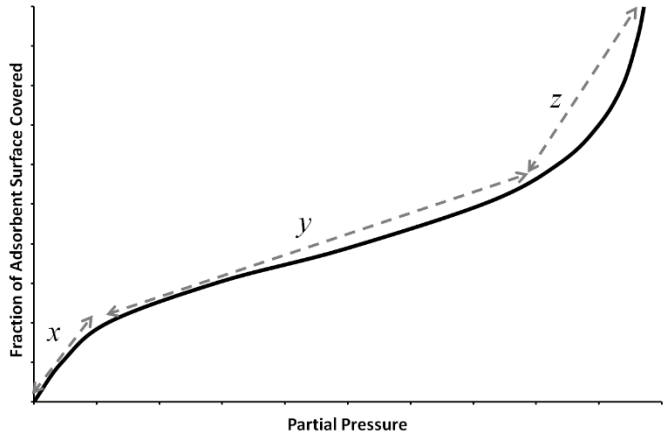

Figure 2-11 – Indicative Type II isotherm (sigmoid isotherm) with key sections (marked x, y, z) identified.

Moisture will desorb from paper as temperature increases. This can be explained thermodynamically by considering the energy of the system. (2-8) shows the change in Gibbs free energy[1] of a system (with *H* the system enthalpy, *T* the temperature, *S* the system entropy, and *G* the Gibbs free energy of the system). When adsorbed to the solid insulation, moisture molecules are constrained in movement and thus in arrangement, and so the entropy of the system reduces ($\Delta S<0$). As a result, (2-8) becomes (2-9).

$$\Delta G = \Delta H - T\Delta S \quad (2\text{-}8)$$

$$\Delta G = \Delta H + T|\Delta S| \quad (2\text{-}9)$$

Adsorption of moisture by cellulose is a thermodynamically spontaneous process, therefore the change in Gibbs energy is negative ($\Delta G<0$) and so a release of enthalpy ($\Delta H<0$) during adsorption is a consequence of (2-9) – i.e. adsorption is an exothermic process.

[1] The Gibbs free energy describes the thermodynamic potential of a system, it is minimised at chemical equilibrium. Therefore any thermodynamic state above the minimum value will attempt to move toward equilibrium in order to minimise the value of *G*.

Exothermic processes are less prolific at higher temperatures, in accordance with le Chatelier's principle[2] [104].

This means that moisture leaves paper as transformer temperature increases. Fortunately, the liquid insulation capacity for moisture increases and may take up the moisture released [105]. Note though that there is a lag between conductor / solid insulation temperature rise and the resultant liquid temperature rise [23, 106]. If moisture is released from solid insulation beyond the liquid moisture capacity then moisture may exist as free water within the transformer, which can be particularly dangerous [107]. This may also occur if a sudden drop in temperature follows a period of high loading (as the moisture that had previously left solid insulation into the liquid can no longer be held in the liquid, but is unable to return quickly to the paper (due to its being dispersed around the total volume of liquid) . Temperature within transformer windings is not uniform, and so this means that moisture content in the solid insulation can vary with position [68].

A final notable feature of sorption phenomena is that there is hysteresis between the adsorption and desorption processes. Therefore, one would expect different answers if desorption or adsorption isotherms were used, and as bubbles are a desorptive process it is not appropriate to use adsorption data to represent bubbling. The hysteresis is a feature of the thermodynamically irreversible sorption process [16] (moisture can be desorbed after adsorption, or vice-versa, but work must be done to the system to enable this change). Caution should thus be exercised when using isotherm data [13].

2.4.4 Preparing Transformer Insulation for Service

The transformer paper insulation is dried by vapour phase drying [43]. The intention is to dry the insulation as much as possible (<0.5% [31, 57]) without degrading the DP too much. It was shown in [56, 57] that reducing water content is preferable to maintaining higher DP, and additional drying is therefore beneficial to the transformer lifetime.

As well as insulating liquid (which is free to move around the transformer), the cellulosic insulation is also impregnated with the liquid. This provides a vital duty of filling voids which would otherwise be available to gases (usually air) which weaken the dielectric strength of the paper. Even if the voids are evacuated but not filled with liquid insulation, the dielectric strength of the insulation is reduced compared to when impregnated [43].

[2] le Chatelier's principle states that when a system under equilibrium is perturbed, the system will adjust to minimise the effects.

Impregnation is done with dry liquid under vacuum after drying of the cellulose. Before being entered into service, the insulation must adhere to relevant standards which indicate the conditions which ensure safe and reliable operation, for example, mineral insulating oils are covered by IEC Standard 60422 [108].

2.5 TRANSFORMER FAILURES

Transformers are crucial assets within the electricity network. Failure of transformers can lead to loss of customer connection to the grid and cause stability issues across the network as a whole. Loss of a transformer can be a costly event, especially when it occurs unexpectedly (i.e. before the asset can be phased out of service as part of a replacement regime). Costs include the replacement transformer, charges levied for lost customer hours, and lost revenue [109]. Secondary impacts are to society where loss of power results in reduced economic output, and vulnerable people being put at increased risk.

To avoid failures, condition monitoring of the transformer is usually carried out. Monitoring is normally done by assessing the insulating oil through numerous tests. These tests vary in their utility and their development, but currently this is seen as the best method available. Testing of solid insulation is not an option as once in service the windings of the transformer are considered inaccessible, therefore the paper insulation condition (the most commonly used metric of transformer lifetime) is inferred from the results of analyses conducted on the oil. If results of oil analyses show reason for concern then action can be taken to rejuvenate or mitigate the transformer.

2.5.1 Causes

There are many mechanisms for transformer failure. Surveys which collate data on transformer failure often divide failures into categories. Common categories include: mechanical; lightning / switching impulses; ageing; electrical / short circuit; overloading; and more besides [110, 111]. Failures can also be ascribed to particular components of the transformer, with the most common failure points tending to be the windings, [on-load] tap changer and bushings [110-113]. In [109] the cause most commonly found as the source of transformer failures in a study of 94 transformer failures over a period of 5 years (1997 – 2001) was insulation failure.

Often, causes of failure may conflate, for example in bubbling the fault may be ascribed to either ‘high overload’ (the cause of the bubble), or to ‘flashover’ (the cause of

the failure when the weakness in the insulating material is exploited). In this thesis, failure through bubbling is generally considered to be caused by high overload (the root cause). As detailed later, the mechanisms for actual formation of the bubble are limited by this definition and so this should be borne in mind throughout. However, the value of this study is not diminished by only focussing in on bubbles formed through high temperature events within the transformer.

2.5.2 Thermal Behaviour and Failure

The study of thermal behaviour of a transformer is challenging. A transformer has a profile of temperature which varies with location. The temperature mostly increases with increasing height. The temperature is also higher closer to the windings. The windings are the main contributor to temperatures within the transformer as they provide heat into the system (in the form of resistive (and other) losses).

The temperature profile can also be affected by the cooling regime of the transformer, which is either natural or forced flow, the height of the radiator, and other factors such as ambient conditions (temperature and weather).

2.5.2.1 Modelling Transformer Temperature

To calculate the temperature within the transformer, the location of the temperature must therefore be established. Most commonly the temperature considered is the HST. In the standard practice, this temperature is assumed to appear at the very top of the winding structure, with temperature decreasing linearly down to the bottom of the winding. A gradient is assumed between the oil and the winding temperature (with the winding temperature being the higher), and so the oil at the bottom of the windings is the lowest temperature part of the transformer insulation system. The HST is constructed by considering consecutive temperature rises above ambient temperature, bottom oil temperature and top oil temperature. This is shown by the thermal diagram displayed in Figure 2-12 [23].

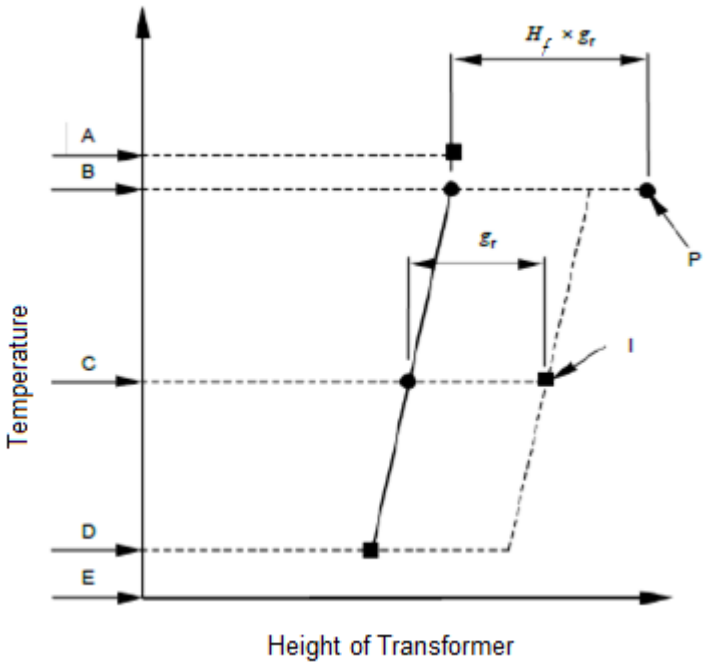

Figure 2-12 – Transformer thermal diagram [23]. Solid line shows the liquid insulation temperature at different heights within the transformer; dotted line shows the winding temperature at equivalent height.

In taking this model to be accurate (or at least representative), the HST can be calculated assuming it occurs at the top of a winding. Modifications may be necessary to account for specific situations [114]. The HST is normally considered to be the most dangerous point (thermally) within a winding as it is the point at which the effects of high temperatures are likely to be felt most. For this reason, both IEC and IEEE provide HST calculation methodologies in their respective loading guide standards [22, 23]. Note that the validity of many of these assumptions has been challenged in previous literature, for example in [115-117], but some studies have shown good agreement of calculations with these methods to actual temperature measurements made during overload tests [106].

2.5.2.2 Effects of Temperature on Insulation Failure

There is a lot of effort placed on the understanding of the transformer thermal performance. This is due to the strong influence that temperature has on transformer performance and an even greater effect on transformer insulation life.

As the temperature of the copper winding conductor increases, so too does the resistance of the copper (at ~4% K^{-1}), and as a consequence the resistive losses also increase (further increasing the temperature). Due to the increased resistance, the transfer of energy

across the transformer is less efficient, with [118] showing a 10% increase in resistive loss when temperature rises from 70ºC to 100ºC.

The lifetime of solid insulation within the transformer is coupled to the temperature. For NTUP systems, a relationship is thought to exist where increasing the temperature by approximately 6–10°C causes a doubling in the rate of degradation [62, 119]. This is based on the energy required to break bonds between cellulose units within the cellulose chains. The ageing process through degradation of cellulosic insulation results in the generation of many by-products, among which are acids and, importantly, water. Once the cellulose chains are broken enough, the degree of polymerisation (DP, the average length of the chains, as described by the total monomer units in a polymeric chain) reduces to a point at which failure of the transformer becomes likely. This point is variously set as a value of DP = 200 [23, 45], 50% retained tensile strength [22], 25% retained tensile strength [22], or interpretation of functional life tests [22]. At this point the transformer is likely to be taken out of service so as not to suffer a catastrophic failure.

The generation of by-products from the ageing process can cause further problems for the transformer insulation system. Acid and water can both catalyse the degradation process [46, 61, 120]. Acids can also migrate into the insulating liquid, increasing its capacity for moisture and thus reducing the dielectric performance of the system [90]. Exceedingly high temperatures can damage the paper directly, generating gaseous by-products such as carbon monoxide, carbon dioxide, methane and ethane. As previously mentioned, generation of gases is not a favourable situation for transformer insulation integrity.

With increasing temperature, as a general rule, polar by-products move from paper into oil. The reverse process occurs, albeit usually much more slowly, as temperatures reduce. The movement of material into the oil with temperature causes problems for the monitoring of transformer condition described above, with temperature correction factors commonly needing to be employed when analysing test results [121]. Moisture is one of the impurities that desorbs from paper to oil during temperature rise. At high temperatures, this moisture may leave the solid insulation as a vapour bubble (in contrast to molecular desorption from paper and absorption into the oil). This bubbling procedure can occur quite effusively, with multiple bubbles generated from a small nucleation point [55, 67, 122].

2.6 BUBBLING PHENOMENA AND EARLY BUBBLING STUDIES

2.6.1 Thermodynamic Description of a Bubble

Bubbles herein relate to vaporised media within a bulk fluid. Bubbles of gas within transformers are dangerous as they affect the dielectric strength of the bulk fluid within which they exist. The electrical withstand strength of insulating oil is significantly reduced by the presence of bubbles [123]. This reduction means that, especially in areas of high electric field strength, there is a risk of partial discharge (PD) occurring. This can lead to a flashover event, particularly in cases where a stream of multiple bubbles is present. However, it is not easy to ascribe failure of a transformer to the presence of bubbles as there is no evidence left behind for post-mortem analysis to uncover [34]. There are publications which do attribute failures to bubbles that have been generated [124] but without pointing to any specific cases. Studies such as [122] have shown that applying vacuum to remove bubbles post-generation gives a partial recovery of the withstand strength of the liquid insulation, and again, it can therefore be difficult to prove weakening of the insulation occurred if time is allowed for bubbles to leave the system (e.g. into the headspace). One of the mechanisms of transformer failure listed in [125] is bubbles, with three different proposed causes of bubbling suggested.

Bubbles can occur through a number of mechanisms:

- Bubbles may be formed either homogenously or heterogeneously. Homogenous bubbles form within the bulk fluid only, whereas heterogeneous formation occurs at an interface (either the interface between solid and liquid insulation or between liquid insulation and the vapour space). Heterogeneous bubbles are usually much less demanding in terms of the energy required to form as the interface acts as a nucleation site and are therefore much more common [126, 127].
- Bubbles can be caused by high temperatures or by reduction in pressure [128]. Within a transformer, high temperatures tend to occur at the solid insulation, with energy coming from the conductor with which it is in direct contact. A loss of pressure could occur for numerous reasons, but a particularly pertinent case is when during operation a transformer is subjected to rapid cooling (e.g. by rainfall onto the external tank walls) which reduces the oil temperature which in turn increases the oil density. The reduction in volume as a result

causes dissolved gases to bubble out of the oil in order to fill the space. The material of the bubbles from the former is likely to be material sorbed in the paper, whereas in the latter case it is from gases already dissolved in the oil. Both cases can be viewed as an alteration in the vapour pressure equilibrium state of the system.

- Bubbles can be formed by altering the saturation level for a material dissolved within the transformer oil. This can occur due to changes in temperature and / or pressure [127]. Note that for some materials (e.g. nitrogen) an increase in temperature results an increased solubility, whereas for other materials (e.g. carbon dioxide) the solubility in oil decreases with increasing temperature [129].
- Bubbles may be spontaneous or non-spontaneous. Non-spontaneous bubbles require some form of mechanical input, e.g. sparging. Spontaneous bubbles occur because of the thermodynamic preference of the system.

The bubbles considered within this study are heterogeneous, spontaneous bubbles caused by elevated temperatures, specifically focussed on ebullition of moisture from the solid insulation.

2.6.1.1 Role of Surface Tension in Bubble Formation

In order for a bubble to form, the internal pressure (p_{int}) of the bubble must balance the external pressure (p_{ext}), plus the pressure to maintain the surface of the bubble, and overcome any pressure losses such as friction [102]. The last of these concerns is normally considered negligible. Equation (2-10) shows this pressure balance. Rearrangement of (2-10) to give (2-11) indicates that surface tension (σ) is involved in the pressure gradient term (Δp), which acts as the driving force for maintenance of a bubble (balancing the internal pressure against the external pressure over the bubble surface).

$$p_{int} = \frac{2\sigma}{r} + p_{ext} \qquad (2\text{-}10)$$

As the unit of pressure is equivalent to J/m^2 it represents a specific energy (energy divided by area). Equation (2-11) also leads to the relationship that in order to grow a bubble by a unit radius (r), the energy input per unit area required is equal to twice the value of the surface tension. Note that for each subsequent increase by unit radius the equivalent increase in surface area is larger than before, yet the same amount of energy per unit area (twice the surface tension) is required. Surface tension is therefore a parameter of importance to bubble

energy calculations. Several studies looking at bubbles in transformers, discussed later, use surface tension as a basis for their work.

$$p_{int} - p_{ext} = \frac{2\sigma}{r}$$
$$\Longrightarrow \Delta p = \frac{2\sigma}{r} \quad (2\text{-}11)$$

2.6.1.2 Gibbs Energy Derivation

The Gibbs energy is the free enthalpy within a system and can be used to assess the thermodynamic potential of a system, that is, the maximum amount of reversible work that can be done by the system. At chemical equilibrium (under constant pressure and temperature), a system will minimise thermodynamic potential. This means that equilibrium is the position that it is most difficult for a system to change from without an external perturbation (which is the general understanding of the term 'equilibrium' anyway). In order for a system to spontaneously change, the Gibbs energy must decrease (change in Gibbs energy must be less than zero).

Equation (2-12) shows the fundamental Gibbs energy formula. By following equations (2-12) to (2-18), it can be seen that surface tension is equal to the Gibbs energy per unit area.

$$G_{Bubble} = H - TS \quad (2\text{-}12)$$

$$\partial G_{Bubble} = \partial H - \partial(TS) \quad (2\text{-}13)$$

Given that the change in enthalpy can be described in terms of internal energy, *U*, pressure, *p*, and volume *V* as,

$$\partial H = \partial U + \partial(pV) \quad (2\text{-}14)$$

and the change in internal energy is the summation of change of heat, *Q* and work done, W_d, across an area, *A*,

$$\partial U = \partial Q + \partial W_d = T\partial S - p\partial V + \sigma\partial a \quad (2\text{-}15)$$

then by substitution the change in Gibbs energy can be written as

$$\partial G_{Bubble} = T\partial S - p\partial V + \sigma\partial a + p\partial V + V\partial p - T\partial S - S\partial T \quad (2\text{-}16)$$

$$\partial G_{Bubble} = V\partial p - S\partial T + \sigma\partial a \quad (2\text{-}17)$$

Rearrangement, and taking pressure and temperature to be constant (indicated by subscript symbols) yields,

$$\left(\frac{\partial G_{Bubble}}{\partial a}\right)_{p,T} = \sigma \tag{2-18}$$

This concept can be thought of as the escaping tendency of molecules at the surface (the escaping tendency is the likelihood of the molecule to leave the surface into the gaseous phase, often termed the 'chemical potential', which is the Gibbs energy [130]). A higher value of surface tension suggests that molecules have more energy at the surface, which must be provided from the bulk material (or externally input without being taken up by the bulk material) to prevent the loss of molecules (and hence, loss of the surface) into the gaseous phase.

By considering the Gibbs energy at the bubble surface, rather than of the whole bubble, it is possible to develop an equation for the enthalpy at the surface of a bubble, which is dependent on only two properties; temperature and surface tension. This is shown in equations (2-19) to (2-22), starting with the fundamental equation for change of Gibbs energy.

$$\partial G_{Surface} = V\partial p - S\partial T \tag{2-19}$$

$$\left(\frac{\partial G_{Surface}}{\partial T}\right)_{p} = -S \tag{2-20}$$

Substitution with (2-18) gives,

$$\left(\frac{\partial \sigma}{\partial T}\right)_{p,\mathrm{a}} = -S_a \tag{2-21}$$

Substitution of (2-18) and (2-21) into the fundamental enthalpy equation reduces to,

$$H_a = G_a - TS_a = \sigma - T\left(\frac{\partial \sigma}{\partial T}\right)_{p,\mathrm{a}} \tag{2-22}$$

The result that enthalpy of a bubble surface (over a defined area) can be described by surface tension and temperature, reducing as temperature increases, leads to the possibility of different energy demands for different oil types, as they have different surface tension values (as will their surface tension dependence on temperature). If there are large differences in the surface tension values of different liquid insulators, then this may give an

advantage in terms of survival of high-overload scenarios for particular liquid insulation which has greater surface tension.

2.6.1.3 Generation of Bubbles inside Transformers and how they lead to Failure

The presence of bubbles within the insulating fluid will reduce dielectric strength [123], thus potentially leading to breakdown and failure. There are several steps required for this failure to occur, shown in Figure 1-3.

Each of the stages in the process shown in Figure 1-3 contributes to the failure, and by removing any stage, failure is unlikely to occur. Thus, it is possible to protect a transformer from failure by removing or mitigating against each stage independently (which is much simpler than mitigating the entire pathway). However, the more stages which are moderated against, the more layers of protection are built in, and the less likely a transformer is to failure due to a bubbling event.

This is still a difficult task however. Some of the stages seem easy to prevent at first sight. For example, high temperature can be avoided by operating the transformer without overloading it, but transformers *do* run over-temperature, at overload conditions on occasion; it is sometimes deemed necessary to do so. Other stages, such as bubble release seem to be more difficult to control, yet some researchers have recognised that there are things within the transformer that may contribute to bubble release [34, 131].

2.6.2 Early Studies on Transformer Bubbling

Previous authors have addressed bubbles in transformers, covering various areas. [132] found that electrically stressed insulation (oil impregnated paper) would gassify, and that the amount of ‘stress’ that needed to be applied was inversely related to the moisture content of the insulation. A study by Kaufmann in 1977 looked at bubbles forming through two of the mechanisms described in Section 2.6.1: rapid external cooling and short term overloading [122]. This study also aimed to specify how gasification of material in a transformer can affect breakdown strength within a transformer insulation system.

Kaufmann’s work began by using a 37.5 kVA transformer with unaged TUP and mineral oil insulation. The main focus for this set of experiments was to load the transformer at overloaded conditions, and then to simulate rainfall on the transformer tank (by spraying water at a specified rate). Bubbles were witnessed in some experiments, mostly when in

overloaded condition coupled with high rainfall [122]. The bubbling intensity was seen to depend strongly on the loading condition.

Further testing where an increase in load to exceedingly high levels (rising from 1.75 p.u. to 3.00 p.u.) was done, without rainfall simulated. Bubbles were witnessed and so these were deemed to have been caused purely by the temperature increase.

Bubbles in [122] formed solely from the solid insulation irrespective of whether the temperature was rising or falling. This was attributed to the lack of 'agitation' of the oil. Indeed, without a pump to provide mechanical work, it is much more difficult to form bubbles without a nucleation point. Kaufmann points out that the oil in his study was 'saturated with gas' [122]. It is therefore likely that super-saturation did occur, but that gases simply escaped at the interface between the oil insulation and the gas head space, which is much easier to achieve than bubbling within the bulk [128].

Kaufmann conducted a material analysis of the bubbles formed in his study and found carbon dioxide and carbon monoxide to be present. Due to the high overload conditions used in some of the tests, this material could have been evolved during the test or could have been released from extant dissolved gases in the oil. The insulation moisture condition before the tests are not provided, although as the system is described as 'new' the moisture content is likely to have been low. The solid insulation was also 'vacuum-impregnated' with the insulating fluid, which again implies that the insulation system was dry before the test began. Thus moisture bubbles would be difficult to generate in these tests.

Kaufmann then repeated the tests for a transformer placed under voltage stress (the initial tests were performed with the secondary terminal shorted to minimise the voltage stress). These tests showed a similar bubbling performance and so Kaufmann remarks:

'From the observations made here it was concluded that voltage stress had no effect on bubble formation.' [122].

This is an important consideration for future testing as it helps to simplify the experimental design.

Kaufmann then continued the study by making use of miniature coils, which were useful as they increased the visible area of the coils compared to the transformer used initially. From the tests on the smaller coils, two important observations were made. Firstly, bubbles generated during the tests were witnessed as 'stuck' in between layers / turns, or beneath the winding. This trapping of bubbles increases the likelihood that a fault could

occur as a result of their presence in an area of high electric field strength. Secondly, the breakdown voltage of the system was measured. It was noted that a decrease in breakdown strength was observed after bubbling occurred. The samples were then degassed and a partial recovery of the breakdown strength ensued, thus confirming that bubbles / gases within the transformer oil reduce the dielectric performance of the transformer insulation system [122].

The next step in transformer bubbling research was performed by Heinrichs in 1979 [131]. This study reduced the scale of the experiment drastically compared to Kaufmann's earlier work [122]. Heinrichs used a test tube to represent the transformer tank and a heating element to represent a winding, his full set-up is displayed in Figure 2-13 [131]. Kraft paper (one layer only) is wrapped around the heating element, replicating the solid insulation wrapped around the conductor. The type of oil used in these tests is not specified, but mineral oil is assumed based on the time and location of the investigation.

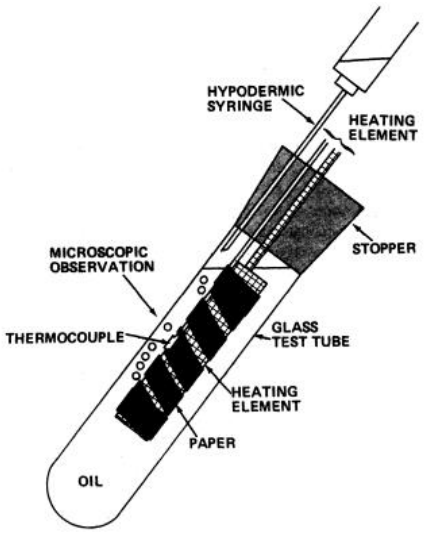

Figure 2-13 – Experimental set-up used by in [131].

Heinrichs describes the purpose of these experiments with the following statement:

> *'…the generation of gas bubbles is related to the thermal limitations of the oil-paper system under overload conditions at typical operating stresses.'* [131],

and this work thereby continues from the understanding of Kaufmann that overload conditions are of significant importance for transformer bubbling.

During preparation of the samples for the experiments, the oil and paper insulation was dried under vacuum, leaving the insulation system almost completely without moisture and gas [131]. This again means that the bubbles formed through these tests are likely to be formed from the products of decomposing solid insulation. The chemical analysis carried

out shows this too, with methane, carbon monoxide and carbon dioxide all present, as well as water.

One of the interesting features that Heinrichs noted is the size of bubbles in the tests, appearing at between 25 and 50 μm [131]. The performance of the system was evaluated with and without the presence of vibration at the resonant frequency of a transformer (120 Hz used, resonant frequency of US based system). It was found that bubbles were released at smaller size under the influence of this vibration [131], however it is not stated if these conditions influenced the release time of the bubbles.

This experiment used a cyclical temperature profile, with each subsequent 'peak' getting progressively lower. The initial peak was 160°C, rising over a period of around one hour from 90°C. This is a reasonably slow rate of temperature rise (on average approximately 1 K/min), but the high temperature condition was then maintained for an extended period (approximately one hour). Bubbles were found in the region of 130 – 160°C (measured as the surface temperature of the heating element) [131]. The author then recommended that a maximum operational limit of 140°C should be introduced into the loading guides [131]. The wording of the most recently published IEEE and IEC loading guides suggests that this advice was adopted and still exists today [22, 23].

This work shows that the transformer insulation system can be scaled down for analysis of bubbles, although there are some difficulties in achieving a representative system when construction is done manually – air bubbles were noticed being released from insulation during the early phase of the experiment and this may have influenced the final results [131].

A 1980 paper by McNutt et al. [133] also reported a 140°C figure for their first observation of bubbles from sample coils, even for relatively dry samples (<0.5% moisture content in paper). These were described as 'streams of tiny bubbles' [133]. In that paper, the authors noted that bubbles evolved more quickly and at a larger size as temperatures increased, before reducing after a period of time.

Further work by Kaufman, with colleague McMillen in 1983 looked into the necessity behind bubbling research by conducting a study assessing how the withstand capability of the insulation is affected by bubbles generated from overloading [34]. The investigation began by assessing the loading conditions which caused bubbling to occur for a set of model coils. The coils had a single layer of TUP wrapped around a copper conductor of layer type

construction. These windings were then placed into a tank with an observation port. Five such coils were made, with one being fitted with thermocouples acting as a temperature guide only. The test does not specify the oil type used, and so again, mineral oil is assumed, but the system is vacuum impregnated and is dried such that the insulation is thought to be at a similar condition as a new transformer. The presence of bubbles was measured by PD measurement at low voltage [34].

The tests were performed by applying a load profile established as per the information presented in Table 2-2. The loading values equate to a steady state temperature, also shown in Table 2-2, and the system was allowed to reach these temperatures on each occasion. The test indicates a movement from 'full load' to a 'moderate overload' and then a rise from 'normal loading' to a 'severe overload'. During the first stage (full load to moderate overload), the rate of temperature rise is sedate at 1.33 K/min, whereas for the second stage (normal load to severe overload) the rate of temperature rise is more drastic at 5.17 K/min. Both stages occurred for a period of thirty minutes. Bubbles were only witnessed visually during the second stage, although even during this stage, temperatures in excess of 180°C were required, however the PD measurement identified a reduction in the dielectric strength of the insulation much earlier than this. The tortuous nature of the winding design is blamed for this discrepancy [34].

Table 2-2 – Summary of temperature and load profile for bubbling experiments in [34].

Step	Load (per unit)	Steady State Temperature (°C)	Rate of Temperature Rise in First Thirty Minutes (K/min)
1	1.00	100	–
2	1.54	180	1.33
3	0.50	45	–
4	2.25	225	5.17

During these tests, bubbles were seen to increase in ferocity as temperature continued to rise, and the bubbles were formed at locations such as at the winding leads [34].

Kaufmann and McMillen performed a DGA of the oil after their tests (bubbles were not collected for analysis), as with [131] they found increases in both water and carbon dioxide [34]. As was the case in [122], recovery of the dielectric strength in [34] occurred some time after the overload condition was stopped. Bubble generation also ceased almost immediately on loading returning to normal (i.e. before temperature had reduced significantly) [34].

Having established the bubbling performance of the model coils, fifteen 25 kVA transformers were put into testing. These transformers were insulated with TUP, and there

were transformers representing core-from, shell-form, and 'modified shell-form'. Some of the test objects were aged, others unaged. Radio noise measurements were used to detect bubbles, as well as visual observation. It was found from this that there is potential for bubbles to be withheld in the interstices of the winding (witnessed as a difference in time between bubble identification through the radio noise measurement and the later visual observation). It was also seen that bubble generation stopped almost instantly once the current (i.e. the heat source) was stopped [34].

Later in the 1980s, work turned from an experimental basis to more theoretical analysis with McNutt et al. [134] and Fessler et al. [135] publishing mathematical models for bubble evolution in transformers.

The former of these two works identified three mechanisms for bubble formation within the transformer, and they accord with those already identified above. The first mechanism considered is that the blanket gas dissolves into the insulating fluid and then a change within the system causes super-saturation to occur. It was shown that if moisture content is also considered, either a drop in load or an increase in load can cause the concentration of nitrogen dissolved in oil to overcome the equilibrium state and hence the nitrogen will tend to leave the oil, with bubble formation the result. Consideration of other dissolved gases has shown not to have large influence on the expected temperature needed for bubbles given that they appear in much smaller quantities than nitrogen does [134].

The second mechanism identified is from directly degrading the cellulosic insulation. The by-products of cellulose breakdown are various, with [74, 120] listing many of them. The degradation of cellulose occurs through any of three main methods: oxidation; hydrolysis; and pyrolysis [50]. Pyrolysis occurs at high temperatures (usually considered to be above 140°C [46]) and does not require reactants to be present; it degrades the cellulose by direct cleaving of the inter-monomer bonds. Hydrolysis is accelerated greatly by the presence of acids and / or water [46, 50], and takes place at a lower temperature than pyrolysis. Oxidation is normally considered to be the origination of transformer insulation ageing due to the low temperature required [50] and the abundance of oxygen in the atmosphere and in some species of impurity found within the insulation oil [31], although this process can be significantly retarded by use of inert blanket gases.

Carbon monoxide and carbon dioxide are considered to be the most common gases evolved from the decomposition of cellulose. In order to establish the bubbling tendency of

gases evolved through the decomposition of cellulosic material in oil, the same partial pressure treatment as above for nitrogen is applied [134]. The finding from this modelling is that bubbling from the second mechanism does not need to be paid any credence below temperatures of 150°C [134].

The third mechanism identified is that of moisture within the cellulose insulation being evaporated [134]. This last mechanism is only treated in conjunction with other mechanisms within their study however.

The second of these papers focussed on mathematically derived bubble predictions firms the understanding of the localised requirements for bubble formation thus:

'Conditions in the local oil adjacent to the conductor surface are suitable for free gas bubble evolution when the summation of the partial pressures of the dissolved gasses and water vapour exceed the total static pressure at that point.' [135].

This statement clearly identifies that the partial pressure of material dissolved within the insulation is an important parameter, and that the combination of such material may be crucial in establishing bubbling likelihood. One limitation of the description is that when considering 'local oil adjacent to the conductor' there is no account taken for motion of the oil, which of course would occur for cooling purposes, and so the scenario is condensed to an instantaneous situation.

Reference [135] essentially advances on [134] by updating some of the assumptions used in that work. For example, up to date water solubility and water equilibrium results as well as updated thermal decomposition information were introduced. In the paper, the authors rearrange an empirically derived formula for moisture content in paper (shown in (2-23)) to give a formula for water vapour in paper (as in (2-24)), with the vapour pressure key to their investigation. This formula would later be adopted by other authors and go on to form the basis for BIT calculations used to set temperature limitations. Unfortunately, an error in the transposition of (2-23) into (2-24), as identified by [136], means that the later formula is flawed. Equation (2-25) indicates the corrected form provided in [136].

$$W = (2.173 \times 10^{-7}) p_v^{0.6685} exp^{\frac{4725.6}{\vartheta}} \tag{2-23}$$

$$p_v = (5.8869 \times 10^{9}) W^{1.4495} exp^{\frac{-6996.7}{\vartheta}} \tag{2-24}$$

$$p_v = (9.28 \times 10^{9}) W^{1.496} exp^{\frac{-7064.8}{\vartheta}} \tag{2-25}$$

where p_v is the vapour pressure of water (in mmHg) at temperature ϑ (K) and water content in paper W (g moisture / g dry paper).

Key outcomes from [135] show that the temperature required to generate bubbles can be elevated by using a membrane conservator system instead of a nitrogen blanket (due to a reduction in the dissolved gas content). Further, bubble formation can be greatly influenced by location – higher static head of oil over the conductor also elevates the temperature required for bubbling.

From these initial works into bubbles, the most significant finding is the temperature for bubbling to occur was anchored to be 'approximately 140°C'. The importance of vapour pressure of the dissolved material was firmly established. Mostly, studies centred on new, dry insulation, and the composition of bubbles was generally that of the blanket gas, or of gases formed directly from the decomposition of the cellulosic insulation. The experimental studies range widely in scale, with [131] working at the test tube level, [122] working on real size transformers, and [34] working somewhere between the two with model coils and transformers. It was shown that reasonable accuracy can be attained through mathematical models in [134] and [135], although the variety of potential cases for bubbles are so numerous that modelling of this type (summation of vapour pressure for different transformer scenarios) makes setting of a standard temperature difficult. The authors of those papers settled on a range of 130 – 150°C as likely to form bubbles.

2.6.3 Continued work on Transformer Bubbling

After the initial work described above from [34, 122, 131, 134, 135], there was loose accord between experimental data and mathematical models. Also, variation in insulation condition (as described by the moisture and gas content) was given little credence. This changed with the publication of [137]. This study conducted a series of experiments on a model coil, investigating the BIT considering a range of values for two parameters which the authors considered vital: the moisture content in paper (% mass of moisture / mass of dry paper) and the gas content in liquid (%). The moisture content in paper covered the range 0.3% to 8.0%, and gas content in liquid ranged from 0.45% to 12.3%. This range for the parameters is impressive, and covers the two extreme conditions for both parameters, however only 26 experiments were carried out making it difficult to analyse either parameter alone.

The graph in Figure 2-14 shows the experimental results of tests done at gas content of 8.8% (in orange) and 1.0% (in blue), thereby showing both the influence of moisture content in paper on BIT, and how the influence of moisture is affected by gas content in liquid [137].

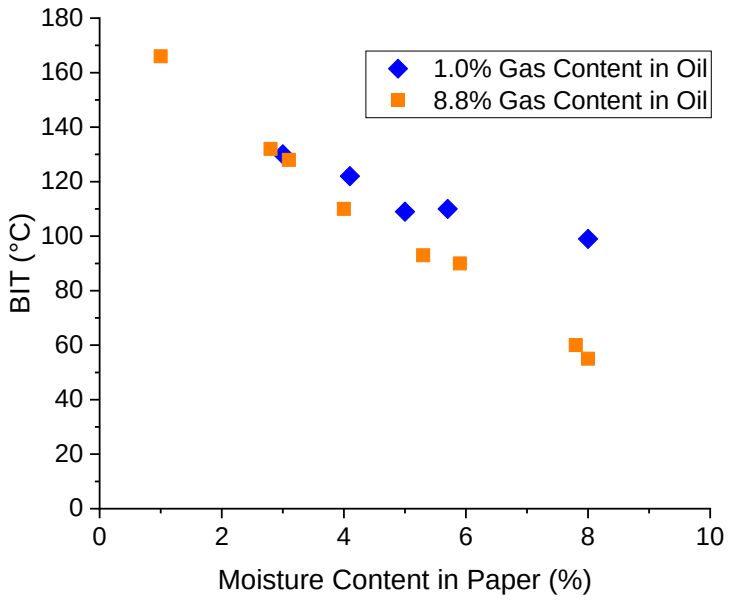

Figure 2-14 – Comparison of variation of BIT with moisture content in paper at gas content in liquid of 1.0% (blue diamonds) and 8.8% (red squares) [137].

It is clear that the temperature needed to form a bubble in the system is affected by the moisture content present in the paper insulation. There is a negative relationship between the amount of moisture and the temperature required. This relationship holds irrespective of the gas content in liquid. Values of 1.0% and 8.8% for gas content in liquid represent a reasonably degassed system and a system saturated with nitrogen at moderate temperature. The BIT difference between systems at these values of gas content in liquid is exaggerated by increasing moisture content in paper. For dry paper, where the moisture content is around 3.0%, there is no discernible difference in BIT whether the gas content is high or low. However, at moisture content in paper of around 5.8%, the difference in BIT is approximately 20 K.

The outcome from the experiments in [137] is the development of a formula that predicts BIT based on inputs of moisture content in paper, gas content in liquid, and pressure. The formula is constructed in two parts, as shown in (2-26). Ignoring the second term, the formula is seen to be the rearrangement of (2-24) for temperature. The second term is then a fitting factor of arbitrary type to correct the formula to the experimental data, consisting of γ, the gas content in liquid (%).

Recalling that (2-24) was erroneous, the formula should be used with caution, despite it fitting the original data well. The formula appears as standard guidance in IEEE Standard C57.91 [22] and in IEC Standard 60076-14 [71], and is discussed in more depth later in this chapter. This is the foremost knowledge that pervades the industry on transformer bubbling [80].

$$\vartheta = \frac{6996.7}{(22.454 + 1.4495 \ln W - \ln p_v)} - \left(exp^{0.473W} \left(\frac{\gamma^{1.585}}{30} \right) \right) \quad (2\text{-}26)$$

While [137] studied bubbles using a scaled down system of model coils, [55] went further and reduced the problem to a heated tube wrapped with paper, shown in Figure 2-15. The same conclusion, that moisture has a large influence on BIT is found from the experiments of [55] with BIT reducing for wetter paper insulation. In a related study, [138], the same author shows that the temperature can be achieved through dielectric losses in the insulation, with wetter insulation contributing more to this effect than drier insulation.

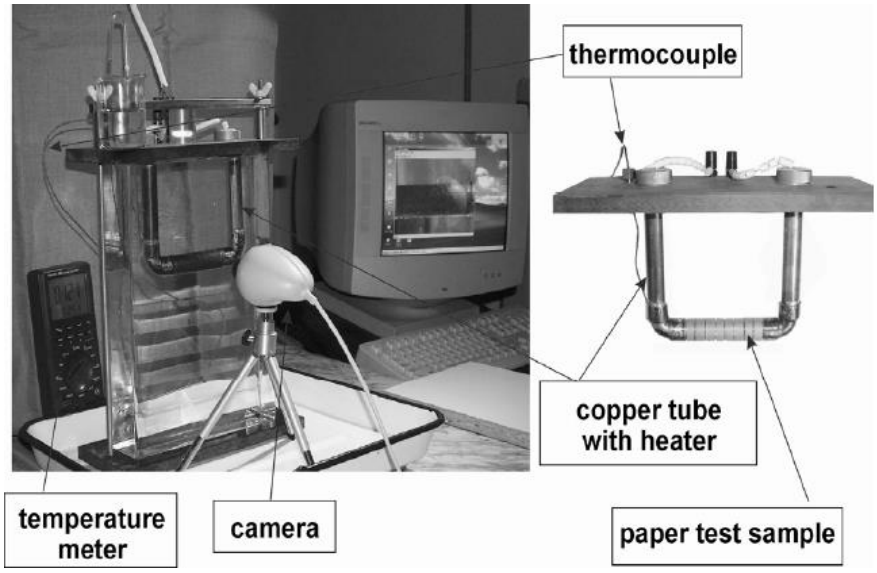

Figure 2-15 – Experimental set-up used in [55].

Evaporation of water from the solid insulation became the main interest of transformer bubbling experiments. In [102] the bonding nature of cellulose and water is described. At approximately 2% moisture by weight, the bonds are weaker van der Waals forces which require less energy to break than the more strongly bonded moisture that forms the initial 2% (approximate value) of moisture in the paper. This concept is used to explain the relationship between water content in paper and bubble inception temperature [102].

The structure of paper is also used to explain the mechanics behind bubble formation in the transformer environment. It has previously been stated [34], and shown [55], that

bubbles tend to form from the winding and not in the bulk oil. How this occurs is postulated by [102] as follows: the cellulosic insulation surface has capillaries across it, the capillaries act as a germination point for bubbles, retaining evaporated moisture and preventing it from simply migrating into the insulating fluid. Once enough moisture is trapped in a capillary it can combine and push out of the capillary as a bubble. This process reduces the energy necessary to form a bubble.

Similar to [55], [102] used a heated tube wrapped with insulating paper to represent the winding conductor. This was immersed in oil within a flask. The set-up is shown in Figure 2-16. The results of the experiments in [102] allowed a BIT formula to be created. The formula takes on a different format to that of [137], and is shown in (2-27) for standard Kraft paper and mineral oil.

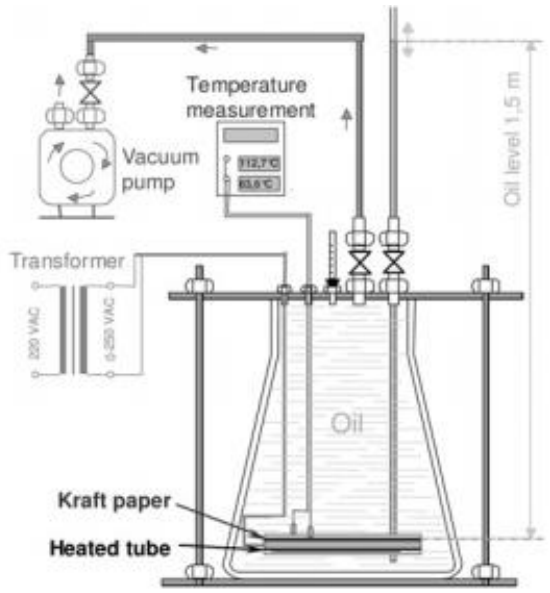

Figure 2-16 – Experimental equipment used in [102].

$$\vartheta = 195.5\mathrm{e}^{-0.11186W} \tag{2-27}$$

Figure 2-17 shows the agreement between the two systems for comparable conditions as moisture content is varied. The oil in [102, 139] is assumed to be gas free (in lieu of any other information) and so a value of 0.0% is chosen for γ in (2-26).

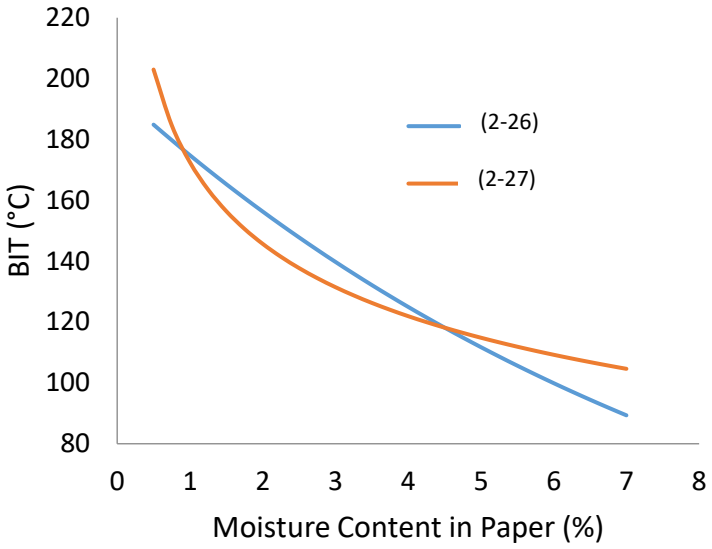

Figure 2-17 – Comparison of BIT prediction at varying moisture content in paper between (2-26) and (2-27), under the same assumed conditions.

A paper by Perkasa et al. returned to the use of a model coil to investigate bubbles formed from transformer insulation [140]. The basis for bubbling is the same as in equation (2-10), but the authors also identify that the oil properties, including moisture capacity, viscosity and other thermal parameters as being influential. The study reinforces earlier knowledge that BIT is coupled strongly with moisture content in paper, but also opens discussion on how the time to bubble inception (tBI) should also be included in analysis. In previous work such as [34] commentary on tBI is provided, but only insomuch as to mention that bubbles do not occur instantaneous to the increasing of load, nor even necessarily to attainment of a certain temperature threshold. The analysis of [140] takes this further and suggests that the oil is being saturated in this period, and so the assumptions of [134, 135] may need to be adjusted. The mathematical models calculate the temperature based on the fluid saturation characteristics, but allow no time for equilibration to occur and so, especially in the non-steady state scenario, the temperature is likely to need to be at or beyond the calculated temperature for some period.

The authors of [140] provide further analysis in [33] where tBI is plotted against moisture content of paper. This data shows a similar result as with BIT – increasing moisture content in paper not only reduces BIT, but also reduces tBI.

Perkasa also introduced the idea of a two-stage mechanism for bubble formation, with a stark change in gradient of the BIT versus moisture content in paper plot at approximately 2% [33]. In the area where the paper insulation is drier, the BIT reduces rapidly with

increasing moisture, whereas for wetter paper, the gradient is gentler. This could imply that a change in the mechanism is at play, and this could possibly be linked to the nature of the moisture-paper bonding, as suggested by the discussion on bonding in [102].

The most recent work published in this area is by Gao et al. [141]. Pictures are presented in their report which clearly shows the location of bubble formation within the experiment, being the overlap point of the outer wraps of the paper. This is concordant with images in [55, 102] and also aligns with the physical description of [102] which suggests that capillaries are conducive to bubble formation. The presence of a site for the bubble to attach to during the initial stage reduces the energy requirement for formation and encourages growth of the bubble [128].

Further bubbling investigation in [141] considered the effect of multiple successive overload scenarios. It was found that in each subsequent overload, the BIT increased. The reasoning is that the earlier overloads had dried out the paper (and there was not sufficient time between overloads for remoistening) and so the BIT accorded to the 'new' moisture content in paper. This is an important result – not only does it imply that the transformer becomes more resilient to failure through [moisture] bubbling in successive overloads, it also shows that the drying of paper due to higher prior transformer operating temperature affects BIT. Indeed, the mal-distribution of moisture across the solid insulation due to the existence of a temperature profile [68] means that bubbles may be less likely to occur at the HST (considered to be the location of the driest solid insulation) than at another location which is wetter, such is the link between moisture content in paper and BIT.

This outcome can be problematic to the design of experiments. The temperature measurement in all of the experiments considered so far has been the HST. This is the easiest, and arguably most sensible, temperature with which to describe the behaviour of the system, even with regard to bubbling. However, an understanding of the temperature and moisture profiles of the paper insulation are also desirable such that when describing a bubble event as occurring at a given temperature, the reality is not obfuscated by such a description. Hence, average or single moisture values, and HST figures should be treated with the necessary caution. Due to the temperature at the HST and its locale however, it is still considered most prudent to use this as the location of measurement in bubbling experiments.

The five studies mentioned in this section which have investigated bubble inception for systems of standard Kraft paper and mineral oil used a variety of experimental techniques,

and comparison of their experimental apparatus can provide an insight into differences seen between the outcomes. Table 2-3 provides an overview of the experimental equipment and methods used by each research team.

Table 2-3 – Selected features of different bubbling experiments.

Feature \ Researchers	Oommen & Lindgren [137]	Przybylek [55]	Koch & Tenbohlen [102]	Perkasa et al. [33]	Gao et al. [141]
Heating source	Coil	Heater within Copper Tube	Heated Tube	Coil	Heater within Copper Tube
Oil:paper ratio	Not Stated	Not Stated	Not Stated	212:1	1276:1
Moisture in paper range (%)	0.3 – 8.0	1.46 – 6.98	1.1 – 5.1	1.0 – 6.0	1.5 – 5.5
Gas in oil content range (%)	0.45 – 12.3	Degassed (assumed)	Gas saturated	Degassed	Degassed
Number of paper layers	Not Stated	1 (assumed [54])	4	4	2
Temperature rise technique	Rapid initial increase in temperature	Not Stated	Varied rates of temperature rise (2, 3 & 6 K/min)	Step change in current (100% → 163% 'rated' value)	Varied rates of temperature rise (2 - 16 K/min)
Monitoring technique	Partial discharge / visual	Visual (camera)	Visual (video recording)	Visual observation	Visual (high magnification camera)

2.6.4 Considerations beyond Moisture and Gas Content

There are more parameters to consider than simply the amount of moisture and gas within the insulating solid and insulation fluid. This section of the report addresses several key parameters which have been given less coverage, but can have a great influence on the BIT. They may also provide some explanation for discrepancies seen in temperatures among the current studies as in Table 2-3.

2.6.4.1 Effect of Paper Insulation Age

A key consideration has been found to be the age of the paper, described through the DP value of the paper. DP describes the average number of cellulose monomers per chain in the solid insulation. This decreases over time due to the natural ageing processes which have already been described above. Change in DP is important to BIT for several reasons: it affects the number and distribution of capillaries / pores on the paper surface, it influences the hydrophilicity of the paper, it can change the ratios of cellulose:hemicellulose:lignin and crystalline:non-crystalline regions, existence of [polar] impurities (degradation products) can reduce the energy for bubble inception and provide nucleation sites, and indeed the degradation of paper itself will generate moisture.

There has not however been a clear outcome from the investigations into the effect of paper insulation age on BIT. Two studies, [55] and [102] looked into this phenomenon. Both compared new paper to aged paper and found different responses for BIT: [55] found that BIT reduced with ageing; [102] found the opposite.

From [55], formulae are presented akin to (2-26) (albeit without the second term, a gas free system is thus presumed). Below the equations for new paper (DP = 1357) and aged paper (DP = 341) are shown in (2-28) and (2-29) respectively.

$$\vartheta = \frac{10880}{(30.544 + 3.156 \ln W - \ln p_v)} \tag{2-28}$$

$$\vartheta = \frac{16210000}{(3.747 + 4497 \ln W - \ln p_v)} \tag{2-29}$$

Evidently there is a huge change in the mathematical description of the data between the new and aged cases, with big differences in coefficients. The decrease in BIT is explained by [55] as being related to the decrease in moisture sorption capacity of the aged paper, indicating that moisture is less strongly bound in aged paper. The reason for this might be that the locations for moisture to bond to paper are taken up by other species, or that the bonding sites are themselves destroyed through the ageing process.

A lower affinity for moisture (lower hydrophobicity) means that an increase in temperature can drive out the moisture from the paper more easily than in new paper at the same moisture content, leading to bubbles forming at lower temperatures. Reference [50] provides counter-evidence that moisture can be bonded even more strongly to paper by the presence of some degradation products, such as acids. This could also be affected by the selection of liquid impregnant.

The author of [55] also publishes results of the impact of paper ageing on BIT in [54]. The data shows the results for four DP values (representing different stages of the insulation lifetime) and there is a consistent trend of BIT reducing with age for the same value of moisture content in paper. This is strong evidence for the argument that ageing of transformer insulation reduces BIT. The original work is reported to come from [142] although an English language version is not available to this author and hence details are omitted herein.

One potential reason for the difference in trend between [55] and [102] is that in [102] the paper ageing process was done at high temperature (130°C) and a high relative humidity

(RH), close to 100%, and this may have led to hornification of the paper. This difference in the ageing mechanism can affect how the paper holds moisture and should mean that results are treated with caution.

More work is needed in this aspect of BIT. The ageing of paper is a natural process, and description of moisture content is valuable, but wet paper is rarely new paper. Therefore being able to describe the BIT in terms of the moisture content of paper and the DP of the paper seems to be a prerequisite for an accurate BIT prediction. In [137] (which established (2-26), the formula used in the current standards) the change of age of the paper was not considered when changing the moisture content, even as far as 8% which is an extreme condition even for an aged transformer. The moisture content in paper of a transformer is considered 'dry', 'wet' or 'excessively wet' by IEEE Standard 62 [143], based on the ranges shown in Table 2-4.

Table 2-4 – Transformer moisture classifications [143].

Classification	Moisture Range
Dry	0 – 2.0%
Wet	2.0 – 4.5%
Excessively Wet	> 4.5%

A further complication when considering the impact of solid insulation age is that the transformer solid insulation does not age uniformly, due mainly to the non-uniform temperature profile over the height of the windings [23, 139]. This uneven temperature profile means that the ageing profile also competes with uneven moisture distribution [68] leading some studies to suggest that the location of the HST may not be the primary source of bubbles, and, while bubbling is an undesirable situation for a transformer to operate under, the fact that moisture is released from paper is a positive factor for reduction in ageing [144].

2.6.4.2 Effect of Liquid Insulation Age

Not only the age of the paper insulation, but also the age of the liquid insulation is assessed in [102] which compared a virgin mineral oil (Shell Diala D, total acid number (TAN) = 0.016) against a service-aged mineral oil (Shell K 6 SX from a transformer put into service in 1965, TAN = 0.48). The age of liquid insulation can be variously described through its acidity value, its dielectric dissipation factor, or its interfacial or surface tension value, among others [108, 145, 146]. The acidity is used in [102], but from analysis presented above (e.g. equation (2-18)), the surface tension is an important factor when considering bubble formation.

The findings of [102] showed that ageing of liquid insulation reduces the BIT. Figure 2-18 shows the comparison, and an average difference of 14 K is observed across the full range of moisture content tested.

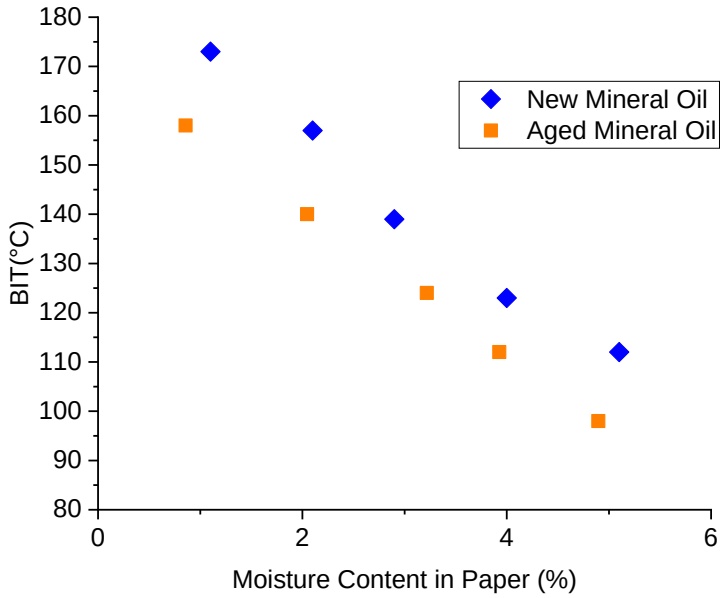

Figure 2-18 – Comparison of BIT for NTUP with new mineral oil versus NTUP paper with aged mineral oil [102].

That the BIT reduced when acidity increased is expected, but does not describe the reason for this. Some of the acid from the oil is likely to have migrated into the paper and this may have reduced the energy needed to desorb moisture from the paper. Also important is that the presence of acids will have reduced the surface tension of the oil, and this will also have reduced the energy requirement to generate a bubble. Interestingly, the moisture capacity of oil increases with age [147] (in [102] it is approximately triple the capacity of the new oil). This would be anticipated to increase the BIT as more moisture can move from paper to oil. It is likely that both of these factors, and more besides, are involved in behaviour witnessed and the interplay of all factors may be difficult to isolate.

2.6.4.3 Effect of Dissolved Gas Content

Early mathematical models considered dissolved gases to be the primary factor influencing BIT, with some attention given to products of cellulose degradation and to evaporation of moisture [134, 135]. In [137] however there is a shift to moisture being the main bubble source. From the results of experiments shown in [137], reproduced in Table 2-5, there are several BITs that are significantly below 100°C [shown in **bold type**]. The low temperature bubble results are all from experiments with relatively high gas content which

suggests that the bubbles in these tests could be formed from dissolved gases rather than evaporating water.

Table 2-5 – Results of BIT tests from [137] showing test conditions (moisture content in paper and gas content in liquid), the observed BIT, and the predicted BIT based on (2-26). Test results shown in bold are below 100°C.

Test Number	Test Conditions	Observed BIT	Predicted BIT	Test Number	Test Conditions	Observed BIT	Predicted BIT
	C (%), γ (%)	°C	°C		C (%), γ (%)	°C	°C
1	0.3, 0.45	220	224	14	4.0, 8.80	110	113
2	0.3, 1.48	215	215	15	3.0, 1.00	130	130
3	0.6, 8.15	209	191	16*	5.0, 1.00	109	111
4	0.5, 9.95	209	192	**17**	**8.0, 1.00**	**99**	**98**
5	0.4, 9.68	204	209	**18**	**8.0, 7.70**	**60**	**64**
6	0.4, 11.0	209	209	**19**	**8.0, 8.80**	**55**	**53**
7	0.4, 12.3	211	208	20	4.1, 1.00	122	119
8	1.5, 1.90	158	153	21	5.7, 1.00	110	108
9	1.1, 9.70	160	164	**22**	**5.9, 8.80**	**90**	**91**
10	2.3, 9.70	131	134	23	3.1, 8.80	128	124
11	1.6, 1.56	152	151	**24**	**5.3, 8.80**	**93**	**98**
12	1.6, 9.73	158	149	**25**	**7.8, 8.80**	**60**	**58**
13	1.0, 8.80	166	168	26	2.8, 8.80	132	128

*The moisture content for test 16 is given as 3.0 in [137] but calculation suggestions that the true value is 5.0, as shown here.

That there are results far below 100°C (as in tests 18, 19 and 25) indicates that a distinction between different bubble inception mechanisms could be necessary. High gas content in liquid appears to be difficult to fit for, by splitting the tests into 'high gas content' tests (above $\gamma = 2.0\%$) and 'low gas content' tests (below $\gamma = 2.0\%$) and then averaging the difference between the observed and predicted results the low gas content tests fit better (average deviation of 2.0 K for low gas content versus average deviation of 5.1 K for high gas content).

As already shown in Figure 2-14, increased gas content in liquid can reduce BIT for the same moisture content in paper. A greater amount of gases dissolved in the oil increases the partial pressure, making it more likely that evaporated moisture can form a bubble. Therefore gas content in liquid is a factor that should be accounted for in BIT studies;

experimenters should be clear however as to which bubble formation mechanism is under study, and a catch-all formula may not be realistic to achieve.

No other study to date has looked into the influence of gas content on BIT in any great detail. Figure 2-14 shows that based on the BIT predictions of (2-26) gas content becomes more influential at higher moisture contents, and as the likely transformer moisture range is low, starting at 0.5% [124] and ending around 4.5% (per description in Table 2-4), the impact of gas content in liquid is mitigated and further study may only be of secondary, or even tertiary importance.

2.6.4.4 Effect of Rate of Change of Temperature

Comment has been made above that the calculations carried out in some studies assume an instantaneous generation of bubbles once certain criteria are met, or that steady state conditions are experienced for a prolonged period. Long term stable conditions are rare within a transformer, especially when considering overload situations. It has been found by some studies such as [102, 141] that not only the achievement of certain criteria is important for understanding bubbling, but so too is the manner in which those criteria are attained.

The main concept investigated is the rate of change of temperature (RoCoT). The RoCoT varies based on the final load, the difference in initial and final loads, the thermal mass of the system, the materials used, the environmental conditions, and for a multitude of other reasons. One of the difficulties in defining the RoCoT is that the temperature response to load is non-linear.

In the scenario of a transformer operating in the real world, there are two ways in which the load may increase. Either it can rise in a stepped manner, for example as the result of a failure of a parallel transformer, or it can rise more gradually in response to increasing demand (in the UK this rise is often seen in the evenings, as shown by the ‘base final’ loads in Figure 2-19 [148]).

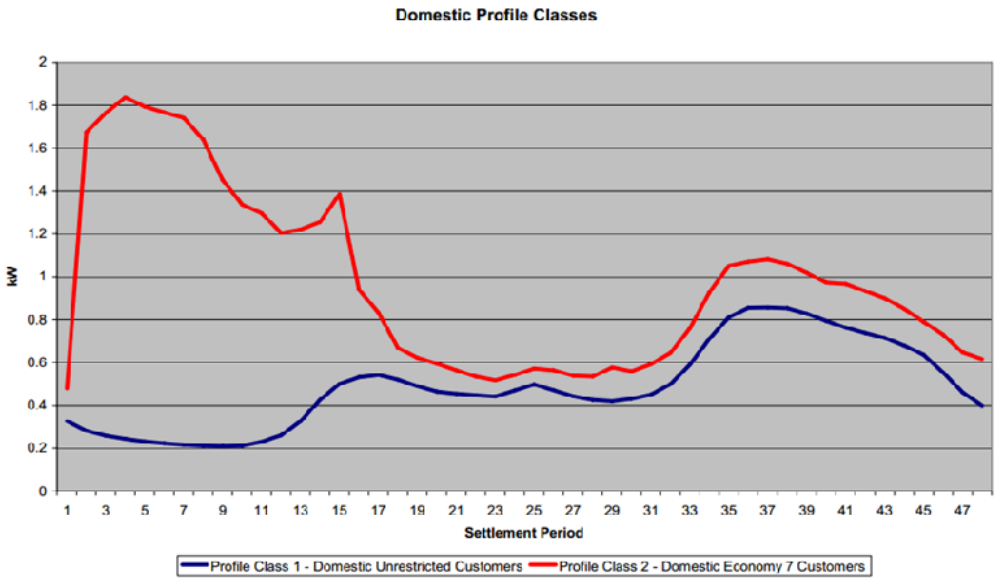

Figure 2-19 – Daily load profiles of domestic customers (in kW) based on ELEXON data [148].

It has been shown by [102] and [141] that a greater RoCoT generates bubbles at a lower temperature than at a lower RoCoT when all other parameters (especially moisture content) remain the same. Figure 2-20 shows the trends from both studies. Both lines appear to approach an asymptotic value, although it is not possible to conclude the existence of a minimum temperature / maximum RoCoT from this data.

Interestingly, despite being the wetter of the two samples (5.4% moisture content in paper versus 5.1% moisture content in paper), [141] has higher BIT, although the two datasets appear to converge as RoCoT increases. This implies that different systems can have different BIT values.

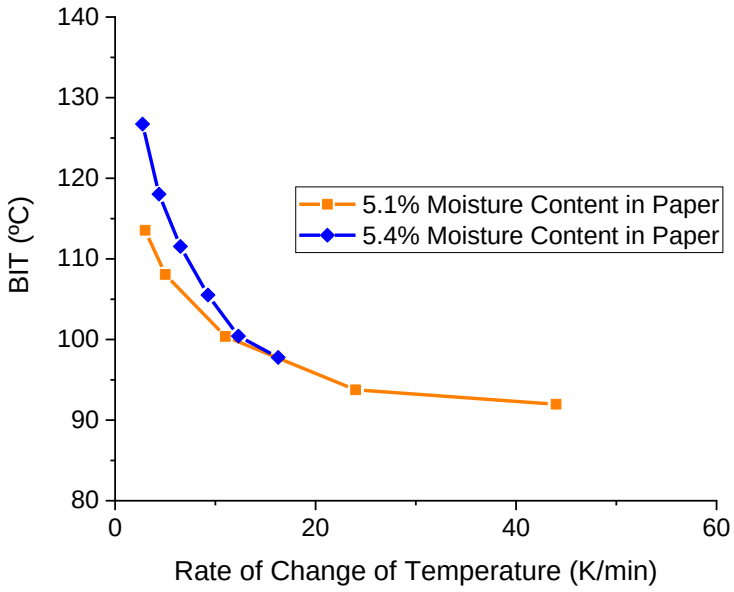

Figure 2-20 – BIT vs RoCoT from [102] (5.1% moisture content in paper) and [141] (5.4% moisture content in paper).

Reference [102] concluded that '*Only a steep temperature increase causes bubble emissions (>3 K/min).*' and suggested that for RoCoT lower than this value the moisture does not form a bubble, but rather it migrates into the oil. As with absolute temperature, the setting of a value to suit all systems should be treated with caution. Przybylek conducted experiments in [55] with a RoCoT of 2 K/min, theoretically no bubbles should have occurred based on the limit set in [102], but this was not seen to be the case because bubbles did form.

Based on Figure 2-20, it could be presumed that the RoCoT is a determiner between experiments – greater RoCoT should result in a lower BIT. Figure 2-21 shows the results of BIT against moisture content in paper from [55] (in red), [102] (in green), and [54] (in blue). These results represent 2 K/min, 3 K/min and 6 K/min respectively.

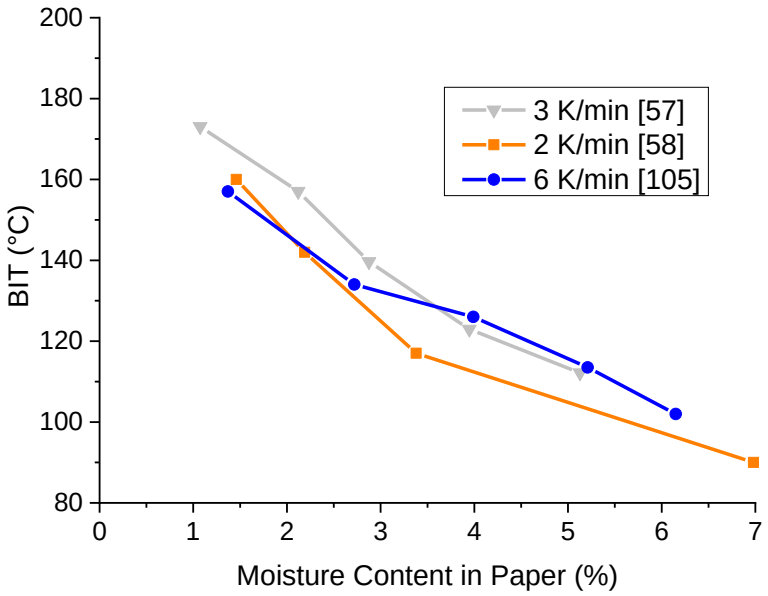

Figure 2-21 – Comparison of BIT results varying with moisture content in paper for different RoCoT [54, 55, 102].

As can be seen, the BIT and the RoCoT do not accord with the findings of [102, 141] that a higher RoCoT causes lower BIT, in fact there is no discernible relationship between these two factors. It is likely that the results shown in Figure 2-21 are accurate, but their validity is limited to being system-specific. Thus it would be incorrect to state that there is certain RoCoT required for BIT, and more investigations into this area should be carried out before further deductions can be made.

2.6.5 Alternative Paper Insulation Studies

The type of solid insulation is a consideration which has not received enough attention in bubble formation studies. The work of [137] and [102] make it clear that the paper surface and the moisture content in paper are key to the understanding of bubbling within transformers. This is further supported by [55] and [102] who link the ageing condition of the paper to the BIT.

Therefore, one would expect that different types of solid insulation would have different BIT performance. Two studies have delved into this concept: [102] compared standard Kraft paper with a TUP; [54] contrasted the performance of standard Kraft paper to Aramid insulating paper. Chemical treatment with compounds containing nitrogen is normally used to upgrade the insulation [43, 46, 50]. The addition of nitrogen has been stated as the reason for the reduction in hydrophilicity of the insulation.

The BIT for TUP in [102] showed the same behaviour as standard Kraft paper in that higher moisture content resulted in lower BIT. However, the gradient of the trend is steeper for TUP, as shown in Figure 2-22.

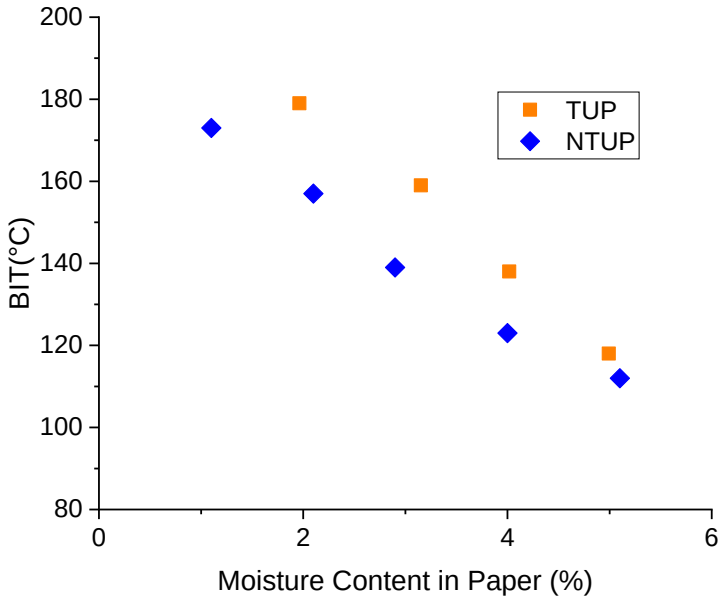

Figure 2-22 – BIT comparison between TUP and NTUP with varying moisture content in paper [102].

If the RS of the paper insulation is used instead of the moisture content, the BIT is always higher for TUP (Figure 2-23). The reduction of BIT with increased RS is also less severe for TUP than standard Kraft paper in these experiments [102].

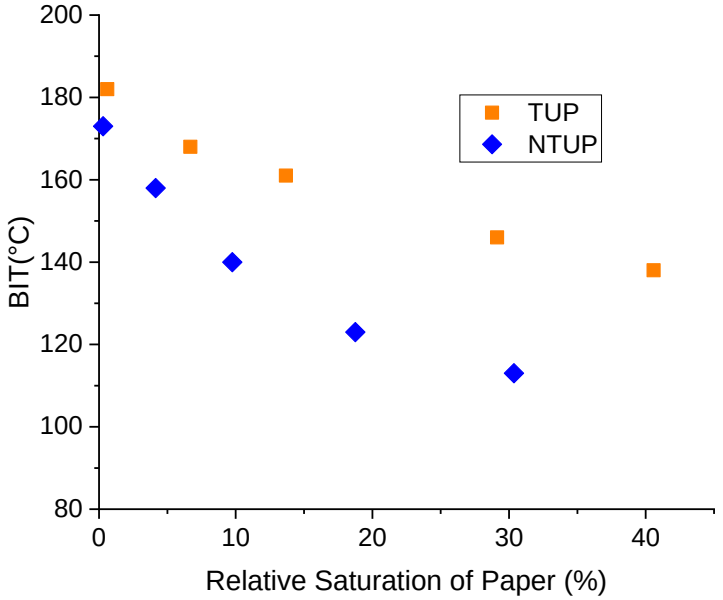

Figure 2-23 – BIT Comparison between TUP and NTUP with varying relative saturation of paper [102].

The affinity for water of Aramid insulation is also shown to be lower than standard Kraft paper in [54]. From Figure 2-24, the shape of the curves for standard Kraft paper and

Aramid paper are similar, with Aramid paper showing the lower BIT. The difference is quite significant (approximately 18 K). However, the use of RH [of the environment that paper is conditioned in] in place of moisture content of the paper brings the BIT of the materials much closer together, as per Figure 2-25. As, under the same environmental conditions, Aramid paper will contain less moisture than standard Kraft paper, and as Aramid insulation generates less moisture through its decomposition at the same point in the transformer life, it is not necessarily appropriate to compare the two materials at equivalent moisture content.

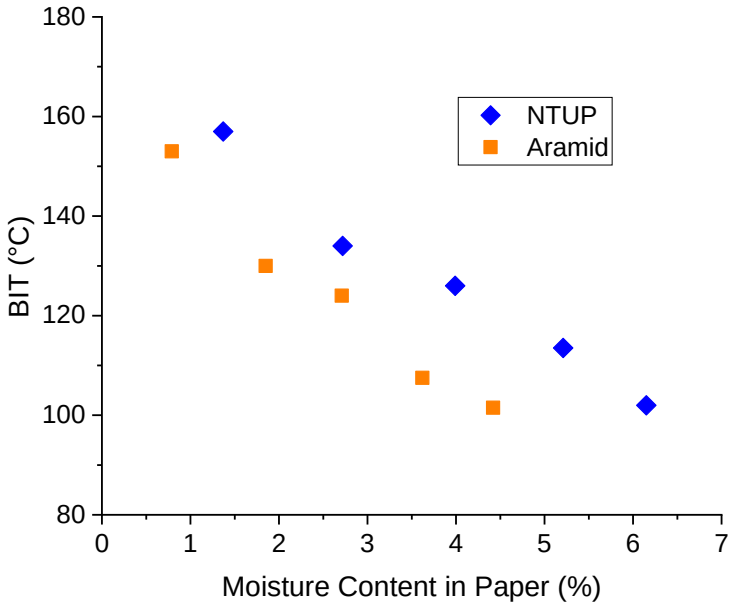

Figure 2-24 – Comparison of BIT for NTUP and Aramid paper with varying moisture content [54].

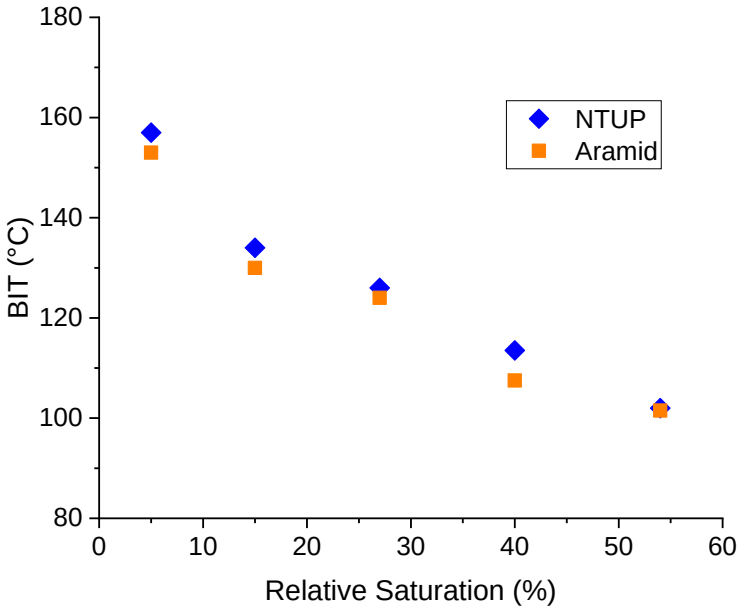

Figure 2-25 – Comparison of BIT for NTUP and Aramid paper with varying RH [54].

It is not possible to draw definitive conclusions from the studies conducted on different paper insulation materials. The two main studies have shown conflicting results [54, 102].

One outcome from both studies however is that not only the moisture content of the paper on a mass of moisture per mass of dry paper basis, but also the RS of the paper can provide insight into the relative bubble inception performance of insulation materials.

2.6.6 Alternative Liquid Insulation Studies

Traditionally, mineral oils are used as the insulating fluid within a transformer. When new, mineral oil is a poor solvent for water and acids [50, 149]. As the oil becomes aged, both the acidity and moisture capacity are seen to rise [124]. However, water has much greater solubility in alternative oils such as synthetic and natural esters, and these insulating fluids commonly test as more acidic [31, 150]. Some authors have postulated that the increased solubility of water in an insulating liquid may influence the BIT as more moisture can be dissolved into the oil during the overload, thus preventing any bubbles from forming [105, 124].

Different fluids also differ in their surface tension. As has been shown by equations (2-11) and (2-18), the surface tension is a key parameter in determining the energy required to form and maintain a bubble. This therefore has been another reason proposed by some researchers that would predict different BIT for bubbles evolved from solid insulation when the liquid insulation changes [102, 140].

Other properties of the insulating fluid that can be considered important to the BIT are the thermo-physical properties such as density, thermal capacity, viscosity and thermal conductivity, and how these properties change with temperature. These parameters are worthy of consideration because they affect the cooling performance of the transformer, and so the same energy input (i.e. the same losses in the winding) leads to different temperatures (including the HST) with different fluids [151, 152].

Variation of BIT between oil types has been covered in two studies. The first of these compared a mineral oil with synthetic ester [153]. The findings indicate that synthetic esters have a higher BIT than mineral oil at the same moisture content in paper. The author attributes this to the greater polarity of synthetic esters compared to mineral oils which results in a stronger bonding between the moisture and oil-impregnated paper before the overload, hence more energy is needed to desorb moisture [153]. It is also mentioned that the increased moisture solubility of synthetic ester over mineral oil allows more moisture to desorb before the partial pressure increases sufficiently to form a bubble [153]. The study is

limited to moisture content in paper values of 3% and above, and this makes a full assessment difficult.

An elevation of BIT was also witnessed for a natural ester compared to a mineral oil (Diala B) in [33]. The temperature difference ranged from 6-13 K, with the temperatures appearing to diverge as moisture content in paper increased, as seen in Figure 2-26. The same two-stage behaviour of a drastic change in gradient at approximately 2% moisture content in paper is seen in both fluids.

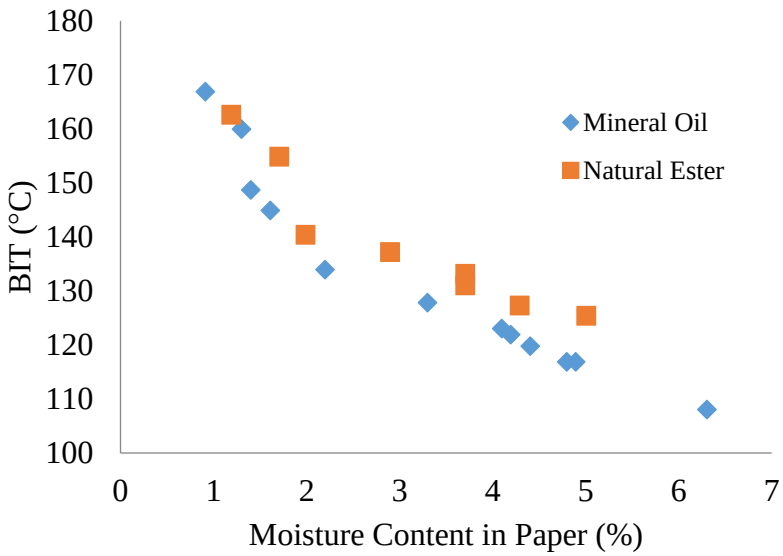

Figure 2-26 – BIT comparison between mineral oil and natural ester [33].

A seemingly contradictory result is that the tBI between the two oils is similar [33], as shown in Figure 2-27. The significance of this is that the same amount of energy is applied to the system in both cases (the test method is to apply a constant overload of 260 A to the winding). Therefore it can be concluded that the difference in temperatures is not due to a higher temperature requirement, but rather the same energy input resulting in a higher temperature in the natural ester in this system. The authors of [33] quote the kinematic viscosity and the density as probable parameters of influence here, and also quote [154] which lists thermal conductivity, specific heat capacity and viscosity as the factors which govern the performance of a fluid as a coolant.

From the data of these studies into bubble formation with alternative fluids, the consensus appears to be that higher BITs are seen when using alternative fluids (esters) compared to mineral oil. The reason behind this is most likely to be due to the different

cooling performances of these fluids, rather than any inherent bubble retarding abilities, nor even due to their increased capacity for moisture, although this cannot be ruled out entirely.

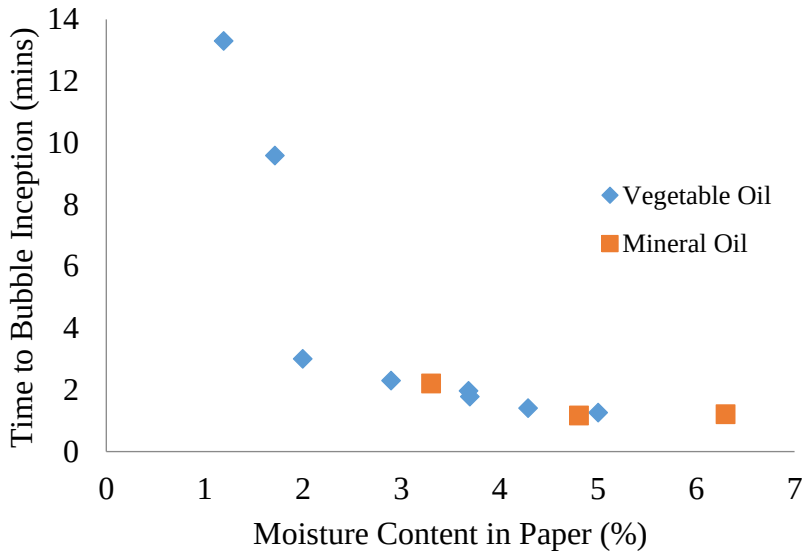

Figure 2-27 – tBI inception comparison of mineral oil and natural ester [33].

Further work looking at the bubble formation performance (e.g. BIT and tBI) would be welcomed for alternative fluids. Indeed, the usage of alternative insulating fluids is becoming more prevalent [85], and the improved thermal, safety and environmental performance is often quoted as a key differentiator for these products [85, 101, 140, 155]. No studies have yet been conducted into the performance of GTL oils, and this should also form part of future investigations.

A summary of the reasons that previous authors have proposed for the observed differences in BIT between insulating liquids are given below:

2.6.6.1 Polarity of the Liquid Insulation

Ester liquids have a higher polarity than mineral oils, and resultantly they have a higher attraction for water molecules. The ester liquid used in [153] was seen to have a higher temperature for bubble inception than the mineral oil. It is suggested that the liquid which is impregnated in the paper insulation plays a role in restricting the release of moisture molecules from the paper. As ester liquids have a higher affinity for the water, greater energy (and thus higher temperature) is needed to release the water molecules when esters are used compared to when mineral oil is the insulating liquid.

2.6.6.2 Moisture Capacity of the Liquid Insulation

An alternate theory based around the polarity of the liquid insulator suggests that as more polar liquids can hold more moisture, the formation of bubbles is retarded when they are used. The idea is that as the moisture is released from the paper with increasing temperature it is absorbed and carried away in the liquid, thus preventing any bubbles from forming. This concept was introduced in [105].

2.6.6.3 Different Thermal Characteristics of the Liquid Insulation

In [33] it is pointed out that mineral oils and natural esters have different thermal characteristics. The discussion focused on the viscosity of the two liquids, with the ester showing a much higher kinematic viscosity (8 mm^2/s versus 2 mm^2/s, at 100°C) than the mineral oil. Viscosity affects cooling performance of the liquid [73], particularly in naturally cooled systems (systems where the fluid moves via buoyancy rather than mechanical means). Hence, different values of viscosity (and other thermo-physical properties) will result in different temperature response to the same energy input.

2.6.6.4 Surface Tension of the Liquid Insulation

Literature, including [102], clearly describes the pressure balance required for a bubble to exist within a medium. Equation (2-10) clearly shows this balance. Note the role of the surface tension in this balance; it represents the additional energy per surface area that needs to be generated to maintain the bubble. Thus liquids with different surface tension can be expected to perform differently in respect to their tendency to form bubbles. This has only been investigated through [102] by comparing aged mineral oil which has a comparably higher acidity than new oil, and it is assumed that his has a consequent influence on its surface tension. Indeed, the aged oil showed a reduction in the bubble inception temperature however it is not conclusive that this is due to the reduction in surface tension (or indeed that there even was such a reduction).

It is clear then that there is not a complete understanding of why the selection of liquid insulator affects the BIT. Any of these reasons, or an interplay of some (or even all) of the proposed mechanisms could be the reason for the variation in BIT seen in these studies.

2.6.7 Bubbles from Different Sources

2.6.7.1 Bubbles Caused by Other Gases Generated in Insulation

From the works conducted since the turn of the millennium, the most important factor in the transformer bubbling phenomenon has been identified as the moisture content of the paper insulation. Therefore the bubbles that form are generally considered to be either wholly or primarily water vapour.

Heinrichs established through chemical analysis that other gases can contribute to the bubble. He found that hydrocarbon materials can be generated and released from cellulose-mineral oil insulation systems at high temperatures when the test was conducted in a low moisture environment [131]. Gao et al. also witnessed this [141]. Theoretical analysis also confirms that the pre-existence or the evolution of such material can generate bubbles under the right thermal conditions [134]. The fact that bubbling which occurred at temperatures around 160°C during ageing tests in [144] led to a reduction in the paper ageing rate, strongly suggesting that the bubbles were, at least mostly, formed of water, even at relatively high operating temperature (reduction of paper water content is likely to reduce the ageing rate by slowing the hydrolysis reaction, whereas release of other gases due to paper decomposition would not be expected to lead to a similar reduction in ageing rate).

2.6.7.2 Bubbles Caused by Cooling Transformers

Generally, work conducted in recent years has been focused on the generation of bubbles in transformer insulation through elevated temperatures. Bubbling can be brought about from reduction in temperature, as investigated experimentally in [122] and shown mathematically in [134]. Bubbles formed this way are likely to be the blanket gas / atmospheric gases, or dissolved gases formed as by-products of ageing processes. There have not been any defined criteria set to prevent bubbling through this mechanism.

2.6.7.3 Bubbles Formed by Hot Metal in Contact with Liquid Insulation Only

A feature of the studies in [33, 102, 153] is that they only considered the systems with paper insulation involved. Previous studies have shown that BIT is strongly coupled with the water content of the paper insulation, and so comparing the influence of liquid insulation type in this situation is important and useful. However, IEC Standard 60076-7 also provides guidance on loading for situations of metal surfaces in contact with mineral oil only: short-time emergency loading (30 minutes) has a maximum allowable temperature of 180°C

(contrast 140°C where cellulosic insulation is present) [23]. Within available literature, only [133] appears to have considered bubbling directly from high temperature metal in contact with insulating liquid. A temperature range much higher than 180°C was used in [133] (250 – 350°C), producing no visible gas bubbles. However, only one liquid was tested, presumably mineral oil but termed 'transformer oil', and only at one condition.

2.6.7.4 Free Water Formation Caused by Cooling Transformers

Bubbles within transformer liquid insulation are dangerous as they reduce the dielectric strength of the insulation and this can lead to failure, as explained above. Another concern is the formation of 'free water', i.e. water that is not dissolved in the oil but forms a distinct phase [147], sometimes described as the 'emulsion state', as in [156, 157]. Water of this form can lead to dangerous flashover events. While the dielectric strength of water is higher than that of vapour, it is still lower than the insulating fluid [90]. Formation of a free water phase within a transformer can be more likely to cause failure as it is likely to prevail for a longer period than bubbles (which collapse or move into the head space), and as the water can be a continuous phase (distinct from the insulating liquid) it has higher likelihood of contacting two conducting points than does a stream of bubbles.

Free water can be brought about by rapid external cooling of the oil whilst the transformer remains energised. When the conductors of the transformer run hot, moisture is forced out of the solid insulation and into the liquid insulation. The liquid insulation has limited capacity for moisture (especially in the case of mineral oils), but this capacity increases with temperature. Figure 2-28 shows how the solubility of water in a mineral oil and a natural ester rise dramatically with increasing temperature [105].

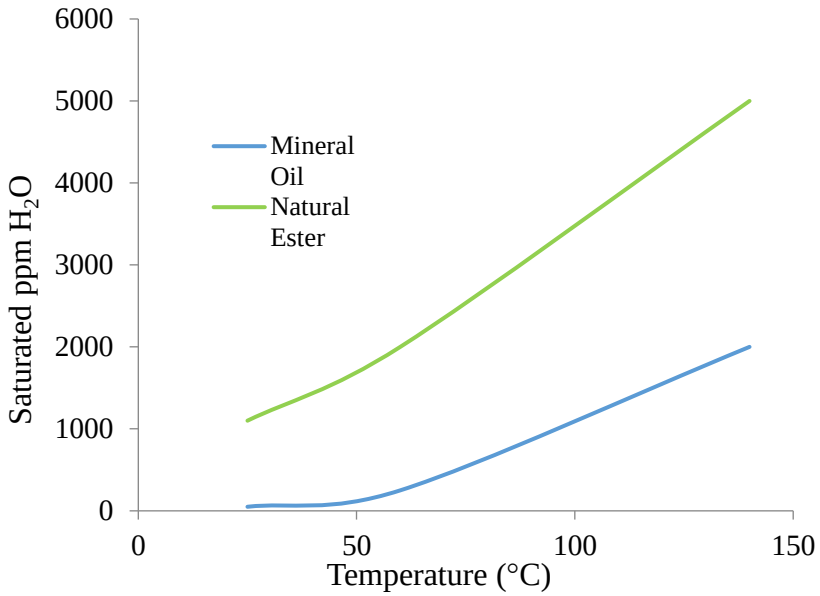

Figure 2-28 – Saturation limits of mineral oil and natural ester, variation with temperature [33].

Free water can thus occur when the insulating liquid is at or near to saturation and its temperature is decreased rapidly. When the temperature reduces quickly (especially when the conductor, and so too the solid insulation, temperature is kept high), the moisture cannot return to the solid insulation fast enough, and so it precipitates out of the insulating fluid into a distinct phase. The rate of diffusion of moisture from liquid to solid insulation is slower than the reverse under conditions of similar temperature behaviour [149, 158], and is only worsened by the scenario described here. However, during experiments of this nature, [122] does not report any free water formation. In contrast, [33] saw water droplets forming as temperature continued to increase after generation of bubbles was witnessed.

2.6.8 Bubble Inception Formula

As seen in equations (2-26) – (2-29), previous researchers have attempted to predict BIT through formulae. Finding an accurate and comprehensive formula is something of a holy grail, and as seen throughout this literature review, there are many factors which must be accounted for when estimating the temperature a bubble will form at within a particular system. Any successful formula(e) should account for the moisture content in paper, the insulation materials and their age, the transformer loading situation, the cooling set-up, and more factors besides.

The most widely utilised formula currently is (2-26) from [137] found in both [22] and [71], which is re-presented below. The formula consists of two parts. The quotient of

the first term is based on work from [135]. The latter term is a fitted factor to correct the formula to the experimental data of [137].

$$\vartheta = \frac{6996.7}{(22.454 + 1.4495 \ln W - \ln p_v)} - \left(exp^{0.473W} \left(\frac{\gamma^{1.585}}{30} \right) \right) \quad (2\text{-}26)$$

There is an error within this formula however. Considering the fit of the formula to the data of [137] (i.e. Table 2-5), it is not surprising to find that there is good agreement. However, when considering the physics behind the system, the error (followed through from [135]) becomes obvious. Reporting just the value calculated by the first term provides the comparison in Table 2-6.

Plotting the data from [137], as the difference between experiment and estimation from Table 2-6 for each experiment as in Figure 2-29, it can be seen that the formula commonly over-predicts the temperature (a negative value for the difference) when using only the part of the formula built from rearrangement of moisture concentration. This is clearly nonsensical – essentially showing that it requires more energy to desorb moisture than it does to desorb it as a bubble. It has already been shown (e.g. in (2-18)) that there is an energy 'cost' associated with maintenance of a bubble (related to surface tension) and so the energy for desorption as a bubble must require extra energy.

Situations where the formula under-predicts the temperature significantly tend to be those with high gas content in oil, which skews the outcome, and as identified above, bubbles in this situation may be formed through different mechanisms than ebullition of moisture.

Table 2-6 – Results of BIT tests from [137] showing test conditions (moisture content in paper and gas content in oil), the observed BIT, and the predicted BIT based on only the first term of (17).

Test Number	Test Conditions	Observed BIT	Predicted BIT	Test Number	Test Conditions	Observed BIT	Predicted BIT
	W (%), γ (%)	ºC	ºC		*W* (%), γ (%)	ºC	ºC
1	0.3, 0.45	220	224	14	4.0, 8.80	110	120
2	0.3, 1.48	215	215	15	3.0, 1.00	130	130
3	0.6, 8.15	209	192	16*	5.0, 1.00	109	96
4	0.5, 9.95	209	193	17	8.0, 1.00	99	100
5	0.4, 9.68	204	211	18	8.0, 7.70	60	101
6	0.4, 11.0	209	211	19	8.0, 8.80	55	99
7	0.4, 12.3	211	210	20	4.1, 1.00	122	119
8	1.5, 1.90	158	153	21	5.7, 1.00	110	109
9	1.1, 9.70	160	166	22	5.9, 8.80	90	108
10	2.3, 9.70	131	138	23	3.1, 8.80	128	129
11	1.6, 1.56	152	151	24	5.3, 8.80	93	110
12	1.6, 9.73	158	152	25	7.8, 8.80	60	100
13	1.0, 8.80	166	170	26	2.8, 8.80	132	132

*The moisture content for test 16 is given as 3.0 in [137] but calculation suggestions that the true value is 5.0, as shown here.

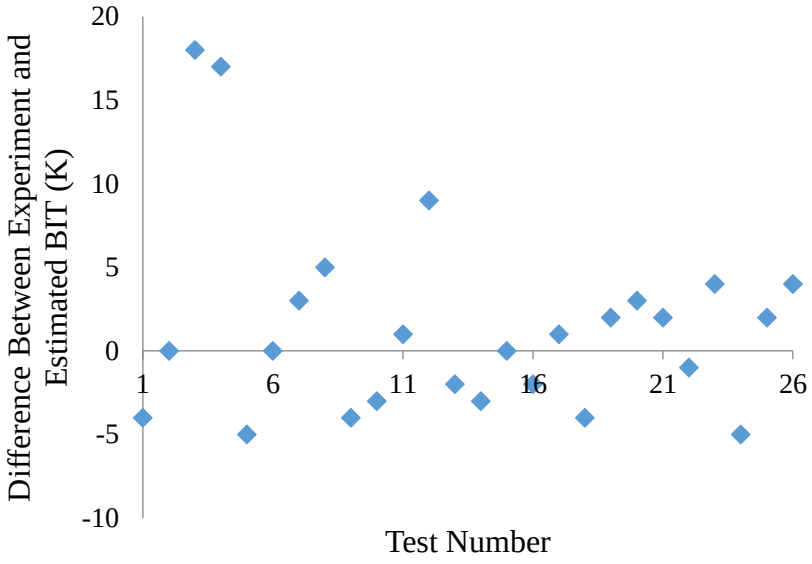

Figure 2-29 – Difference between experimental and estimated BIT for different tests from [137].

An outcome of this is that the latter part of the formula is negative (to reduce the overshoot), and is usually small. A list of the calculated values of the second term for each

experiment is provided in Table 2-7. The correction term cannot be negative (mathematically impossible) and so the calculation can only be reduced by using it (due to the negative sign in the equation).

Table 2-7 – Calculated values of the correction factor from (2-26).

Test Number	Test Conditions	Correction Term	Test Number	Test Conditions	Correction Term
	W (%), γ (%)	ºC		W (%), γ (%)	ºC
1	0.3, 0.45	0.017	14	4.0, 8.80	7.187
2	0.3, 1.48	0.109	15	3.0, 1.00	0.179
3	0.6, 8.15	2.033	16*	5.0, 1.00	0.284
4	0.5, 9.95	2.614	17	8.0, 1.00	0.483
5	0.4, 9.68	2.328	18	8.0, 7.70	12.282
6	0.4, 11.0	2.851	19	8.0, 8.80	15.177
7	0.4, 12.3	3.404	20	4.1, 1.00	0.234
8	1.5, 1.90	0.310	21	5.7, 1.00	0.325
9	1.1, 9.70	3.477	22	5.9, 8.80	10.603
10	2.3, 9.70	5.382	23	3.1, 8.80	5.775
11	1.6, 1.56	0.2352	24	5.3, 8.80	9.455
12	1.6, 9.73	4.280	25	7.8, 8.80	14.702
13	1.0, 8.80	2.846	26	2.8, 8.80	5.329

*The moisture content for test 16 is given as 3.0 in [137] but calculation suggestions that the true value is 5.0, as shown here.

More work is needed to develop this formula. It would be of huge benefit to transformer owner / operators to have a reliable method of predicting BIT, but given the number of parameters involved and the innumerable ways in which these parameters interact with each other means that it may not be possible to have a single, simple formula for all cases. While it is obvious that the experimental and predicted data fit well, this is not surprising as the formula was fitted on the experimental data. The industry should not feel compelled to follow the guidance of a formula that is incorrect in construction, but which fits a set of data (26 points) well.

2.7 BUCHHOLZ RELAY

Aside from preventing bubbles in the first instance (e.g. by having dry insulation and operating below defined thermal limitations), a protection device is also provided for a

power transformer in the form of an liquid-gas actuated relay, also known as a Buchholz relay [37]. A US patent application for a precursor device was granted as early as 1939 [159].

The operation of this safety device is relatively simple, with a float switch first sending an alarm and then tripping the transformer out of service when generated gas displaces the oil level within the device. The Buchholz relay is fitted to the top pipe of a transformer, usually leading to the conservator tank, making use of the rising tendency of gases within the more dense insulating liquid [160]. The distance between the relay and the fault location is ideally minimised to ensure appropriately quick activation of the protection [72].

This device will prevent the likely catastrophic failure during rapid generation of gasses (e.g. through overpressure or dielectric failure). However, the result of such an absolute measure means that despite the protection of the asset from further damage, the outcomes of loss of downstream supply or increased loading of in-parallel assets still occur. Thus activation of the Buchholz relay is undesirable and it is much preferable to prevent bubble generation in the first instance.

The device is designed primarily for conditions of very high temperatures such as during a short circuit event, where high amounts of gas can be generated as cellulose decomposes aiming to prevent over-pressurisation which could even lead to tank explosions [72]. Thus it may not be optimised for generation of moisture bubbles. It is also worth noting that the device only activates when the oil level in the device itself is displaced. This requires generation of sufficient gas quantity [119] (e.g. from thermal decomposition of cellulose) although history shows that the relay can activate in the incipient stages of a fault [37]. Most importantly however, Buchholz relay operation requires this gas generated to be motive. As described in [34], it has been witnessed in certain experiments that trapping of gases within the windings can occur, and other areas of the transformer (for example, angle rings) may also cause entrapment. As this entrapment can take place in areas of high electric field, concerns over dielectric failure during bubble formation remain realistic even in the presence of the Buchholz relay.

2.8 SUMMARY OF LITERATURE

The investigations conducted into transformer bubbling so far have led to a point where the following is well understood:

- Transformers are key network assets, their failure can be costly. Transformer failure is more probable at elevated temperatures for numerous reasons.
- BIT is a possible failure mechanism influenced by increasing loads.
- BIT is strongly linked to the moisture content of the solid (paper) insulation (higher moisture content gives a lower BIT),
- tBI is strongly linked to the moisture content of the paper insulation (higher moisture content results in a lower tBI),
- Surface tension is a parameter involved in the energy of a bubble.

There is also much that still remains unclear about bubble formation. The below list shows the factors which are not so well understood:

- Type of liquid insulation, two studies have shown that there is potentially higher BIT in esters than mineral oil, but a consistent underpinning reason has not been established.
- Types of solid insulation, the two studies conducted so far have shown contradictory results.
- Insulation age, it has been shown that the age of insulation may affect the BIT, but there have been contradictory results published.
- Gas content of oil appears within the formula used in loading guide standards, however gas content in oil appears to be of minimal consequence and may actually relate to a different bubbling mechanism.
- RoCoT is an important factor which must be kept consistent within a single experimental series to ensure self-consistent results. It has been seen that comparison across different experiments shows irregularities and this is a concept worthy of more investigation.
- Formulaic representation of bubbling inception within the transformer system is complicated, relying on many variables, and requiring explicit definition of the mechanism being modelled.

There is therefore great benefit to be had in further testing of the impact on bubble formation of alternative insulation materials and the impact of RoCoT, considering the relationship between RoCoT, transformer temperatures and loading profiles.

3 MODELLING STRATEGY FOR TRANSFORMER LOADS AND TEMPERATURES

3.1 INTRODUCTION

The majority of work conducted so far by other authors into the bubbling behaviour of transformers has been experimental. However, Chapter 4 relies on modelling of loads based on the model provided in [161, 162], and modelling of transformer temperatures based on the formula presented in [42]. MATLAB R2019a is the software environment for coding and simulations. Assessment of bubbling in transformers is then conducted on these temperature profiles, also in MATLAB. Figure 3-1 shows the pathway followed to get from load profile to bubble assessment, encompassing these three stages of modelling.

Later, Chapter 7 analyses the bubble formation formula and suggests improvements to its structure. The analytical section is done mostly by fitting existing data for transformer insulation bubbles to different equations using OriginPro 8.5.1. Comparison of the formula 'as is' and the newly developed version is done by reassessing the potential for bubble formation as in Chapter 4.

The purpose of this chapter is to outline the strategy used to create the transformer load and temperature profiles which are then used in the analyses of Chapters 4 and 5. The profiles are generated in Chapter 4. Within this chapter, the focus is on the rationale behind the modelling strategies, that is, why these models were selected, their benefits, and any limitations.

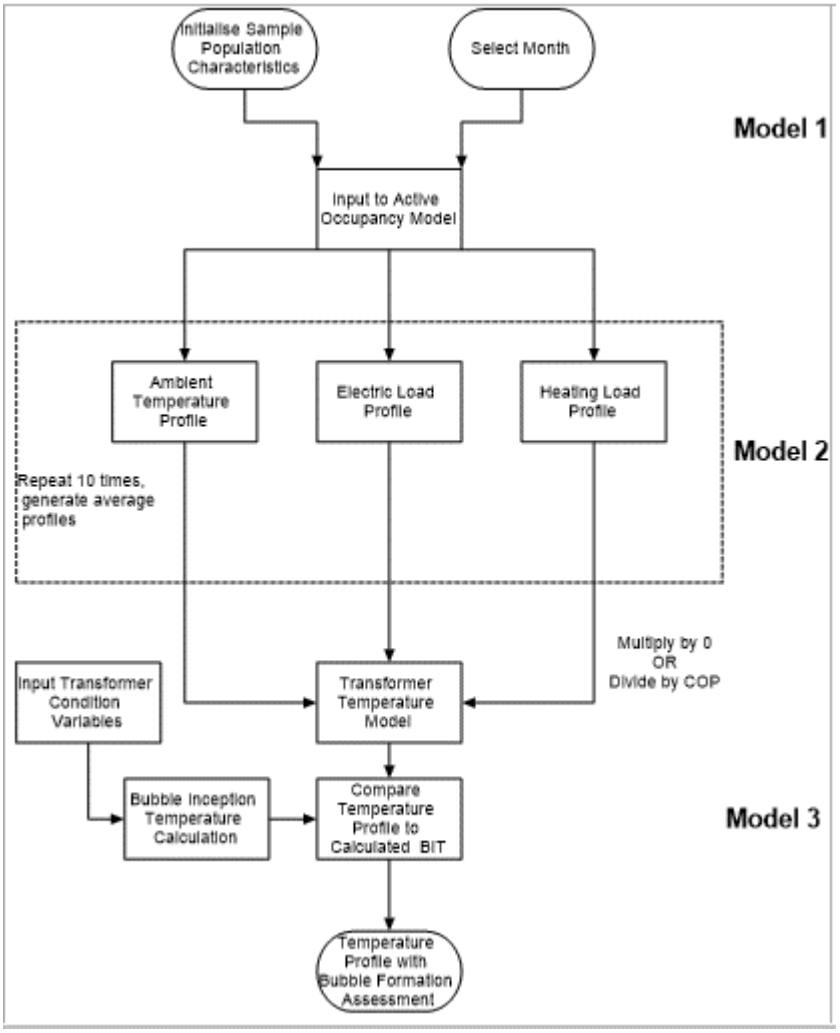

Figure 3-1 – Flow diagram showing steps involved in performing BIT analysis for a transformer load profile (COP – coefficient of performance of electric heat pump).

3.2 BACKGROUND TO ELECTRIFICATION OF HEATING

Improvements in the UK electricity generation profile have seen a reduction in GHG emissions, with emissions from the power sector down by 68% compared to 1990 [11]. This change is mainly due to a shift in reliance on gas instead of on coal, but it has also been boosted by installation of wind and solar generation, as well as improvements in efficiency.

In the UK, transportation accounts for around 40% of end energy usage [163] and is responsible for 23% of emissions, with the total amount rising since 2012 [11]. Cars are the main contributor at 14% of UK emissions [17]. Transport is a large contributor around the globe, figures quoted for the US show transport as being responsible for 28% of energy usage [164]. Heating also accounts for over 40% of end energy use in the UK, the majority of which is used at the domestic level [165]. Domestic users are also the most susceptible to changes in ambient temperature, strongly influencing the demand for heating [163].

Thus, the 'electrification' of both the heating and transport vectors is proposed as a method of reducing emissions, taking advantage of the progress in and promise of further reducing emission from electrical generation. The main technologies proposed are electric heat pumps (EHPs) and electric vehicles (EVs) for the electrification of heating and transport, respectively [17, 19, 165]. Both of these technologies are (primarily) implemented at the home, i.e. at the distribution level. EV charging is estimated to occur at domestic residence for between 50% and 80% of instances [166]. While issues such as lack of space (certainly in population dense countries such as the UK) may limit the uptake of EHPs, it is most likely that they will also be located at the home. EHPs can provide domestic space heating and hot water, their usage in multi-resident dwellings (such as blocks of flats) can also therefore be problematic.

Whether or not the tactic of electrification is inherently sound is not a focus of this thesis – rather, the main motivation is to consider electrification of demand and its impact on load, and to identify any change in risk to the network. It is important though to consider what impact these technologies may have on network assets to ensure that well-meaning changes do not result in serious impacts elsewhere. Note that likelihood of electrification seems high, with the sale of petrol and diesel cars (including hybrids) to cease by 2040 [167], and the connect of new-build houses to the gas network no longer being allowed from 2025 [168]. Therefore, the load modelling strategy used in this thesis is to assume wholesale adoption of EHPs, and thus to convert all heating demand (which was previously provided

by the gas network) to an electrical demand, using a sensible coefficient of performance (COP) for the calculation. The thermal impact of this added load on a transformer is then assessed.

3.3 LOAD MODELLING – MODEL 1

It is necessary to have a realistic load profile which can provide an input for calculation of transformer temperatures. The relationship between load and temperature is non-linear, much as the relationship between temperature and insulation lifetime is also non-linear. As the voltage on either side of the transformer does not vary by much (+ 10% / − 6% for distribution systems [169]), changes in load can equally be seen as changes in current, following (2-3). The main losses in a transformer occur in the windings as load losses, also called I^2R losses [37]. For this reason, it is common to work on the basis that a change in load causes a change in temperature in a squared relationship. Other factors, including thermal time constants and the weather conditions, can also influence the temperature profile. Thus, to calculate transformer temperatures one needs estimates of the value of such factors and an estimate or measurement of load. This, added to the fact that the load profile is never fixed (unless off), and calculation depending on the immediate thermal history of the transformer plus the ambient conditions, makes calculating temperature accurately in real time somewhat difficult.

For the purposes of this study, it is necessary to generate a load demand based on domestic users. This requirement comes from the discussion around which low carbon technologies can cause the greatest change to load profiles of transformers. Technologies employed at the distribution level have the potential to alter the load demand on distribution transformers. The focus will be the influence of conversion of heating demand from gas to electric source.

In order to achieve this, a model is needed which can generate a ‘base electrical load’ (i.e. the electrical demand of users for appliances that are currently electric-sourced, e.g. televisions, lighting, etc.), and also a heating demand. These model outputs need to be temporal and to be on a fine enough time interval to allow transformer temperatures to be calculated. Such a model exists in [161], an ‘integrated thermal-electric demand’ model based on a ‘four-state active-occupancy’ methodology with ‘high temporal resolution’. It has been adopted for many previous published studies.

Breaking down these terms, high temporal resolution means that the time step is small, with outputs on a minute-by-minute basis. This allows the temperature profile of the transformer to be assessed across each minute of a day, and hence the fullest picture of the thermal response of the transformer – dilution of the load profile brings inaccuracies to the transformers life assessment and to fault identification. The description of the model as an active occupancy model indicates that it determines usage based mostly on the activities of people at the home which use electricity; the four states relate to the status of personnel in houses as active / inactive (awake or asleep) and present / absent (i.e. at home or not). This treatment of the model helps to account for the 'randomness' of electricity usage [170].

Further, the model assigns a number of occupants to each dwelling. A key aspect of this model is to apply a coordination between persons within the same residence [170]; that is, their energy use is not independent (two people in the same residence would not both turn a living room light on, and they can only have one temperature setting on the heating, as examples). The occupancy data, i.e. the number of people per household, is generated stochastically by the model.

Finally, based on this input data, the model determines energy demands, thermal (gas heating) and electric, via a Markov chain analysis. This demand output can be interrogated on a dwelling-by-dwelling basis, or as a combined demand. The model also allows for inclusion of solar panels. The electricity developed through the use of solar panels would be taken off the total demand, leaving a net demand across the transformer. Within this analysis however, the number of houses with solar panels was forced to zero (i.e. no houses had solar panels). This allows for the analysis to be a 'worst case' in terms of demand, and also accounts for the highly plausible case where residents are unable to afford solar panels after purchasing EHPs (which would be a necessity with the cessation of gas connections).

The number of dwellings selected for this study is 90. They are connected to a transformer assumed to be at the 11 kV/400 V level, with a rated capacity of 200 kVA, therefore a per unit load can be calculated by dividing by this capacity.

3.4 TEMPERATURE MODELLING – MODEL 2

Transformer temperature is related to the load that is being transferred across the windings; more specifically, it is related to the current and the losses generated as a result of this. That said, the temperature is a complex parameter to calculate and is dependent on many factors. For the work done in this thesis, a model for calculating transformer temperature

was developed in MATLAB, following the methodology described in the 2005 version of the IEC 60076-7 loading guide [42]. This loading guide was updated in 2018 [23], but the only major change to the calculation of transformer HST calculation is to move the explanation of the difference equation from an annex to the main body of the standard. There is no difference in the final calculation of temperature between these two standards, and so the validity of the original work is preserved.

Thus, the majority of the discussion presented here is based around the 2005 guide without fear of loss of accuracy or relevance. One study determined that the IEC calculation method gives 'reasonable accuracy at load increase' compared to measurements made on real transformers [106].

3.4.1 Theoretical Construction of Transformer Hot-spot Temperature Model

To calculate transformer temperatures, the process outlined below from [42] is followed. The basis of the calculation is the diagram shown in Figure 3-2 [23]. In this depiction of transformer temperatures, the y-axis is the height of the transformer winding, and the x-axis shows the temperature. It is then clear that an assumption of this construction is that temperature rises along the height of the transformer. The diagram also shows that the temperature rise is linear with height. The solid line passing points B, C and D represents the temperature of the liquid insulation, with point A representing the 'top oil temperature'. (Note that the 'top oil temperature' is a commonly used term, but it applies equally to other insulating liquids such as esters, wherever 'top oil temperature' is used, the intention is to imply 'top liquid temperature', but this is awkward and uncommon parlance. The reader can assume that the concept applies to all liquids equally.) The dotted line parallel to the solid line for liquid insulation temperature indicates the winding temperature. The fact that it is parallel shows that there is an assumption of a constant temperature gradient between the liquid insulation and the winding throughout the height of the winding. This is denoted as g_r with units of K. To calculate the hottest spot within the transformer, it is recognised that there is an increase of the gradient between the top oil and the winding at that location, and so a factor, *Hf*, is applied. Multiplication of g_r by *Hf* gives the increased gradient needed to calculate the HST, indicated as point 'P' on the figure.

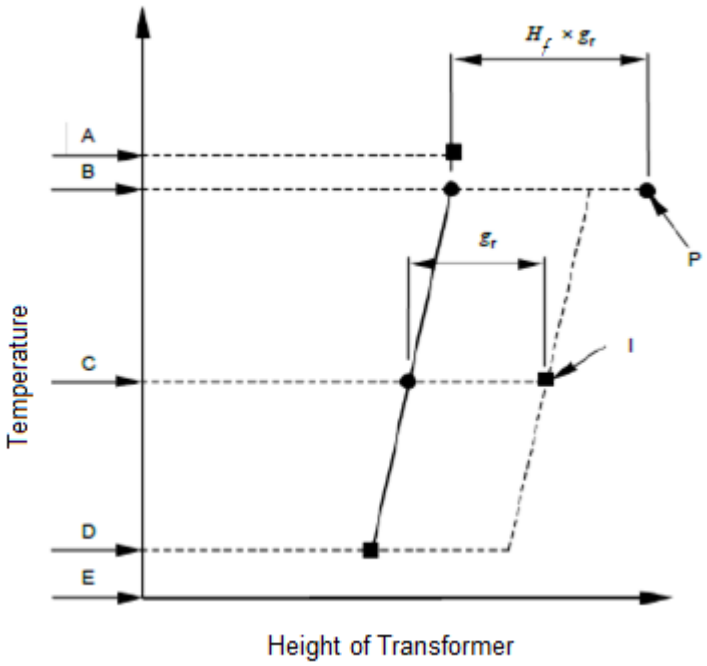

Figure 3-2 – Transformer Thermal Diagram adapted from [23]. Solid line shows the liquid insulation temperature at different heights within the transformer; dotted line shows the winding temperature at equivalent height.

Thus, the calculation of the HST can therefore be split into five main tasks:

1. Establish the ambient temperature profile,
2. Calculate the top oil temperature rise above ambient (i.e. how much hotter is the top oil than the ambient temperature),
3. Determine the gradient between the liquid insulation and the winding temperatures,
4. Calculate or estimate a factor to apply for the hot-spot temperature rise,
5. Sum the ambient temperature, top oil temperature rise over ambient, and HST rise over top oil temperature.

3.4.2 Formulation of Transformer Hot-spot Temperature Model Equations

This process is shown in equations (3-1) – (3-3), which is known as the difference equations solution method from Annex C of [42]. Ultimately, the aim is to have a mathematical description for point 5 from above, which can be written as (3-1). *T* is temperature in K, with the subscripts *h* standing for hot-spot, *amb* for ambient, *o* for oil and Δ indicating a temperature difference.

$$T_h = T_{amb} + \Delta T_o + \Delta T_h \tag{3-1}$$

The HST of a transformer is linked to the ambient temperature. Treatment of ambient temperature in this manner may not be fully representative as it does not account for a thermal time constant for the insulation system to respond to changes in ambient temperature, instead assuming that changes occur instantaneously. A model that accounted for this was developed in [115], improving on the IEEE model (error of 0 ±0.4 K versus 1.5 ±15.0 K) compared to measured top oil temperature data from a transformer operating at low loading. A separate study, [116], stated a maximum error in calculated top oil temperature of transformer experiencing higher loading of 1.7 K. For the purposes of this study however, it is assumed that the impact is minimal, and as transformer design will need to conform to the standards, it is thought best to run the temperature and bubble generation analysis using the method as described in [42].

To obtain the HST, the first step is to write out the equation that describes the oil temperature rise above ambient temperature at the next time step (i.e. the next calculation point, which is at a point one minute further along), shown in (3-2). As the time step within the work in this thesis is one minute, the time step value, $\Delta t = 1$. Selection of the time step is important, it should be no greater than half of the smallest time constant used within the calculation (and always as small as practicable). For transformer HST calculation, this will be the winding temperature constant which usually ranges from 4 to 10 minutes (shown later). A one minute time step ensures that this criterion is always met.

Calculation of the oil temperature rise includes accounting for the load. Load is given as a load factor, κ, calculated as the actual current divided by the rated current (i.e. the per unit current), which is roughly equivalent to the actual power divided by the rated power. It is more accurate to use the current for these calculations as it is current, i, which appears in the equation for power loss, Equation (2-7).

In (3-2) subscript o indicates oil, subscript t indicates that the value is at the present calculation time step, $(t-1)$ indicates that a value is at the previous time step, and subscript r indicates that the value is calculated at the rated value of the transformer. The value R describes the ratio of load losses to no-load losses. The quotient before the brackets is a term that accounts for the delay in time taken for the oil to respond to changes in load (which can be large, in the order of hours) with τc_o being the oil time constant, and k_{11} a constant specific to the transformer design, but usually with a value ≤ 1. x is the oil exponent, which also usually has a value ≤ 1.

$$\Delta T_{o,t} = \frac{\Delta t}{k_{11}\tau c_o}\left[\left[\left[\frac{1+R\kappa^2}{1+R}\right]^x \Delta T_{o,r}\right] - \Delta T_{o,t-1}\right] + \Delta T_{o,t-1} \quad (3\text{-}2)$$

Equation (3-2) essentially shows that the top oil temperature rise above ambient temperature is a function of the top oil temperature rise above ambient temperature of the previous time step, with an additional term. The additional term calculates how the oil temperature responds to the change of load between time steps. A known value, the top oil temperature rise above ambient at rated load ($\Delta T_{o,r}$) is multiplied by a factor relating the loss ratio to the instantaneous per unit loading of the transformer – essentially, the rated response is adjusted to account for the actual amount of energy being generated as losses, which is then adjusted by the thermal time response.

The next stage is to calculate the HST rise above the top oil temperature. This is done through equation (3-3). The HST rise above oil temperature has two components, the first relates to how quickly the temperature of the winding responds to the change in load. The second component is subtracted from the first, and reflects how the oil cooling reacts to the winding temperature change in response to loading change.

$$\Delta T_{h,t} = \left[\frac{\Delta t}{k_{22}\tau c_w}\left[k_{21}\kappa^y \Delta T_{h,r}\right] + \Delta T_{h1,t-1}\right] - \left[\frac{k_{22}\Delta t}{\tau c_o}\left[(k_{21}-1)\kappa^y \Delta T_{h,r}\right] + \Delta T_{h2,t-1}\right] \quad (3\text{-}3)$$

The term reflecting the winding response multiplies the load factor (raised to a winding exponent, usually >1) by the rated HST rise above the top oil temperature, and a constant, k_{21}. This is all then divided by the winding time constant τc_w (which has the order of minutes) multiplied by a further constant, k_{22}. The changes in winding response and cooling effect on winding temperature calculated at time *t*, are then added to their respective previous time step values (indicated by $\Delta T_{h1,t-1}$ and $\Delta T_{h2,t-1}$) before the cooling effect is subtracted from the winding temperature increase. The constants k_{11}, k_{21}, and k_{22} are not given physical meaning, but could be determined from an extended temperature-rise test if the HST is measured using optical fibre.

Finally, to establish the HST at time *t*, the two values calculated in (3-2) and (3-3) are summed, and then added to the ambient temperature of the same time step, as in (3-1).

3.4.3 Bubble Inception Temperature Modelling

Bubble inception temperatures will be calculated against the formula of [22, 71], shown in Equation (2-26). The equation requires inputs of moisture content in paper, gas content in oil, and system pressure. A range of moisture and gas values will be tested, with a typical system pressure chosen. There are no other inputs to the equation.

To identify points of potential risk of bubble formation on the transformer temperature profile, the minute-by-minute transformer temperatures are compared to the BIT calculated for the chosen conditions, where the transformer temperature is higher, this presents a risk.

3.5 SUMMARY

The aim of Chapter 4, to determine the extent to which adoption of LCTs could impact transformer thermal performance, is done through modelling. The modelling is conducted through three stages: firstly, loads are established using the active occupancy model of [161] in Model 1, load is then converted to transformer HST by Model 2, and finally potential bubble situations are identified through Model 3.

The process by which a 'typical' residential area can be examined for the potential impact of electrification of heating via these stages of modelling is shown in Figure 3-1. The results of these simulations are given in Chapter 4.

4 SIMULATION OF CHANGES TO TRANSFORMER LOAD, TEMPERATURE AND BUBBLE RISK UNDER LOW CARBON TECHNOLOGY FUTURE

4.1 INTRODUCTION

The aim of this chapter was to assess transformers for their risk of bubble formation based on the formula provided in [22, 71]. This was done in two stages: firstly on the present-day loading scenario; and secondly for a future scenario which includes the electrical demand generated by electrification of heating. The load profiles for both cases were created using an 'active occupancy' model presented in [161, 162]. Finally, results of a BIT analysis for the two cases (base electrical load and added electrified heating demand) is conducted for a number of transformer material conditions.

4.2 AMBIENT TEMPERATURE PROFILE – MODEL 1

To allow calculation of the transformer temperatures, a profile of ambient temperature is required. A profile is generated within the model of [161] and this was run ten times with the average (mean) profile used for this investigation. This was performed for both a 'winter' scenario (January 15th) and 'summer' scenario (July 15th) in a location in Sheffield, which is roughly central to the UK. This location is chosen to allow for comparison of the simulated temperatures with a local weather station for which averaged data is available on a monthly basis from 1883 to present (excluding some war years). The generated temperatures were compared with the respective average monthly temperature from the weather station and were found to be consistent. Figure 4-1 shows both of the ambient temperature profiles which are used in these transformer temperature calculations.

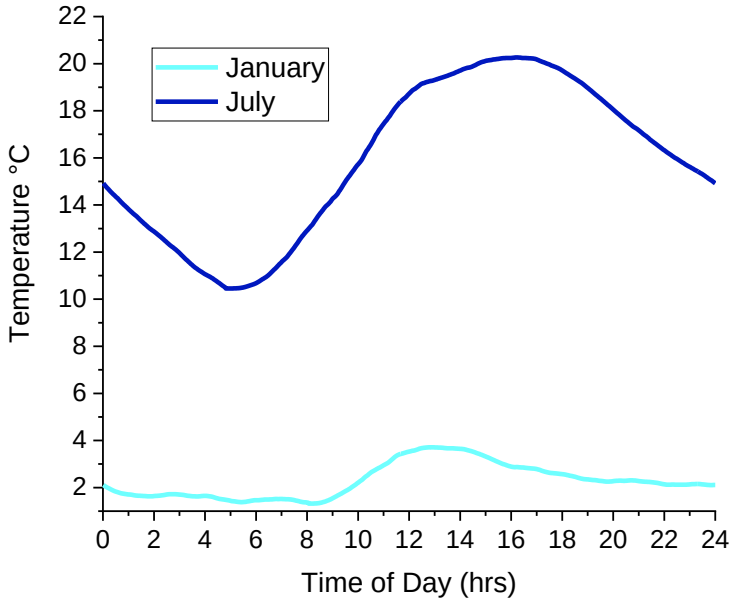

Figure 4-1 – Generated ambient temperature profiles for January and July days.

The two situations are interesting. Clearly, a summer day is likely to be hotter than a winter day, and so in summer the ambient temperature contribution to HST is more significant. However, the electricity demand in summer in the UK is generally lower than in winter [171]. Despite increases in air conditioning loading in some cities such as London, the load used for heating and lighting in winter, coupled with shorter daylight hours means that electricity demand is still higher in the winter [165]. Therefore, both cases are considered within the HST modelling to compare the impact of hotter ambient temperatures versus increased loading demand, which is particularly significant when electrification of heating is also accounted for.

4.3 Generation of Base Electricity Demand – Model 1

In order to establish a temporal thermal profile of a transformer, the demand from users connected to the transformer must be known at suitable time intervals. To determine the electrical load from appliances in the house, the active occupancy model [161] was utilised.

Outputs from the model vary according to the input data. Chiefly, the time of year and the geographical location can impact results significantly. Colder months in colder locations will see higher usage of gas and electricity. Warmer months may have high demand for electricity if air conditioning is present, but note gas demand should expect to be down, and other electrical usage is likely to reduce as well. However, running the model for the same day, in the same location, even with the same occupancy distribution can lead to different results due to the stochastic nature of the four-state active occupancy model.

In order to mitigate the risk of a particular profile being an extreme case (e.g. very high demand, very low demand, or high / peaks), the model will be run for the same inputs ten times. The average (mean) electrical demand profile is selected from these ten profiles to ensure that a representative profile is used for the analysis. Figure 4-2 shows the minimum, maximum, mean, and medium profiles for the winter case (January), and Figure 4-3 shows the same for the summer case (July). As 'maximum' and 'minimum' profiles may not exist, i.e. no single profile is highest for the duration of the entire day, the maximum and minimum profiles shown are the mean ±1 standard deviation. The shape of each profile is similar, with peaks at the expected time points (the profiles show the usual features of low overnight usage, an early morning peak, which drops slightly but remains steady for most of the day, then a large evening peak, dropping off again as night comes). The median and mean profiles match well, implying that there is a symmetrical distribution of the profiles, and that there is no real 'outlier' case.

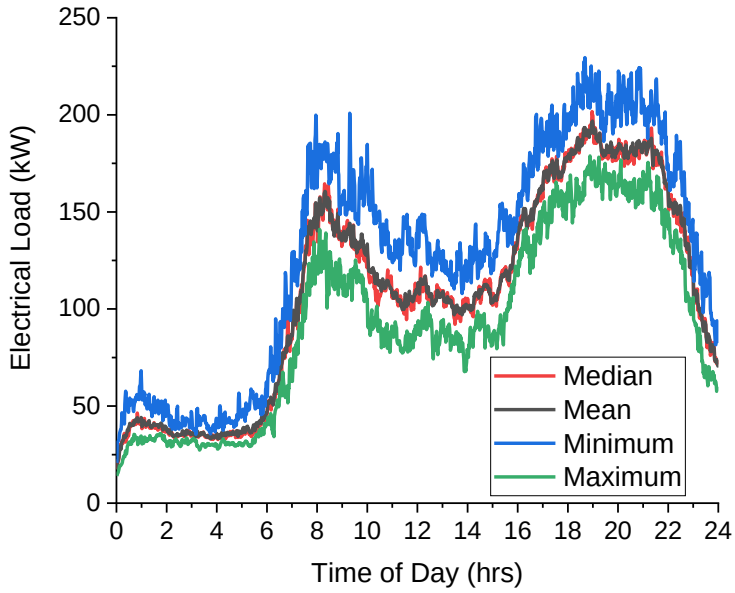

Figure 4-2 – Mean, median, maximum and minimum electrical load profiles for January.

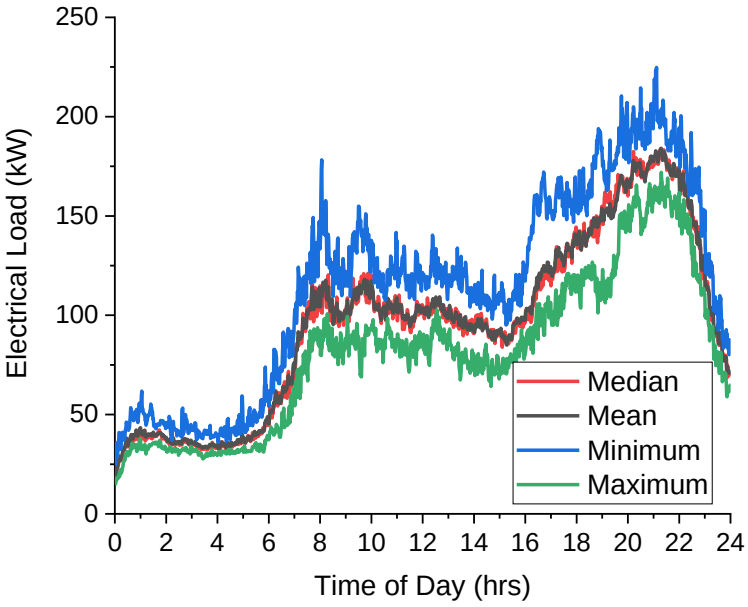

Figure 4-3 – Mean, median, maximum and minimum electrical load profiles for July.

A comparison of the electrical demand to be used in this analysis (i.e. the mean plots of Figure 4-2 and Figure 4-3) for winter and summer is shown in Figure 4-4. The overall and peak demands are lower in summer, as expected. Morning peak is higher for January, but the value of the evening peak is similar (though it starts earlier and lasts longer for January).

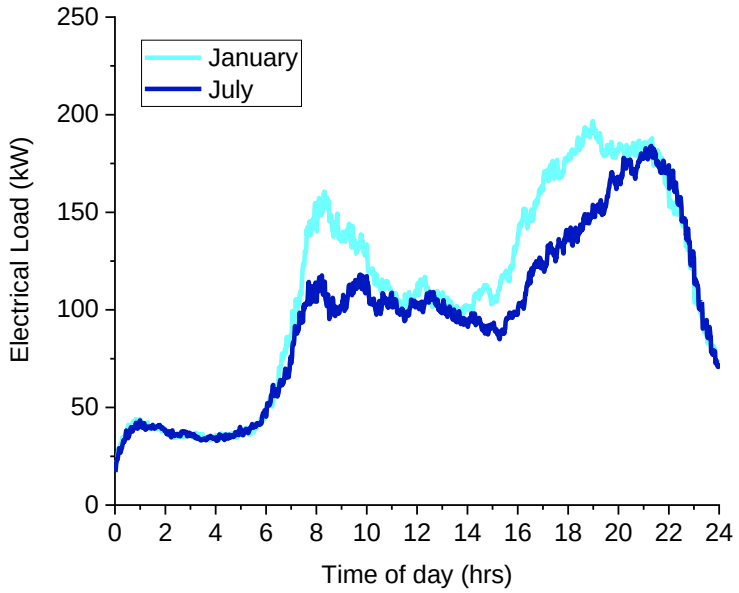

Figure 4-4 – Base electrical load profiles of January and July days.

4.4 Electrification of Heating – Model 1

Emissions from buildings are mostly due to the use of fossil fuels for heating. Building emissions contribute up to 17% of the total UK domestic emissions [17]. The majority of the heating comes from residential buildings [17].

In terms of decarbonisation, electrification of heating is the preferred method. The UK government has proposed that approximately 17 – 19 million homes will be heated (space and water heating) through use of heat pumps [17]. Heat pumps are a technology used to 'pump' heat in the reverse direction than is thermodynamically natural (i.e. they move heat from cold to hot, not the other way round). To do so, they require electrical power input. A key advantage of the heat pump, beyond that of it being an electrically powered method of heating, is that it outputs more heat energy than the electrical energy input. The efficiency of a heat pump is described by its COP, which is calculated from (4-1) with $P_{in,\ elec}$ and $P_{out,\ heat}$ representing the electrical power input and the output power as heat, respectively. The COP should be greater than 1, and the larger the COP, the better the heat pump performance.

$$\mathrm{COP} = \frac{P_{out,\ heat}}{P_{in,\ elec}} \qquad (4\text{-}1)$$

Several factors can influence the COP, including the type of demand and the ambient temperatures. A 'seasonal' COP (SCOP) has thus been defined in some texts, rather than using an average value throughout the year. Particularly, in winter (cold) months, the large temperature differences reduce the EHP efficiency, while in summer (warm) months, the

EHP demand is for domestic hot water supply more than for space heating which has a higher efficiency [172].

4.4.1 Base Heating Demand

Heating demand was calculated within the model per dwelling in the same way as electricity, with key input parameters of ambient temperature and the active occupancy status of the residences on a stochastic basis, accounting for the varying temporal use of heating by users and the ambient temperature. The heating demand calculated for both the summer and winter months are shown in Figure 4-5, plotting the kilowatt hour demand of gas against time of day. Similar to the electrical demand profile, the overnight demand is low, with an early morning peak in usage, followed by a relatively constant loading throughout the day and evening. January demand is unsurprisingly higher than in July due to the cold weather in winter.

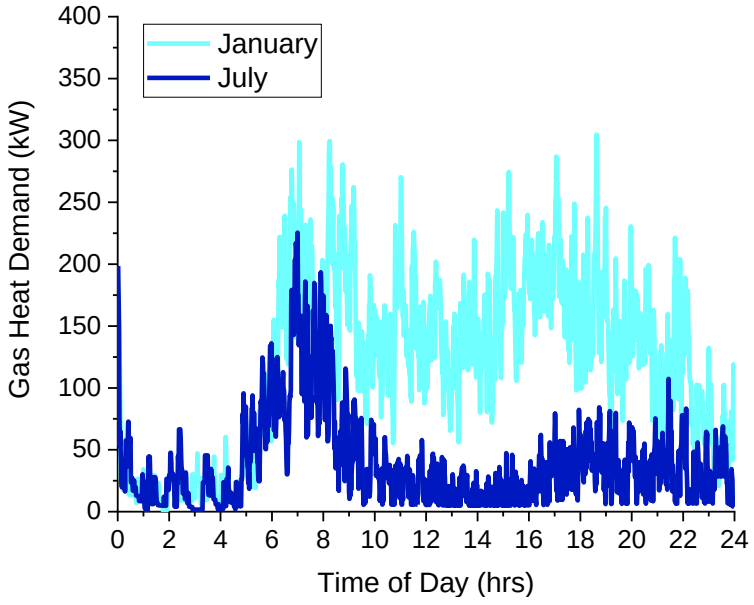

Figure 4-5 – Gas demand for January and July days.

4.4.2 Electrified Heating Demand

The heating demand was electrified by assuming that the gas demand shown in Section 4.4.1 (which was generated stochastically on a per minute per house basis, and then summed for a total demand per minute) is shifted entirely over to electric duty in the form of EHP. The COP used for the calculation is 1.5, chosen as a typical value for the time of year based on figures from large study for the UK government [173].

Dividing the loads in Figure 4-5 by the COP converts the load to electricity demand: as the COP is >1, the energy demand reduces. Figure 4-6 shows the heating electrical demand for heating. The minute-by-minute electric heating demand is then added to the base electrical demand from Figure 4-4, and this final load profile of the transformer inclusive of heating demand is shown in Figure 4-7. This combined profile of heating and base electrical loads is much higher than the base load, particularly in the winter (January) case.

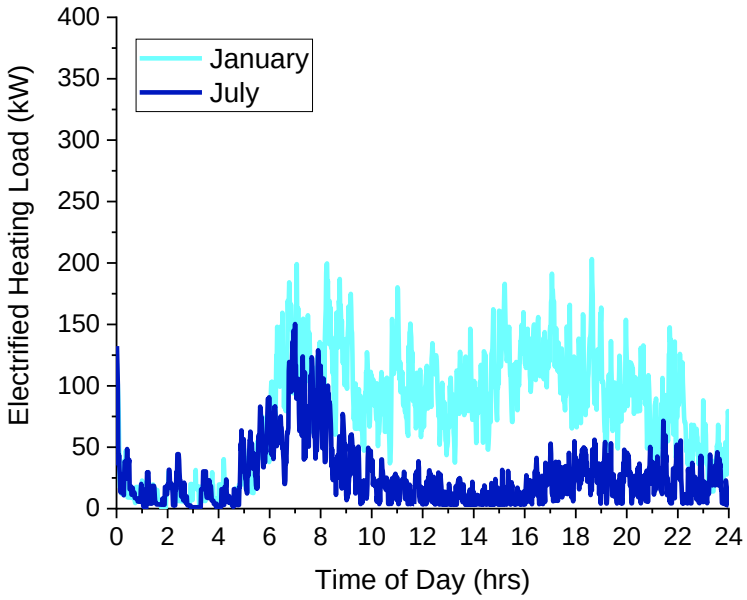

Figure 4-6 – Heating load converted to electric load by COP = 1.5, for January and July days.

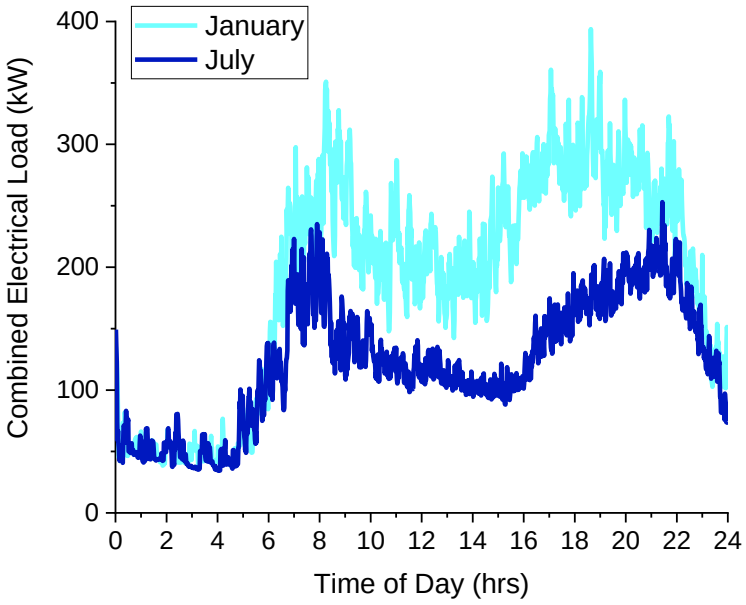

Figure 4-7 – Combined electrified heating load and base electrical load for January and July days.

4.5 TRANSFORMER TEMPERATURES – MODEL 2

The temperature profiles of a transformer before and after the electrification of heating load are shown in the following sections. The temperatures are calculated using the HST formula shown in (3-1). The load profiles from Sections 4.3 and 4.4 are used as inputs to the calculation. The ambient temperature used is described in Section 4.2. All other input parameters to the equations are given in Table 4-1, and are the standard parameters suggested in Table K.1 of [42] for the type of transformer under study. Using these parameters allowed the model to be verified against the output provided in [42] which confirms the accuracy of the temperature outputs.

Table 4-1 – Transformer thermal parameters used in temperature model.

Parameter Description	Parameter Symbol	Value in model (from [42])
HST rise above top oil temperature, at rated load (K)	$\Delta\vartheta_{hr}$	23
Top oil temperature rise above ambient temperature, at rated load (K)	$\Delta\vartheta_{or}$	55
Thermal model constant	k_{11}	1
Thermal model constant	k_{21}	1
Thermal model constant	k_{22}	2
Ratio of load losses to no-load losses	R_L	5
Oil thermal time constant (minutes)	τ_{Co}	180
Winding thermal time constant (minutes)	τ_{Cw}	4
Oil exponent	x	0.8
Winding exponent	y	1.6

4.5.1 Temperature Profile of Base Electrical Demand

The transformer is assumed to connect 90 domestic residences. A house in the UK is typically assumed to have an after diversity maximum demand (ADMD) of 1.5 kW, where

the ADMD is the maximum coincident electrical demand averaged over the number of connected houses, it therefore accounts for the non-coincidence of loads that would occur if the maximum demand of each house was summed instead, resulting in a lower combined peak value estimation. As a result, the transformer in this study is sized at 200 kVA, being the next standard size of transformer suggested in [174], that could service this load (90 residences operating at 1.5 kW ADMD requires at least 145 kVA).

Based on this size selection, and using the parameters from Table 4-1, the ambient profiles in Figure 4-1, and the load profiles generated in Section 4.4.1, a HST profile is created for a transformer. Figure 4-8 shows the HST profiles generated for these input parameters.

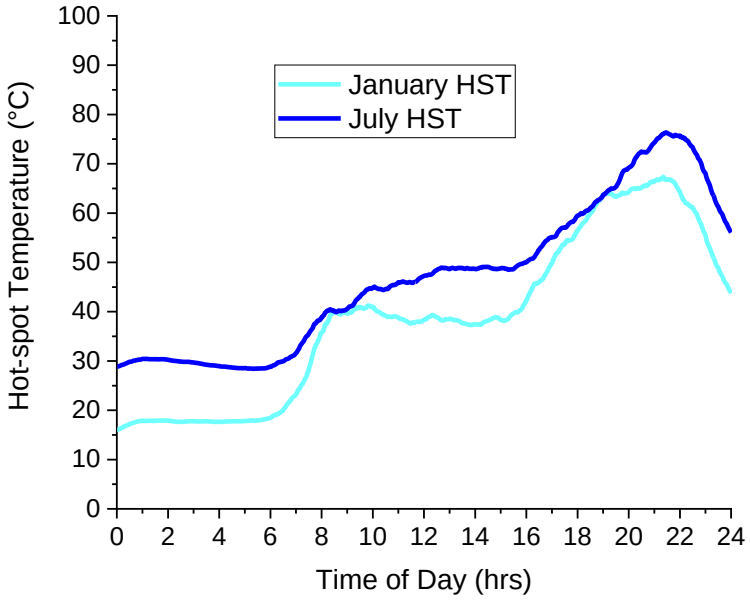

Figure 4-8 – Hot-spot temperatures of January and July base electric loading cases.

The temperatures are generally low (always below 98°C rated temperature), reflecting the low per unit loading of the transformer. This is common in UK transformers and would result in a long transformer insulation life with few occasions for high temperature failures.

The July case has a higher peak temperature, and the peak occurs slightly later in the day. The higher peak is mainly driven by the higher ambient temperature, and the delay in the peak is likely due to longer daylight hours (meaning people are away from the house for longer and turn lights on at home later). However, the shape and magnitude of the two curves are quite similar.

The difference caused by the thermal time constant of conductor and liquid insulator can be seen by comparing the HST and the top oil temperatures. The HST is much more

sensitive to the changes in load, whereas the top oil temperature follows the ambient temperature more closely. Figure 4-9 shows this for January, and Figure 4-10 for July. This highlights the benefits that can be gained from having a good liquid insulation cooling system to remove heat quickly.

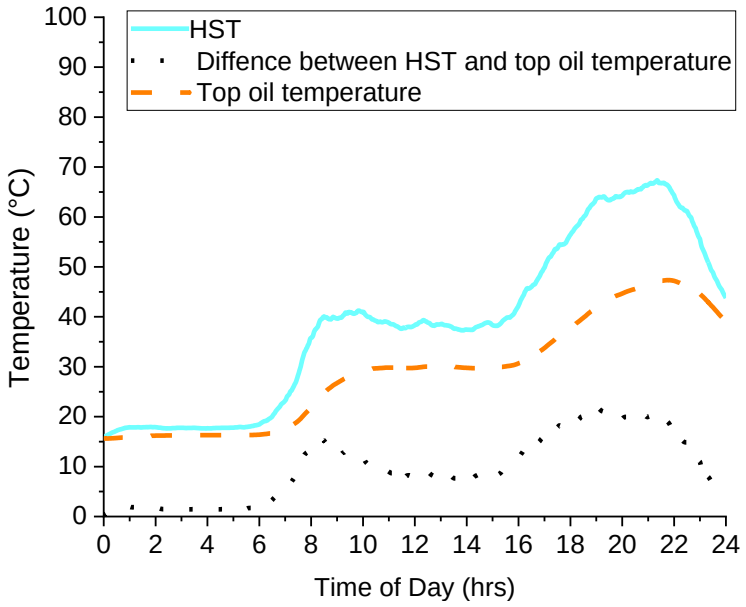

Figure 4-9 – Hot-spot and top oil temperatures for January base electric load case.

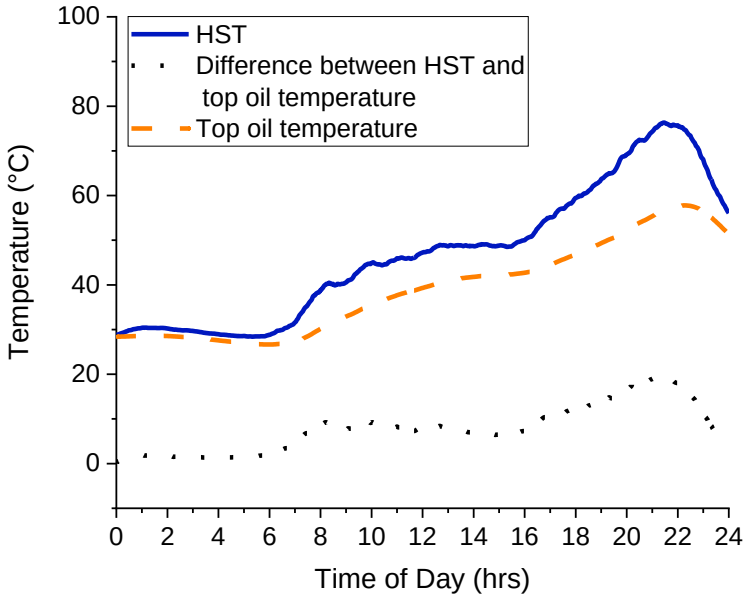

Figure 4-10 – Hot-spot and top oil temperatures for July base electric load case.

4.5.2 Temperature Profile Inclusive of Electrified Heating Demand

Inclusion of the electrified heating demand (i.e. adoption of heat pumps to replace gas-heating demand, at a SCOP of 1.5, as described in Section 4.4.2) into the model is done

using the same parameters from Table 4-1. Figure 4-11 shows the HST profile for both the summer and winter cases.

The temperatures are much higher than in the equivalent base case, but the highest temperatures still reflect peak loads, and they thus occur at a similar time of day (i.e. mid-morning and evening). The overnight loading is still low in both cases, and so the transformer temperatures tend back towards ambient, with winter temperatures becoming lower than summer, a trend which reverses from around 07:00 when load starts to increase again.

The peak temperatures for the January case go way beyond the rated temperature, in excess of 98ºC for more than seven hours of the day. While the July case remains below the rated conditions, the temperatures are still higher than without the added heating load. Therefore the ageing profile of insulation in both summer and winter with added heating load would be quickened.

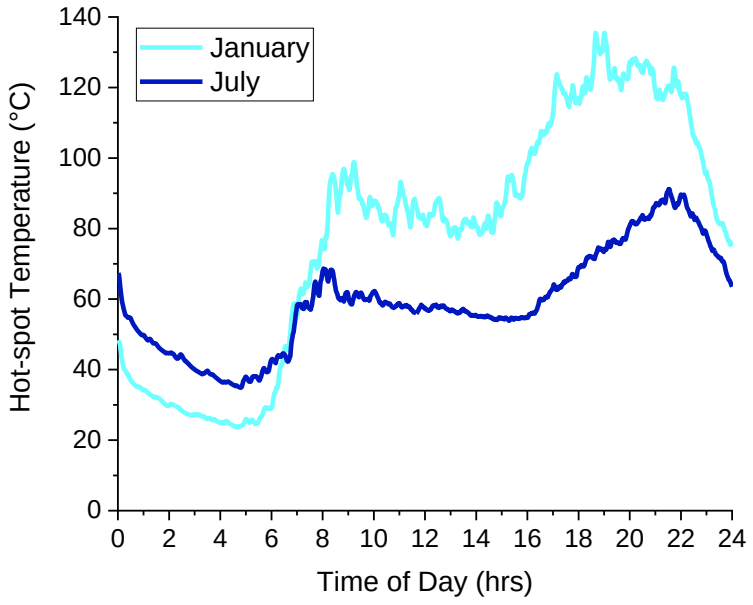

Figure 4-11 – Hot-spot temperatures for January and July days inclusive of electrified heating loads.

On first inspection, these profiles suggests that bubble formation is not a concern – temperatures get close to, but never reach 140ºC, and thus do not breach the overarching statement within [23]. However, further analysis can be done by calculating a specific BIT value based on the transformer insulation condition, which is presented in Section 4.6.

4.6 Assessment of Likelihood of Bubble Formation – Model 3

4.6.1 Bubble Formation Assessment for Various Transformer Insulation Conditions

The IEC standard 60076-14 [71] provides a formula for calculation of the temperature of bubble formation, shown in Equation (2-26). Additionally, IEC standard 60076-7 advises that temperatures should remain below 140°C to avoid bubble formation, later stressing that this temperature is valid for paper insulation at 2% moisture content [23]. Although even in the case with added heating load temperatures are always lower than 140°C (suggesting that risk of bubbling is low), the formula indicates that the actual temperature of bubble formation is specific to the transformer condition.

Hence, in Table 4-2 the BIT for four different transformer conditions are described, representing different stages of a transformer lifetime. The first condition is a new transformer that has been transported and prepared correctly. The moisture content of the paper insulation will be low, in the order of 0.5% [37] at this initial stage. Accordingly, the associated BIT is very high.

Over time, moisture ingress to the transformer occurs through ageing and ambient ingress. This can lead to the situation such as described in [23] where a transformer attains 2% moisture. In Table 4-2 the BIT calculated for 2% moisture is done with 0% gas content in oil because the standard does not specify the gas content – any increase in the gas content would reduce the BIT. In certain situations the amount of moisture within the transformer can increase beyond 2%, for example in the case of a failed or saturated desiccator on free-breathing transformers. [143] states that >4.5% moisture in paper should be classified as ‘excessively wet’ and so it is unlikely that many transformers will reach this condition even by end of life. However, to consider the impact of high moisture content in the paper insulation, a value of 4% is selected (which would be classified as ‘wet’). Two cases are considered, one where the gas content in the oil is 8%, representing a figure close to saturation (temperature and species dependent) and also the maximum value used in [137] from which the formula used to calculate BIT was developed. The other case considers a significant reduction in the gas content, which may be caused by regeneration of the oil (the paper moisture content is assumed unchanged as for mineral transformers only around 1%

of the total transformer moisture is commonly found within oil [31], and so drying of solid insulation would not be likely to occur on a large scale.

From Figure 4-11 it is apparent that the first two cases in Table 4-2 would not be at risk of bubble formation as the maximum HST is lower than the BIT shown. While these two cases can operate safely with the added heating load, the insulation would experience accelerated ageing.

Table 4-2 – Representative transformer conditions and calculated BIT.

Transformer Condition Description	Water Content in Paper (%)	Gas Content in Oil (%)	Bubble Inception Temperature (°C)
Newly Installed	0.5	1.0	205
Description from Standard [23]	2.0	0.0	147
Transformer Near End of Life	4.0	8.0	116
Transformer Near End of Life after Partial Degassing	4.0	4.0	120

The temperature profiles from Figure 4-11 are plotted in Figure 4-12 and Figure 4-13 for the last two conditions described in Table 4-2, with red circles showing the time points where temperatures could be high enough to cause bubbling (i.e. where the transformer temperature is greater than the calculated BIT).

Given the worsened condition of the insulation in the case of Figure 4-12 (i.e. more degraded oil condition), the BIT is lower (Table 4-2) and thus the period of potential bubble inception is extended compared to Figure 4-13. Under the transformer conditions of the cases in Figure 4-12 and Figure 4-13, the formula does not predict bubbling during the morning peak, only during the higher, evening peak period. From these calculations, there is a total time of 305/1440 minutes where the transformer is at risk during the January day profile for the worst conditions (Figure 4-12), starting at about 17:00, extending through beyond 22:00.

For the reduced gas content case (Figure 4-13), the BIT period also occurs from just after 17:00, until approximately 22:00, though the temperature is only intermittently above the calculated BIT (a total period of 199/1440 minutes exists where the HST is greater than the BIT for this case).

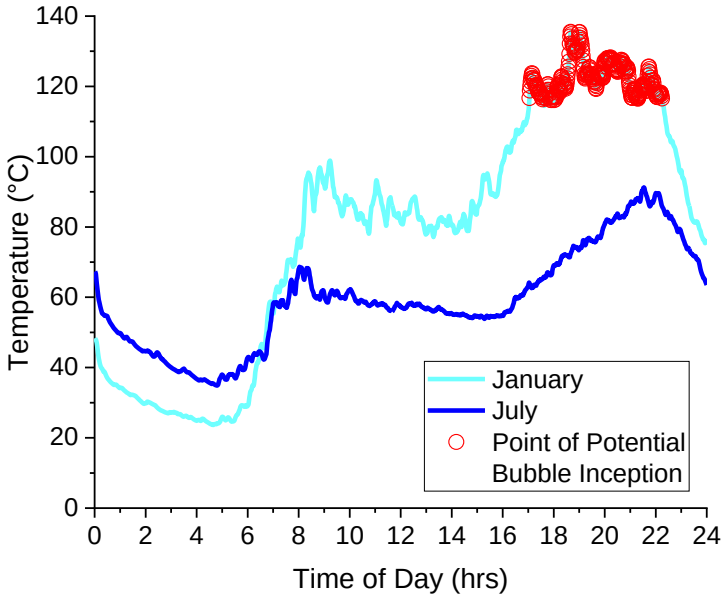

Figure 4-12 – Points of potential bubble formation identified for a transformer with 4% water content in paper and 8% gas content in oil.

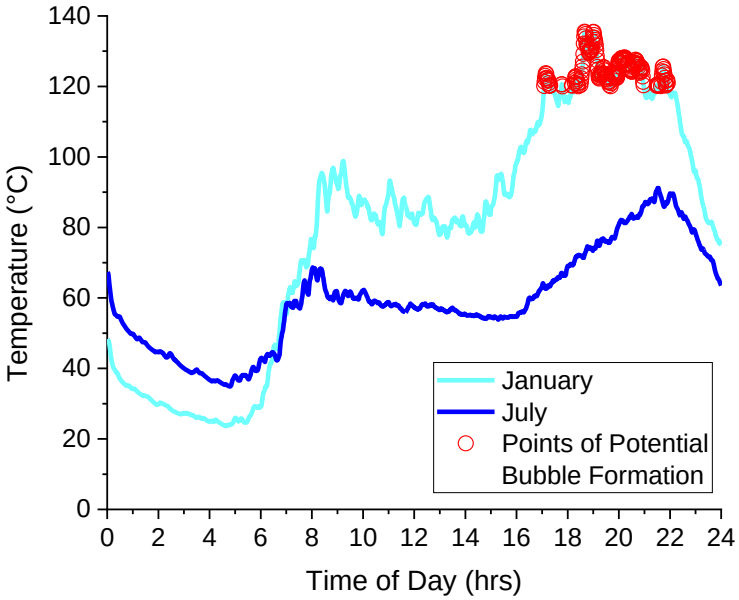

Figure 4-13 – Points of potential bubble formation identified for a transformer with 4% water content in paper and 4% gas content in oil.

4.6.2 Sensitivity to Changes in COP Value

As the assessment herein is done based on the load that EHPs add to the transformer, it is important to consider what happens if the EHP performance (i.e. COP) improves (i.e. increases). As the technology develops, this is a trend that would be expected. A fair choice for an average annualised value (contrast SCOP) for COP is 2 [172, 175]. Thus, Figure 4-14 and Figure 4-15 how the HST and BIT assessment for the same calculation as in Figure 4-12

(i.e. worst insulation conditions), but considering a COP of 2, and 1.75 (halfway between 1.5 and 2), respectively. Only January temperature profiles are plotted as July profiles did not present bubbles in the lower COP case.

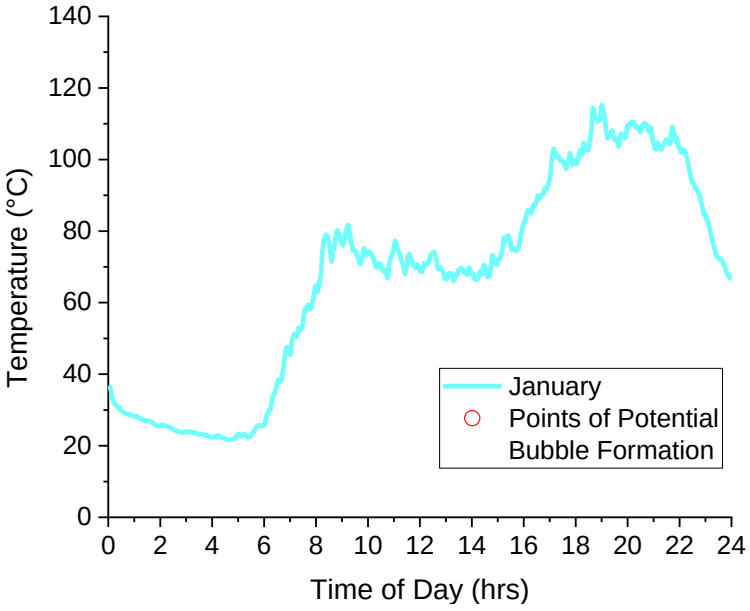

Figure 4-14 – Points of potential bubble formation identified for a transformer with 4% water content in paper and 8% gas content in oil, where COP for load calculation is 2.

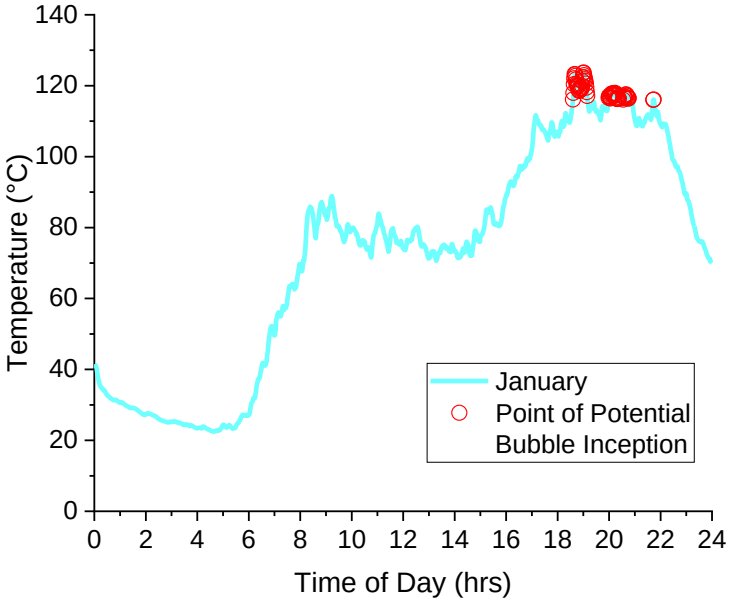

Figure 4-15 – Points of potential bubble formation identified for a transformer with 4% water content in paper and 8% gas content in oil, where COP for load calculation is 1.75.

As the figures show, there is much lower risk (less time) where bubble formation in the transformer is feasible when the COP is greater and the transformer load profile reduces. In this case, when a COP of 2 is used, the temperatures reduce enough that bubble formation is never likely, even under this 'worst case' insulation condition assessment. With a COP of 1.75, the transformer is still at risk, though now only for 75/1440 minutes.

4.7 SUMMARY

The results of this chapter show that under present loading situations (i.e. before addition of electrified heating load), transformers are unlikely to reach temperatures high enough for bubble formation. However, considering future loading cases may see an increase in load profile that elevates temperatures inside the transformer enough that, particularly for transformers in poor condition, they could pose a risk of bubbling for time periods of minutes to hours. Risk seems to be dominated during the winter months, where demand (both heating and electrical) is higher.

The load profile used in this study was the average from a number of simulated profiles. As a comparison, the winter transformer HST profile generated using the highest load profile from these simulations (Figure 4-2) is shown in Figure 4-16. BIT is identified based on the same basis as Figure 4-12 (4% moisture content in paper and 8% gas content in oil, BIT = 116°C). The maximum temperature is only higher by a few Kelvin, but this load profile does have the impact of extending the period during which the transformer is at risk of bubbling to 351 minutes (up from 305 minutes in Figure 4-12). This shows that normal fluctuations in electrical demand can also have an important effect on transformer HST when coupled with electrified heading load.

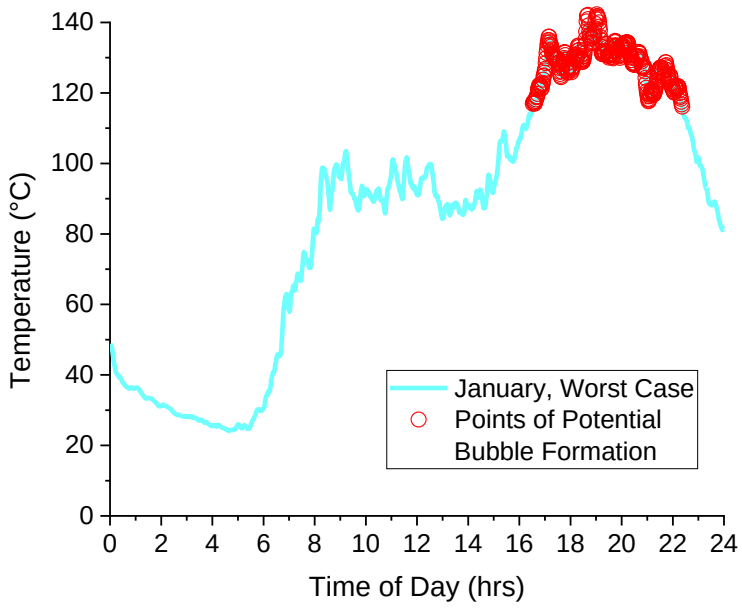

Figure 4-16 – Points of potential bubble formation identified for a transformer with 4% water content in paper and 8% gas content in oil, considering the 'worst case' January electrical loading scenario (COP = 1.5).

It is also worth noting that this work assumed complete uptake of EHPs. Supply of heating energy demand is moving from gas to electric means – that is certain. How it shifts from gas to electric is not as firm. EHP carry with them a massive benefit in that they have a COP >1. However, not every user will be fortunate enough to take up EHP, they require large spaces, are costly, and may not be optimal for multi-resident dwellings such as blocks of flats (though much work is going into this). Instead, these users may need to switch to electrified heating in the form of resistance heating, where efficiencies may be close to unity, but certainly never above it. The impact on loads in this scenario is would be even worse.

This chapter has considered the impacts on the thermal capacity of transformers due to high instances of electrification of heating. Work by Gao [117] looked in a similar way at the influence to load profiles from adoption of EVs, viz the increase of load through domestic EV charging. The timing of the load increase coincides with peak times, as can be seen in Figure 4-17.

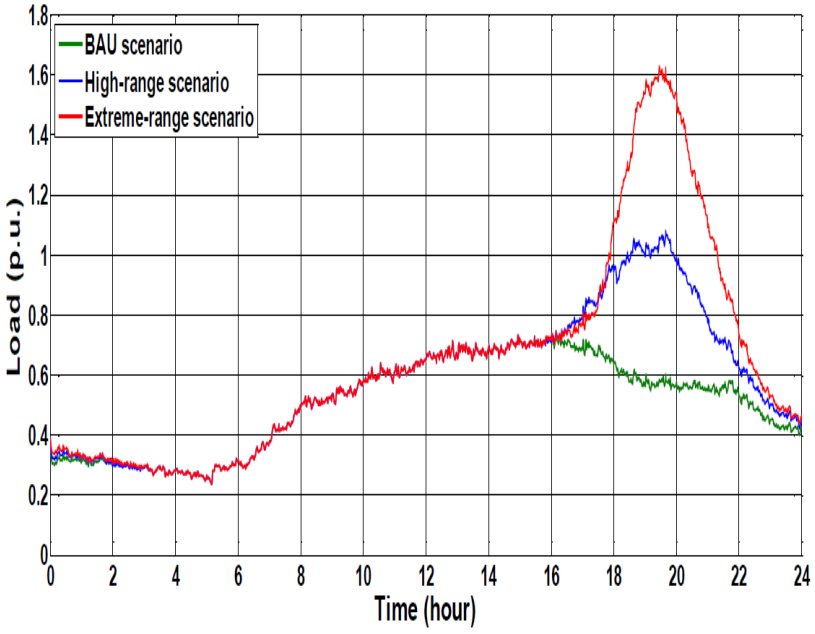

Figure 4-17 – Per unit load profile including EV charging loads from [117]. (BAU - business as usual).

Note that the main impact of electrified heating and EV charging is at the existing peak times. This is the least optimal time for additional loading, and the confluence of these two factors could be catastrophic. Without controlled charging / usage, there is a real chance that the network assets will be unable to handle the additional loading, as shown by the increased potential for transformer high temperature failures shown here.

The assessment within this chapter is made against the formula for BIT presented in [22, 71] which only requires inputs of the moisture content in paper, gas content in oil,

and the system pressure. It does not account for factors such as the RoCoT, and the formula outputs only BIT, there are no other considerations such as time included. While that may be a raw assessment of bubbling, it is aligned with the present guidance, and thus reflects the best estimate that a transformer operator could currently make.

5 BUBBLE FORMATION IN LIQUID INSULATION

5.1 INTRODUCTION

There have been several experimental studies into bubble formation conducted by previous authors. The lessons learnt from previous studies were applied in the development of this experimental set-up, which was later used for the investigations that form Chapter 6. This chapter describes the bubble formation tests in liquid only insulation and also some of the considerations that were found to be important during the development of this set-up.

The experimental set-up deployed for this study was a small scale test that utilised a heating element to represent metallic parts that generate heat within a transformer. The heating element was then placed into a test-tube containing one of three types of insulating liquid (mineral oil, GTL, or synthetic ester). The condition of the liquid was varied in order to test the possibility of bubble formation against the guidance of [23] under several transformer-like scenarios.

There are several metrics by which the materials under test are to be compared in their performance with respect to bubbling. Accordant to the existing common interpretation of bubble performance seen in literature and termed within the transformer loading guides, temperature is the primary metric. Temperature is reported at the time of bubble inception (i.e. when a bubble can first be identified during the germination phase).

Secondarily, the time taken for the bubble inception to occur from the onset of power delivery to the heating element (and thus from the point of temperature rise within the insulation) are also noted. The time to bubble inception was also reported in [33, 105] but has not generally been considered as a main parameter of concern.

Different materials are used as the insulation within transformers. It is vital to understand how these materials perform under the multitude of stresses that a transformer insulation system experiences to give transformer designers, suppliers and purchasers the best information with which to select the best material for their application. This also serves to help transformer operators make use of the asset without placing it into compromising situations. Therefore, the experiments in this chapter can provide operators with more detailed guidance on the limits of operation faced by transformers, specifically in answer to

the risk of bubble formation in areas of the transformer which do not have solid insulation, but that may reach high temperatures.

5.2 EXPERIMENT MATERIAL SELECTION

The tests in this chapter cover three types of liquid insulation, those selected are: Gemini X (mineral oil), Diala S4 ZX-I (GTL oil), and MIDEL 7131 (synthetic ester). These are three of the most common types of liquid used as insulation within transformers. Current knowledge regarding bubbling within transformers is based mainly on mineral oil. There is a push to move away from mineral oil towards materials that are deemed to be safer for the environment, that extend the lifetime of the transformer, and that are lower risk (e.g. reduced risk of fires) [85]. It is thereby expected that GTL and synthetic ester insulation liquids will become more prevalent within the transformer market in the near future. It is important to ensure that the understanding of bubbling within transformers based on mineral oil translates well between liquid types. The variation of the material characteristics on some key parameters should be considered. Table 5-1 shows relevant thermo-physical properties and moisture capacity of the materials.

Table 5-1 – Selected thermo-physical properties of different insulating liquids.

Property \ Liquid	Gemini X (Mineral Oil)	Diala S4 ZX-I[#] (GTL)*	MIDEL 7131 (Synthetic Ester)
Kinematic viscosity, cm^2/s (40ºC)	0.09 [176]	0.1 [89]	0.28 [100]
Specific Heat Capacity, J/kg.K (25ºC) (typical values)	1860 [177]	2200 [118]	1880 [177]
Thermal Expansion Coefficient, K^{-1}	~8 x 10^-4 [82]	-	~8 x 10^-4 [82]
Density, g/cm3	0.88 (20ºC) [88]	0.81 [89]	0.97 (20ºC) [100]
Moisture Capacity, ppm (20ºC)	50 [178]	50 [178]	2100

[#]The designator ZX-I indicates that the insulation is a fully inhibited (X) insulating oil (Z) which conforms to IEC standard (I) and will therefore be dropped from the name of this insulating liquid for the rest of the report.

[*]For properties which are not available for Diala S4, they have been assumed similar to Gemini X values.

Moisture content is an interesting parameter in discussions of bubble formation, and has been noted as possible parameter of interest when considering differences between liquid insulators. This is further complicated by the fact that the liquid insulation moisture content changes (generally capacity increases) with temperature and also commonly with ageing [178].

The different thermal characteristics of the liquids (most notably the viscosity, but also the specific heat and thermal expansion) mean that their response to the same power input is also different. This is shown later through experiment in Section 5.4.2.4.

It is also important to keep in mind that the liquid insulation within a real transformer moves through the entire enclosure, whereas the paper / other solid insulation is static. Thus, liquid insulation may be heated at different locations within the transformer and the potential of bubble formation there needs consideration. It is this factor that forms the basis for the tests within this chapter.

5.3 EXPERIMENTAL SET-UP

5.3.1 Purpose

The purpose of these experiments is to test the performance of different insulation materials in respect to high temperature bubbling in a simplified but representative manner. Testing is conducted on different insulation materials. The small-scale nature of the experiments is used to abstract issues such as bulk liquid volumes, cooling channels, and moisture variation, while allowing a reasonably realistic assessment of the response of each material to varying conditions.

Within this chapter, the main parameters of interest are the BIT and the time to bubble inception (tBI) of three insulating liquids, tested against the guidance set out in [23]. IEEE Standard 60076-7 suggests that

> *'Bare metallic parts, except windings, which are not in direct thermal contact with cellulosic insulation but are in contact with non-cellulosic insulation (for example, aramid paper, glass fibre) and the oil in the transformer, may rapidly rise to high temperatures. A temperature of 180 °C should not be exceeded.'[23]*

therefore these tests serve to validate this criterion.

Four different conditions were tested for each of the three liquid types, these conditions are shown in Table 5-2. They represent four different stages of the liquid preparation procedure (outlined in Section 5.4.4), but each condition also represents a different situation that may occur in reality within a transformer. The situations that the tests represent at different conditions are given in Table 5-2.

Table 5-2 – Conditions of liquid insulation tested in absence of solid insulation.

Liquid Condition	Preparation Stage	Representative Situation
Fully processed	Fully prepared.	New transformer.
Gasified	Filtered and dried, not degassed.	Nitrogen blanketed transformer, liquid is fully gas saturated / close to gas saturation.
Higher particulates	Dried and degassed, not filtered.	Degraded liquid insulation with presence of particulates.
Moistened	Filtered and degassed, then moistened.	Moistened liquid insulation after a period of service life or moisture ingression

For the ‘moistened’ condition, multiple stages of moisture content are tested to find the lowest percentage saturation required to form a bubble.

5.3.2 Test Cell Construction

The test cell consists of several major parts, which can be grouped into the following categories: sample, sample support, ancillaries.

For the liquid-only tests conducted in this chapter, the sample consists of a heating element with a thermocouple affixed, immersed in insulating liquid. The thermocouple is secured in place at a position 2.5 cm from the top of the heating element with copper wire to fix it to the surface of the sample. The heating element was immersed into 38 ml of liquid insulation, irrespective of the liquid type under test.

The sample support structure is in place to hold the sample and the liquid insulation required for testing. The main support items are the glass test tube, silicone rubber stopper, and stainless steel washer supports. These materials were selected due to their known compatibility with the materials under test (solid and liquid insulation) and their stability when operating at the temperatures required in these tests.

The silicone rubber stopper has a hole to allow the heating element cables and the thermocouple to pass through, and is pierced separately by a needle, used to allow the pressure to balance during heating of the sample (as the liquid insulator expands, the head space is allowed to escape through the needle to prevent pressure build up). The needle relieves to atmosphere only; gas is not collected in these experiments.

The washers are fitted to the heating element top and base, avoiding the thermocouple head. The purpose of the washers is to maintain the position of the heating element during the test and to provide a consistent position throughout testing and across tests. The lower washer is positioned in line with the base of the parallel section of the test tube to ensure a consistent height among tests, as shown in Figure 5-1. The upper washer has a gap to allow

the thermocouple to pass through, and also to aid with oil expansion. Examples of the two washers are shown in Figure 5-2. This support structure is held in place by a clamp stand.

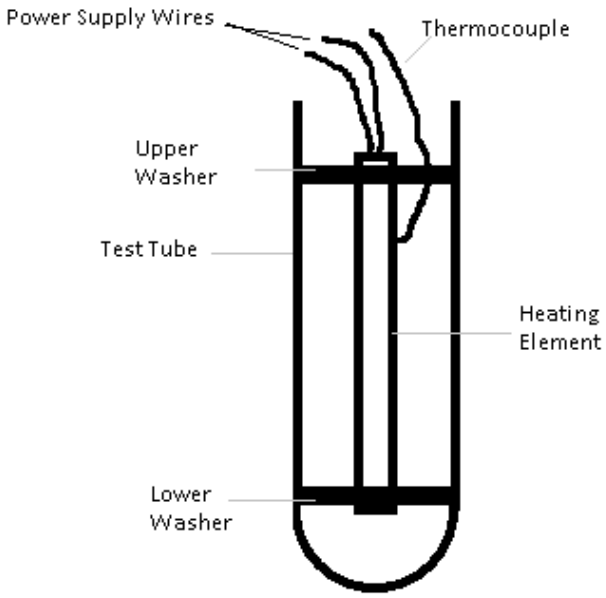

Figure 5-1 – Indicative drawing showing locations of washers supporting heating element, ensuring consistency of positioning between tests (not to scale).

Figure 5-2 – Two styles of washer used within test, with upper washer (with gap cut to allow thermocouple to pass) shown on the left, and lower washer on the right.

The power supply to the heating element was provided using a variac with maximum supply of 240 V. Power supply was controlled by using a proportional-integral-derivative (PID) controller (OMEGA CN7800) with a relay switch. Finally, the ancillary equipment which allows the experiment to be monitored is described in the following section.

5.3.3 Monitoring of Test Cell

The main requirement for monitoring is to allow for capture of the point of bubble inception. This is done by recording the sample from the front and back using DSLR (digital single-lens reflex) cameras. The intention in doing so is to have essentially 360° coverage of

the sample, shown diagrammatically in Figure 5-3. The recordings are made for 30 minutes, in accordance with the test procedure described in Section 5.4.3.

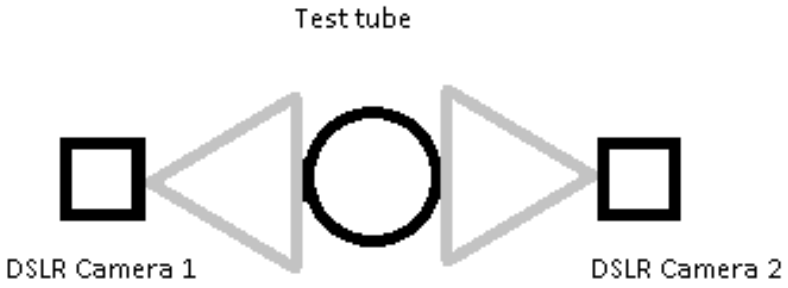

Figure 5-3 – Overhead view of camera arrangement, showing ~360 degree capture of sample.

Voltage is continuously measured using a voltmeter (TENMA 72-7735) which enables the correct setting of power input for tests, in accordance with the procedure of Section 5.4.1. Additionally, current and temperature are recorded for the duration of the test. Current is recorded with an ammeter (TENMA 72-8720), via direct link to a computer. The temperature of the heating element is measured using a Type-K thermocouple (Nickel-Chromium / Nickel-Alumel) which has accuracy of at least ±2°C. The thermocouple feeds an input to the PID controller which logs data directly to a computer.

5.3.4 Determination of Appropriate Orientation of Test Cell

Originally, it was thought that the pressure relief provided by the needle may be compromised during the test if a vertical system was used, that is, there was concern that the expansion of the insulating liquid during the test may cause it to rise above the needle tip. This could have resulted in either ejection of hot liquid from the system, or more likely simply prevention of the pressure from being balanced causing an undesirable build up within the test cell. As the test cell was not designed to be pressurised, this could result in a catastrophic failure. Therefore it was initially decided to run the tests at an angle of 30° from vertical. This arrangement could ensure that liquid rose up along the lower wall of the test tube, leaving the upper part free for gas to relieve through the needle.

Experience gained through conducting initial tests found that the liquid did not rise sufficiently over the course of the experiment to cause an issue, and thus a truly vertical arrangement of the cell was adopted instead.

Vertical testing was preferable as it is easier to control the location of the heating element, and thus to maintain consistency in the thermal profile of the heating element and

the sample across tests. Finally, video capture of the test was simplified by the vertical positioning, as a clamp stand was used to support the test tube in position, rather than a wooden support as was used for the 30° angle tests.

To ensure that the sample is in the same location across all tests, the arm of the clamp stand is checked as being parallel to the workbench before each test; thus once held by the clamp, the test tube must be perpendicular to that surface (i.e. it is vertical at 90°) and so the heating element is consistently placed in each test.

5.4 BUBBLE INCEPTION TEST PROCEDURE

5.4.1 Selection of Power Input

The primary requirement of the power input used for these tests was to be able to obtain at least the ultimate temperature of 180ºC in order to test the liquid against the limit set out in the standard [23]. Trial and error testing showed that at a power input of approximately 13 W was the minimum required to achieve this. However, the time taken to reach 180ºC was long and the rate of temperature rise slow. Given the remarks in [102] that a minimum RoCoT is necessary for bubble formation, the power input was increased.

As shown in Chapter 4, the IEC Standard 60076-7 provides a winding thermal time constant of 7 minutes for most transformer designs, with a range of 4 – 10 minutes given [23]. Increasing the power input to 20 W moved the system to a ‘winding’ thermal time constant of close to 6 minutes and initial tests showed that bubbles formed from samples under this profile. This also means that just over half of the test duration is spent at 180ºC (this ultimate temperature is achieved in just under 15 minutes). Figure 5-4 shows the profile of the HST for the power input of 20 W.

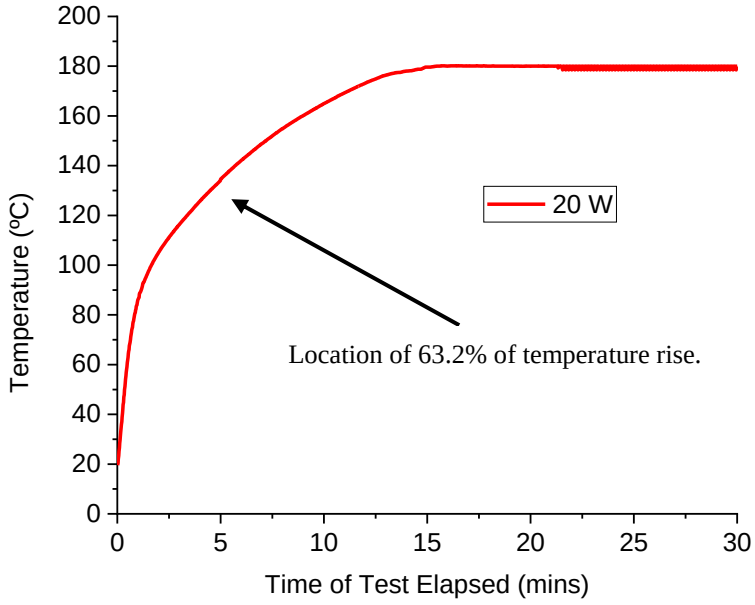

Figure 5-4 – Heating element temperature profile (measured 2.5 cm from top) in Gemini X for 20 W power input, with 63.2% achieved temperature rise identified.

5.4.2 Validation of Temperature Profile

5.4.2.1 Full Temperature Profile

One of the interesting phenomena studied in these tests in the variation of temperature across the heating element. Measurements were made at 1 cm intervals from 2.5 cm to 8.5 cm along the same surface of the heating element (distances measured from the top of the heating element). A thermocouple was secured at each location. The full profile for 20 W power injection is shown in Figure 5-5. The profile shows that the temperatures at 2.5, 3.5 and 4.5 cm are similar, with 3.5 cm approximately 1ºC higher. This meant that measurement could be made at 2.5 cm as planned without losing accuracy. The location of this measurement location is of particular importance to tests on solid insulation, on which more detail is given in Section 6.3.2.

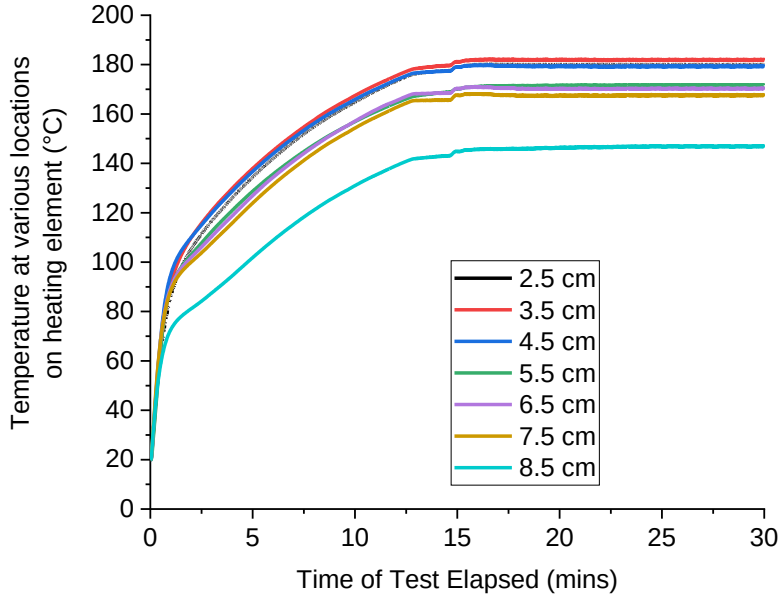

Figure 5-5 – Temperature profile over the length of the heating element in Gemini X for 20 W power input.

It is also seen from Figure 5-5 that the bottom of the heating element is significantly cooler, with a difference apparent within the first two minutes of the test. This is due to the circulation of the liquid insulation, with coldest liquid sinking to the bottom.

The reason that the hottest spot does not occur at the very top of the element is that the heat generating resistance wire is not present until around 2.2 cm from the top of the heating element: heat is generated in the lower part of the heating element, but will still conduct upwards to the top of the metal surface. This is not an issue for the experiment, but does require the thermocouple to be placed lower than 2.2 cm from the top of the heating element (it is located at 2.5 cm, as already detailed).

Bubbles are expected to form first at the top of the sample, which is the hottest section (and also has the lowest static head). Figure 5-5 shows that there is a significant proportion at the top of the sample which is at high temperature.

5.4.2.2 Repeatability of Temperature Profile

A temperature profile was generated, showing the temperature of different locations on the heating element over the duration of a thirty-minute test at 20 W power input, shown in Figure 5-5. The test was repeated using the same sample on a different day, and Figure 5-6 shows the temperature at 2.5 cm (i.e. the location of the measurement in the tests) from both tests. It is seen that the two curves are basically indistinguishable.

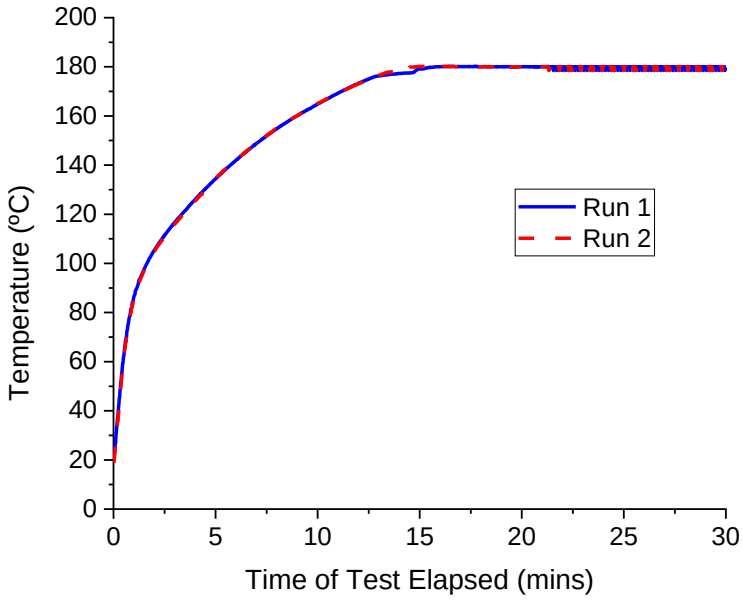

Figure 5-6 – Plot of repeated temperature measurement tests at 2.5 cm location on heating element in Gemini X insulating liquid for 20 W power input .

This outcome is necessary for the success of the experiments in this work. It ensures that tests are comparable and means that BIT in tests can be established from this reference temperature profile.

5.4.2.3 Influence of Ambient Temperature on Heating Element Temperature Profile

The ambient temperature of the laboratory is not controlled, and therefore temperatures may differ by several Kelvin between tests as the testing period extends over several months. The initial temperature of the sample may also then differ by this amount between tests (as the test begins at ambient conditions), and colder ambient temperatures will cool faster than hotter temperatures. It is found that the small variation of starting temperature is not important for the testing temperatures; the difference is subsumed almost immediately due to the input of energy to the system. An initial difference of a few Kelvin is not large in comparison to the energy input to the system throughout the test.

In Figure 5-6, the temperature of the test which starts at a lower temperature (blue line) catches up to (or at least does not lag behind) the test with higher initial temperature (red line). The difference in initial starting condition is visible in Figure 5-7. The initial difference of 2.4 Kelvin is subsumed within 2 minutes of the test, and the profiles are a similar shape.

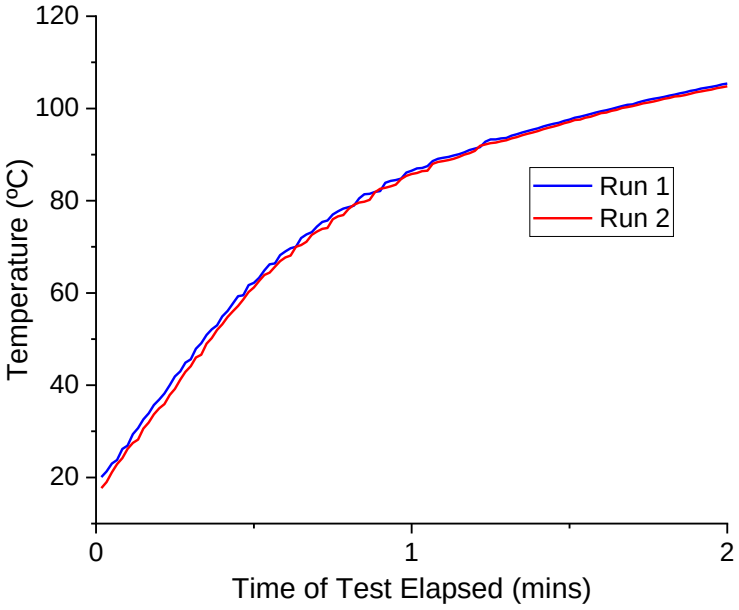

Figure 5-7 – Zoomed temperature profile showing several Kelvin different in starting temperature.

5.4.2.4 Temperature Profile of Alternative Insulators

The three liquid insulators have different thermal properties (with some shown in Table 5-1). The key relevance to this study of this fact is that the temperature response of the three liquids to the same power input will differ. Figure 5-8 plots the temperature profiles of each of the three liquid types for a 20 W power input.

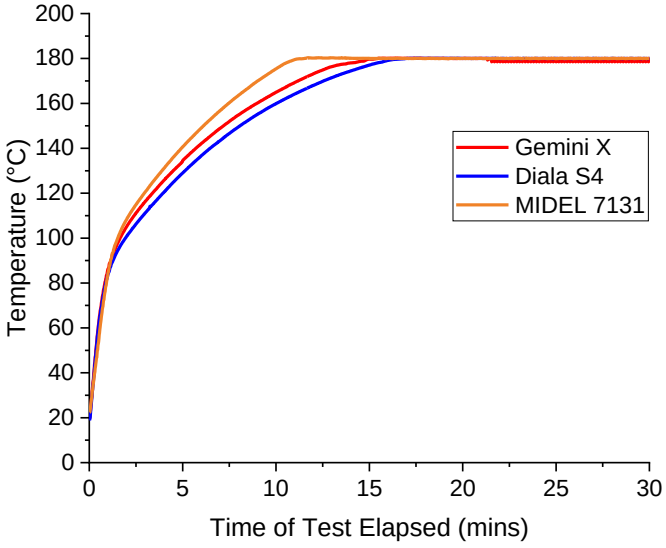

Figure 5-8 – Temperature profile of heating element at 2.5 cm of three different insulating liquids in response to same 20 W power injection.

There is a notable difference in the time taken to reach 180ºC, with the synthetic ester liquids rising fastest in temperature followed by the hydrocarbon liquids, which have more

similar trends. Differences are noticeable after approximately 2 minutes. All three liquids control well at 180ºC once it has been attained, and there is no overshoot beyond 180ºC in any of the liquids.

5.4.3 Test Duration

The tests are conducted for thirty minutes from the moment that power is applied. This is in line with the short term overload period advised in [23], and means that there is a consistent period allowed between liquids and conditions. Tests are continued to thirty minutes even if a bubble occurs during the test to allow observation of the continued bubbling behaviour (if any) of the liquid insulation during such an overload test.

5.4.4 Liquid Insulation Pre-processing Procedures

Before use, liquid insulation is prepared in accordance with best laboratory practice, and aiming to replicate the processes that would be undertaken with real transformer liquid due to enter service.

5.4.4.1 Filtering

For use in a transformer, the contamination of the insulating liquid by particles should be minimised. High particulate count can lead to increased likelihood of failure through partial discharges and breakdown, although as with bubbles, it can be difficult to provide exact evidence showing particulates as the cause of a failure post-event [179].

Hence, in order to achieve conditions of low particulate contamination for these experiments, liquid insulation is filtered through a 0.2 μm nylon gauze filter. It is typical to report contamination levels as the count of particles >5 μm per 100 ml of liquid [179]. Each liquid has its own filter (to avoid cross-contamination). Liquids are filtered into pre-cleaned bottles and sealed with caps to prevent recontamination during storage. Filtering is aided by pulling vacuum on the filter.

5.4.4.2 Drying

After filtration, the liquid insulation is dried by purging with dry nitrogen gas. Purging is conducted at 1 l/min of nitrogen for 1 hour per litre of liquid for mineral oil and GTL, and for 1.5 hours per litre of liquid of synthetic ester. Drying was conducted for these periods to ensure that moisture content in the liquid was <10% RS at room temperature (esters have a longer period due to their increased viscosity and the higher amount of absolute moisture to be removed from them). This provides a consistent starting point for the tests, and accords

with both the specification for liquid used in new transformers [108] and best practice [37]. After drying, samples were degassed at <5 mbar pressure (room temperature) to remove as much dissolved nitrogen as possible. A period of 30 minutes was sufficient for this stage of the process as bubbles were no longer observed leaving the liquid after this period.

5.5 Testing of Material Conditions

To fully describe the conditions of the liquids under test, the following laboratory tests are carried out on liquid samples.

5.5.1 Particulate Matter Tests

The particle count of the liquid insulation is measured by a method known as 'light blocking', using a HIAC ABS-2, Automatic Bottle Sampler and HIAC 8000A Liquid Particle Counter (both from Hach). This method works by shining light of known intensity through the liquid as it flows; particles present within the liquid will block the light and thus the light leaving the liquid will be reduced in intensity, and this is the measurement made. According to [179], this is by far the most commonly used method in laboratories.

To perform the test, the automatic sample takes a 10 ml sample of prepared liquid and shines light from a laser diode through it, making a measurement of the received light intensity as explained above. The test is repeated twice and results are provided in on cumulative and differential count bases for particle size ranges up to 100 μm. The cumulative count is deemed of most importance for this work, and total particulate count should be less than the advised upper limits.

Within this work on bubble formation, it is important to monitor particulate content for three main reasons: firstly, to maintain conditions as close to expected reality as possible; secondly, to ensure that samples are as repeatably conditioned as possible; and finally because it is thought that the presence of small particles may aid bubble formation by providing a site for nucleation [126]. The last of these concepts is tested in Section 5.6.3 where filtering has not taken place.

5.5.2 Moisture Tests

Moisture is determined through coulometric Karl Fischer (KF) titration from the electrochemical generation of iodide ions (I^-) from water (H_2O) and iodine (I_2). Coulometric titration is known to detect smaller concentrations than volumetric titrations [180], which is particularly important for dry paper and dry mineral oil measurements. The equipment used

for the test is the 831 KF Coulometer and the 832 Thermoprep. KF titration is critically reviewed in [181].

Moisture content of the liquid insulation is measured before the bubbling test using coulometric KF titration. For these moisture measurements, the liquid insulation is assumed to be in equilibrium, i.e. it is equally dry at all locations.

To test the amount of moisture present in the liquid, 3 ml samples are pipetted into 9 ml glass headspace vials and sealed by crimping on aluminium caps. The mass of the 3 ml sample is measured using XB 120A Presica weighing scale (Precisa Instruments Ltd, Switzerland). The caps have a butyl rubber septum which is pierced by a needle during the titration. The vial containing the sample is placed into an oven at 140^{o}C, and as the temperature increases, moisture is evaporated from the paper sample and is transferred through the needle to the titrator where the amount of moisture present is measured. The titrator reports the amount of moisture present based on 1 g of sample and this is corrected to the actual mass by dividing the reported value by the measured mass of liquid, giving a final result in ppm.

5.6 Results of Liquid-only Bubble Formation Tests

5.6.1 Fully Processed Liquid-only Tests

The tests showed that for any of the liquid insulation type tested, the fully processed conditions (i.e. conditions as per Section 5.4.4) never saw bubbles form during the testing procedure (shown in Section 5.4). Each liquid was tested on three occasions.

This is an important result as it confirms that the guidelines of IEC Standard 60076-7 [23] are sufficient to protect the transformer from bubbles when transformer liquid insulation is new. It is also useful because IEC Standard 60076-7 applies to mineral oil transformers, but the criterion does not require specificity for GTL oil, natural esters or synthetic esters based on the results of these tests - the same limitations can be safely applied.

5.6.2 Gasified Liquid-only Tests

The gas content of the liquid insulation is a parameter included within the formula of [22, 71], and was varied within the tests of [137]. However, it seems that only at exceedingly high gas in oil content coupled with high moisture content in paper was there a notable effect in previous tests.

Bubble Formation in Liquid Insulation

As suggested in [134], once the local partial pressure increases above the system pressure, gases will bubble out of the liquid insulation, and this may occur as a combination of different gases. The tests of [131] show that gases can evolve from paper insulation in similar tests with paper and oil insulation, and the cases evaluated in [134] show that the generation of gaseous material from paper can contribute to bubble formation in transformers. However, [134] also shows that temperature increases can generate bubbles directly from gases pre-existent within the insulating liquid.

Therefore tests were conducted on samples of insulation liquid (for each of the three liquids mentioned) where the liquid was filtered and dried, but not degassed – i.e. the liquid was essentially saturated with nitrogen gas without presence of paper insulation (saturation of nitrogen within the insulating liquids is ~70,000 ppm).

No bubbles were observed for any of the liquids tested, with each liquid tested twice for gasified conditions. The implication being that the nitrogen gas dissolved in liquid was either held more tightly within the liquid, or that bubbles could not form without the nucleation point provided by the paper insulation. Note that the Ostwald's coefficient for nitrogen is positive [182], indicating increasing solubility within increasing temperature.

5.6.3 Higher Particulate Count Liquid-only Tests

To obtain the samples with higher particulate content, the liquids were not filtered during the preparation stage. All other stages of preparation were adhered to as in Section 5.4.4. The particulate matter within the liquids with and without filtering is shown in Table 5-3. Note though that synthetic ester, even without filtering, had a particulate count that did not exceed the limit of a count of 1,000 particles of ≤5 μm per 100 ml suggested for new installations (i.e. those undergoing factory acceptance tests) in [179]. All other liquids fall within the 'normal' classification for particulate condition before filtering, i.e. GTL and mineral oil were both above the 'low' threshold. After filtering, the particulate count was always below that threshold. Therefore, these tests (particularly on GTL and mineral oil) compare bubbling likelihood for these liquids at start-up (after filtering) to the likelihood through-life (pre-filtering).

Table 5-3 – Particulate matter count for liquids before and after filtering with 0.2 μm gauze

Liquid Type	**Particulate count after filtering (<5 μm / 100 ml)**	**Particulate count before filtering (<5 μm / 100 ml)**
Mineral Oil	345	11370
GTL Oil	445	4190
Synthetic Ester	185	445

Bubbles were not evolved from the liquid insulation during these tests (with each liquid tested twice in the unfiltered condition), suggesting that even though a potential nucleation site was present for the bubble tests when more particulates were present, sufficient material (moisture or gases) was not available to generate bubbles.

5.6.4 Moistened Liquid-only Tests

Tests were conducted on liquid-only samples for each of the four liquids considered within the study, at various relative moisture contents. Calculation of RS in this section is always considered against the room temperature saturation capacity. The moist samples were obtained by pipetting small amounts of moisture into large containers of the liquid, and then stirring (using a magnetic stirrer at ~400 rpm) for five days to ensure assimilation.

The synthetic ester liquid did not bubble, even at approaching 100% saturation (final value tested: 99% RS). The mineral oil and GTL tests had bubbling start at 78% RS. Two tests were conducted at each condition, and the BIT results are summarised in Table 5-4.

Table 5-4 – Results of bubble tests on moistened liquid-only samples.

Liquid	Test Number	Relative Saturation (%)*	Bubble Inception Temperature (°C)	Time to Bubble Inception (sec)
Gemini X	1	78	101	103
	2	78	109	138
Diala S4	1	78	92	75
	2	78	94	82

*RS calculated based on KF titration measurement and moisture capacity shown in Table 5-1.

The bubbles seen during these tests were small and infrequent, but did continue to form throughout the tests. The bubbles also formed at the surface of the heating element, indicating that a nucleation point was required.

A relative moisture content as high as 78% within transformer insulation liquid is likely to be uncommon. One scenario where it could occur would be a high loading situation followed quickly by a low loading situation or outage. Here, the moisture leaves paper into liquid as the transformer heats up during the high loading period, and then the moisture tries to reverse direction during the cooler period. Unfortunately, the return of moisture to paper is a much slower process, and even formation of free water is a plausible outcome [183]. If a second high load occurs, this could then cause bubbles to form from oil in contact with hot bare metal and so this is something operators should be wary of, despite the relatively low

probability. Such cases are purported to have led to failure of transformers, even leading to fire and explosion.

5.6.5 Summary of Liquid Insulation Results

Results of the liquid-only tests conducted in this chapter are given in Table 5-5. For liquid-only tests, it was shown that the conditions of the insulation need to be severe in order to form bubbles. This gives the important information that the solid insulation must be the most critical source of bubbling from the tests where solid and liquid insulation is present. The only condition tested under which bubbles formed was high moisture content, in excess of 78% RS (room temperature basis). This is not likely to be a common situation within a transformer. However, a period of high temperature will drive moisture from the solid insulation into the liquid insulation. The process for moisture returning to the solid insulation is slow and therefore the liquid insulation moisture saturation would be increased once the high temperature period ends. A high temperature event after this could then evolve bubbles away from the solid insulation. IEEE Standard C57.91 suggests a higher temperature limit during short term emergency loading of 200°C for 'other metallic hot-spot temperature (in contact and not in contact with insulation)' [22], but this was not used during these tests. Note that this condition was only present in hydrocarbon-carbon based liquids, and the ester liquid tested did not show bubbles up to 100% RS.

Table 5-5 – Summary of liquid-only test results (times, *t*, and temperatures, ϑ, shown are averages of all results).

Condition / Liquid	Fully Processed	Gasified	High Particulate Count	High Moisture Content
Gemini X	No bubbles formed.	No bubbles formed.	No bubbles formed.	Bubbles formed at 78% RS: ϑ = 105°C t = 121 s
Diala S4	No bubbles formed.	No bubbles formed.	No bubbles formed.	Bubbles formed at 78% RS: ϑ = 93°C t = 79 s
MIDEL 7131	No bubbles formed.	No bubbles formed.	No bubbles formed.	No bubbles formed up to 99% RS.

5.7 SUMMARY

Experiments have formed the backbone of previous research into bubbles, and there is still much to be uncovered about the mechanism of bubble formation within transformers. This chapter has described some of the main considerations when designing an experiment

for looking at transformer insulation bubbling, and explains the rationale for selections made for the tests that were conducted. This experimental set-up is further utilised and developed in Chapter 6. Results of tests of bubble formation in systems with liquid insulation not in contact with solid insulation are also detailed for a number of important cases.

Tests are on a test-tube scale, where a load is applied to a resistive heater in order to replicate the thermal rise of a transformer at peak load conditions. The tests look for 'failure' in terms of bubble formation (identified visually), during a 30 minute duration (testing the short term overloading limitations of [42]). Different liquid insulation materials are tested across a range of conditions.

Key considerations for experiments are: the capture of 360º of the sample; initial conditions liquid insulation; the variables and parameters which need to be measured.

Results of tests on liquid insulation in absence of solid insulation are presented, summarised in Table 5-5. The results show that it is difficult to form bubbles under such conditions; only in particularly wet hydrocarbon-based liquids did bubbles form. Saturation with gas, or contamination with particles, did not generate bubbles, and nor did bubbles form from liquid in fully processed condition (under the temperature profile shown in Figure 5-4). This is a positive result for transformer operation, meaning that the areas where hot solid insulation is not present are at low risk of bubbling, and following the temperature guidance of [23] can protect transformers from bubbles in areas of liquid contact with hot metal.

6 IMPACT OF LOADING AND SOLID MATERIAL SELECTION ON BUBBLE FORMATION

6.1 INTRODUCTION

Chapter 5 established an experimental set-up and tested liquid insulation for likelihood of bubble formation. This chapter develops the experimental design further, to include solid insulation, and then tests two types of solid paper insulation for likelihood of bubble formation. Also in this chapter, the effects of different load profiles on bubble formation are analysed. This chapter further analyses the mechanism of bubble formation, honing in on how the moisture behaves between insulation media, and how that is influenced by the thermal profile of the system.

The experiments within this chapter are done using mineral oil (Gemini X), allowing the focus to be on the solid insulation. Two types of solid insulation are compared, non-thermally upgraded paper (NTUP), and thermally upgraded paper (TUP). Full details of these insulation materials are provided in Table 6-1.

Low carbon technologies are being installed to replace traditional carbon-based sources of generation and to reduce or displace electricity demand. These changes should result in a reduction of GHG emissions; however they may also cause a change in load profile. The load profile of a transformer is tantamount to its performance: load and temperature are intertwined, and temperature is considered to be a key factor in how quickly insulation ages and thus how long the transformer can be put to useful service. For this study, changes in load (and thus temperature) profile are considered because the impact on bubbling can be profound.

As a result, a better understanding of the limitations of transformer thermal capacity is gained, with specific insight of the differences in bubbling behaviour among materials and against the loading demand placed on the transformer.

6.2 EXPERIMENTAL MATERIAL SELECTION

Two types of solid insulation were selected for the experimental work of this study. They are both Kraft papers, one of which has been thermally upgraded. The majority of the paper insulation, and the majority of the hot solid insulation, within a transformer would be one of these two papers in most cases. This is the most active part of the solid insulation with

respect to moisture, and as it is in direct contact with the windings, it is liable to attain high temperatures, thus being the most likely site for generation of bubbles.

Relevant material characteristics of the two papers are shown in Table 6-1. Figure 6-1 (a) shows the NTUP and Figure 6-1 (b) shows the TUP. The brown colour is the natural colour of the paper; the blue colour is a dye which indicates the thermal upgrading. The influence of the dyeing can be seen in the value of the conductivity of the aqueous extract in Table 6-1, where the TUP is significantly higher. The paper type is IEC type 5A2-2H1 for NTUP and IEC type 5B2-2H1 for TUP [184] and was supplied by WEIDMANN Electrical Technology AG.

Table 6-1 – Average values for the material characteristics of non-thermally upgraded paper insulation and thermally upgraded paper insulation, based on IEC Standard 60554-3-5 unless otherwise stated.

Characteristic	NTUP	TUP
Thickness (µm)	48	51
Grammage* (g/m^2)	40	43
Tensile Strength (Nm/g)		
• Machine Direction	107	104
• Non-machine Direction	53	53
Degree of Polymerisation#	>1000	>1000
Water Absorption (mm/10 min)	7	7
Conductivity of Aqueous Extract (mS/m)	3.3	4.8
Nitrogen Content† (%)	0.0	3.0

*Grammage calculated as density / thickness.
#Degree of polymerisation tested in-house following method based on American Society for Testing and Materials (ASTM) [185] and IEC [186] standards.
†Nitrogen content determined by supplier using Kjedhal method.

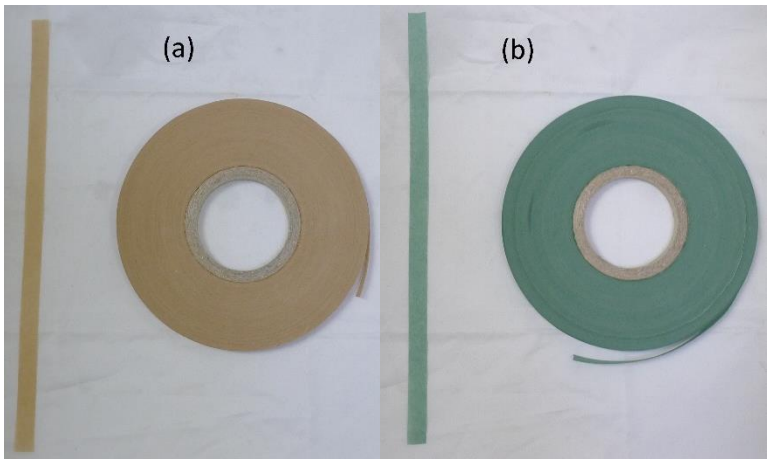

Figure 6-1 – (a) Non-thermally upgraded Kraft paper and (b) thermally upgraded Kraft paper used in experiments.

These two types of paper insulators are commonly used in transformers, and so investigation into their performance is appropriate. It is noted that the majority of experimental work to date on the bubbling performance of paper insulation has been done on NTUP, and so it is also helpful to compare the performance of TUP to ensure that the understanding of bubbling

maps between paper types. The main difference between the two materials (colour notwithstanding) is the nitrogen content (i.e. the proxy for the amount of thermal upgrading agent added). The paper used herein has a relatively high degree of thermal upgrading [48], in the expectation that this will give the clearest results if any differences do exist.

6.3 EXPERIMENTAL SET-UP

6.3.1 Purpose

The experiments in this chapter test two types of solid insulation: NTUP and TUP. The tests are conducted across a range of values for moisture content in paper, and look for the BIT and tBI. As before, the small-scale nature of the experiments is used to abstract issues such as bulk liquid volumes, cooling channels, and moisture variation, while allowing a reasonably realistic assessment of the response of each material to varying conditions.

6.3.2 Test Cell Construction

6.3.2.1 Paper Wrapping Technique

The test cell itself is similar to that described in Section 5.3.2, however, the sample now includes two layers of paper, wrapped around the heating element. This is shown in Figure 6-2. The location of the thermocouple is identical to that in the liquid-only tests, however, it is now wrapped with two paper layers as well. As seen in Figure 6-2, the paper is secured to the heating element by use of three turns of copper wire. Excess paper is wrapped beyond the bottom copper fixing of the sample, and this is used later for measurement of the initial sample moisture content. Individual layers are self-abutting, and the upper layer overlaps the inner layer by 50%.

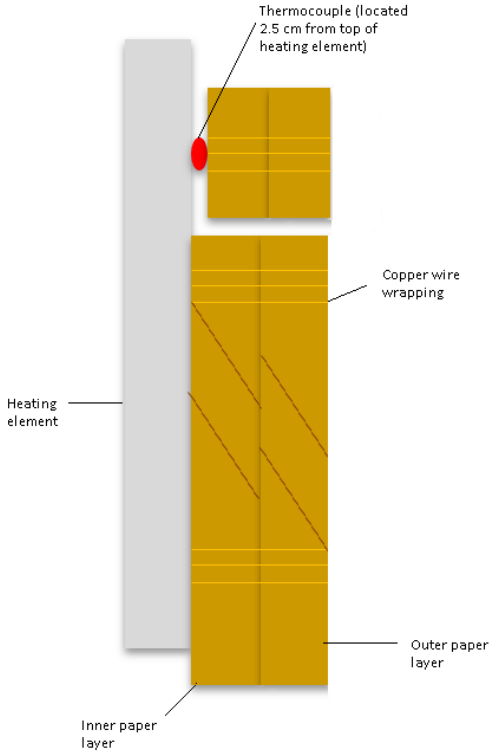

Figure 6-2 – Axisymmetric axial cut through of sample, showing paper wrapping technique (where dark brown lines show the locations of overlaps). Red dot indicates the thermocouple location. (Drawing is approximate - not to scale).

Two pieces of paper, each 1.5 cm wide and 12 cm long, are cut to be wrapped by hand in a 50% overlapping method (that is, the outer layer overlaps the inner layer by 50%; individual layers are self-abutting), shown for an NTUP sample in Figure 6-3. Two layers of paper of these dimensions have a combined mass of approximately 0.14 g (based on grammage from Table 6-1). The volume of liquid used in the tests is 38 ml (irrespective of the liquid selection, and so the mass varies slightly based on density values in Table 5-1). This means that the oil:paper ratio is in the region of 1:271 (mass:volume basis). This is at the high end of typical values, and as a small section of paper is removed pre-test, the actual value during tests will be higher than this.

The thermocouple is secured 1 cm above the sample area (in the same location as in the liquid-only tests, meaning that the temperature measurement and the temperature of the sample can be consider as per the measurements shown in Figure 5-5. When the upper and lower washers are added, they are placed such that they do not contact (and hence do not influence) the sample area.

Figure 6-3 – Example of paper wrapping.

Repeatability in the construction of samples is important so as to ensure that differences do not influence results of bubble formation tests. Figure 6-4 and Figure 6-5 show a selection of prepared samples for NTUP and TUP, respectively.

Figure 6-4 – Consistency in construction of wrapping technique of NTUP samples.

Figure 6-5 – Consistency in construction of wrapping technique of TUP samples.

6.3.2.2 Validation of Number of Solid Insulation Layers

The solid insulation of a transformer winding would typically consist of multiple layers of paper wrapped around the copper conductor. In order to best identify the mechanism of bubble formation within transformer insulation systems, the number of paper layers had to be determined.

Initial tests (at 13 W power input) on samples of a single layer of paper failed to produce bubbles, even at high moisture content. Thus, a second layer was added. Tests at 13 W then saw production of bubbles at elevated temperatures.

Due to the increased difficulty of manual wrapping, additional layers are not desirable. Added layers also make it more difficult to view the mechanism of bubble formation, particularly through inner layers. Initial tests at 20 W also showed that increasing the number of layers (from two to six) produced a slight increase in BIT, as shown in Figure 6-6.

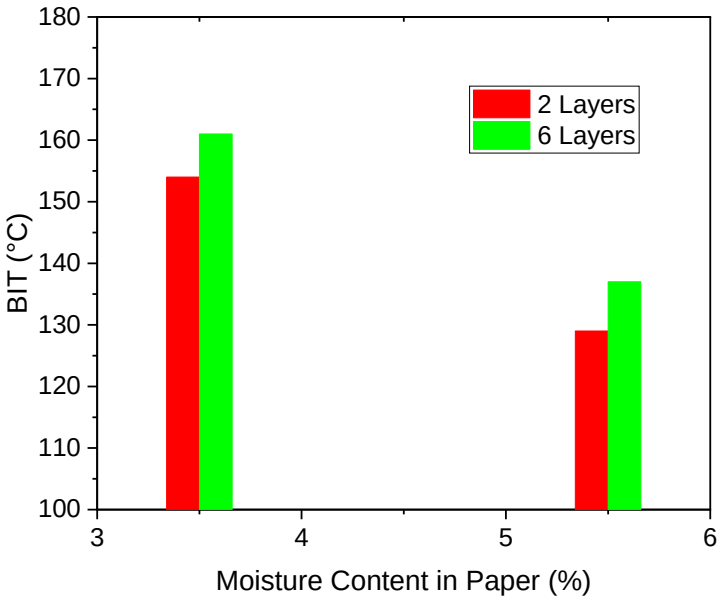

Figure 6-6 – Initial BIT results for 2 layer and 6 layer paper wrapped sample tests.

It was therefore determined that in order to best identify the mechanisms that drive bubble formation within transformer insulation that two layers of paper insulation per test would be optimal.

6.3.3 Monitoring of Test Cell

As with the liquid-only tests, the positioning of the DSLR cameras for capturing bubbles as they release is important. Figure 6-7 shows an example of the image capture for a TUP sample.

Figure 6-7 – Camera recording of TUP sample, at beginning of test.

6.4 BUBBLE INCEPTION TEST PROCEDURE

6.4.1 Test Duration

For the experiments involving paper insulation, two durations of test will be conducted: a) thirty-minute tests and b) bubble only tests. The thirty-minute tests last for the full 30 minutes, following the profile of Figure 5-4, irrespective of bubbling behaviour. In contrast, bubble only tests will last only until the first bubble is observed (i.e. always less than 30 minutes), at which point the power supply is turned off.

Both tests have advantages. Primarily, this can be as follows:

- Thirty-minute tests match with the short term overload guidelines and thus show the bubbling risk over such conditions,
- Bubble only tests allow for assessment of how material conditions have changed in the period only up until the first bubble formed, giving insight into formation mechanisms.

6.4.2 Selection of Power Input

For tests which allow comparison between NTUP and TUP, the same profiles is used as in Figure 5-4. However, tests are also conducted in this chapter to uncover the influence of the load profile on the results. In order to investigate the impact of increased loading, two further profiles were established, of 26 W and 32 W power injection. The temperature profiles associated with these power inputs are shown in Figure 6-8, along with the 'base load' of 20 W for comparison. The time constant for both of these profiles was accordantly shorter (i.e. they represent a faster rate of temperature rise). These profiles are controlled in the same manner as the 20 W profile, with 180ºC maintained once achieved, until a total experimental time of 30 minutes is attained. Note that the time taken for the HST to reach 180ºC is 8 minutes and 5 minutes for the 26 W and 32 W profiles respectively (though note that the 32 W profile shows a slight overshoot in temperature and settles back to 180ºC just before the 26 W profile at approximately 8 minutes).

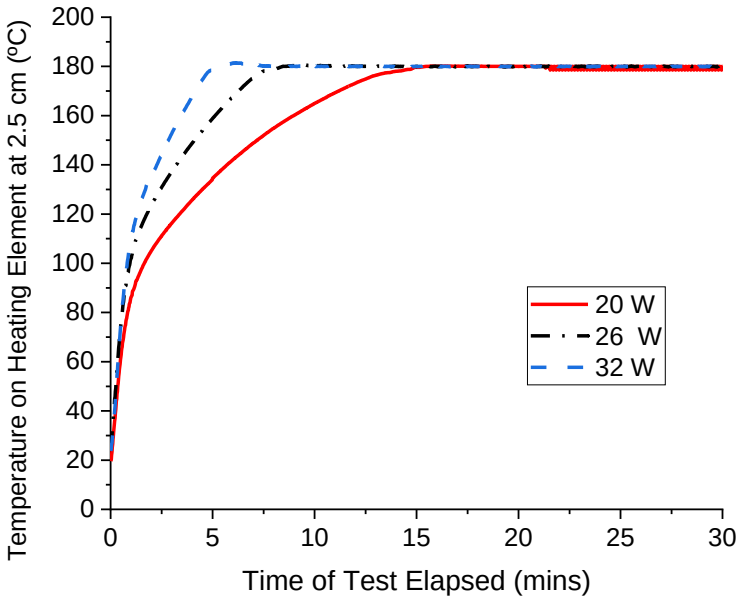

Figure 6-8 – Heating element temperature profiles of three levels of power input.

6.4.3 Paper Sample Pre-processing Procedures

6.4.3.1 Paper Insulation Drying and Impregnation Procedure

Paper insulation is dried in a vacuum oven for 48 hours at 105°C and <5 mbar. NTUP moisture content is <0.5% and TUP <0.3% after drying under these conditions. However, re-exposure to the atmosphere would result in re-moistening of the paper, and potentially lead to air entering between paper layers or between the inner layer and the heating element.

Either of these situations would be undesirable in terms of the control of the bubbling within tests.

Therefore, after drying of the paper insulation, liquid (pre-processed already, per Section 5.4.4) is introduced to the oven without breaking vacuum to impregnate the paper. The impregnation also takes place under a vacuum (<5 mbar) for a further 48 hours, but at a temperature of 60°C. This lower temperature ensures that the liquid insulation does not thermally degrade, that any potentially volatile additives (such as oxygen inhibitors) are not extracted unwarrantedly, and it also means that the paper insulation is not exposed to high temperatures for longer than necessary, thus ensuring the integrity of the initial degree of polymerisation (DP), yet it is still sufficient to ensure that the liquid is reduced enough in viscosity to aid with the impregnation of the paper insulation.

Impregnation ensures that gaps and capillaries in the paper are filled with liquid, and hence cannot be filled with air or moisture (or anything else) once the vacuum is lifted after drying is complete. This is a particularly vital stage in the processing of samples for bubble formation. The liquid and paper insulation are considered ‘dry’ and ‘gas free’ at the end of this procedure. Figure 6-9 shows some NTUP samples in Gemini X immediately after the impregnation stage.

Figure 6-9 – NTUP samples immediately after impregnation with Gemini X, before re-moistening.

6.4.3.2 Sample Moistening Procedure

Once fully prepared, dried and impregnated, the samples (heating element wrapped with paper, immersed in liquid) are moved to desiccators prepared at different relative

humidity (RH) in order to produce samples of different paper moisture content. Figure 6-2 shows the RH and moisture content relationships used in this study. The desiccators were prepared using saturated salt solutions or silica gel balls, as indicated in Figure 6-2. The sample moistening takes place at room temperature. These conditions represent the full range of moisture values that a transformer may experience throughout its life [143].

Table 6-2 – Sample moistening conditions. Moisture contents shown for paper samples impregnated with Gemini X, small deviations occur for other liquids.

Relative Humidity of Desiccator (%)	Approximate Resultant NTUP Paper Moisture Content (%)	Approximate Resultant TUP Paper Moisture Content (%)	Material used for Desiccator Preparation
Dry	<0.5	<0.3	Direct from vacuum oven
7	1.5*	0.5#	Silica Gel
13	2.9	2.0	Lithium Chloride
26	4.5	3.2	Potassium Acetate
30	5.1	4.1	Super-saturated Potassium Acetate

*Assumed value based on Oommen's curve [187] (7% RH samples not tested).
#7% RH TUP samples not tested, value assumed based on differences to NTUP at other RH values.

A period of 28 days was long enough to moisten 3 mm thick pressboard to 97% saturation at room temperature in [188] and so samples for these tests are left for at least 30 days to ensure they reach equilibrium. A 'before test' sample is tested for moisture content for each sample.

6.5 Testing of Material Conditions

6.5.1.1 Degree of Polymerisation

It is well understood that temperature accelerates reduction of cellulose DP. The tests conducted on paper samples are done with the temperature profile given in Figure 5-5, and this is above transformer rated temperatures for the majority of the test.

It could therefore be considered that the change of DP over the test could influence the BIT results. Calculation suggests that any influence would be negligible. Using a formula from IEEE Standard C57.91 [22], given in Equation (6-1), change in DP can be calculated. This equation allows for the calculation of a dimensionless 'accelerated ageing factor' (F_{AA}) which is a multiplicative factor describing how the ageing of the paper progresses compared to the ageing expected at the rated temperature (i.e. 1 per unit life). To do so, the equation finds a ratio between the energy and temperature component of the reaction rate formula (i.e. the exponential of reaction energy divided by the ideal gas constant, *B*, divided by

temperature, ϑ) at two conditions, the rated condition (subscript *r*) and the actual HST (subscript *h*).

$$F_{AA} = e^{\left[\frac{B}{\vartheta_r} - \frac{B}{\vartheta_h}\right]} \tag{6-1}$$

Annex I of [22] provides a list of possible values of *B*, which differ depending on the end of life criterion selected. A *B* value of 11,720 is shown for end of life criterion 'DP = 200' from [189], a criterion which is in common use today. Using this value, and temperatures of 98ºC and 180ºC, F_{AA} is evaluated to 304. This factor is large, meaning that ageing of insulation is greatly accelerated (expected outcome for such high temperature).

However, despite the acceleration of ageing suggested by this accelerated ageing factor, the total time of the test is short, and so the loss of DP is mitigated. For the thirty-minute test, the equivalent ageing period is approximately 150 hours. Assuming a final DP of 200, the expected life of a transformer operating at constant rated load is 150,000 hours [22]. Therefore, the reduction of DP experienced in the test can be estimated (by assuming that DP reduces linearly in this region [31]) as:

$$\frac{Equivalent\ Ageing\ Period}{Total\ Lifetime} \times (Initial\ DP - Final\ DP)$$

$$= \frac{150}{150{,}000} \times (1000 - 200) = 0.8$$

This is a minor reduction in DP, and even allowing for a slightly faster initial rate of DP depletion, the reduction is in the order of tens (even a 100-fold acceleration of the initial rate would lead to a decrease of only 80 DP, which is still relatively insignificant). There is a limitation to this method of calculation as it assumes that the ageing mechanism does not alter (and so *B* is maintained) across the temperature range. As the actual HST diverges further from the rated value, the calculation will become less accurate. However, as an indicative calculation, this shows that the ageing of the paper throughout this test is not sufficient to cause concern about the impact on BIT, particularly as this is a 'worst case' assessment, considering 180ºC for the entire 30 minutes, whereas bubbles will be expected to form early within the test and at temperatures below 180ºC.

To confirm whether this calculation is accurate, a selection of the samples will be tested for DP, using a viscometric method based on ASTM [185] and IEC [186] standards. The test involves dissolving paper in copper(II) ethylenediamine (cuen) solution and measuring the residence time of the solution against a blank (containing no paper).

6.5.1.2 Moisture Tests

The testing of moisture is of paramount importance to this investigation. Determination of the initial and final conditions of the solid insulation has two purposes. Firstly, the initial moisture content is the value plotted against the times and temperatures for bubble formation and therefore this value must be captured. Secondly, the change from starting moisture to final moisture can be analysed to give a picture of the moisture behaviour within the insulation.

As for the tests of liquid insulation, moisture of paper samples is determined through coulometric Karl Fischer (KF) titration. Samples are taken before and after bubble inception tests. The inner and outer layers are both tested.

Before the test, moisture samples are cut from the bottom of the sample, below the actual test area (indicated in Figure 6-2). To mitigate against the potential for ingress of moisture or air to the samples when cutting the moisture test section away, the process is conducted within a container of liquid insulation (of the same conditions as for the test, i.e. room temperature, dried and degassed). All efforts are made to minimise the time taken for this process without damaging or altering the sample.

After the test, the sample area is cut into four pieces: upper and lower sections of the inner and outer layer. Paper insulation is sampled 15 minutes before the bubble test for the before test sample. The after test samples are taken as soon as the sample cools to 40°C, which is achieved approximately 15 minutes after the test under natural cooling in air. This sampling split is shown in Figure 6-10.

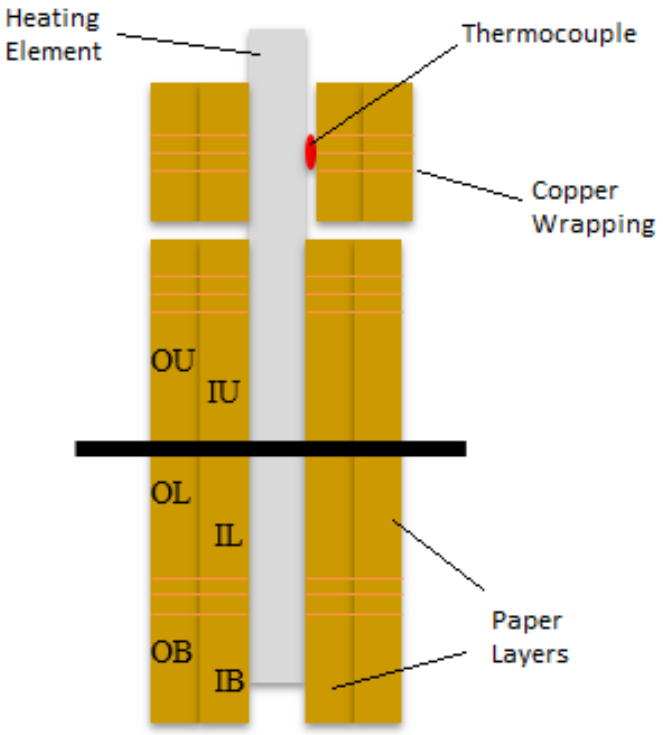

Figure 6-10 – Arrangement of sampling locations for paper moisture content samples. OU – outer layer upper piece (post-bubble test sample), IU – inner layer upper piece (post-bubble test sample), OL – outer layer lower piece (post-bubble test sample), IL – inner layer lower piece (post-bubble test sample), OB - outer layer bottom piece (pre-bubble test sample), IB – inner layer bottom piece (pre-bubble test sample). Not to scale.

Once cut, samples are placed into 6 ml glass headspace vials and sealed by crimping on an aluminium lid. The lid has a butyl rubber septum which is pierced by a needle during the moisture test. The testing procedure is based on IEC Standard 60814 [190]. The vial containing the sample is placed into an oven at 140ºC, and as the temperature increases, moisture is evaporated from the paper sample and is transferred through the needle to the titrator where the amount of moisture present is measured. This amount is reported as a parts-per-million (ppm) value on an assumed sample weight of 1 g. This must be adjusted to the actual mass of paper used in the test, on a dry basis.

To obtain the mass of paper on a dry basis, it is first washed with heptane to de-oil the paper. The paper is then dried in an oven at 80°C to remove any heptane or moisture. The mass is then obtained using an XB 120A Presica balance (Precisa Instruments Ltd, Switzerland). Due to the small mass of paper used in the moisture tests (~0.1-0.2 mg), weighings are repeated until three concordant measurements are achieved. Concordance is assumed as a range of 0.5 µg. The value of moisture given by the KF titration is divided by the mass of paper in grams to give the final moisture content of the paper.

6.6 Results of Tests on the Influence of Material Selection and Loading on Bubbling Performance

Within the following sections, the results of the experiments with paper insulation are detailed.

6.6.1 Comparison of Solid Insulation Bubbling Performance

The first comparison conducted in this chapter is between NTUP and TUP, with tests conducted over a range of moisture contents, at 20 W power input. Two metrics are recorded from these tests, the bubble inception temperature (BIT) and the time to bubble inception (tBI).

It was considered that different liquid insulators will provide less impact on the bubbling mechanism than solid insulators, in line with findings of [102, 105, 153]. The results shown within this chapter are all conducted with Gemini X insulating oil. Additionally, tests at high moisture content in paper values were conducted with each of the four liquid insulators with NTUP, the results of these tests are plotted in Annex A.

The comparative results of NTUP and TUP are shown in the following sections. Tests on dry paper (NTUP, <0.5% and TUP <0.3%) were conducted in all cases, but bubbles were not generated with these conditions, furthering the case that moisture is the key parameter of interest.

6.6.1.1 BIT against Moisture Content of Paper

Figure 6-11 plots the BIT of NTUP and TUP samples in Gemini X against moisture content in paper, for power input of 20 W. The plot shows the expected result that drier samples form bubbles only at higher temperatures, and that this is true for both types of paper. Most of the BIT results are below 140ºC.

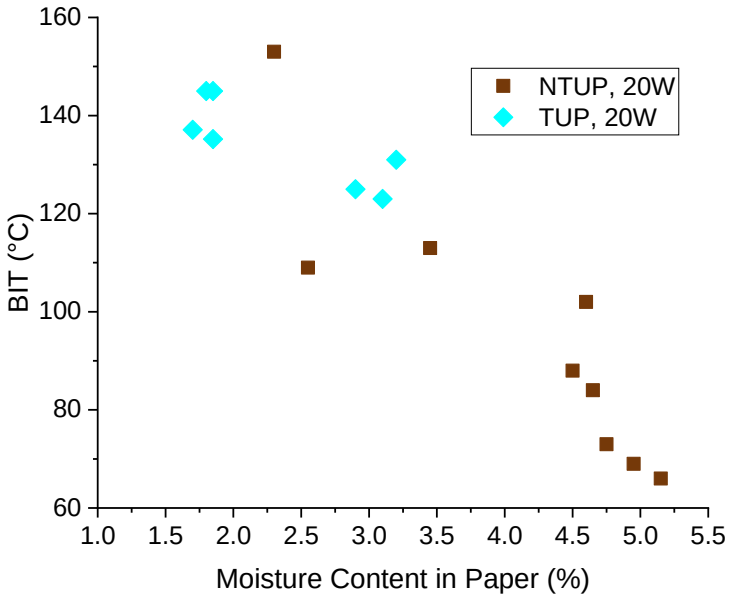

Figure 6-11 – Comparison of temperature attained at formation of first bubble against moisture content in paper for NTUP and TUP samples at 20 W power input.

6.6.1.2 BIT against Relative Humidity of Conditioning Environment

In contrast to Figure 6-11 which uses moisture content in paper, Figure 6-12 plots the same BIT of NTUP and TUP in Gemini X but instead of using the absolute moisture content, plots the BIT against the RH used to prepare the samples. Due to its lower hydrophilicity, the TUP has a lower maximum saturation and so has a higher RS than NTUP for the same absolute moisture content.

In this case the TUP BIT is higher than the NTUP at equivalent position on the x-axis, whereas they appeared similar when absolute moisture content was used. This is consistent with the findings of [102] for NTUP and TUP (shown in Figure 2-23) but contrary to [54] for Aramid insulation and NTUP (shown in Figure 2-25).

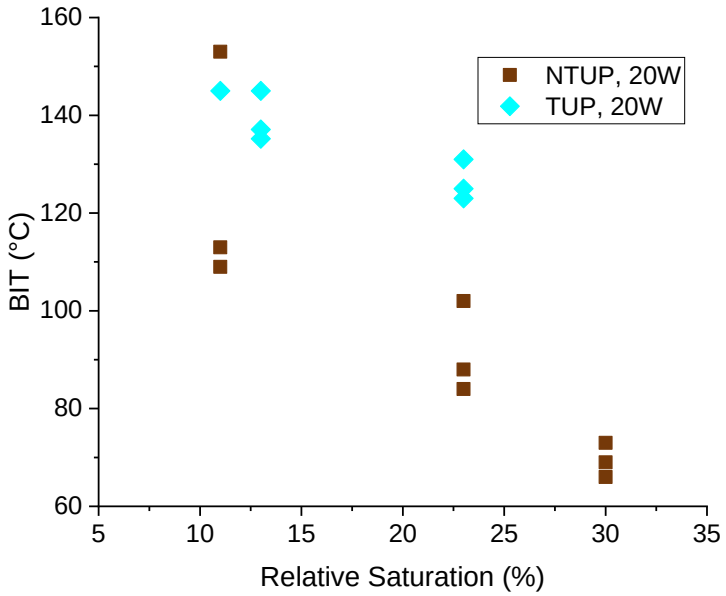

Figure 6-12 – Comparison of temperature attained at formation of first bubble against relative saturation of paper for NTUP and TUP samples at 20 W power input.

6.6.1.3 tBI against Moisture Content of Paper

The time taken from the point where power injection to the sample began until the formation of the first bubble was measured. The tBI results (in seconds) against moisture content in paper for NTUP and TUP are plotted in Figure 6-13 for tests conducted at 20 W. As the power input and the insulating liquid are the same in these tests, the temperature profile is the same (i.e. per the 20 W temperature profile of Figure 5-4). It takes a longer time for a bubble to form for drier samples.

As the temperature profiles in these tests are equivalent, the time taken to obtain the same temperature is the same, thus, as with the BIT results (shown in Figure 6-11), the tBI appears to be part of the same trend for both types of paper insulation. However as the rate of temperature rise is non-linear, with a rapid initial rise that tails off as the temperature approaches 180ºC. As a result, the slope of a straight line fitted through the tBI results is flatter than one fitted through BIT results (this is best observed by comparing NTUP results against RS, i.e. Figure 6-12 and Figure 6-14).

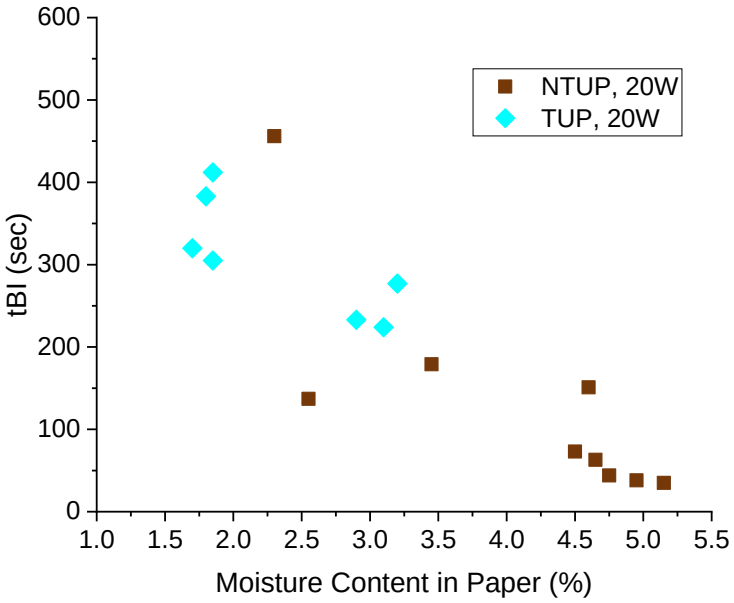

Figure 6-13 – Comparison of time taken for first bubble to form against moisture content in paper for NTUP and TUP samples at 20 W power input.

As the power input is constant during the initial phase of the test (i.e. until the temperature is near 180ºC the power input is 20 W, thereafter the power input is controlled by PID controller to maintain 180ºC), time is a proxy for the total energy added to the system: power multiplied by time equals energy. Therefore, it appears from Figure 6-13 that same amount of energy is required to form a bubble from NTUP or TUP for the same absolute moisture content in paper. This again ties in with the matching temperature profiles.

6.6.1.4 tBI against Relative Humidity of Conditioning Environment

As for BIT, the tBI is replotted against the RS of the paper insulation, Figure 6-14. As before, the results of the two types of paper stratify when plotted on this basis, with TUP needing a relatively longer time (and hence a greater amount of energy input) before a bubble forms when conditioned to the same RH environment.

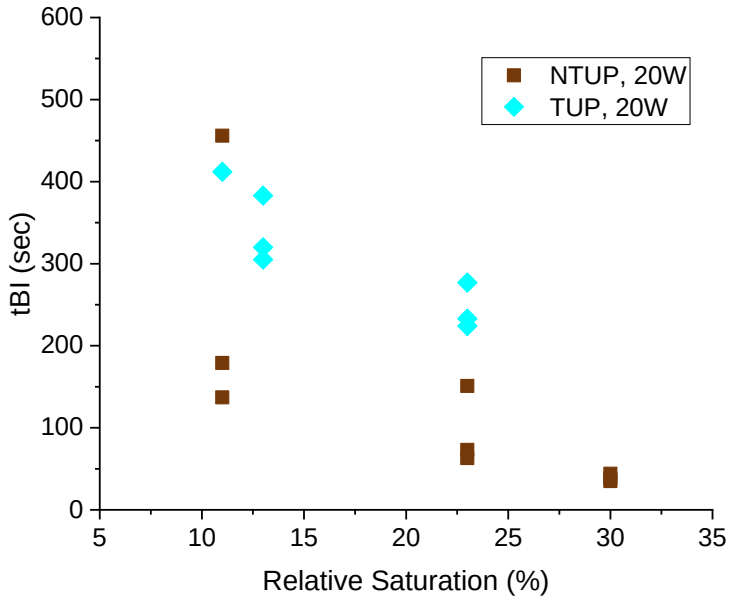

Figure 6-14 – Comparison of time taken for first bubble to form against relative saturation of paper for NTUP and TUP samples at 20 W power input.

6.6.1.5 Summary of Solid Insulation Results

Section 6.6.1 investigated the influence of changing moisture content on BIT and tBI for two commonly used solid insulation materials, NTUP and TUP. Moisture content was seen to have a strong influence on the BIT and tBI. Higher moisture content resulted in lower BIT and shorter tBI. Due to the non-linear adsorption isotherm for moisture and cellulose, the apparent change seems more drastic when using absolute moisture content rather than RS (absolute moisture content is the more common metric for transformer solid insulation, for both bubbles and moisture discussions in general). Bubbles could not be evolved from very dry paper samples for either material.

The selection of solid insulation material has an impact on BIT and tBI, with TUP resisting bubbling better than NTUP, particularly when comparing them at the same RS (one data point for NTUP appears to have a very high BIT / long tBI, and may be erroneous). Interestingly, in tests with both materials, BIT was observed as lower than 140ºC in several of the tests.

6.6.2 Effect of Magnitude of Step Increase in Load

The experiments in Section 6.6.1 were conducted using a step load increase of 20 W, described by the profile shown in Figure 5-4. In experiments using Gemini X, 180°C was attained after a period of about 14 minutes. This section examines what happens with the

same liquid insulation, but with a greater step change in load and the resultant faster rise of temperature of the system.

Two alternative profiles are considered in addition to the 20 W profile: 26 W and 32 W. Under a power input of 26 W, the temperature rose to 180°C after approximately 8 minutes, as shown in Figure 6-8. For a power input of 32 W, 180C was obtained after just 5 minutes, with the full profile also shown in Figure 6-8.

6.6.2.1 BIT against Moisture Content of Paper

Plotting the BIT against moisture content for NTUP (Figure 6-15) and TUP (Figure 6-16) allows for assessment of the influence of step change in load on BIT.

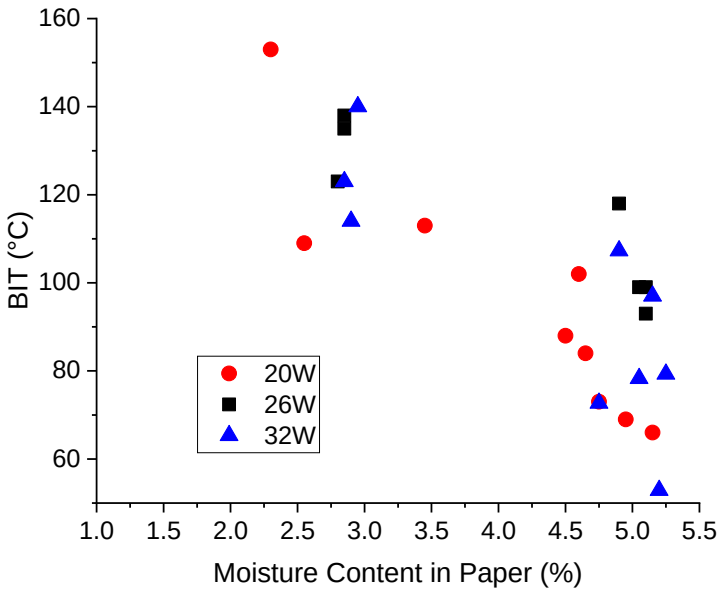

Figure 6-15 – Temperature attained at formation of first bubble for NTUP tests in Gemini X, for three power inputs.

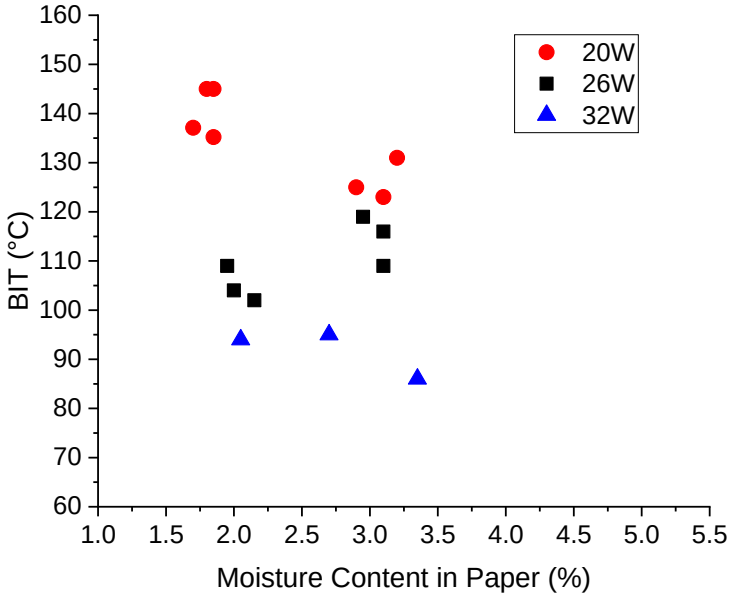

Figure 6-16 – Temperature attained at formation of first bubble for TUP tests in Gemini X, for three power inputs.

From Figure 6-16 (for TUP), there is a noticeable trend, with higher power input tests generating bubbles at lower temperatures than lower power tests. The NTUP results of Figure 6-15 do not show this difference however, with the BIT for all three power levels overlapping.

6.6.2.2 tBI against Moisture Content of Paper

Likewise, plotting the tBI for bubbles generated at under different power input profiles against moisture content in paper for NTUP (Figure 6-17) and TUP (Figure 6-18) helps to assess the influence of the load change.

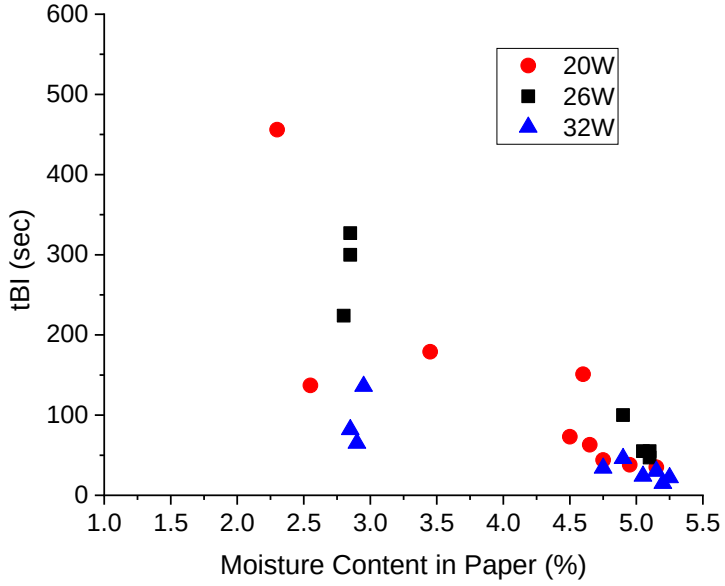

Figure 6-17 – Time taken for first bubble to form for NTUP tests in Gemini X, for three power inputs.

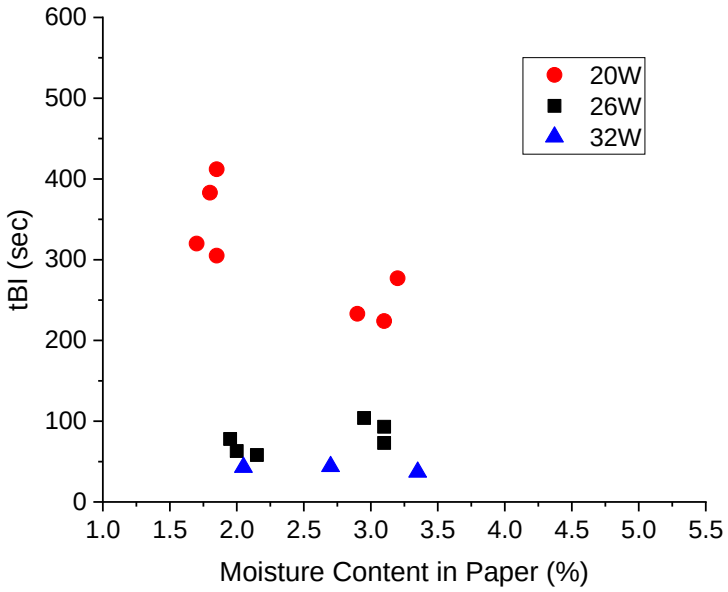

Figure 6-18 – Time taken for first bubble to form for TUP tests in Gemini X, for three power inputs.

There is clustering of the results of very moist NTUP samples in Figure 6-17, where all results seem indistinguishable, with bubbles occurring very rapidly. For TUP, a similar stratification of the results is present in Figure 6-18, as for BIT results in Figure 6-16.

6.6.2.3 Summary of Increased Step Loading Results

Section 6.6.2 tested the BIT and tBI of NTUP and TUP samples at three levels of power input: 20 W (base case, as per Section 6.6.1), 26 W, and 32 W. Results for TUP samples showed a clear effect, where higher power input resulted in shorter tBI and higher BIT, with the difference resulting from equivalent absolute increases in power reducing in magnitude. This outcome suggests that at the threshold power necessary for bubble formation (for this system, somewhere around 13 W), small increases in power can lead to large reductions in the tBI. This may also be inferred from the temperature profiles, for example in Figure 6-8, the 32 W and 26 W profiles are more similar than the 26 W and 20 W (though it is worth repeating here that the same absolute magnitude, rather than relative magnitude, of power increased is used for each step increase). NTUP results showed more scatter, potentially due to the comparatively higher absolute ‘wetness’ of those samples.

The conclusions drawn here must be linked back to the results of Chapter 4, where the electrification of energy demand was investigated. The case considered there was of electrification of heating, but as remarked, there is also the potential of coincident electrified transportation. While no allowance was made for the rate of temperature rise in Chapter 4 (rather, simply following the calculation provided in [71]), the results of this section show

that coincident load could increase transformer temperatures while also reducing the BIT threshold through increase rate rise, placing the transformer at ever increased risk.

6.6.3 Comparison of Controlled Temperature Rise to Step Increase in Load

The temperature profiles of Figure 5-8 all allowed the temperature to rise naturally, with a steep initial rise and a slower increase as the temperature approached 180°C, the PID controller begins to operate at around 175°C, and continues to control at 180°C for the remainder of the test.

The tests at 20 W constant power input had an average temperature rise (calculated as 180°C minus the initial temperature, divided by the total time taken to reach 180°C once power is turned on) of approximately 13 K/min. However, this is not representative of the temperature rise at most points of the heating period, with the initial rate much higher, and later rate much lower.

A set of tests were conducted on samples of NTUP with Gemini X to consider the influence of temperature rise rate. The PID controller was reprogrammed to control the temperature rise to 40°C within the first minute, then to rise at a constant 13 K/min until 180ºC was reached (180ºC was then maintained for the remainder of the test, as before). The initial point of 40°C on the constant temperature rise profile was chosen to account for the different potential starting temperatures (i.e. ambient temperatures) and as the PID controller could not act quickly enough to reliably maintain the temperature at a set-point lower than this. Figure 6-19 shows the different temperature profiles of a 20 W constant power injection profile and a 13 K/min constant temperature rise profile. It was necessary to set a power injection slightly greater than 20 W for the constant temperature rise test to ensure that the rate of temperature rise could be maintained at the high temperature end of the test.

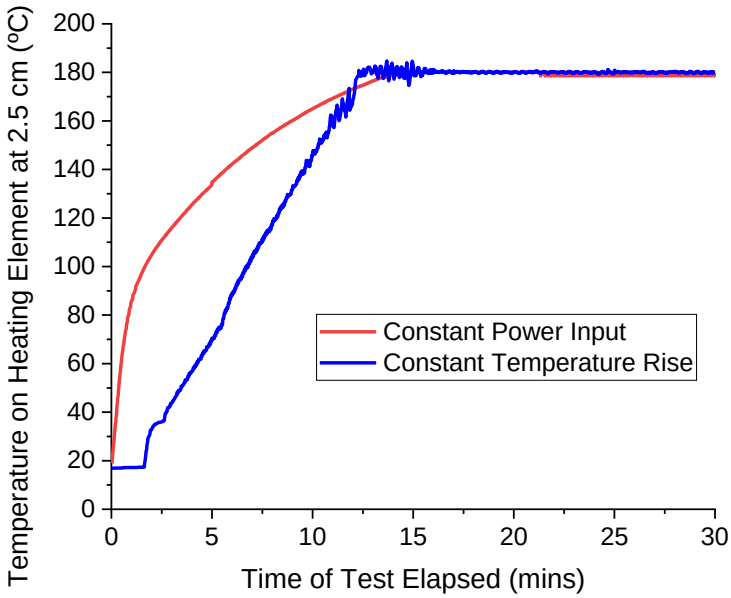

Figure 6-19 – Temperature profiles for constant power input and constant temperature rise tests.

6.6.3.1 BIT against Moisture Content of Paper

Figure 6-20 plots the BIT for the constant power input case (20 W) and for the 'equivalent' constant temperature rise case (13 K/min).

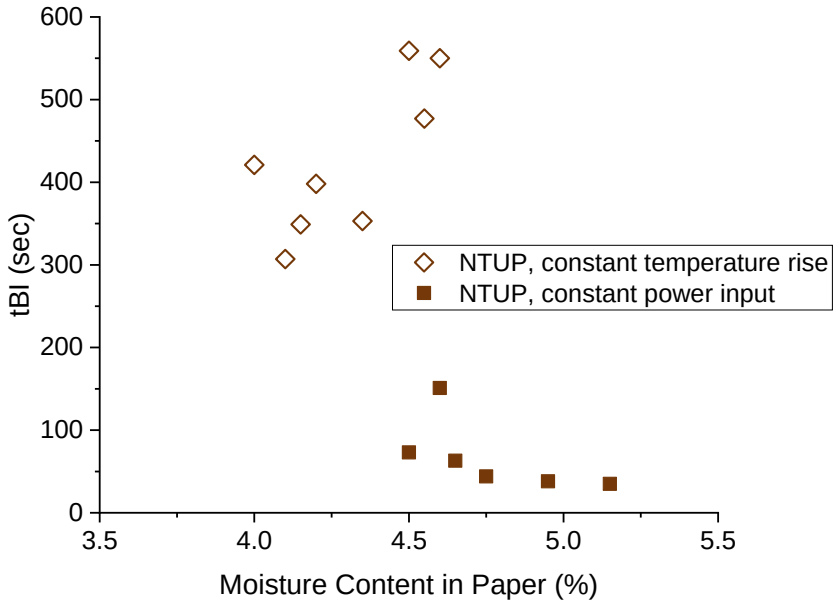

Figure 6-20 – Comparison of temperature attained at formation of first bubble against moisture content in paper for NTUP with constant power input profile, 20 W (solid squares) and constant temperature rise profile, 13 K/min (empty diamonds).

The constant temperature results show an unusual trend where higher moisture content samples attained a higher temperature at bubble inception. The results of the five samples at around 4 – 4.5% moisture content in paper seem to match the trend of the constant power input results.

6.6.3.2 tBI against Moisture Content of Paper

Figure 6-21 plots the tBI for the constant power input case (20 W) and for the 'equivalent' constant temperature rise case (13 K/min).

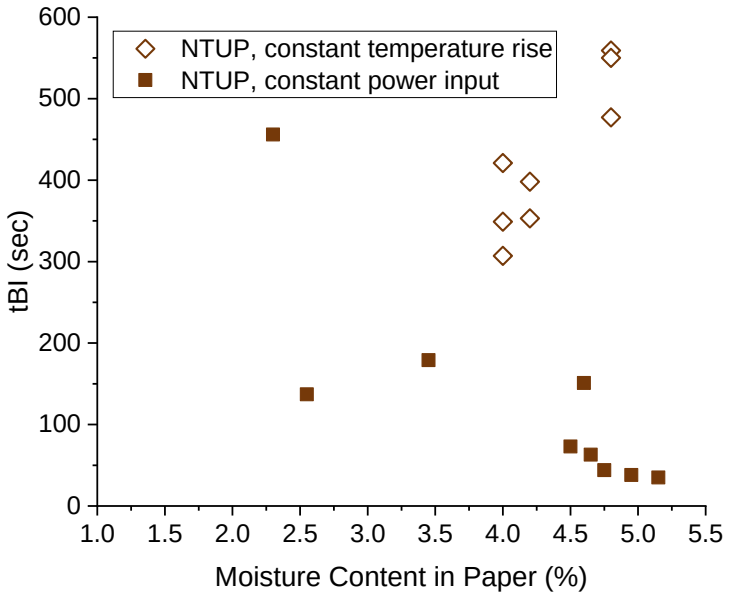

Figure 6-21 – Comparison of time taken for first bubble to form against moisture content in paper for NTUP with constant power input profile, 20 W (solid squares) and constant temperature rise profile, 13 K/min (empty diamonds).

Although the constant temperature rise results show (necessarily) the same unexpected trend of longer tBI for higher moisture content samples, this graph also shows an interesting phenomenon: the time taken for bubble inception is much greater (in the order of 5 – 10 minutes) for the constant temperature rise case than the constant power input case.

The implication is that the slower initial rate of the constant temperature rise case compared to the constant power input case delays the onset of bubbles – i.e. a more gradual temperature rise, even at the same average rate, delays the onset of bubbles, potentially providing more time for the transformer operator to act to prevent the worst case scenario.

It is worth pointing out specifically that even the results for moisture content in paper of around 4 – 4.5% which showed similar BIT have an elevated tBI compared to the constant power input case.

6.6.3.3 Power against BIT

An interesting plot which begins to explain the results of Sections 6.6.3.1 and 6.6.3.2 is shown in Figure 6-22, where the BIT of the constant power input and constant temperature rise samples against the energy input calculated at the time of the first bubble generated are shown.

For constant power input samples, this is a straightforward calculation of power multiplied by time, with power a known value (as bubbles form in advance of any PID controller action). For constant temperature rise tests, the calculation is somewhat more complicated, given that the PID controller is working from the first moment, adjusting the power input to maintain the temperature rise value. Therefore the power is calculated from current measurements multiplied by the voltage measurement at intervals up to the point of bubble inception. These power calculations are then multiplied by the time step of the intervals and are then summed to give the total energy input to the system until the first bubble is formed.

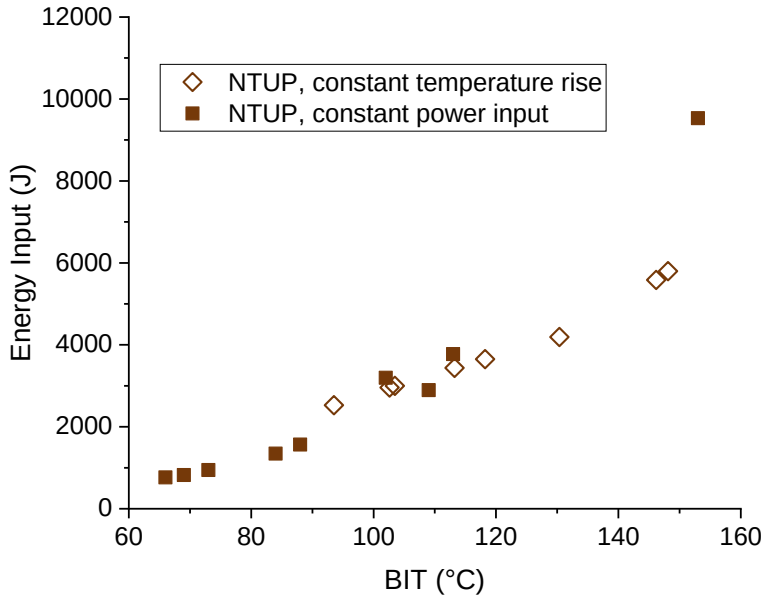

Figure 6-22 – BIT recorded for constant power input (20 W) and constant temperature rise (13 K/min) against the total energy input to attain that temperature.

As Figure 6-22 shows, the energy input required to achieve a certain temperature (here, the BIT, but it is arbitrary which temperatures are selected in reality, i.e. there is nothing special about points of BIT on the temperature profile), is the same across the two tests. Thus, while the constant temperature rise tests may have taken longer to form bubbles, the energy input to generate bubbles is the same, for otherwise similar conditions.

6.6.3.4 Summary of Temperature Rise Rate Results

Tests were conducted on two profiles of the same average rate of temperature rise, but which followed greatly different paths to attain the same ultimate temperature.

Bubbles were observed in both cases at similar temperatures, however the tBI varies significantly between the two cases. On further inspection, the calculation of energy input

showed that the net energy added to the system in both cases were identical, with the profile of initial slower rate of temperature rise (i.e. initially lower power injection) taking longer.

6.7 Findings Regarding the Mechanism of Bubble Formation

6.7.1 Changes in DP during Test

Despite the calculation of Section 6.5.1.1 predicting that DP would not change significantly during the bubble formation tests, DP tests on actual samples of NTUP impregnated and immersed in Gemini X mineral oil showed a more marked reduction of DP (after 30 minutes, following the profile of Figure 5-5). As Figure 5-5 shows, there is a temperature profile along the heating element, and thus also along the sample – this temperature profile is considered to be greater than the temperature profile across paper layers of the sample (particularly for the case considered here of two layers). Therefore, the sample was divided into two sections, upper and lower, which were tested independently. Two cases are considered, a sample prepared at 11% RS, and one prepared at 26% RS. Figure 5-2 summarises the results.

Table 6-3 – Results of DP tests on samples of NTUP in Gemini X, prepared at 11% RS and 26% RS, taken from samples tested for 30 minutes (initial DP = 1000).

Sample Condition	DP after 30 minutes
Upper section, 11% RS	823
Lower section, 11% RS	870
Upper section, 26% RS	670
Lower section 26% RS	734

The fact that DP reduces by the order of 200 – 300 shows that the tests operate outside the applicable range of the formula or its parameters. A value of around 800 DP would not be considered ‘aged’, and is likely due to the depletion of the amorphous region which would have limited influence on the physical parameters of the paper (see Figure 2-5 and associated discussion for fuller details). The DP of the (hotter) upper section is lower in both cases tested, which follows the theory. Interestingly, the influence of moisture content had the greater effect on the depletion of DP than temperature: at such high temperatures, one might assume that pyrolysis is the dominant mechanism breaking down the cellulose structure, but the effect of moisture here strongly indicates that hydrolysis is also still an important factor.

6.7.2 Drying of Paper during Test

The moisture content value can be useful in understanding the bubbling mechanism. It is useful in two aspects: firstly, does the amount of moisture released from paper before a

bubble forms vary based on the initial value; and secondly, is there a difference between paper types in terms of how much moisture is dried from the paper during the bubbling process.

6.7.2.1 General Observations of Paper Insulation Drying

Moisture content in paper of the sample was tested before and after the tests, as per the sampling split shown in Figure 6-10. Figure 6-23 plots the average final moisture content of the paper insulation post-test for thirty-minute and bubble only tests for comparable initial moisture content of paper (for 20 W NTUP tests), and Figure 6-24 plots the same for TUP samples (also at 20 W). In all cases, the moisture remaining in the paper insulation after 30 minutes of the test is close to the 'dry' condition achieved when preparing the samples. Contrastingly, after bubble only tests NTUP samples (where tests tended to last <2 minutes) are hardly changed with moisture content very close to initial values. TUP samples (which take in the order of 5 minutes) show a more significant decrease in moisture content, yet still remain significantly higher in moisture than the 'dry' condition or after a thirty-minute test.

Comparison between moisture content in paper after thirty-minute tests and 'bubble only' tests provides the obvious conclusion that the paper is drier after longer tests. The result that the bubble only tests are still close to the initial paper insulation moisture content after a bubble was observed indicates that there is not a requirement for large amounts of moisture movement to form a bubble, i.e. bubbles can form from a reasonably small amount of released moisture.

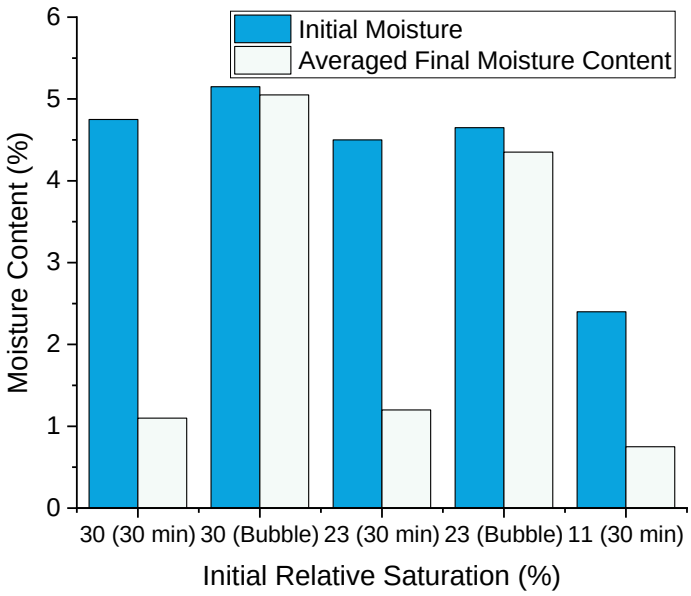

Figure 6-23 – Change in absolute moisture content between initial value and average post-test value for NTUP samples tested at 20 W, shown by relative saturation of paper and type of test (30 minutes or bubble only, shown in brackets).

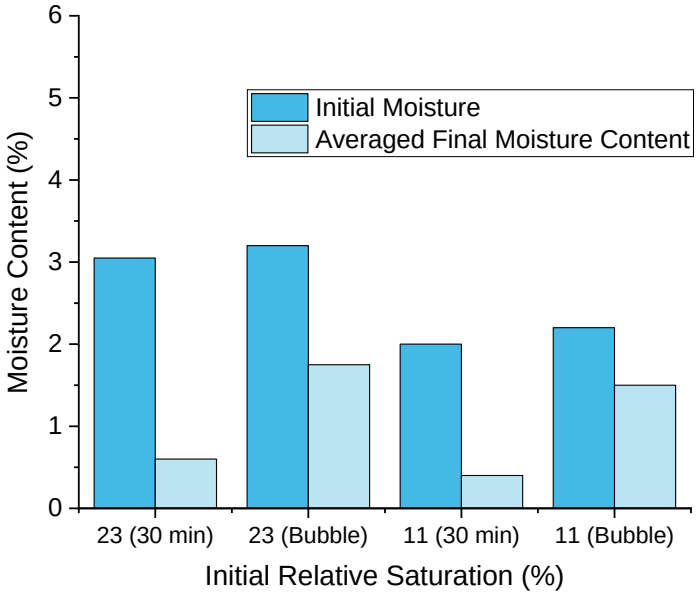

Figure 6-24 – Change in absolute moisture content between initial value and average post-test value for TUP samples tested at 20 W, shown by relative saturation of paper and type of test (30 minutes or bubble only, shown in brackets).

6.7.2.2 Observations of Differences in Insulation Drying with Height of Sample

Another expected outcome is found in the pattern of drying, where the lower section of the sample is usually found to have higher moisture content than the upper section at the end of the thirty-minute tests (Figure 6-25). The upper section is at higher temperature (as shown by Figure 5-5, for 20 W NTUP tests), and as the drying process is temperature driven, this is a sensible outcome. For bubble formation tests conducted for 30 minutes, both the upper and lower sections are almost fully dried. For bubble only tests, the time taken for a

bubble has an impact on the degree of drying, but the samples remain relatively moist and there is no clear trend across tests regarding upper or lower segments being wetter or drier.

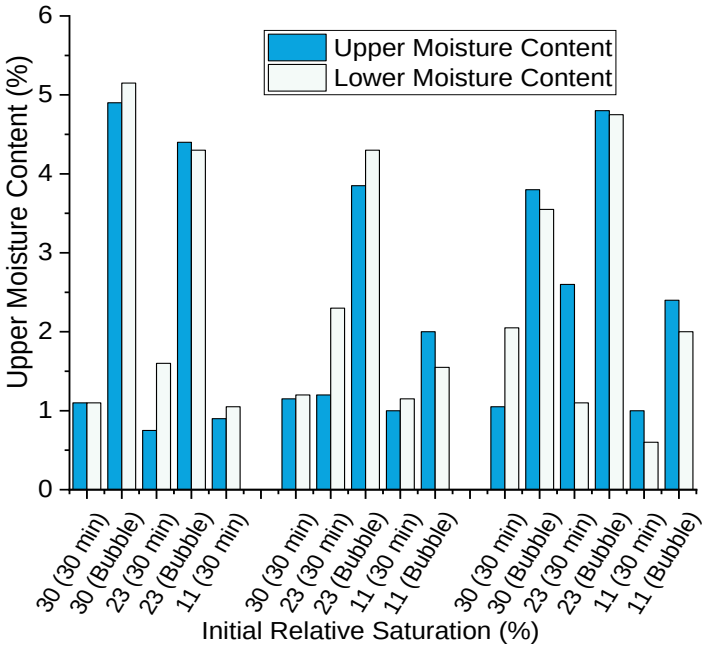

Figure 6-25 – Final moisture content of upper and lower paper insulation segments post-test for NTUP samples tested, shown by relative saturation of paper and type of test (30 minutes or bubble only, shown in brackets), for 20 W, 26 W and 32 W input (left to right respectively).

6.7.2.3 Observations of Differences in Drying between Insulation Layers

The observation of paper insulation drying between layers provides an unexpected result. Figure 6-26 shows how inner layers dried faster than outer layers over thirty-minute tests. Moisture at the inner layer moves into the outer layer (which both start at the same moisture content) while moisture from the outer layer moves into the insulating liquid. The results show that the latter process, of moisture moving from outer layer to liquid, is slower than the inner layer moving to the outer layer in these tests, even with the release of bubbles.

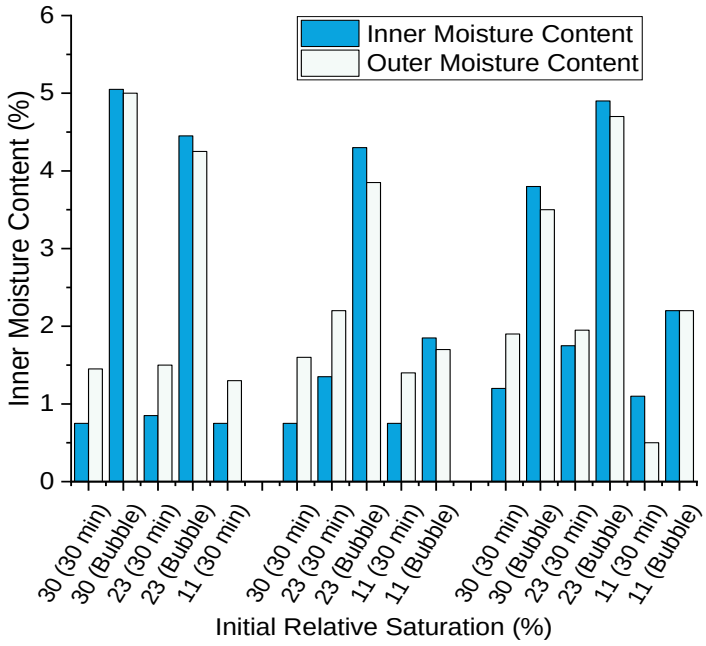

Figure 6-26 – Final moisture content of inner and outer paper insulation layers post-test for NTUP samples tested, shown by relative saturation of paper and type of test (30 minutes or bubble only, shown in brackets), for 20 W, 26 W and 32 W input (left to right respectively).

There are a few explanations behind this, but the most important factor is the relative rate of diffusion between the layers. As seen in Section 2.4.3.2, moisture leaves cellulosic paper insulation as temperature rises. The inner layer is adjacent to the heating source, and so (on its inner surface, at least) will be at the same temperature as the metal surface of the heating element; the outer layer will be at a slightly lower temperature (by a few Kelvin). There is thus a balance between temperature driven and media driven diffusion of material. Conversely, in the early stages of the test (i.e. up to the first bubble) the moisture of the inner layer is higher than the outer layer, which may be linked to the dryness of the liquid insulation at the beginning of the test.

6.7.3 Liquid Insulation Moistening during Test

Throughout the test, moisture leaves paper insulation in one of two ways: either it passes on a molecular level, absorbed into the liquid insulation, or it leaves into the headspace as a bubble. To challenge the concept that bubbles only occur when liquid insulation reaches saturation, the moisture content post-test was measured for both thirty-minute and bubble only tests. Moisture tests are conducted in accordance with Section 5.5.2, with a 24 hour ‘equilibration’ period allowed under sealed conditions after paper insulation is removed.

Impact of Loading and Solid Material Selection on Bubble Formation

For Gemini X tests, all samples began with <5ppm moisture content in liquid. Figure 6-27 shows the amount of moisture in the liquid insulation after bubble only tests. The moisture content has increased in all tests, from <5 ppm to ~20 ppm. There appears to be little variation in this value (approximately ±5 ppm is not large given the small measurement and the equipment limitations).

Figure 6-28 shows the amount of moisture in liquid insulation after the thirty-minute tests. Comparing Figure 6-28 to Figure 6-27 shows that more moisture transferred from paper to liquid insulation in the thirty-minute tests, as expected. Many samples showed moisture values close to fully saturated (based on 20ºC, Table 5-1) in the thirty-minute tests. The importance of this result however is that although over the course of a thirty-minute high-temperature test, liquid insulation will become extremely moistened, this is not a necessary condition for bubbling. Bubbles can form well before this point, with values closer to 30 – 40% saturation (based on 20ºC values, which are not reflective of the test conditions) observed. High values for final liquid moisture content were seen for all conditions, with slightly lower values recorded for the lowest starting moisture in paper conditions (11% RS).

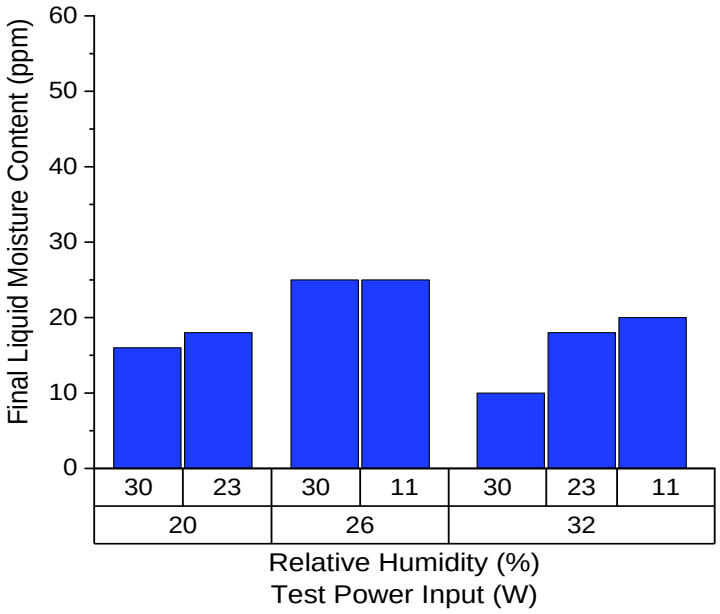

Figure 6-27 – Post-test moisture content in Gemini X insulating liquid for bubble only tests, shown by initial paper insulation relative saturation and test power input (for NTUP tests).

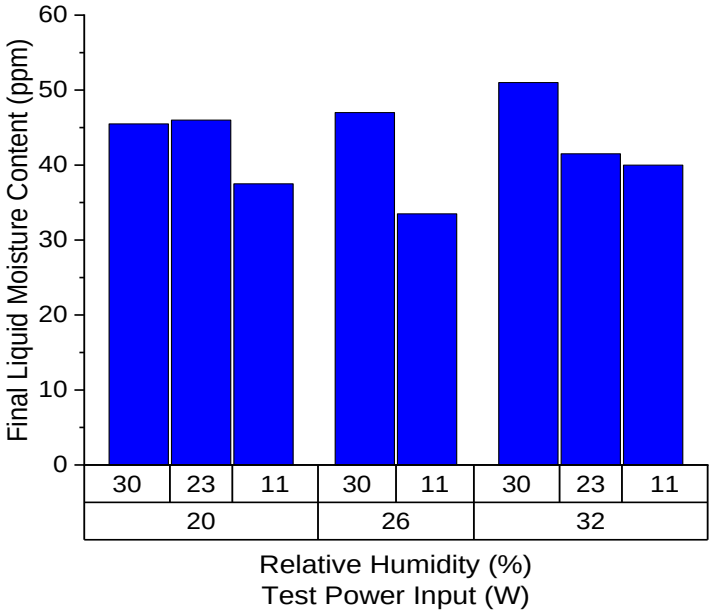

Figure 6-28– Post-test moisture content in Gemini X insulating liquid for thirty-minute duration tests, shown by initial paper insulation relative saturation and test power input (for NTUP tests).

Final moisture content in liquid (for bubble only and thirty-minute tests) appears to be independent of power input used in the test. There is a relationship between the length of the test up to the bubble and the post-test moisture content in liquid, as shown in Figure 6-29.

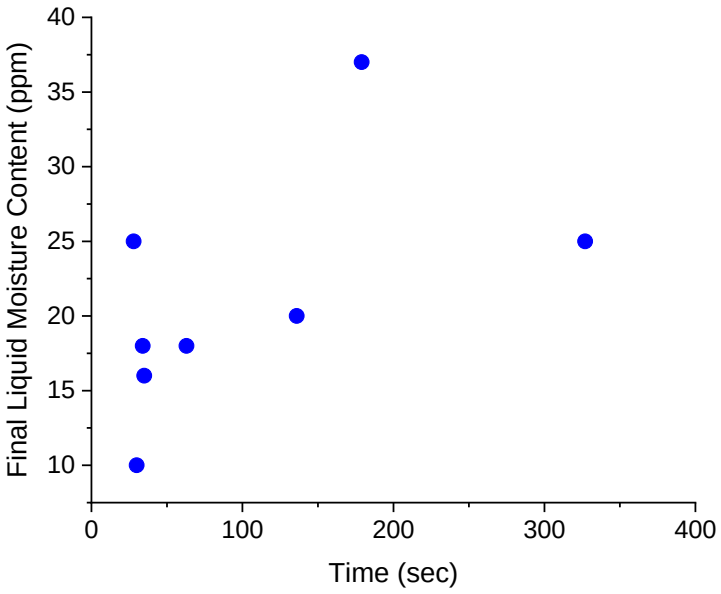

Figure 6-29 – Post-test moisture content in Gemini X insulating liquid for bubble only tests against tBI (for NTUP tests).

6.7.4 Observation of Pooling Behaviour

During the tests, constant recording of a 360º view of the sample was maintained. Interesting aspects of the bubble formation process were observed. In almost all cases where at least one bubble formed and released, it was preceded by a phenomenon herein termed ‘pooling’. Pooling appeared immediately precedent to bubble formation, at the location from where a bubble formed. The pooling was the point where moisture which was released from the inner layer accumulated beneath the outer layer, presumably as a result of the different rates of thermal and media led diffusion of the two layers. The beginning of this process is shown within the red circle in Figure 6-30.

Figure 6-30 – Example of pooling behaviour beginning on 26% relative saturation TUP sample, 26 W test.

The pooling consistently appeared first near the top of the sample (hottest section of the sample). Bubbles tended to release at the ridge of adjacent turns of the outer layer, and in some instances secured at this location. Figure 6-31 shows bubbles releasing from this location (highlighted by a red circle), local to the original pooling (also within red circle).

Figure 6-31 – Example of bubbles releasing from overlap of paper insulation on 26% relative saturation TUP sample, 26 W test.

This pooling phenomenon accords with the above understanding, and, when considered alongside the descriptions of moisture behaviour in Sections 6.7.2 and 6.7.3,

begins to explain the bubble forming mechanism in transformer insulation. It appears that inner layers of paper insulation release moisture rapidly, and this forms pools in between layers (this is already a dielectric weakness which could place the transformer at risk). As the moisture cannot progress easily between subsequent layers, the continued addition of moisture and energy leads to formation of bubbles.

As paper insulation is tightly bound, it is likely that bubbles only form at the two outermost layers, but moisture will be provided from inner layers. This could explain why slightly higher BIT was observed during initial tests involving additional layers, Figure 6-6. What may *actually* have been observed was a greater tBI, and a higher BIT was recorded as a result - further tests would need to be conducted to confirm this conclusion. Equally, the temperature of the outermost layer is lower than the HST of the heating element surface by several Kelvin, so the temperature at the location of bubble formation (between layers 5 and 6) may have been at the same temperature as at the location of the bubble formation for the 2 layer tests (between layers 1 and 2).

6.7.5 Observation of Continued Pooling and Bubbling after Initial Bubble

The analysis presented within this chapter is, for the most part, related to the test up until the formation of the first bubble. This presents the point at which the transformer can be considered at high risk of dielectric failure. However, a majority of the tests conducted continued for the full 30 minute test period, and so there is a some additional insight to be gleaned from those tests (in addition to the information introduced in the above sections on changes in moisture).

The recordings are made for the entirety of the tests, and so the continued pooling and bubbling behaviour of samples can be followed. Figure 6-32 shows this progression, with pooling occurring gradually further down the sample as time progresses, until at the very end of the test, the sample is very dry and pools cover less of the sample. The pools are always between layers, and bubbles are seen lower and lower with time, but always releasing from the overlaps of the paper. A crude estimate of typical bubble size at point of release for this test suggests a bubble diameter of approximately 0.5 mm, this is an order of magnitude higher than those identified in [131] (though bubbles in [131] were not moisture bubbles and so less material would have been available), but the range of ‘barely visible to ¼″’ of bubble size (assumed to be moisture bubbles) in [122] matches perfectly.

Figure 6-32 – Progression of pooling and bubbling in sample with time for 26% relative saturation TUP sample, 26 W test. Capture at 30 seconds, 3 minutes, 5 minutes and 27.5 minutes after first bubble from left to right.

6.7.6 Summary of Moisture Behaviour during Tests

Following the moisture in paper and liquid insulation has not previously been done in tests on bubbling in transformer insulation. The results have provided insight into the mechanism of bubble formation. Firstly, it was seen that moisture appears to build up in between layers during rapid, high temperature events, and that this trapped moisture, with continuing addition of moisture and energy resulted in formation of bubbles which released at points of paper overlapping. It was also seen that the condition of the liquid insulation does not play a significant role, with bubbles able to form in liquid with remaining capacity for moisture.

Bubbles, and the prerequisite pooling, appeared at the hotter locations of the sample first. This accords with the theory that the thermal driver for the movement of moisture between layers.

6.8 DISCUSSION

6.8.1 General Remarks

The results of this chapter were broken down into two subsections: the influence of solid material selection and loading on BIT and tBI which is a direct assessment of what the system status is at the time of failure; and the observations of the mechanism of bubble formation, which focusses in on the formation characteristics.

It was shown that bubbles formed from both TUP and NTUP samples at temperatures below the 140ºC threshold set in the standards. Therefore, caution should be taken when working to this operating restriction. Unsurprisingly, bubbles formed near the top of the sample, where temperatures were highest and so reached the BIT first.

Further, it was seen that TUP samples resisted bubbling better than NTUP samples when compared on the same RS of paper, with quite a large difference in BIT. This finding is critical; TUP is known to resist thermal ageing better than NTUP, and ages at the same rate for rated conditions at 12ºC higher (in mineral oil) [71]. However, the increased thermal operating point would have been null if the TUP was at risk of bubbling at 'low' temperatures.

From the plot in Figure 6-22, it is shown that the BIT was reasonably independent of the pathway taken to attain it. That is to say, for the same total energy input, the BIT was equal, despite a different duration taken (i.e. different applied power, rate of energy input), for the same materials.

From the latter section, it was observed that bubbles are formed by the migration of moisture from inner layer to outer layer occurring too quickly: once moisture leaves the inner layer, it is trapped physically, but not chemically beneath the outer layer. Bubbles then form due to the continued addition of energy and moisture, and release at the point of least resistance (i.e. they release at paper overlaps – bubbles do not force / permeate their way through layers directly). This formation mechanism supports the finding of initial tests in Section 6.3.2.2 where samples with more layers had a higher BIT (and longer tBI) – it is likely that the reason behind this is that moisture from inner layers takes longer to reach the outermost layer (and the further from the heat source a layer is, the lower its temperature will be, also reducing the driver behind the moisture migration). The inability to generate bubbles in samples of just a single layer also supports this mechanism of bubble formation (as there was nowhere to 'trap' the moisture where it could accumulate and form bubbles).

The fact that the moisture is higher in outer layers than inner layers thirty-minute tests further suggests that bubbles are forming from moisture that comes from the inner layers.

6.8.2 Comments on Behaviour of Water during Tests

Bubbles in transformers are driven by two aspects: the thermal behaviour of the system and the behaviour of moisture within the insulation.

Moisture moves from the inner paper layer to the outer paper layer, and from outer paper layer to the liquid insulation, driven by the temperature profile of the system (both the vertical and axial temperature profiles). Wet outer layers (which are cooler than inner layers) present a barrier to liquid leaving the inner layers, causing a build-up of liquid between layers that leads to bubbling.

A period of 30 minutes at high temperature is enough to dry the samples of almost all moisture, however, when bubbles formed, paper insulation was still wet. In contrast, at the end of such tests, liquid insulation is essentially saturated, but at the point of bubble formation, while the liquid insulation has gained moisture, it is still less than 40% saturated (on room temperature basis) in these tests.

6.8.3 Use of BIT or tBI?

The results of the experiments presented throughout this chapter showed that there are two ways of analysing the weakness of an insulation system to bubbling: temperature and time. Both of those values are linked to the energy added to the system.

For a system experiencing a known thermal (load → temperature) profile, the time and temperature can be considered equivalent. However, when comparing across thermal profiles, they are not, given the different temperature response to different thermal inputs.

It is recommended to continue using temperature as a guideline for protecting transformers against potential failure through bubble formation, but it is also worth considering the net energy input. For example, taking Figure 6-22, the two different temperature profiles led to bubbles forming at equivalent ultimate temperatures, however, the time taken to achieve that temperature was longer in the system where energy was input at an initially lower rate. This knowledge could help in protecting transformers – low rise rates and more a gradual temperature curve can delay bubble onset and give operators time to act before bubbling occurs.

6.9 SUMMARY

This chapter analysed the influence of the solid insulation (specifically, the influence of thermal upgrading of solid insulation) on the bubble formation metrics. Additionally, the influence of different load profiles is monitored. The temperature and time required for bubble formation is measured to allow comparison between the different cases. Moisture movement within tests is also measured, which gives new insight into the way that bubbles form at the solid insulation within transformer insulation systems.

7 DEVELOPING BIT FORMULAE AND ACCOUNTING FOR CHANGES IN DP

7.1 INTRODUCTION

In this chapter, results from several previous papers are assessed based on a rigorous theoretical foundation of the chemistry and thermodynamics involved in the bubbling process. Data fitting using Origin Pro 8.5.1 was done to fit existing data against proposed bubble inception temperature (BIT) models. The intention is to improve the BIT formulae used in extant standards (i.e. [22, 71]) by increasing specificity to the condition of the transformer insulation, and also the physical mechanism that occurs during bubbling.

Results from Chapter 6 are compared with the developed formula. The chapter concludes by assessing the temperature profiles developed in Chapter 4 for potential bubble inception using an updated formula, and comparing the outcome with that from the formula from [71].

7.2 THEORETICAL ANALYSIS OF BIT FORMULAE

To date, analysis of bubbles has been mostly experimental. A notable exception was the development of a mathematical model for bubble generation [134, 135], which looked mainly at super-saturation scenarios for different theoretical gas generation calculations. Ultimately though, the calculation of BIT is done using the formula proposed by [137] which has a theoretical basis of the desorption isotherm developed in [135]. There are other parameters that should be considered when assessing BIT, chiefly, the degree if polymerisation (DP) of the solid insulation. Further, the use of sorption isotherms is not theoretically sound. Within this section, several improvements are given regarding calculations of BIT based on assessment of existent BIT results available in the wider literature.

This section deals firstly with fittings of the isotherm equation given in [71], providing a method of calculating the BIT as the insulation DP varies. For this work, the description of the sorption isotherm formula from Section 2.6.3 is relied upon, and the formula in its base form (developed in this chapter) is helpful.

Thereafter, an alternative equation (enthalpy equation) is analysed in much the same way, and is then treated further through an analysis of how the parameters of that equation

vary where different insulation materials are used. This equation is developed from the form of equation (2-27).

7.2.1 Sorption Isotherm Formula

7.2.1.1 Description of the Sorption Isotherm

The sorption isotherm is currently the formula in use within the transformer industry, and is the formula given in Equation (2-25). It relies on the water content of the solid insulation, the gas content of the liquid insulation, and the system pressure to calculate expected BIT.

As remarked in Section 2.4.3.2, a Type II isotherm is observed for adsorption of moisture by cellulose. While this is described by a formula of the type shown in equation (2-25), the numbers in the equation are specific to the materials used in [135] (from where the formula originates).

It is useful to look at the construction of the isotherm equation from first principles, which begins from reaction kinetics. By considering that an adsorbed molecule represents a successful reaction (i.e. the successful formation of an OH-H_2O (at the mono-layer) or H_2O-H_2O bond (in poly-layers)), the isotherm can be formed from a reaction rate equation, such as (7-1). This shows how the amount of water (W) that will be in the cellulose changes with respect to the system pressure (p) raised to the power n^{-1}, and multiplied by a reaction rate constant, K. n is a value which describes the system topology, which can be influenced by many factors. Essentially this details the difference in bonding energy at different adsorption layers, or the difference in adsorption affinity among sites if the 2-, 3-, 6- OH bonding theory is preferred.

$$W = Kp^{\frac{1}{n}} \tag{7-1}$$

The rate constant, K, can be further described by (7-2), which shows an exponential reliance on the specific energy (i.e. energy divided by Boltzmann constant or universal gas constant) needed to form the adsorption bonds, B, divided by the system temperature, T. This indicates that at higher temperature, more reactions will take place (which follows the theory outlined in Section 2.4.3.2). K also has a constant, A, which represents the frequency of the effective collisions. The A value is seen to be very important to the variation of BIT with DP.

$$K = A\mathrm{e}^{\frac{B}{T}} \tag{7-2}$$

Substituting with this expanded form of *K*, (7-1) becomes (7-3). Rearrangement for temperature as in (7-4) allows for calculation of the isotherm temperature for known conditions of *p* and *W*, which is the familiar form of the equation as already shown in equation (2-25) (ignoring the additional correction term added in [137]).

$$W = A\mathrm{e}^{\frac{B}{T}}p^{\frac{1}{n}} \tag{7-3}$$

$$T = \frac{nB}{nln(1/A) + n\,ln\,W - ln\,p} \tag{7-4}$$

Note that the coefficients of [135, 137] should be those of [136], shown here as (7-5). Table 7-1 shows how the coefficients of (7-5) correlate with its algebraic form, (7-4). The cause of this change in coefficients is described in Section 2.6.2. As this formula is being used to indicate the BIT instead of the isotherm temperature, the symbol ϑ is used instead of *T*.

$$\vartheta = \frac{7064.8}{22.95 + 1.4959\ln W - \ln p} \tag{7-5}$$

Table 7-1 – Relation of values in bubble inception formula, (5) to rearranged form of Freundlich Formula, (4).

Parameters	Value
A	2.173×10^{-7}
B	4722.8
n	1.4959
nB	7064.8
$n\ln(1/A)$	22.95

7.2.1.2 Variation of BIT with Insulation Ageing

An experimental assessment of the variation of moisture equilibrium with insulation ageing condition was done in [139], considering desorption isotherms at temperatures much lower than those at which bubbles form. In the specific application of isotherms for moisture equilibrium modelling, the *A* parameter of (7-4) was found to depend on degree of polymerisation (DP) of the paper insulation. Thus, if the isotherm equation is applied to BIT, the same phenomenon should be observed.

Results in [55] showed that the ageing condition of the paper insulation, defined by its DP value, affects the BIT. New parameters were fitted to (7-4) for the new paper data in order to find the *A*, *n* and *B* values applicable to the specific paper insulation used in the study. This fitting for BIT of new paper (DP = 1357) from [55] is shown in (7-6).

$$\vartheta = \frac{10880}{30.544 + 3.156 \ln W - \ln p} \qquad (7\text{-}6)$$

This gives $A = 6.26\text{x}10^{-5}$, $n = 3.156$ and $B = 3447.4$. The n value is much higher than from [135] (1.4959), whereas the B value is lower (4722).

In [55], the results of BIT for aged paper were fit against the original formula, allowing n, B, and A to vary. This fitting for BIT of aged paper (DP = 341) from [55] is shown in (7-7). Note that from plotting of the curve, the $n\ln(1/A)$ term appears to have been misreported and the formula should actually appear as (7-8). It is also noted that the formula is originally presented with a plus sign before the pressure term, but this would violate the rearrangement (per rearrangement of (7-3) to (7-4)), following the physical reality that increased pressure should increase BIT.

$$\vartheta = \frac{16210000}{3.747 + 4497 \ln W + \ln p} \qquad (7\text{-}7)$$

$$\vartheta = \frac{16210000}{37470 + 4497 \ln W - \ln p} \qquad (7\text{-}8)$$

Considering (7-6) and (7-8), there does not appear to be any specific trend in the parameters found from the curve fitting and the DP value of the samples.

Returning to the underpinning description of the formula from Section 7.2.1.1, n is a value that is specific to the adsorption bond uniformity, and it is assumed that ageing through hydrolysis (the main ageing mechanism) has little to no influence on either the ratio between 2-, 3- and 6- located OH on cellulose monomers (shown in Figure 2-10), nor the ability of mono-layers and poly-layers to form, it seems sensible to suggest that the value of n should remain unchanged as the cellulose ages. Equally, because the bonds formed are the same (OH - H_2O) during adsorption irrespective of paper DP, the energy of formation should be unaffected by the ageing process (especially if the influence of other ageing by-products is discounted), so the value of B should remain constant as well.

This leaves only A able to vary with ageing. In (7-2), A is a pre-exponential factor for the rate constant, K, which can be described as showing 'the number of effective collisions per second', where 'effective' requires the collision to occur 'in the correct orientation' [104] and with sufficient energy to react [191].

When cellulose ages, its amorphous region is attacked first [49, 65, 192] and this is the form of cellulose which holds moisture most easily [66, 193]. Indeed, several studies have

shown that aged paper is capable of holding less moisture than unaged paper [55, 67-69, 77]. The proportions of amorphous and crystalline regions define the CI, with higher crystalline prevalence giving a higher CI.

If the amorphous region is depleted, resulting in a reduced accessibility of sites, it is reasonable to assume that the value of A is also affected, as the frequency of effective collisions is impacted. Smaller values of A in (7-4) result in lower BIT which is the expected outcome for bubbling in aged paper insulation [55]. This process is depicted by the flow chart in Figure 7-1.

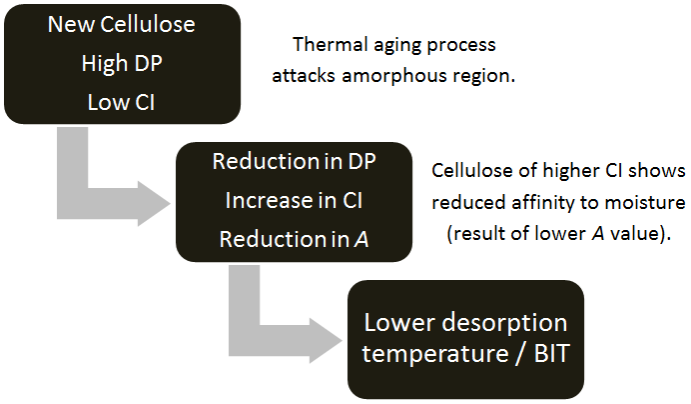

Figure 7-1 – Flow chart describing the reduction in A with ageing, and its effect on BIT.

Therefore, (7-4) is used to refit the data from [55] to improve (7-8), with n and B held constant from (7-6). This is presented in (7-9), showing that the A value has decreased in the aged paper. Figure 7-2 shows the original fitting of (7-8) compared to (7-9) on the data from [55]. There appears to be no advantage of the original fitting as both formulae fit the experimental data well; however the construction of (7-9) has a more sound theoretical basis.

$$\vartheta = \frac{10880}{32.05 + 3.156 \ln W - \ln p} \qquad (7\text{-}9)$$

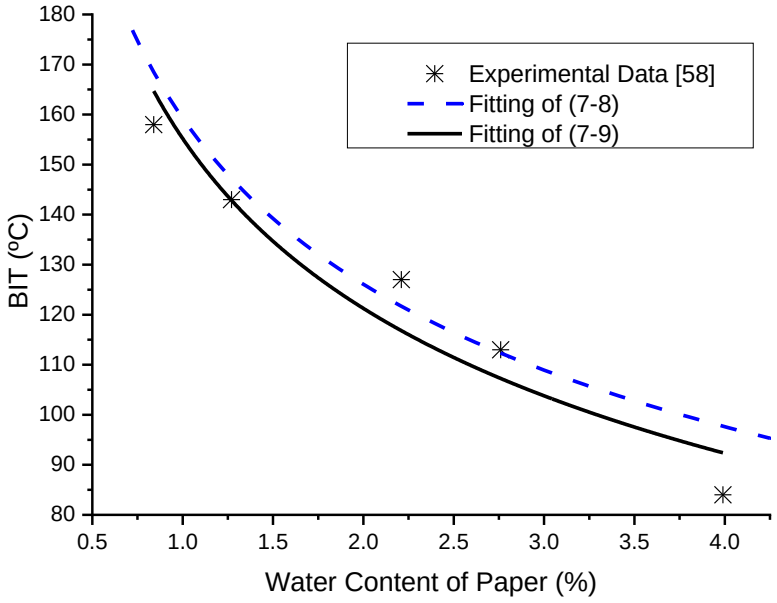

Figure 7-2 – Comparison of fitting between (7-8) and (7-9) against experimental data for aged paper from [55].

In addition to the work in [55], the same author published [54], which has results of BIT against moisture content of paper plotted for four values of DP (1360, 670, 464, and 272). Using (7-4) to fit these data, the *A* values and *n*ln(1/*A*) values are shown in Table 7-2. As in [55], because the system is gas free, the final term of equation (2-25) is not included in the fitting.

Table 7-2 – *A* and *n*ln(1/*A*) values against DP from data fitting on BIT plots in [54] with self-consistent *n* and *B* values.

DP	***A***	***n*ln(1/*A*)**
1360	7.33E-5	35.97
670	5.71E-5	36.92
464	4.03E-5	38.23
272	2.98E-5	39.37

As can be seen from Table 7-2, the *A* value decreases as DP decreases, as per prediction. The initial rate of change of *A* is fast, with amorphous regions attacked preferentially (thus raising the CI) which occurs over the first few chain scissions. Once the amorphous content is depleted, the crystalline regions are harder to degrade, and this will slow down the rate of decrease of *A*. Therefore, an exponential fitting of decay of *A* with DP^{-1} was used, shown in Figure 7-3. This generates (7-10), with $R^2 = 0.96$. The formula for *A* can then be input into (7-4) giving (7-11),

$$A = (9.3 \times 10^{-5}) e^{\frac{-339.1}{DP}} \qquad (7\text{-}10)$$

$$\vartheta = \frac{10880}{3.156\ln\left(\frac{1}{(9.3\times10^{-5})\mathrm{e}^{\frac{-339.1}{DP}}}\right) + 3.156\ln W - \ln p} \quad (7\text{-}11)$$

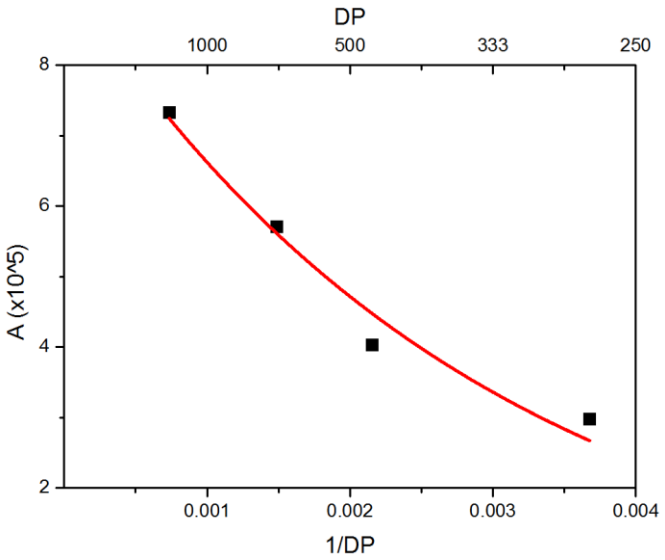

Figure 7-3 – Plot showing variation of *A* value with DP.

As mentioned, the *n* and *B* values are specific to the paper insulation selected. Varying these parameters shows how sensitive the fitting for the values in Table 7-2 is to their selection. Table 7-3 shows a summary of fittings for various cases. The formulae shown therein would directly replace (7-10) in (7-11), as would the appropriate *n* and *B* values.

Table 7-3 – *A* value fitting for various values of *n* and *B*.

Case	*n*	*B*	Fitting Relationship to *A*
n and *B* from (7-5)	1.4959	4722.8	$(3.7\times10^{-7})\mathrm{e}^{\frac{-331.5}{DP}}$
Small *n* from [135]	1.2799	4722.8	$(1.7\times10^{-7})\mathrm{e}^{\frac{-331.4}{DP}}$
Small *B* from [135]	1.4959	4211.6	$(13.0\times10^{-7})\mathrm{e}^{\frac{-334.2}{DP}}$
Large *B* from [135]	1.4959	4952.6	$(2.1\times10^{-7})\mathrm{e}^{\frac{-330.4}{DP}}$
n and *B* from [55]	3.156	3447.4	$(8.8\times10^{-5})\mathrm{e}^{\frac{-340.8}{DP}}$
n and *B* from [54]	3.778	3567.3	$(9.3\times10^{-5})\mathrm{e}^{\frac{-339.1}{DP}}$

When using different parameters, the pre-exponential factor changes accordingly to account for the changes in the formula caused by the adjustment of either the *n* or *B* value. However, the coefficient within the exponential term is relatively constant despite the changing conditions, indicating that while desorption characteristics may change, dependence on DP is consistent and reasonably unaffected by the selection of *n* and *B*.

7.2.2 Alternative Formula: Sorption Enthalpy

Rather than looking at bubbles as a change in the sorption isotherm state, bubbling temperature can be calculated by making use of an equation related the enthalpy for desorption of moisture from cellulose – bubbling is an aggressive form of desorption. Previously, a formula using this basis has been proposed by [102], as explained in Section 2.6.3. The base form of the equation is shown in (7-12) with α and β representing coefficients. β is a decay constant which causes temperature to reduce for wetter samples, and α is a pre-exponential temperature factor. This is derived from the desorption energy equation, (7-13), which relates the sorption energy of bonded water (Q_s) to the latent heat of water (i.e. the energy needed to vaporise pure, free water, L_r) and a value that reduces as the water content increases [194]. Essentially, (7-12) is (7-13) divided by the universal gas constant, after L_r has been taken away from Q_s.

$$\vartheta = \alpha e^{-\beta W} \qquad (7\text{-}12)$$

$$Q_s = \bar{R}_m \alpha e^{-\beta W} + L_r \qquad (7\text{-}13)$$

The equation in (7-12) is neat, because it allows the enthalpy to become very large as water content reduces toward zero, reflecting the difficulty of removing moisture completely, which is anecdotally well documented [56, 195]. Further, as the water content becomes very large, the energy flattens off to a constant value, which represents the point where moisture bonded in distant poly-layers becomes indistinguishable from free water (i.e. the desorption energy is close to the vaporisation energy of pure water).

Use of this equation in [102] was flawed, as the authors used temperatures based in Celsius instead of Kelvin for the parameter fitting. The first six entries in Table 7-4 show the original parameters from [102] and the parameters on an absolute temperature basis for a variety of conditions (aged insulation materials and TUP in addition to the usual new NTUP and new mineral oil).

For the form of BIT equation shown in (7-12) to be useful, not only should it have a theoretical basis and use parameters on the correct temperature basis, but it should also fit to other data. Data from [55] for insulation in the new condition (DP = 1357) is seen to have similar parameters to those from [102]. Likewise, the α and β values for new paper (DP = 1360) in [54] are similar. These parameters are summarised in Table 7-4.

Table 7-4 – α and β values for various data sets, materials, and material conditions (dashed line separates relative and absolute temperature fittings).

Source \ Parameter	Materials	Description	α	β
[102]	New NTUP New mineral oil	Original fitting on relative temperature basis (°C)	195.5	0.11186
[102]	New TUP New mineral oil	Original fitting on relative temperature basis (°C)	237.7	0.13718
[102]	Aged NTUP Aged mineral oil	Original fitting on relative temperature basis (°C)	178.0	0.07338
[102]	New NTUP New mineral oil	Revised fitting on absolute temperature basis (K)	464.4	0.03817
[102]	New TUP New mineral oil	Revised fitting on absolute temperature basis (K)	499.6	0.04866
[102]	Aged NTUP Aged mineral oil	Revised fitting on absolute temperature basis (K)	447.2	0.02444
[55]	New NTUP (DP = 1357) New mineral oil	New fitting on absolute temperature basis (K)	445.2	0.03097
[55]	Aged NTUP (DP = 341) New mineral oil	New fitting on absolute temperature basis (K)	451.3	0.05768
[54]	New NTUP (DP = 1360) New mineral oil	New fitting on absolute temperature basis (K)	454.4	0.03540
[54]	Aged NTUP (DP = 670) New mineral oil	New fitting on absolute temperature basis (K)	452.5	0.04103
[54]	Aged NTUP (DP = 464) New mineral oil	New fitting on absolute temperature basis (K)	443.0	0.04709
[54]	Aged NTUP (DP = 272) New mineral oil	New fitting on absolute temperature basis (K)	446.5	0.06040
[141]	New NTUP New mineral oil	New fitting on absolute temperature basis (K)	457.8	0.03842
[33]	New NTUP New natural ester	New fitting on absolute temperature basis (K)	446.0	0.02455
[33]	New NTUP New mineral oil	New fitting on absolute temperature basis (K)	440.2	0.02514
[153]	New NTUP New synthetic ester	New fitting on absolute temperature basis (K)	447.5	0.02141
[153]	New NTUP New mineral oil	New fitting on absolute temperature basis (K)	439.1	0.02116

However, as with the isotherm formula, it is also interesting to see how the parameters of the sorption enthalpy formula respond to changes in DP. When considering the aged paper (DP = 341) used in [55], the α value (451.3) is relatively unchanged as compared to the value for new paper given in Table 7-4, whereas the β value is markedly higher (0.05768).

For the range of DP values studied in [54], the α and β values are given in Table 7-4. The α values show minor scatter against DP, however the β values have a linear relationship with DP, as in (7-14), with R^2 >0.999. The plot of 1/DP versus β is shown in Figure 7-4.

$$\beta = 0.029 + \frac{8.58}{DP} \qquad (7\text{-}14)$$

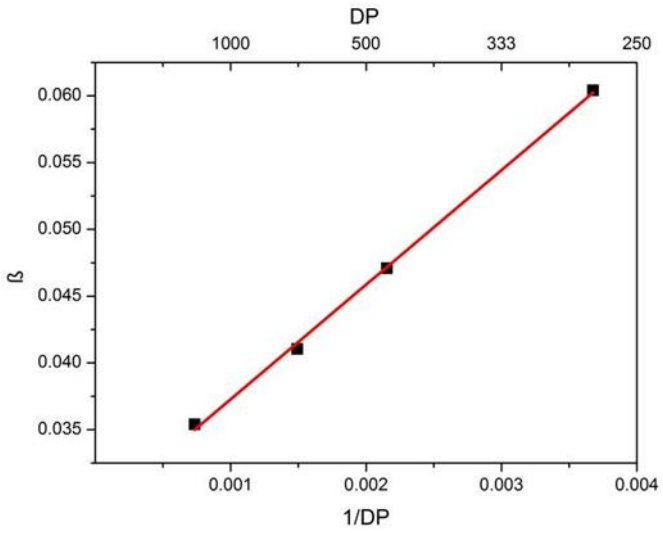

Figure 7-4 – Plot showing how β value varies with DP.

Thus, (7-12) can account for DP by substitution with (7-14) for β, as in (7-15).

$$\vartheta = \alpha e^{-\left(0.029+\frac{8.58}{DP}\right)W} \qquad (7\text{-}15)$$

The inference that β is dependent on DP whereas α is independent of DP assists in further understanding the physical meaning of the equation. The indication is that β describes how moisture influences the decay of BIT. When *W* is close to zero, the temperature is unaffected by the size of β. As moisture content increases, β becomes more influential. Lower DP systems have a reduced moisture saturation capacity, and are seen from Table 7-4 to have a greater β value. Therefore materials which have a large β value will adsorb moisture less strongly, and will have a lower absolute moisture content for the same RS than materials of smaller β.

On the other hand, α seems to be fixed at around 450 K (177°C), which suggests that there is an asymptotic limit on temperature as *W* tends to zero. This is sensible, with no moisture present, formation of moisture bubbles must be impossible, and hence the temperature given by α indicates the temperature at vanishingly small (unobtainably so in practice) moisture content in paper. The definition of 'vanishingly small' is, of course, arbitrary. For a newly installed transformer, one may expect a moisture content of the solid insulation to be less than 0.5% [31, 57], for such conditions and a β value calculated for a DP = 1200 (typical of newly installed insulation [60]), the exponential term would be 0.982, meaning that the temperature would be around 442 K (169°C).

Note that for [102], β was smaller in the lower DP case, instead of following the rising trend of Figure 7-4. This would suggest the opposite trend of moisture influence with ageing. However, as discussed within that study itself, the cellulose structure may have been altered during ageing (hornified) and this may have affected the outcome.

7.2.3 Material Comparisons

Fitting of the sorption enthalpy equation to results available in literature for alternative liquids from [33] and [153] shows how those materials influence the BIT as well. The solid insulation used in both of these studies is new NTUP. Both studies reported that the BIT for ester liquids was elevated compared to mineral oil.

Fitting of the desorption energy equation to the data for natural [33] and synthetic [153] esters produces the coefficients in Table 7-4. It is seen that the β value between mineral oil and ester for both cases is relatively unchanged suggesting that the dependence of BIT on moisture content in paper is unaffected by the liquid insulation selection (i.e., the cellulose moisture saturation capacity is dominant for β).

Conversely, the α value for the esters was higher than for the mineral oil in comparative experiments, indicating that there is a BIT elevation due to the change from mineral oil to ester liquid. The difference between ester and mineral oil α values matches with the differences identified in the BIT in those studies. Note that the β values of each liquid (ester and mineral oil) in both of studies are lower than that seen in all of the other data sets analysed.

The elevation of α may be explained as follows: the actual bond between cellulose OH group and H_2O molecule may be influenced by the surrounding material, especially in the case of materials of more polar nature such as the natural ester and synthetic ester used in [33] and [153], respectively. Insulating liquid impregnated in the cellulose may act as a force pulling inward, strengthening the adsorptive bond, and thus raising the BIT. This behaviour is similar to that of acids within paper which has been shown to increase the resistance of cellulosic paper to drying processes [50].

7.3 Discussion on the Theoretical Analysis of BIT Formulae

7.3.1 General Remarks

In summary, this study has shown that there is a significant requirement to update the formula in place for prediction of BIT: firstly, the errors found in the formula as supplied in the standards should be corrected; and secondly, the use of desorption isotherms needs great care when assessing bubble formation.

It is apparent that not all data available in literature shows the behaviour modelled by the formula as currently employed in the standards. It is shown in this study that improvements may be made by using a formula based on desorption enthalpy instead of sorption isotherms. This alternative is based on a better representation of bubbling activity yet it requires fewer input variables (there is no pressure term), in spite of which, accuracy of BIT prediction is not reduced.

It is important to keep in mind that irrespective of the formula in place, this study has emphasised the need for predictions of BIT to be sensitive to material conditions – particularly the saturated moisture capacity of cellulose or DP.

The dependence of DP has been shown for both of the equations based on data available from existing studies. The theoretical basis for the coefficients used in the two equations is discussed, showing how they can be used and altered in order to incorporate transformer insulation types and conditions. This will help to develop a loading guide which accounts for these features of transformer insulation.

7.3.2 Comments Regarding Formulae Selection

The sorption enthalpy equation for calculating BIT appears to be able to fit well against several data sets available in literature, and has the advantage of only requiring two parameters (α and β) and one variable (moisture content in paper) as inputs. The β value is shown to depend on DP.

The cellulose-moisture isotherm illustrates their sorption behaviour, showing the equilibrium conditions for a certain temperature. As in [139], the isotherm can be used to monitor how moisture is distributed between cellulose and liquid insulations for given temperatures. Under these equilibrium conditions, variation in distribution is noted as the

ageing condition of the paper changes, and this variation itself is seen to vary at different temperatures. Although a dependence on DP is also seen for BIT, as bubbling is a relatively dynamic process which involves vigorous desorption under rapid temperature rises one should not expect that isotherms are the most suitable depiction of this process.

As a result, it seems that a move from the isotherm formula to the enthalpy formula would be advantageous, and may be developed by further work to the great benefit of transformer operation.

Note that there are restrictions when fitting equations to the BIT data found in existing literature. Most data sets are small (in many cases used within this study, four or five data points for one material / material condition), and fitting across a data set therefore does not necessarily yield high accuracy across the full range. A method considered to combat this was to combine data from different studies, however the range of conditions used in experiments are varied, and not always clearly stated and so this was not done.

7.3.3 Case Study of DP and Isotherm Equation

Considering the same conditions for a transformer near end of life as in Section 4.6 (4% water content in paper, 4% gas content in oil), Figure 7-5 shows how the plot looks using parameters of the BIT equation corrected per [136], i.e. equation (7-5). The BIT calculated with the new parameters is 112°C (compared to 120°C previously). The reduction of BIT by 8 K means that the period for potential bubble inception is extended by two hours.

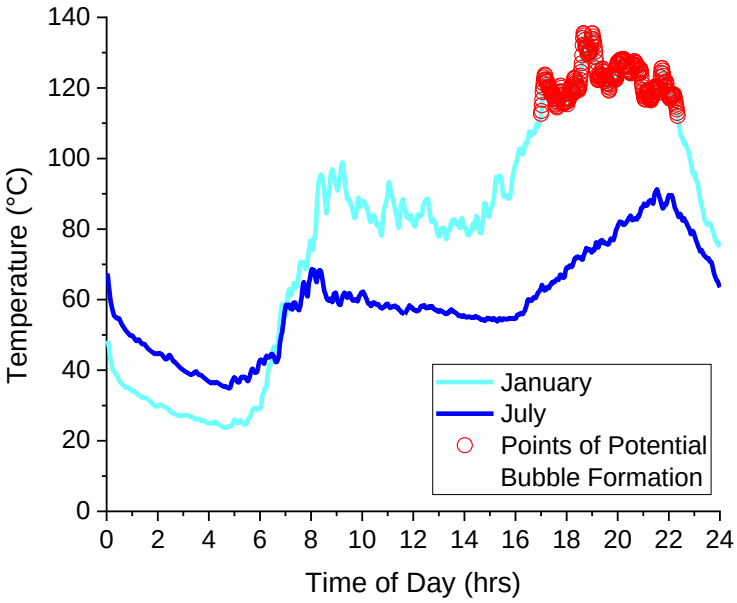

Figure 7-5 – Points of potential bubble formation identified for a transformer with 4% water content in paper and 4% gas content in oil, using updated BIT formula (7-5).

Further refinement can be obtained by using the updated BIT formula based on the inclusion of DP within this equation, as developed in this section (shown in equation (7-16)). By changing DP (but holding other variables constant), the HST profile of Figure 7-5 is reassessed for likely bubbling points.

$$\vartheta = \frac{7064.8}{1.4959\ln\left(\frac{1}{(3.7\times10^{-7})\mathrm{e}^{\frac{-331.5}{DP}}}\right) + 1.4959\ln W - \ln p} \qquad 7\text{-}16)$$

Figure 7-6, Figure 7-7, and Figure 7-8 show how reducing DP from 1000 (BIT = 118°C) to 600 (BIT = 111°C) and then to 400 (BIT = 103°C), respectively, affects the number of points at which the transformer is at risk of bubble formation. The period of potential bubble inception increases as the paper insulation ages. Toward end of life and a 4% moisture content in paper, the DP would be likely to have a value nearer to 400 than 1000, and there is a notable effect of not accounting for this. This demonstrates the importance of including DP within BIT analysis.

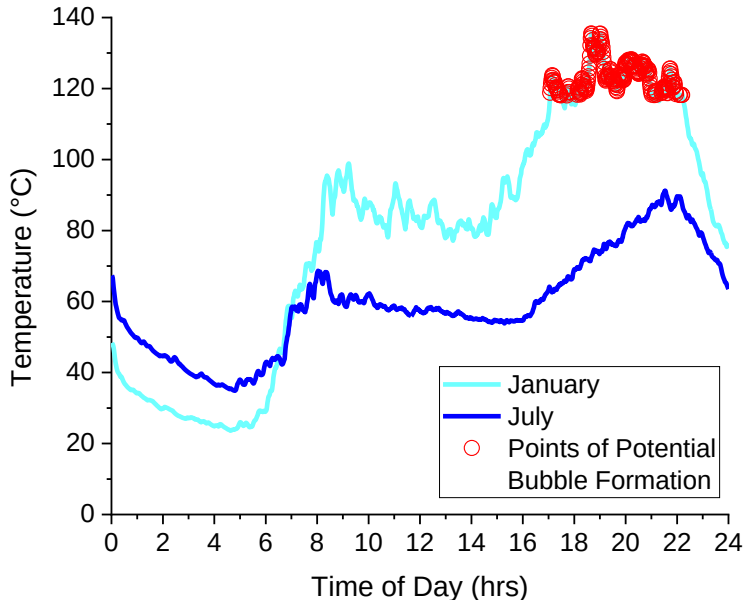

Figure 7-6 – Points of potential bubble formation identified for a transformer with 4% water content in paper and 4% gas content in oil, using updated BIT formula with DP = 1000.

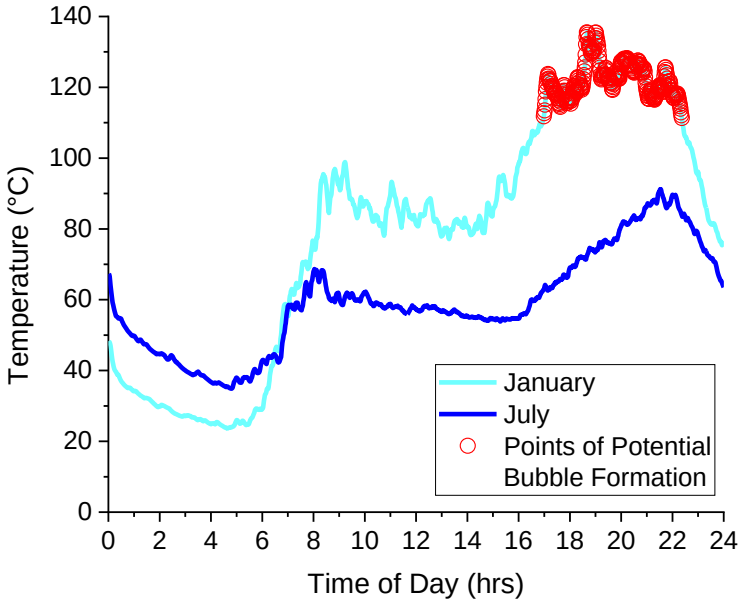

Figure 7-7 – Points of potential bubble formation identified for a transformer with 4% water content in paper and 4% gas content in oil, using updated BIT formula with DP = 600.

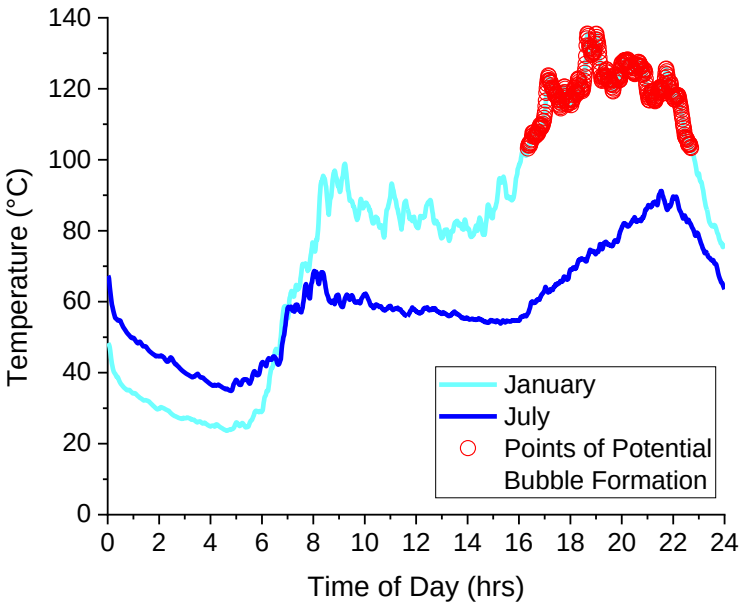

Figure 7-8 – Points of potential bubble formation identified for a transformer with 4% water content in paper and 4% gas content in oil, using updated BIT formula with DP = 400.

7.4 SUMMARY

This chapter has shown the development of an alternative formula for calculating bubble inception temperatures, based on the fundamental thermodynamic process of moisture sorption behaviour within transformer insulation. Both the proposed formula and the original formula are improved by including factors that account for the DP of the cellulosic insulation. The impact of these changes is assessed in a case study comparable to the assessment made in Chapter 4.

8 CONCLUSIONS AND FURTHER WORK

8.1 GENERAL CONCLUSIONS

8.1.1 Bubbling in Transformers

Study of transformer failures due to the formation of moisture bubbles from insulation has been on-going intermittently for more than forty years. New angles and aspects of this topic have been raised, and will continue to do so. The work herein looks at three relevant and contemporary issues (increased loading, alternative material selection, and material condition) and so adds to the available literature. There is also a focus on the mechanism behind bubble formation and this is described through monitoring of moisture in both the solid and liquid insulation media throughout experiments.

The finding that loading and insulation condition impact the time, temperature, and energy required to form a bubble is key information to asset owners / operators and should be factored into the design of new assets as well as being used to protect assets already in service.

The behaviour of moisture within transformers has had an even longer history of study than moisture bubbles, yet still there are impediments to thorough understanding of how it interacts between insulation media, particularly in a dynamic temperature environment. Different materials interact differently with moisture, as can be seen by the results from this study. Thermally upgrading paper has significant benefits to the extensibility of lifetime and / or increasing the loading capacity of a transformer. This work shows that it also offers an increased resistance to bubble formation which is crucial if this insulation is to be allowed to operate at elevated temperatures.

8.1.2 Relevance and Application of Work

The early chapters of this work set the scene for the relevance of this work. It is evident that failures of transformers are events to avoid, and that the impact of failure can be high.

Alternative insulation materials are available to transformer manufacturers, and there are myriad reasons for their selection. An increase in the prevalence of different materials within the transformer fleet is likely, especially as the cost of the newer materials reduces in line with growing production capacity. This presents its own challenges for operators who need to be conversant with numerous condition assessment criteria and a greater breadth of

understanding related to ageing and loading capability of assets fitted with different materials and material combinations. This work goes some way to providing answers to a specific part of this essential knowledge.

Adoption of new technologies is coming. The loading scenarios in this work were based on circumstances where high electrification occurs, and the basis for this is largely related to climate change. It is recognised that there is a small proportion of influential people who do not subscribe to the climate change narrative. For example, under the Trump administration, America has withdrawn unilaterally from the Paris Agreement (effective from 4th November 2020) [196]. Hence some people may dispute the validity of studying such loading cases. However, the need to adapt our electricity networks and to brace them for the stresses of high electrification of energy is still relevant. The UK government is raising legislation to restricts connection of new-build houses to the gas network from 2025 for heating purposes [197]. Similarly, legislation has been in place for a number of years making it difficult for high rise dwellings to be connected to the gas network [198]. The latter of these exists for safety of residents [199], totally abstracted from reduction of GHG emissions. Likewise, EVs are increasing in prevalence, as are charging points. Again, the UK has legislated against sale of new petrol and diesel cars from 2040 (due to be brought forward to 2035) [167, 200], and funding to allow installation of 3,600 new charging points in 2020 has also been committed [201]. There are now more EV charging points than petrol stations in the UK [202]. Indeed, [203] predicted a potential move from the internal combustion engine in cars before the Paris Agreement was conceived, and did so simply by considering market forces and technology. Add in the volatility of fossil fuel prices and their dwindling supply, and the case for electrification is made irrespective of climate change activism.

This document therefore should be taken as a ‘future-proofing’ of transformers, one of the key assets in the power network. New materials and new loads will bring about new challenges.

8.1.3 Summary of Main Findings

In addition to a detailed review of the relevant literature (Chapter 2), a step-by-step description of a modelling strategy that can be used to assess transformer thermal capacity (Chapter 3), and development of an experimental design and philosophy (Chapters 5 and 6), the main findings from this work are:

i. A formula based on an enthalpy basis rather than a desorption basis would hold a stronger theoretical grounding, and such a formula was shown to perform well against previous BIT results. Additionally, the bubble formation formula currently presented in the standards has an error. This should be corrected, and in doing so requires an alteration to the final term, previously dependent on the gas content of liquid insulation. (Shown in Chapters 2 and 7)

ii. Transformer insulation which is more aged has a lower BIT, and this should be accounted for within the bubble inception formula. Including for DP is shown to be more important than including for gas content of the liquid insulation Transformers with insulation of higher moisture content and lower DP are likely to conflate and thus the impact of this should not be ignored, as bubbles may form at several degrees Celsius lower from lower DP insulation. (Shown in Chapter 7)

iii. Future loading scenarios (accounting for electrification of demand) have the potential to put transformers into situations where bubbles are likely to form more often that present loading scenarios. (From results of Chapter 4)

iv. Load impacts bubble inception criteria. A larger step change in load (i.e. a faster rate of temperature rise) makes bubble formation easier and more likely, and thus places a transformer at increased risk. This was particularly prevalent for TUP insulation. (Shown by results in Chapter 6)

v. Material selection is important: solid insulators have different bubble inception performance. Specifically, this study found that thermally upgrading paper insulation resisted bubble formation with a higher BIT for the same RS of paper compared to non-thermally upgraded paper. (From results of Chapter 6)

vi. Solid insulation media is dominant: moisture bubbles form primarily from the solid insulation. The solid insulation holds the majority of the moisture, is at higher temperatures, and is immobile. This study showed that formation within purely from liquid insulation is particularly difficult, and this is a finding which should bring some comfort (Chapter 5). This also allows focus on paper insulation as the best option for combatting bubble formation. The mechanism for bubble formation is described in new detail, with focus on the transition of moisture during tests a key factor. (Shown in Chapter 6)

Referring back to Figure 1-3, the mechanism of failure through bubble formation was broken down into eight segments. The results of this study covered several of them, focusing on the high temperature to formation and release of a bubble from moisture in insulation, and accounting for the effects of ageing. It is important to note that in trying to prevent failure of transformers from bubble formation that if any one of the first seven stages shown in Figure 1-3 can be blocked, then failure will not occur. Advice pervades this thesis, but key messages are to keep solid insulation dry, to account for insulation condition (including ageing condition), and to keep temperatures below the limit calculated by including DP and moisture, as well as material selection.

8.2 FUTURE WORK

This thesis has worked on the problem of bubble formation in transformers due to high temperature overloads. The high temperatures simulated in this work were due to the expected increase in electrical load due to widespread adoption of EHPs. Future work could expand the scenarios around this, including, for example, EV uptake and solar panel installations.

The failure mechanism investigated herein was through the formation of bubbles in the insulation which then present a dielectric weakness within the transformer. There are other life-related aspects of a transformer which are affected by the load / temperature profile of the transformer. Bubble formation was selected for study within this thesis for several reasons, mainly that it is a short-term failure mode, dominated by high-overload temperatures, such as those that may be experienced during future loading scenarios. That said, other mechanisms such as degradation of solid insulation, can also be affected by overload temperatures, and if those overloads are particularly high (as shown to be possible herein) then the effect is not necessarily simple, and so is certainly worthy of further study.

8.2.1 General Suggestions for Additional to Knowledge

There are several routes of further study which can contribute in establishing a more complete understanding of bubbling in transformers by building directly on the experiments and findings of this study:

1. Liquid insulation material condition: this study limited the liquid condition to ‘dry, as new’ whenever paper insulation was included in tests. It would be beneficial to understand how the condition of the material (e.g. wetter, more

acidic, etc.) can influence bubble formation characteristics. This study showed that the solid insulation is the dominant factor for bubble formation, and that liquid insulation did not need to be saturated with liquid before bubbles formed. However it would be helpful to confirm if liquid insulation that is high in moisture content before the test would leave to a reduction in tBI and BIT.

This feature of the insulation can also be related to dynamic loading where in the rise and fall in transformer temperatures affects the moisture distribution between insulation media and this could affect bubbling.

2. Ageing of insulation: within this study, the effect of ageing on bubble inception temperature is developed theoretically. Further experimental validation of the findings would be beneficial.
3. Additional tests conducted at other paper moisture contents would reinforce the findings and conclusions, particularly in the drier region (circa 1 – 2% for NUTP). These tests could include analysis of the substance of the bubbles, particularly for drier samples where less moisture is available and other gaseous material may contribute to the formation of the bubbles.

8.2.2 Development of Large-scale Test Rig

The tests in this study were conducted on a small scale. A limiting factor of this was that it was difficult to make intermediate measurements such as liquid insulation conductivity and temperature measurements. Development of a large-scale test set-up could allow for additional monitoring equipment to be introduced to the sample / test system without compromising the sample quality.

When looking mechanistically at bubbles at the paper interface, the small-scale test had clear advantages, described in Chapters 5 and 6. However, further understanding about the movement of moisture during the tests could be gained by making other observations (such as constantly monitoring the local *and* bulk liquid insulation moisture content).

Another advantage of a larger system is its resistance to inertia – that is to say, small-scale tests were completed after 30 minutes, after which point it was determined that the paper insulation samples were nearly completely dry, and it was decided that further testing would not be beneficial. However, it may be possible to set up a larger scale system which would allow repeated tests on the same sample, which could then allow for longer

scale testing such as application of a daily (or longer) load profile to the sample to see if bubbling resistance is reduced on multiple applications of load (while monitoring factors such as the paper insulation moisture and DP values with time).

8.2.3 Development of Load-Temperature-Moisture-Bubble Model

Clearly the relationship between transformer insulation condition and transformer loading is influential to the bubble characteristics of the transformer insulation. One issue that is faced by the transformer operator when hoping to avoid bubble formation is the inherent link between the key parameters of temperature and moisture. High temperatures drive moisture out of insulation, encourage the breakdown of insulation which creates moisture; and can result in the formation of bubbles. Highest moisture contents tend to be at the coldest parts of the insulation (an advantage in avoidance of bubbles), but sudden high loads or cooling faults can mean that previously cool areas of the transformer may become hot rapidly.

The variety of load profiles that could be applied to a transformer also make this assessment more complex. Other load profiles should be considered, for example uptake of solar panels can reduce daytime demand from the network (due to local production of electricity), but in the evening this is lost. Considered alongside a network of high electrification of heating and transport, there could be a steep evening rise in usage. As shown in Chapter 6 of this thesis, there is a reason for concern when applying larger step changes in loading.

The existing guidance on bubble formation in transformers is to set a temperature beyond which bubbles may form, based almost solely on the moisture content of the insulation. It is apparent from the work of this study that other factors should be considered within the predictive analysis. This works both ways, and there is the potential to free up capacity in some transformers (particularly in new, dry transformers or transformers which may be at continuously high loading) as well as to limit the available capacity of transformers in worse conditions.

Therefore, the ultimate quest of the transformer bubble formation engineer would be to link the load / temperature of the transformer to the moisture migration between its insulation media, and to consider from this the potential for bubble formation for insulation, based on type and condition (e.g. age). Ideally such a complete model would include a

history (at least a recent history) of the transformer conditions and loading. The beginnings of such an idea are discussed in [204].

8.2.4 Moving from Laboratory to Site

The final step to this is the application of live-time monitoring of transformer condition and, ultimately, on allowing a moving limit on its capacity (that may move up or down with time).

Monitoring on the transformer can be difficult and expensive. For direct measurement of temperature, best-in-class is the use of fibre optics. This is a costly method, but there is still uncertainty (that may be reduced, but not to zero, through modelling) in the best location to monitor: the location of the HST is not easy to identify, and may move within the transformer winding depending on the loading or cooling state of the transformer.

Additionally, monitoring of solid insulation is a known difficulty, and work is ongoing to link the condition of the transformer insulating fluid to the condition of the solid insulation [75, 76]. Of course, the relative condition of the two insulating media are linked through temperature, and this adds a further complication when inferring solid insulation condition from liquid insulation condition.

Without accurate information for the temperature, moisture content, and DP of the solid insulation, BIT is always limited to a ‘best guess’ based on the experience of the operators. Of course, engineering should balance the need to monitor and protect the system against financial outlay, but ideally a direct temperature measurement can be made and good information about the material condition held such that decisions such as limitations on the capacity of transformers through-life can be made appropriately.

Thus, the continued work of relating field conditions of moisture content, ageing degree and temperature is needed in order to allow the fullest picture of the transformer failure risk to be developed.

REFERENCES

[1] K. Anderson and A. Bows, "Beyond ‘dangerous’ climate change: emission scenarios for a new world," *Philosophical Transactions of the Royal Society A: Mathematical, Physical and Engineering Sciences,* vol. 369, no. 1934, pp. 20-44, 2011.

[2] Y. N. Harari, *Homo Deus: A Brief History of Tomorrow*. London: Vintage, 2016.

[3] IPCC, "Mitigation of Climate Change–Summary for Policymakers," ed: Cambridge University Press Cambridge, 2007, pp. 1-18.

[4] M. R. Allen, D. J. Frame, C. Huntingford, C. D. Jones, J. A. Lowe, M. Meinshausen, and N. Meinshausen, "Warming caused by cumulative carbon emissions towards the trillionth tonne," *Nature,* vol. 458, no. 7242, pp. 1163-1166, 2009/04/01 2009.

[5] M. New, D. Liverman, H. Schroder, and K. Anderson, "Four degrees and beyond: the potential for a global temperature increase of four degrees and its implications," *Philosophical Transactions of the Royal Society A: Mathematical, Physical and Engineering Sciences,* vol. 369, no. 1934, pp. 6-19, 2011.

[6] "Coal Consumption Affecting Climate.," in *The Braidwood Dispatch and Mining Journal*, ed. NSW, Australia, 1912, p. 4.

[7] "Coal Consumption Affecting Climate.," in *Rodney and Otamatea Times, Waitemata and Kaipara Gazette*, ed. New Zealand, 1912, p. 7.

[8] *Paris Agreement,* United Nations 54113, 2015.

[9] *Kyoto Protocol to the United Nations Framework Convention on Climate Change*, United Nations 30822, 1997.

[10] IChemE. (2019, July/August 2019) UK sets target for net zero emissions by 2050. *The Chemical Engineer*. 16.

[11] Commitee on Climate Change, "Reducing UK emissions: 2019 Progress Report to Parliament," London, UK, 2019.

[12] J. Rogelj, B. Hare, J. Nabel, K. Macey, M. Schaeffer, K. Markmann, and M. Meinshausen, "Halfway to Copenhagen, no way to 2 °C," *Nature Climate Change*, vol. 1, no. 907, pp. 81-83, 2009/07/01 2009.

[13] A. Macintosh, "Keeping warming within the 2°C limit after Copenhagen," *Energy Policy,* vol. 38, no. 6, pp. 2964-2975, 2010/06/01/ 2010.

[14] J. Vidal and A. Vaughan, "Paris climate agreement ‘may signal end of fossil fuel era’," in *The Observer*, ed. UK: Guardian Media Group, 2015.

[15] K. F. Gerdes, Ed. *Carbon Dioxide Capture for Storage in Deep Geological Formations: Results from the CO2 Capture Project. Volume 4: CCS Technology Development and Demonstration Results (2009-2014)*. CPL, 2015.

[16] P. J. Crutzen, "Albedo enhancement by stratospheric sulfur injections: A contribution to resolve a policy dilemma?," *Climatic change,* vol. 77, no. 3-4, p. 211, 2006.

[17] Commitee on Climate Change, "Net Zero: Technical Report," London, UK, May 2019 2019.

[18] D. Calverley, R. Wood, S. Mander, K. Anderson, S. Glynn, and F. Nicholls, "Towards a 2 C future: emission reduction scenarios for Wales," *Report commissioned by the Climate Change Commission of the Welsh Assembly Government,* 2009.

[19] P. Richardson, M. Moran, J. Taylor, A. Maitra, and A. Keane, "Impact of electric vehicle charging on residential distribution networks: An Irish demonstration initiative," 2013.

[20] Commitee on Climate Change, "Reducing UK emissions: 2018 Progress Report to Parliament," London, UK, 2018.

References

[21] S. J. Tee, "Ageing Assessment of Transformer Insulation through Oil Test Database Analysis," The University of Manchester, 2016.

[22] *IEEE Guide for Loading Mineral-Oil-Immersed Transformers and Step-Voltage Regulators*, IEEE Std C57.91-2011 (Revision of IEEE Std C57.91-1995), 2011.

[23] *Power Transformers. Loading Guide for Mineral-oil-immersed Power Transformers*, BS IEC 60076-7:2018, 2018.

[24] "DNO Common Network Asset Indices Methodology," 30/01/2017 2017.

[25] Ofgem, "Companies pay £10.5 million over 9 August power cut," ed. https://www.ofgem.gov.uk/publications-and-updates/companies-pay-105-million-over-9-august-power-cut, 2020.

[26] ENERGO-COMPLEX, "Comprehensive solutions for transformers," *Transformers Magazine*, vol. 7, no. 2, pp. 46-53, Apr 2020 2020.

[27] W. H. Tang, *Condition Monitoring and Assessment of Power Transformers Using Computational Intelligence* (Power Systems). London: Springer London, 2011.

[28] A. Bossi, J. Dind, J. Frisson, U. Khoudiakov, H. Light, D. Narke, Y. Tournier, and J. Verdon, "An international survey on failures in large power transformers in service," *Cigré Electra*, vol. 88, pp. 21-48, 1983.

[29] Cigré, "Cigré Brochure 642 "Transformer reliability survey"," *Working Group A2.37*, December 2015 2015.

[30] Cigré, "Cigré Brochure 735 "Transformer post-mortem analysis"," *Working Group A2.45;*, 2018.

[31] Cigré, "Cigré Brochure 738 "Ageing of liquid impregnated cellulose for power transformers"," *Working Group D1.53;*, 2018.

[32] C. F. Hill, "Temperature limits set by oil and cellulose insulation," *Transactions of the American Institute of Electrical Engineers*, vol. 58, no. 9, pp. 484-491, 1939.

[33] C. Y. Perkasa, N. Lelekakis, T. Czaszejko, J. Wijaya, and D. Martin, "A comparison of the formation of bubbles and water droplets in vegetable and mineral oil impregnated transformer paper," *IEEE Transactions on Dielectrics and Electrical Insulation*, vol. 21, no. 5, pp. 2111-2118, 2014.

[34] G. Kaufmann and C. McMillen, "Gas bubble studies and impulse tests on distribution transformers during loading above nameplate rating," *IEEE Transactions on Power Apparatus and Systems*, no. 8, pp. 2531-2542, 1983.

[35] Cigré, "Cigré Brochure 248 "Guide on economics of transformer management"," *Working group A2.20*, 2004.

[36] A. Allerhand, "Early AC power: The first long-distance lines [history]," *IEEE Power and Energy Magazine*, vol. 17, no. 5, pp. 82-90, 2019.

[37] M. J. Heathcote, *J&P Transformer Handbook*, 13th ed. Elsevier Ltd., 2007.

[38] J. J. Grainger and W. D. Stevenson, *Power System Analysis* (International Editions). Singapore, 1994.

[39] *Modern Power Transformer Practice*. London: Macmillan, 1979.

[40] *Cellulosic papers for electrical purposes — Part 2: Methods of test*, BS IEC 60554-2:2002, 2002.

[41] Cigré, "Cigré Brochure 779 "Field experience with transformer solid insulation ageing markers"," *Joint Working Group A2/D1.46*, 2019.

[42] *Power transformers. Loading guide for oil-immersed power transformers*, BS EN 60076- 7:2010, 2005.

[43] H.-P. Moser, H. Brechna, W. Heidemann, and V. Dahinden, *Transformerboard*. H. Weidmann, 1979.

[44] B. S. Y. H. Matharage, "Ageing assessment of transformer paper insulation through methanol and ethanol detection," The University of Manchester, 2018.

References

[45] C. Krause, "Power transformer insulation–history, technology and design," *IEEE Transactions on Dielectrics and Electrical Insulation,* vol. 19, no. 6, pp. 1941-1947, 2012.

[46] Cigré, "Cigré Brochure 323 “Ageing of cellulose in mineral-oil insulated transformers”," *Task Force D1.01.10;,* 2007.

[47] T. A. Prevost, "Correlation of nitrogen content with aging rate in thermally upgraded conductor insulation," *Doble Engineering Company,* 2004.

[48] T. A. Prevost, "Thermally upgraded insulation in transformers," *Proceedings Electrical Insulation Conference and Electrical Manufacturing Expo, 2005.*, 2005: IEEE, pp. 120-125.

[49] O. H. Arroyo-Fernández, I. Fofana, J. Jalbert, E. Rodriguez, L. B. Rodriguez, and M. Ryadi, "Assessing changes in thermally upgraded papers with different nitrogen contents under accelerated aging," *IEEE Transactions on Dielectrics and Electrical Insulation,* vol. 24, no. 3, pp. 1829-1839, 2017.

[50] L. E. Lundgaard, W. Hansen, D. Linhjell, and T. J. Painter, "Aging of oil-impregnated paper in power transformers," *IEEE Transactions on Power Delivery,* vol. 19, no. 1, pp. 230-239, 2004.

[51] *Cellulosic papers for electrical purposes — Part 1: Definitions and general requirements,* BS 5626-1:1979 / IEC 60554-1, 1977.

[52] DU PONT, "NOMEX Technical Data Sheet Introduction," June 2000.

[53] *Aramid pressboard for electrical purposes - Part 1. Definitions and general requirements,* BS EN 61629-1:1997, 1996.

[54] P. Przybylek, "A comparison of bubble evolution temperature in aramid and cellulose paper," *IEEE International Conference on Solid Dielectrics*, 2013, pp. 983-986.

[55] P. Przybylek, "The influence of cellulose insulation aging degree on its water sorption properties and bubble evolution," *IEEE Transactions on Dielectrics and Electrical Insulation,* vol. 17, no. 3, pp. 906-912, 2010.

[56] G. K. Frimpong and L. Melzer, "Evaluation of mechanical condition of transformer paper insulation after factory drying," *IEEE Electrical Insulation Magazine,* vol. 35, no. 6, pp. 23-32, 2019.

[57] C. Bengtsson, C. Krause, A. Mikulecky, M. Scala, M. Lessard, L. Melzer, P. Hurlet, and C. Rajotte, "Insulation condition during transformer manufacturing," *Electra,* vol. 2018, no. 299, p. 1, 2018.

[58] A. Emsley, "Degradation of cellulosic insulation in power transformers. Pt.4: effects of ageing on the tensile strength of paper," *IEE Proceedings. Science, Measurement and Technology,* vol. 147, no. 6, pp. 285-290, 2000.

[59] H. Gasser, J. Huser, C. Krause, V. Dahinden, and A. Emsley, "Determining the ageing parameters of cellulosic insulation in a transformer," *1999 Eleventh International Symposium on High Voltage Engineering*, 1999, vol. 4: IET, pp. 143-147.

[60] W. J. McNutt, "Insulation thermal life considerations for transformer loading guides," *IEEE Transactions on Power Delivery,* vol. 7, no. 1, pp. 392-401, 1992.

[61] L. E. Lundgaard, W. Hansen, S. Ingebrigtsen, D. Linhjell, and M. Dahlund, "Aging of Kraft paper by acid catalyzed hydrolysis," *IEEE International Conference on Dielectric Liquids, 2005. ICDL 2005.*, 2005: IEEE, pp. 381-384.

[62] V. Montsinger, "Loading transformers by temperature," *Transactions of the American Institute of Electrical Engineers,* vol. 49, no. 2, pp. 776-790, 1930.

[63] F. Clark, "Factors affecting the mechanical deterioration of cellulose insulation," *Electrical Engineering,* vol. 61, no. 10, pp. 742-749, 1942.

[64] P. Przybylek and H. Moscicka-Grzesiak, "The influence of water content and ageing degree of paper insulation on its mechanical strength," *2010 10th IEEE International Conference on Solid Dielectrics*, 2010: IEEE, pp. 1-3.

[65] P. Navard, "The European Polysaccharide Network of Excellence (EPNOE): research initiatives and results," Springer Science & Business Media, 2012, pp. 215-248.

[66] A. Assaf, R. Haas, and C. Purves, "A new iInterpretation of the cellulose-water adsorption isotherm and data concerning the effect of swelling and drying on the colloidal surface of cellulose1, 2," *Journal of the American Chemical Society*, vol. 66, no. 1, pp. 66-73, 1944.

[67] M. Koch, S. Tenbohlen, and T. Stirl, "Diagnostic application of moisture equilibrium for power transformers," *IEEE Transactions on Power Delivery*, vol. 25, no. 4, pp. 2574-2581, 2010.

[68] P. Przybylek, "The influence of temperature and aging of cellulose on water distribution in oil-paper insulation," *IEEE Transactions on Dielectrics and Electrical Insulation*, vol. 20, no. 2, pp. 552-556, 2013.

[69] D. Martin, T. Saha, O. Krause, G. Buckley, S. Chinnarajan, R. Dee, and G. Russell, "Improving the determination of water content of power transformer insulation paper near the end of its functional life," *2016 Australasian Universities Power Engineering Conference (AUPEC)*, 2016, pp. 1-6.

[70] S. P. Hill and J. M. Winterbottom, "The conversion of polysaccharides to hydrogen gas. Part I: The palladium catalysed decomposition of formic acid/sodium formate solutions," *Journal of Chemical Technology & Biotechnology*, vol. 41, no. 2, pp. 121-133, 1988.

[71] *Power transformers. Liquid-immersed power transformers using high-temperature insulation materials*, BS EN 60076- 14:2013, 2013.

[72] ABB Transformers, "Transformer Handbook," *Affolternstrasse*, vol. 44, p. 8050, 2004.

[73] C. Wolmarans and B. Pahlavanpour, "Insulating liquid properties impacting transformer performance," *Transformers Magazine*, vol. 6, no. 1, pp. 104-110, 2019.

[74] S. Y. Matharage, Q. Liu, and Z. D. Wang, "Aging assessment of kraft paper insulation through methanol in oil measurement," *IEEE Transactions on Dielectrics and Electrical Insulation*, vol. 23, no. 3, pp. 1589-1596, 2016.

[75] B. S. Y. Matharage, Q. Liu, Z. D. Wang, G. Wilson, and C. Krause, "Aging assessment of synthetic ester impregnated thermally non-upgraded kraft paper through chemical markers in oil," *IEEE Transactions on Dielectrics and Electrical Insulation*, vol. 25, no. 2, pp. 507-515, 2018.

[76] Z. Yan, S. Y. Matharage, Q. Liu, and Z. D. Wang, "Extraction of low molecular weight acids from transformer liquids using water extraction technique," *2018 12th International Conference on the Properties and Applications of Dielectric Materials (ICPADM)*, 2018: IEEE, pp. 198-201.

[77] D. Martin, T. Saha, R. Dee, G. Buckley, S. Chinnarajan, G. Caldwell, J. B. Zhou, and G. Russell, "Determining water in transformer paper insulation: analyzing aging transformers," *IEEE Electrical Insulation Magazine*, vol. 31, no. 5, pp. 23-32, 2015.

[78] S. Y. Matharage, S. Liu, Q. Liu, and Z. D. Wang, "Investigation on the Acid Removal Performance of Oil Regeneration Sorbent Materials," Cham, 2020: Springer International Publishing, pp. 871-877.

[79] B. Pahlavanpour and I. Roberts, "Transformer oil condition monitoring," 1998.

[80] Cigré, "Cigré Brochure 761 "Condition assessment of power transformers"," *A2.49*, 2019.

References

[81] Cooper Power Systems, "Envirotemp FR3 Fluid - Distribution Transformers in Cold Temperature Environments," Sep 2010 2010.

[82] U. M. Rao, I. Fofana, T. Jaya, E. M. Rodriguez-Celis, J. Jalbert, and P. Picher, "Alternative dielectric fluids for transformer insulation system: progress, challenges, and future prospects," *IEEE Access,* vol. 7, pp. 184552-184571, 2019.

[83] F. Bachinger and P. Hamberger, "Measurement of thermal behavior of an ester-filled power transformer at ultra-low temperatures," *e & i Elektrotechnik und Informationstechnik,* vol. 135, no. 8, pp. 536-542, 2018.

[84] E. Casserly, "The relationship between the physical, chemical, and functional properties of insulating liquids," *2019 IEEE 20th International Conference on Dielectric Liquids (ICDL),* 2019: IEEE, pp. 1-6.

[85] I. Fernández, A. Ortiz, F. Delgado, C. Renedo, and S. Perez, "Comparative evaluation of alternative fluids for power transformers," *Electric Power Systems Research,* vol. 98, pp. 58-69, 2013.

[86] S. A. Azli, M. H. F. Rahiman, Z. M. Yusoff, N. F. Razali, S. S. A. Wahid, and M. S. Ramli, "A review on alternative oils as dielectric insulating fluids on power transformer," *IEEE 15th International Colloquium on Signal Processing & Its Applications (CSPA),* 2019: IEEE, pp. 198-201.

[87] M. Eklund, "Mineral insulating oils; functional requirements, specifications and production," *Conference Record of the 2006 IEEE International Symposium on Electrical Insulation,* 2006, pp. 68-72.

[88] NYNAS, "Product Data Sheet Nytro Gemini X," 2014.

[89] Shell, "Shell Diala S4 ZX-I Technical Data Sheet," 18 August 2014 2014.

[90] N. Lelekakis, D. Martin, W. Guo, J. Wijaya, and M. Lee, "A field study of two online dry-out methods for power transformers," *IEEE Electrical Insulation Magazine,* vol. 28, no. 3, pp. 32-39, 2012.

[91] K. Rapp and A. Sbravati, "Natural ester fluid transforms electrical industry norm," *Transmission and Distribution,* no. 1, pp. 12-15, Feb-March 2020 2020.

[92] Q. Liu, "Electrical Performance of Ester Liquids under Impulse Voltage for Application in Power Transformers," The University of Manchester, 2011.

[93] T. V. Oommen, "Vegetable oils for liquid-filled transformers," *IEEE Electrical Insulation Magazine,* vol. 18, no. 1, pp. 6-11, 2002.

[94] Cargill Inc., "Envirotemp FR3 fluid: Formulated for performance.," October 2016 2016.

[95] J. G. Ford and C. F. Hill, "Dielectric liquid for electrical apparatus," US, 1938.

[96] Cigré, "Measurement of thermal behavior of an ester-filled power transformer at ultra-low temperatures," *A2-111,* 2018.

[97] S. J. Tee, D. Walker, and M. Bebbington, "Experience of synthetic ester filled transformers in SP Energy Networks," *International Conference on Dielectric Liquids (ICDL),* 2019: IEEE, pp. 1-4.

[98] H. Borsi and E. Gockenbach, "Properties of ester liquid Midel 7131 as an alternative liquid to mineral oil for transformers," *IEEE International Conference on Dielectric Liquids (ICDL),* 2005: IEEE, pp. 377-380.

[99] M&I Materials, "MIDEL Selection Guide: Choosing the right transformer liquid for your application," April 2017 2017.

[100] MIDEL, "Dielectric Insulating Fluid Overview," Sep 2014 2014.

[101] E. Pagger, M. Muhr, R. Braunstein, M. Tieber, K. Rapp, and A. Sbravati, "Natural ester FR3 insulating liquid - Very paper friendly," *International Conference on the Properties and Applications of Dielectric Materials,* Xi'an, China, 2018.

[102] M. Koch and S. Tenbohlen, "Evolution of bubbles in oil-paper insulation influenced by material quality and ageing," *IET Electric Power Applications,* vol. 5, no. 1, pp. 168-174, 2011.
[103] P. Hiemenz and R. Rajagopalan, *Principles of Surface and Colloid Chemistry*, 3rd ed. Marcel Dekker Inc., New York, 1997.
[104] P. Atkins and L. Jones, *Chemical Principles: The Quest For Insight*, 4th ed. Basingstoke, UK: W.H. Freeman and Company, 2008.
[105] C. Perkasa, N. Lelekakis, T. Czaszejko, D. Martin, and T. Saha, "Moisture-bubbling of vegetable oil impregnated paper at transformer overload temperatures," *IEEE International Conference on the Properties and Applications of Dielectric Materials*, Sydney, Australia, 2015: IEEE, pp. 76-79.
[106] H. Nordman, N. Rafsback, and D. Susa, "Temperature responses to step changes in the load current of power transformers," *IEEE Transactions on Power Delivery,* vol. 18, no. 4, pp. 1110-1117, 2003.
[107] V. Davydov and O. Roizman, "Moisture assessment in power transformers," *Vaisala news,* vol. 160, pp. 18-21, 2002.
[108] *Mineral insulating oils in electrical equipment. Supervision and maintenance guidance*, EN 60422:2013, 2013.
[109] W. H. Bartley, "Analysis of transformer failures, WGP 33 (03)," *Int. Association of Engineering Insurers (IMIA), 36th Annu. Conf.*, 2003.
[110] X. Zhang and E. Gockenbach, "Asset-management of transformers based on condition monitoring and standard diagnosis [Feature Article]," *IEEE Electrical Insulation Magazine*, vol. 24, no. 4, pp. 26-40, 2008.
[111] M. Wang, A. J. Vandermaar, and K. D. Srivastava, "Review of condition assessment of power transformers in service," *IEEE Electrical Insulation Magazine,* vol. 18, no. 6, pp. 12-25, 2002.
[112] R. Jongen, E. Gulski, P. Morshuis, J. Smit, and A. Janssen, "Statistical analysis of power transformer component life time data," ed, 2007, pp. 1273-1277.
[113] T. Suwanasri, E. Chaidee, and C. Adsoongnoen, "Failure statistics and power transformer condition evaluation by dissolved gas analysis technique," ed, 2008, pp. 492-496.
[114] L. Wang, L. Zhou, H. Tang, D. Wang, and Y. Cui, "Numerical and experimental validation of variation of power transformers' thermal time constants with load factor," *Applied Thermal Engineering*, vol. 126, pp. 939-948, 2017.
[115] B. C. Lesieutre, W. H. Hagman, and J. Kirtley, "An improved transformer top oil temperature model for use in an on-line monitoring and diagnostic system," *IEEE Transactions on Power Delivery*, vol. 12, no. 1, pp. 249-256, 1997.
[116] A. Shiri, A. Gholami, and A. Shoulaie, "Investigation of the ambient temperature effects on transformer's insulation life," *Electrical Engineering,* journal article vol. 93, no. 3, pp. 193-197, 2011.
[117] Y. Gao, "Assessment of Future Adaptability of Distribution Transformer Population Under EV Scenarios," Faculty of Engineering and Physical Sciences, The University of Manchester, Manchester, 2016.
[118] X. Zhang, "Dimensional Analysis Based CFD Modelling for Power Transformers," The University of Manchester (United Kingdom), 2017.
[119] M. Horning, J. Kelly, S. Myers, and R. Stebbins, *Transformer Maintenance Guide*, 3 ed. TMI, SDMyers Inc., 2004.
[120] T. V. Oommen and T. A. Prevost, "Cellulose insulation in oil-filled power transformers: part II maintaining insulation integrity and life," *IEEE Electrical Insulation Magazine*, vol. 22, no. 2, pp. 5-14, 2006.

[121] J. Jalbert, M.-C. Lessard, and M. Ryadi, "Cellulose chemical markers in transformer oil insulation Part 1: Temperature correction factors," *IEEE Transactions on Dielectrics and Electrical Insulation,* vol. 20, no. 6, pp. 2287-2291, 2013.
[122] G. Kaufmann, "Gas bubbles in distribution transformers," *IEEE Transactions on Power Apparatus and Systems,* vol. 96, no. 5, pp. 1596-1601, 1977.
[123] C. Qin, Y. He, B. Shi, T. Zhao, F. Lv, and X. Cheng, "Experimental study on breakdown characteristics of transformer oil influenced by bubbles," *Energies,* vol. 11, no. 3, p. 634, 2018.
[124] Cigré, "Cigré Brochure 349 “Moisture equilibrium and moisture migration within transformer insulation systems”," *Working Group A2.30;*, 2008.
[125] Cigré, "Cigré Brochure 227 “Life management techniques for power transformer”," *A2.18*, 2003.
[126] S. D. Lubetkin, "The nucleation and detachment of bubbles," *Journal of the Chemical Society, Faraday Transactions 1: Physical Chemistry in Condensed Phases,* vol. 85, no. 7, pp. 1753-1764, 1989.
[127] S. D. Lubetkin, "The fundamentals of bubble evolution," *Chemical Society Reviews,* vol. 24, no. 4, pp. 243-250, 1995.
[128] S. D. Lubetkin, D. J. Wedlock, Ed. *Controlled Particle, Droplet and Bubble Formation*. Oxford, UK: Butterworth-Heinemann Ltd, 1994.
[129] A. Muller, M. Jovalekic, and S. Tenbohlen, "Solubility study of different gases in mineral and ester-based transformer oils," presented at the IEEE International Conference on Condition Monitoring and Diagnosis, Bali, Indonesia, 23-27 September 2012, 2012. [Online]. Available: https://ieeexplore.ieee.org/document/6416307/.
[130] J. M. Smith, H. C. V. Ness, and M. M. Abbott, "Topics in Phase Equilibria," in *Introduction to Chemical Engineering Thermodynamics*7 ed.: McGraw-Hill, 2005.
[131] F. Heinrichs, "Bubble formation in power transformer windings at overload temperatures," *IEEE Transactions on Power Apparatus and Systems,* no. 5, pp. 1576-1582, 1979.
[132] Z. Krasucki, H. Church, and C. Garton, "A new explanation of gas evolution in electrically stressed oil - impregnated paper insulation," *Journal of the Electrochemical Society,* vol. 107, no. 7, pp. 598-602, 1960.
[133] W. McNutt, G. Kaufmann, A. Vitols, and J. MacDonald, "Short-time failure mode considerations associated with power transformer overloading," *IEEE Transactions on Power Apparatus and Systems,* no. 3, pp. 1186-1197, 1980.
[134] W. J. McNutt, T. O. Rouse, and G. H. Kaufmann, "Mathematical modelling of bubble evolution in transformers," *IEEE Transactions on Power Apparatus and Systems,* no. 2, pp. 477-487, 1985.
[135] W. A. Fessler, T. O. Rouse, W. J. McNutt, and O. R. Compton, "A refined mathematical model for prediction of bubble evolution in transformers," *IEEE Transactions on Power Delivery,* vol. 4, no. 1, pp. 391-404, 1989.
[136] Y. Du, M. Zahn, B. C. Lesieutre, A. V. Mamishev, and S. R. Lindgren, "Moisture equilibrium in transformer paper-oil systems," *IEEE Electrical Insulation Magazine,* vol. 15, no. 1, pp. 11-20, 1999.
[137] T. V. Oommen and S. R. Lindgren, "Bubble evolution from transformer overload," *Transmission and Distribution Conference and Exposition*, USA, 2001, vol. 1, pp. 137-142.
[138] P. Przybylek, Z. Nadolny, and H. Moscicka-Grzesiak, "Bubble effect as a consequence of dielectric losses in cellulose insulation," *IEEE Transactions on Dielectrics and Electrical Insulation,* vol. 17, no. 3, 2010.

[139] X. Zhang, Z. D. Wang, Q. Liu, P. Jarman, and M. Negro, "Numerical investigation of oil flow and temperature distributions for ON transformer windings," *Applied Thermal Engineering*, vol. 130, 2018 2018.

[140] C. Y. Perkasa, J. Wijaya, N. Lelekakis, and D. Martin, "Preliminary study of bubble formation in vegetable oil filled power transformer," *IEEE Conference on Electrical Insulation and Dielectric Phenomena*, 2013: IEEE, pp. 551-554.

[141] M. Gao, Q. Zhang, Y. Ding, T. Wang, H. Ni, and W. Yuan, "Investigation on bubbling phenomenon in oil-paper insulation," *IEEE Transactions on Dielectrics and Electrical Insulation*, vol. 24, no. 4, pp. 2362-2370, 2017.

[142] P. Przybyłek, "Badania temperatury inicjacji efektu bąbelkowania w izolacji papier-olej," *Przegląd Elektrotechniczny,* vol. 86, pp. 166-169, 2010.

[143] *IEEE Guide for Diagnostic Field Testing of Electric Power Apparatus - Part 1: Oil Filled Power Transformers, Regulators, and Reactors*, IEEE Std 62-1995, 1995.

[144] K. Miyagi, E. Oe, N. Yamagata, and H. Miyahara, "Thermal aging characteristics of insulation paper in mineral oil in overloaded operation of transformers," *Electrical Engineering in Japan*, vol. 182, no. 2, pp. 1-8, 2013.

[145] S. J. Tee, Q. Liu, Z. D. Wang, G. Wilson, P. Jarman, R. Hooton, P. Dyer, and D. Walker, "Practice of IEC 60422 in ageing assessment of in-service transformers," *19th International Symposium on High Voltage Engineering*, Pilsen, Czech Republic, 2015, vol. 423.

[146] Z. D. Wang, Q. Liu, S. J. Tee, S. Y. Matharage, P. Jarman, G. Wilson, R. Hooton, P. Dyer, C. Krause, and P. W. R. Smith, "Ageing assessment of transformers through oil test database analyses and alternative diagnostic techniques," *Proceedings of the 2015 Cigré SC A2 Colloquium*, Shanghai, China, 2015, pp. 20-25.

[147] Y. Du, A. V. Mamishev, B. C. Lesieutre, M. Zahn, and S. H. Kang, "Moisture solubility for differently conditioned transformer oils," *IEEE Transactions on Dielectrics and Electrical Insulation*, vol. 8, no. 5, pp. 805-811, 2001.

[148] Elexon, "Load profiles and their use in electricity settlement," 2013.

[149] E. Mladenov, S. Staykov, and G. Cholakov, "Water saturation limit of transformer oils," *IEEE Electrical Insulation Magazine*, vol. 25, no. 1, pp. 23-30, 2009.

[150] H. Yu, R. Chen, X. Hu, X. Xu, and Y. Xu, "Dielectric and physicochemical properties of mineral and vegetable oils mixtures," *IEEE International Conference on Dielectric Liquids*, Manchester, UK, 2017: IEEE.

[151] X. Zhang, Z. D. Wang, Q. Liu, M. Negro, A. Gyore, and P. W. R. Smith, "Numerical investigation of influences of liquid types on flow distribution and temperature distribution in disc type ON cooled transformers," *IEEE International Conference on Dielectric Liquids*, Manchester, UK, 2017.

[152] A. Santisteban Díaz, F. Ortiz Fernández, I. Fernández Diego, F. Delgado San Román, A. Ortiz Fernández, and C. J. Renedo Estébanez, "Thermal analysis of natural esters in a low-voltage disc-type winding of a power transformer," *International Conference on Dielectric Liquids*, Manchester, UK, 2017.

[153] P. Przybylek, H. Moranda, K. Walczak, and H. Moscicka-Grzesiak, "Bubble effect w układach izolacyjnych papier-ester syntetyczny oraz papier-olej mineralny (Bubble effect in paper – synthetic ester and paper – mineral oil insulation system)," *Przeglad Elektrotechniczny (Electrical Review) (in Polish),* 2013.

[154] D. Martin, "Evaluation of the dielectric capability of ester based oils for power transformers," *University of Manchester, UK*, 2008.

[155] A. Reffas, H. Moulai, and A. Beroual, "Comparison of dielectric properties of olive oil, mineral oil, and other natural and synthetic ester liquids under AC and lightning

impulse stresses," *IEEE Transactions on Dielectrics and Electrical Insulation,* vol. 25, no. 5, pp. 1822-1830, 2018.
[156] V. Aralkellian and I. Fofana, "Water in oil-filled, high-voltage equipment, Part I: States, solubility, and equilibrium in insulating materials," *IEEE Electrical Insulation Magazine,* vol. 23, no. 4, pp. 15-27, 2007.
[157] H. Ding, R. Heywood, P. Griffin, and L. Lewand, "An overview of water and relative saturation in power transformers," *IEEE International Conference on Dielectric Liquids,* 2017: IEEE, pp. 1-4.
[158] D. Martin, C. Perkasa, and N. Lelekakis, "Measuring paper water content of transformers: a new approach using cellulose isotherms in nonequilibrium conditions," *IEEE Transactions on Power Delivery,* vol. 28, no. 3, pp. 1433-1439, 2013.
[159] C. F. Hill, "Protective apparatus for electrical devices," US, 1939.
[160] *Power transformer handbook*. London: Butterworths, 1987.
[161] E. McKenna and M. Thomson, "High-resolution stochastic integrated thermal–electrical domestic demand model," *Applied Energy,* vol. 165, pp. 445-461, 2016/03/01/ 2016.
[162] I. Richardson, M. Thomson, D. Infield, and C. Clifford, "Domestic electricity use: A high-resolution energy demand model," *Energy and buildings,* vol. 42, no. 10, pp. 1878-1887, 2010.
[163] BEIS (DECC), "Energy Consumption in the UK," London, UK, 11/2016 2016.
[164] T. Baxter, "Energy saviours," *The Chemical Engineer*, no. 927, pp. 43-46, Sep 2018 2018.
[165] BEIS (DECC), "The Future of Heating: Meeting the Challenge," March 2013 2013.
[166] UK Power Networks, "Electric Vehicle Strategy," 2019.
[167] "Petrol and diesel car sales ban brought forward to 2035," in *BBC*, ed, 2020.
[168] R. Harrabin, "Gas heating ban for new homes from 2025," in *BBC*, ed, 2019.
[169] "The Electricity Safety, Quality and Continuity Regulations," ed. UK, 2002, p. 14.
[170] E. McKenna, M. Krawczynski, and M. Thomson, "Four-state domestic building occupancy model for energy demand simulations," *Energy and buildings,* vol. 96, pp. 30-39, 2015/06/01/ 2015.
[171] C. Gavin, "Seasonal variations in electricity demand " in "Special feature – Seasonal variations in electricity," Electricity Statistics, March 2014 2014.
[172] A. Stafford, "Long-term monitoring and performance of ground source heat pumps," *Building Research & Information,* vol. 39, no. 6, pp. 566-573, 2011/12/01 2011.
[173] A. S. Jenny Love, Phillip Biddulph, Jez Wingfield, Chris Martin, Colin Gleeson, Robert Lowe, "Investigating Variations in Performance of Heat Pumps Installed via the Renewable Heat Premium Payment (RHPP) Scheme," 2017.
[174] *Power transformers. Part 1: General*, BS EN 60076-1:2011, 2011.
[175] N. Good and P. Mancarella, "Flexibility in Multi-Energy Communities With Electrical and Thermal Storage: A Stochastic, Robust Approach for Multi-Service Demand Response," *IEEE Transactions on Smart Grid,* vol. 10, no. 1, pp. 503-513, 2019.
[176] NYNAS, "Nytro Gemini X Safety Data Sheet," 2015.
[177] MIDEL, "MIDEL(R) 7131 Transformer Fluid Technical Datasheets," December 2010 2010.
[178] T. Gradnik, B. Čuček, and M. Končan-Gradnik, "Temperature and chemical impact on determination of water content in dielectric liquids by capacitive moisture sensors," *2014 IEEE 18th International Conference on Dielectric Liquids (ICDL)*, 2014: IEEE, pp. 1-5.

[179] Cigré, "Cigré Brochure 157 "Effect of particles on transformer dielectric strength"," *Working Group 12.17*, June 2000 2000.
[180] M. Koch, *Reliable moisture determination in power transformers*. Sierke, 2008.
[181] Cigré, "Cigré brochure 741 "Moisture measurement and assessment in transformer insulation –

evaluation of chemical methods and moisture capacitive sensors"," *Working Group D1.53;*, 2018.
[182] J. Jalbert, R. Gilbert, and M. El Khakani, "Comparative study of vapor-liquid phase equilibrium methods to measure partitioning coefficients of dissolved gases in hydrocarbon oils," *Chromatographia*, vol. 56, no. 9-10, pp. 623-630, 2002.
[183] B. Garcia, J. C. Burgos, A. M. Alonso, and J. Sanz, "A moisture-in-oil model for power transformer monitoring - Part I: Theoretical foundation," *IEEE Transactions on Power Delivery*, vol. 20, no. 2, pp. 1417-1422, 2005.
[184] *Cellulosic papers for electrical purposes — Part 3: Specifications for individual materials — Section 3.5 Special papers*, BS 5626-3.5:1995 / IEC 60554-3-5, 1984.
[185] *Standard Test Method for Measurement of Average Viscometric Degree of Polymerization of New and Aged Electrical Papers and Boards*, ASTM D971 4243, 1999.
[186] *Measurement of the average viscometric degree of polymerization of new and aged cellulosic electrically insulating materials*, BS IEC 60450:2004, 2004.
[187] T. V. Oommen, "Moisture equilibrium in paper-oil insulation systems," *1983 EIC 6th Electrical/Electronical Insulation Conference*, 1983: IEEE, pp. 162-166.
[188] H. Gasser, C. Krause, and T. Prevost, "Water absorption of cellulosic insulating materials used in power transformers," *2007 IEEE International Conference on Solid Dielectrics*, 2007: IEEE, pp. 289-293.
[189] W. Lampe, E. Spicar, and K. Carrander, "Continuous purification and supervision of transformer insulation systems in service," *IEEE TRANSACTIONS ON POWER APPARATUS AND SYSTEMS*, 1978, vol. 97, no. 4: IEEE-INST ELECTRICAL ELECTRONICS ENGINEERS INC 345 E 47TH ST, NEW YORK, NY …, pp. 1007-1007.
[190] *Insulating liquids — Oil-impregnated paper and pressboard — Determination of water by automatic coulometric Karl Fischer titration*, BS EN 60814:1998, 1998.
[191] C. G. Hill and T. W. Root, *An introduction to chemical engineering kinetics & reactor design*. Wiley Online Library, 1977.
[192] S. Park, J. O. Baker, M. E. Himmel, P. A. Parilla, and D. K. Johnson, "Cellulose crystallinity index: measurement techniques and their impact on interpreting cellulase performance," *Biotechnology for biofuels*, vol. 3, no. 1, p. 10, 2010.
[193] S. Park, R. A. Venditti, H. Jameel, and J. J. Pawlak, "Studies of the heat of vaporization of water associated with cellulose fibers characterized by thermal analysis," *Cellulose*, journal article vol. 14, no. 3, pp. 195-204, June 01 2007.
[194] A. Mulet, J. García-Reverter, R. Sanjuán, and J. Bon, "Sorption Isosteric Heat Determination by Thermal Analysis and Sorption Isotherms," *Journal of Food Science*, vol. 64, no. 1, pp. 64-68, 1999.
[195] D. F. García, R. D. Villarroel, B. García, and J. C. Burgos, "Effect of the thickness on the water mobility inside transformer cellulosic insulation," *IEEE Transactions on Power Delivery*, vol. 31, no. 3, pp. 955-962, 2015.
[196] *Paris Agreement: United States of America: Withdrawl*, United States of America 54113, 2019.

References

[197] (2019). *Spring Statement 2019: Philip Hammond's speech*. [Online] Available: https://www.gov.uk/government/speeches/spring-statement-2019-philip-hammonds-speech

[198] C. Cook, "Ronan Point: a fifty-year building safety problem," 15 June 2018. Accessed on: 11 June 2020

[199] M. Dowson, A. Poole, D. Harrison, and G. Susman, "Domestic UK retrofit challenge: Barriers, incentives and current performance leading into the Green Deal," *Energy Policy*, vol. 50, pp. 294-305, 2012.

[200] N. Hirst, "Paying for net-zero–The fiscal framework for the UK's transition to low-carbon energy," 2020.

[201] C. Lilly, "On street charge point funding doubled," 21 January 20. Accessed on: 11 June 2020[Online]. Available: https://www.zap-map.com/on-street-charge-point-funding-doubled/

[202] M. Tyrrell. (2019, 11 June 2020). *UK now has more electric car charging points than fuel stations* [Online]. Available: https://www.pesmedia.com/electric-vehicles-charging-points-uk/.

[203] S. Vogel, *Cats' paws and catapults: mechanical worlds of nature and people*. New York, USA: W.W. Norton & Company Inc., 1998.

[204] F. R. de Carvalho Sousa, C. de Jesus Ribeiro, A. P. Marques, and L. da Cunha Brito, "Method for Rating and Analyzing the Combined Effects of Moisture and Temperature on the Oil–Paper Insulation System of Power Transformers by Means of Load Variations," *Journal of Control, Automation and Electrical Systems*, pp. 1-13, 2020.

ANNEX A – 20 W TESTS, NTUP WITH ALTERNATIVE LIQUIDS

Results of tests on NTUP with different liquid insulation. These tests were conducted at 20 W power input. Ester results appear to show higher BIT (Figure A-1) and tBI (Figure A-2), though scatter is large and the number of tests on the alternative (i.e. non-Gemini X) liquids is small.

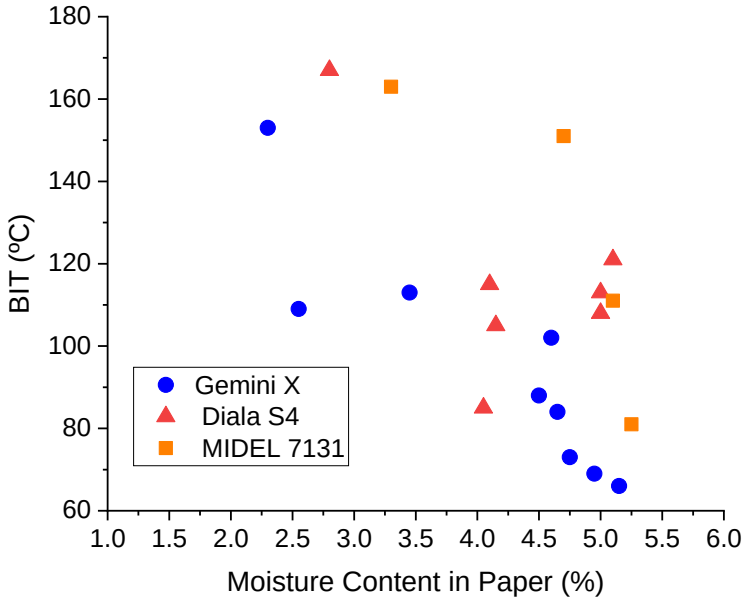

Figure A-1 – BIT Vs moisture content in paper.

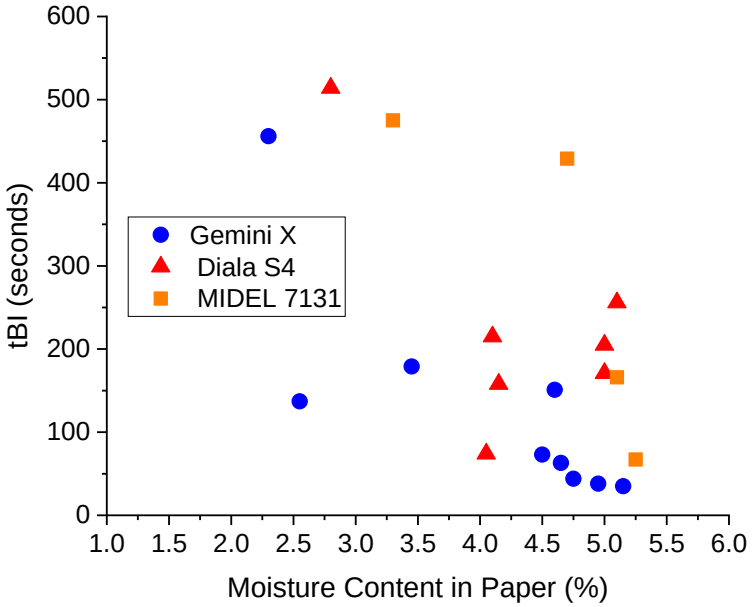

Figure A-2 – tBI Vs moisture content in paper.

ANNEX B – LIQUID INSULATION CHANGES AFTER TESTS WITH ALTERNATIVE LIQUIDS

Changes in liquid insulation moisture content after BIT tests for NTUP with alternative Liquid Insulators, relating to the tests of Annex A. When compared on a ppm basis (Figure B-1), the ester has much more moisture than the mineral oil and GTL (as expected), however, on a relative saturation RS basis (Figure B-2), the mineral oil and GTL are nearly saturated after the tests, whereas ester is less than 20% RS. Across all three liquids, the tests which lasted 30 minutes showed higher moisture content than the bubble-only tests.

Annex B – Liquid Insulation Changes after Tests with Alternative Liquids

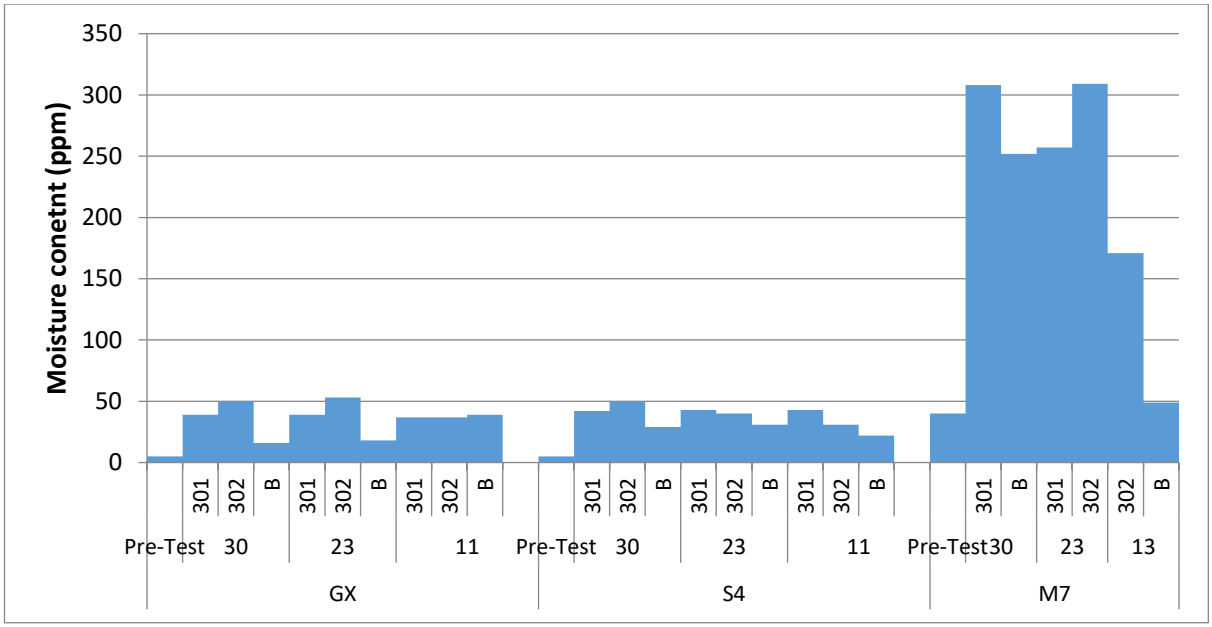

Figure B-1 – Liquid insulation moisture content pre- and post-test (in ppm).

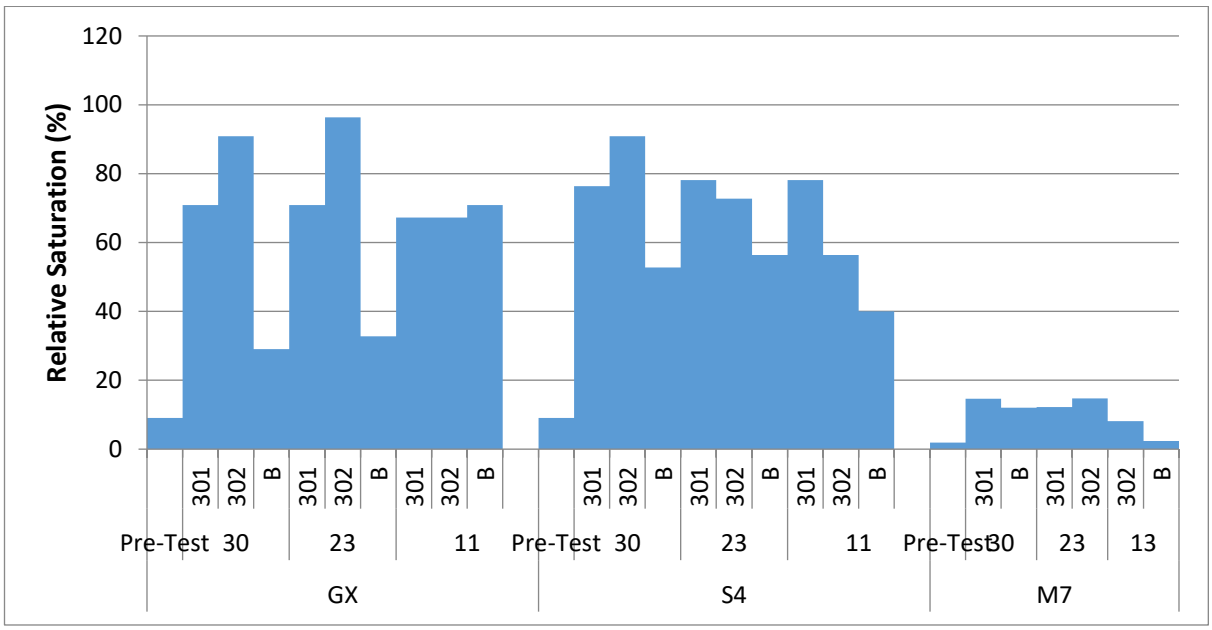

Figure B-2 – Liquid insulation moisture content pre- and post-test (in %RS).

ANNEX C – PAPER INSULATION CHANGES AFTER TESTS WITH ALTERNATIVE LIQUIDS

The change (reduction) in average moisture content of paper from the beginning of the tests to the end of the test in different liquids is compared (Figure C-1). For all liquids, moisture reduced, and reduced by significantly more for longer (30 minute) tests than shorter (bubble-only) tests. Bubble tests appear to have lower average moisture content in paper for ester liquid tests, though this is likely a result of those tests taking longer rather than the inherent differences in the material properties.

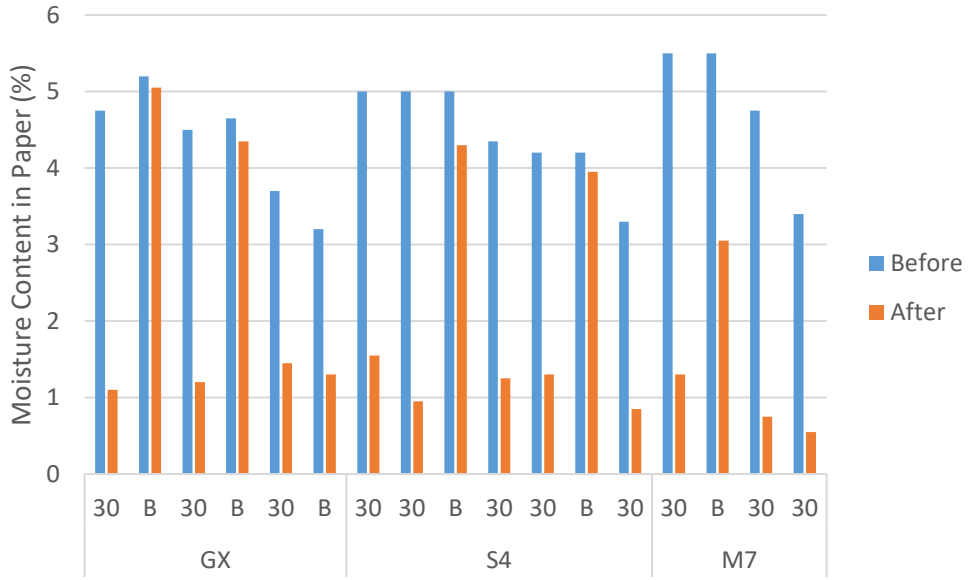

Figure C-1 – Change of moisture content in paper before and after tests on 30 minutes and bubble only tests for NTUP with various liquid insulation

For all liquids, the inner paper layer has higher moisture content than the outer layer for 30 minute tests. Bubble tests show more scatter. This is shown in Figure C-2.

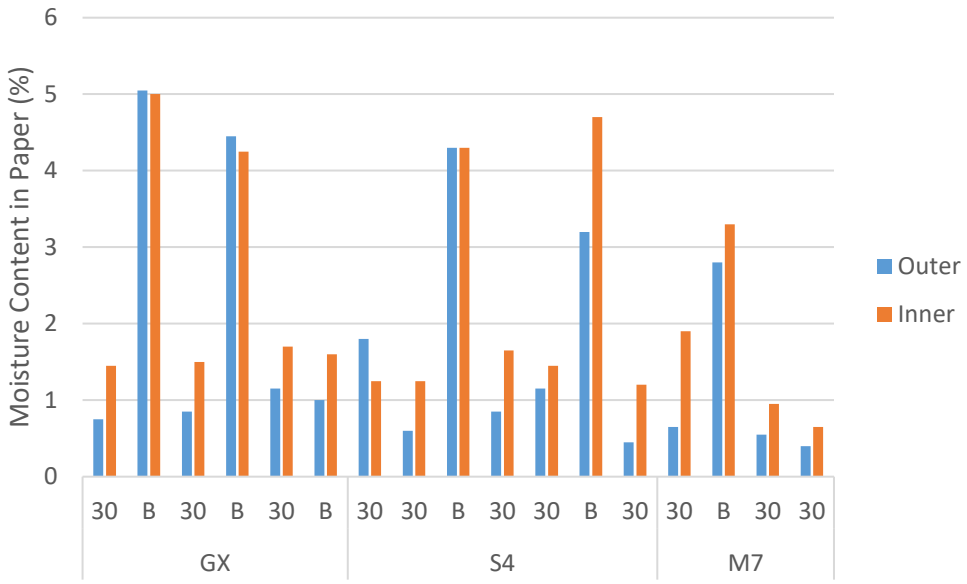

Figure C-2 – Comparison of moisture content in paper in inner and outer layers post-test on 30 minutes and bubble only tests for NTUP with various liquid insulation

In almost all tests, irrespective of the liquid insulation used, the upper part of the paper sample (the part that experiences highest temperatures) had less moisture after the tests (30 minute or bubble-only tests) than the lower section Figure C-3.

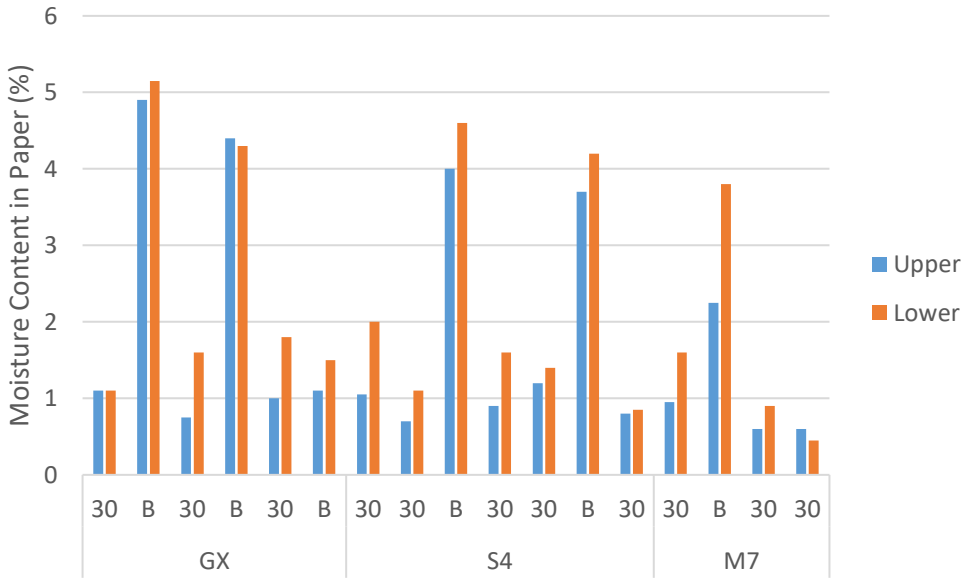

Figure C-3 – Comparison of moisture content in paper in upper and lower sections post-test on 30 minutes and bubble only tests for NTUP with various liquid insulation

ANNEX D – ADDITIONAL MOISTURE TESTS ON TUP SAMPLES

Moisture tests were conducted on the liquid insulation from TUP samples in Gemini X. Figure D-1 shows how the moisture content in liquid post-test is higher for samples of higher starting moisture content in paper, and for higher starting moisture content, the final moisture value of the liquid insulation is also dependent on the tBI. Figure D-2 shows that moisture content in the liquid post-test rises most for 30 minute tests.

Annex D – Additional moisture tests on TUP samples

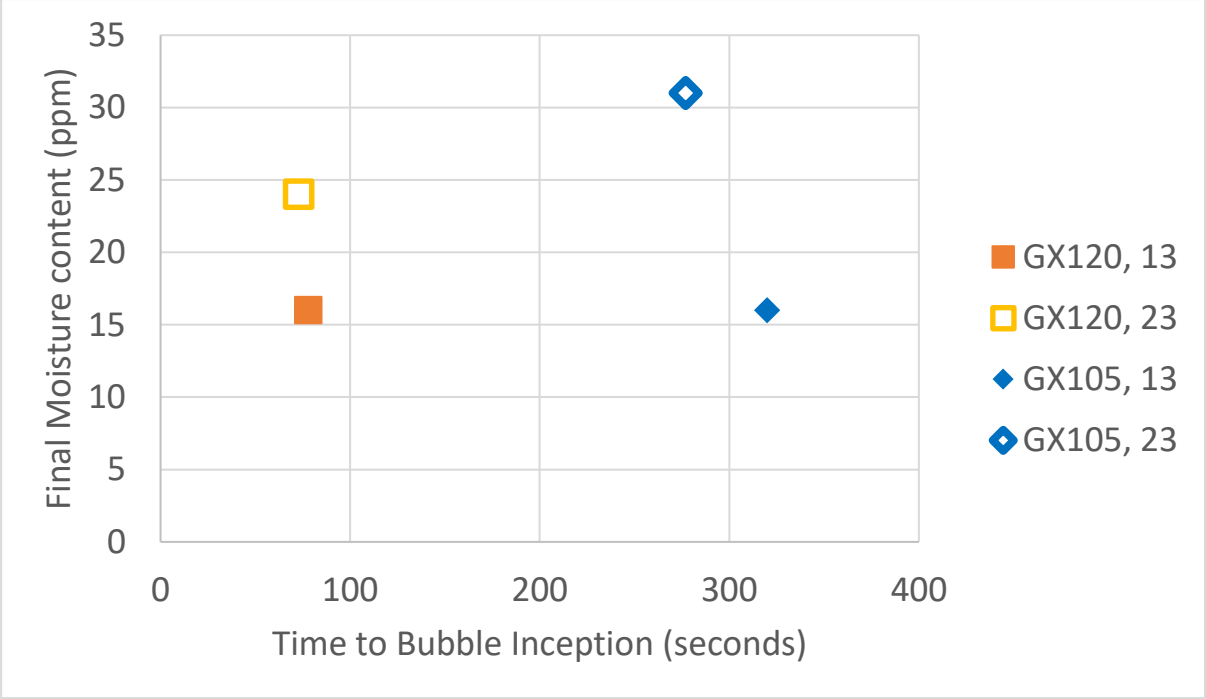

Figure D-1 – Moisture content in Gemini X post-test against tBI for TUP tests (i.e. equivalent to Figure 6-29).

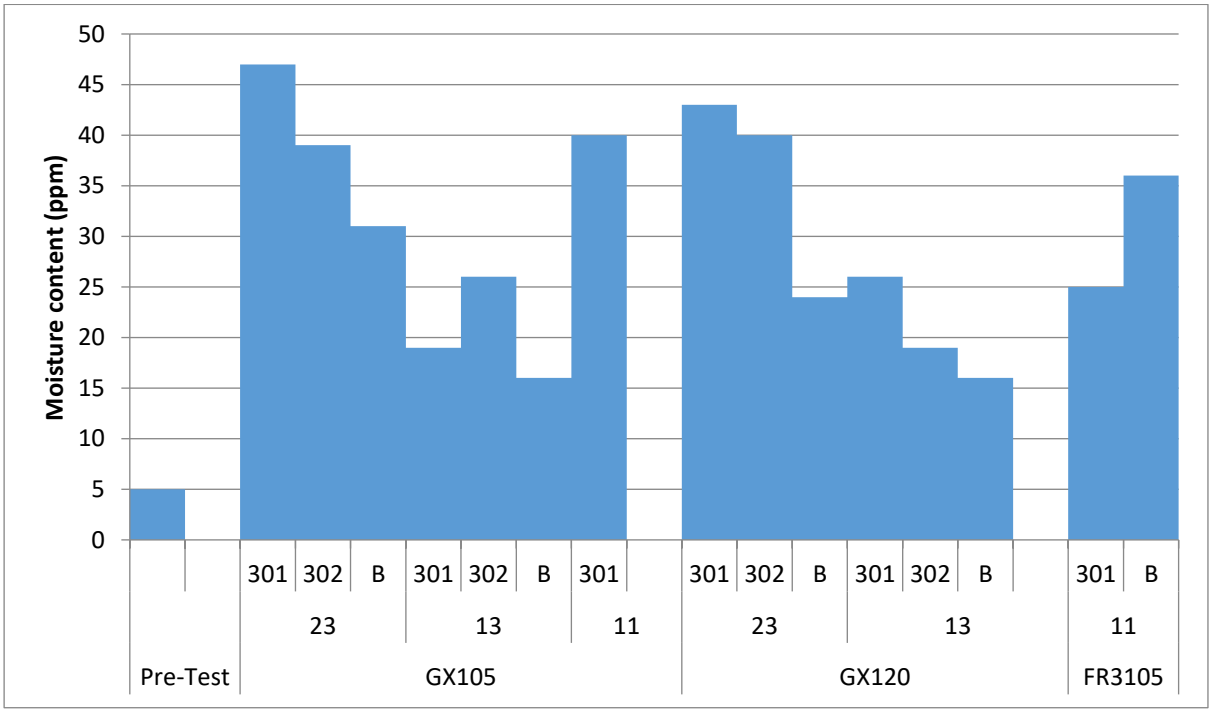

Figure D-2 – Change in Gemini X Moisture for TUP tests (equivalent to Figure 6-27 and Figure 6-28).

ANNEX E – TESTS ON TUP SAMPLES IN GEMINI X ON 13 K/MIN BASIS

Tests on TUP with Gemini X on 13 K/min basis. RS used as only one moisture test complete. Also, three of the four tests represent the same RS, so difficult to draw any conclusions.

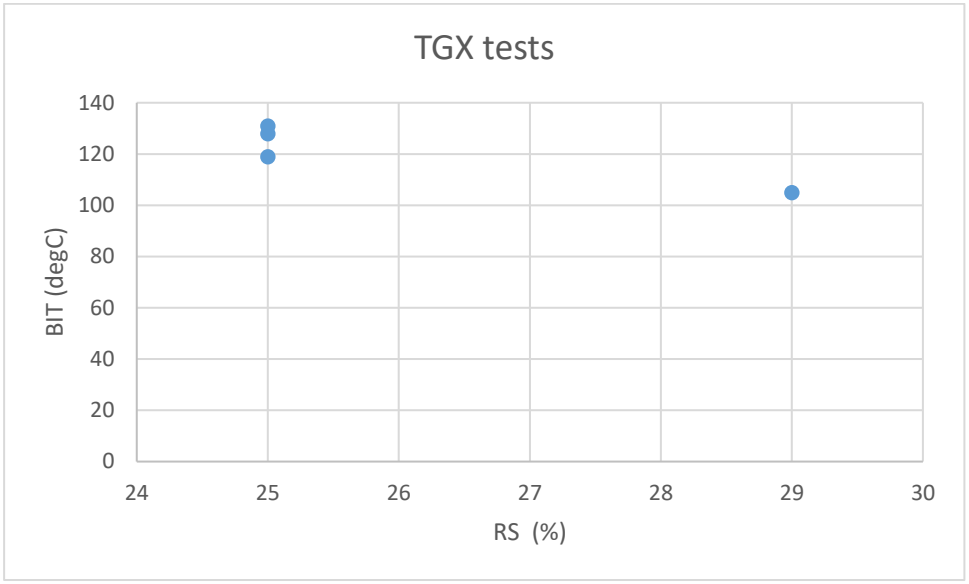

Figure E-1– BIT against relative saturation for TUP samples in Gemini X for 13 K/min rise.

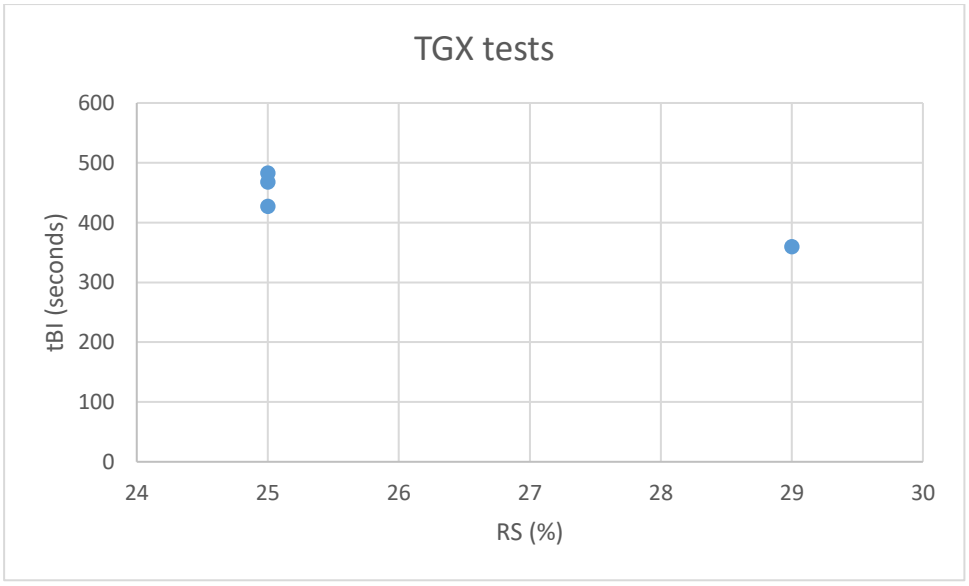

Figure E-2 – tBI against relative saturation for TUP samples in Gemini X for 13 K/min rise.

LIST OF PUBLICATIONS

JOURNALS

[P1] J. Hill, Z.D. Wang, Q. Liu, S. Matharage, A. Hilker, and D. Walker, "Improvements to the construction of bubble inception formulae for use with transformer insulation," *IEEE Access*, vol. 7, pp. 171673-171683, 2019.

[P2] J. Hill, Z.D. Wang, Q. Liu, Ch. Krause, and G. Wilson, "Analysing the power transformer temperature limitation for avoidance of bubble formation," *IET High Voltage*, 2019.

CONFERENCES

[P3] J. Hill, Z.D. Wang, X. Zhang, and Q. Liu, "Effectiveness of using simplified methods to estimate transformer loss of life," *IEEE Power & Energy Society General Meeting (PESGM)*, pp. 1-6, 2018.

[P4] J. Hill, Z.D. Wang, Q. Liu, Ch. Krause, and D. Walker, "Review of experiments investigating transformer insulation condition on bubble inception temperature," *International Conference on the Properties and Applications of Dielectric Materials*, Xi'an, China, 2018. (Best Paper Award).

[P5] M. Han, J. Hill, Z.D. Wang, and P. Crossley, "Thermal Evaluation of Railway Transformer Used in Autotransformer Feeding Systems," *International Energy Conference*, Limassol, Cyprus, 2018.